Application to Food Standards Australia New Zealand for the Inclusion of Maize MON 95275 in *Standard 1.5.2 - Food Derived from Gene Technology*

Submitted by:

Bayer CropScience Proprietary Limited

Level 1, 8 Redfern Road

Hawthorn East, Victoria 3123

14 September 2022

Contents

LIST OF FIGURES

LIST OF TABLES

UNPUBLISHED REPORTS BEING SUBMITTED

Appendix 1. [redacted]. 2021. Amended from TRR0001014: Molecular Characterization of Insect Protected Maize MON 95275. TRR0001330. Bayer CropScience LP. Confidential Business Information

Appendix 2. [redacted]. 2021. Amended from TRR0000933: Updated Bioinformatics Evaluation of the T-DNA in MON 95275 Utilizing the AD 2021, TOX_2021, and PRT_2021 Databases. TRR0001435. Bayer CropScience LP.

Appendix 3. [redacted]. 2021. Amended from TRR0000932: Updated Bioinformatics Evaluation of Putative Flank-Junction Peptides in MON 95275 Utilizing the AD_2021, TOX_2021, and PRT_2021 Databases. TRR0001434. Bayer CropScience LP.

Appendix 4. [redacted]. 2022. Amended from MSL0030830: Segregation Analysis of the T-DNA Insert in Insect Protected Maize MON 95275 Across Three Generations. TRR0001419. Bayer CropScience LP.

Appendix 5. [redacted]. 2021. Demonstration of the Presence of Mpp75Aa1.1 and Vpb4Da2 Proteins in Maize Grain Samples Across Multiple Generations of MON 95275. TRR0000780. Bayer CropScience LP.

Appendix 6 [redacted]. 2021. Amended Report for TRR0001114: Characterization of the Mpp75Aa1.1 Protein Purified from the Maize Grain of MON 95275 and Comparison of the Physicochemical and Functional Properties of the Plant-Produced and *Escherichia coli (E. coli)*-Produced Mpp75Aa1.1 Proteins. TRR0001571. Bayer CropScience LP.

Appendix 7. [redacted]. 2021. Amended Report for TRR0001113: Characterization of the Vpb4Da2 Protein Purified from the Maize Grain of MON 95275 and Comparison of the Physicochemical and Functional Properties of the Plant-Produced and *Escherichia coli (E. coli)*-Produced Vpb4Da2 Proteins. TRR0001572. Bayer CropScience LP.

Appendix 8. [redacted]. 2021. Assessment of Mpp75Aa1.1 and Vpb4Da2 Protein Levels in Maize Leaf, Root, Forage, Grain and Pollen Tissues Collected from MON 95275 Produced in Five Field Sites of United States Field Trials During 2019. TRR0000722. Bayer CropScience LP.

Appendix 9. [redacted]. 2021. Amended from TRR0000931: Updated Bioinformatics Evaluation of Mpp75Aa1.1 and Vpb4Da2 in MON 95275 Utilizing the AD_2021, TOX_2021, and PRT_2021 Databases. TRR0001416. Bayer CropScience LP.

Appendix 10. [redacted]. 2022. Amended Report for TRR0000731: Assessment of the *in vitro* Digestibility of *Escherichia coli*-produced Mpp75Aa1.1 Protein by Pepsin and Pancreatin. TRR0000731. Bayer CropScience LP.

Appendix 11. [redacted]. 2020. Assessment of the *in vitro* Digestibility of *Escherichia coli*-produced Vpb4Da2 Protein by Pepsin and Pancreatin. TRR0000596. Bayer CropScience LP.

Appendix 12. [redacted]. 2021. The Effect of Heat Treatment on the Functional Activity of *Escherichia coli*-produced Mpp75Aa1.1 Protein. TRR0000870. Bayer CropScience LP.

Appendix 13. [redacted]. 2021. The Effect of Heat Treatment on the Functional Activity of *Escherichia coli*-produced Vpb4Da2 Protein. TRR0000871. Bayer CropScience LP.

Appendix 14. [redacted]. 2022. Characterization of DvSnf7.1 RNA Extracted from MON 95275 and Comparison of the Molecular and Functional Properties of Plant-produced and *in vitro*-produced DvSnf7.1 RNA. TRR0000514. Bayer CropScience LP. Confidential Business Information

Appendix 15. [redacted]. 2022. Comparison of DvSnf7.1 RNA from MON 95275 and DvSnf7 RNA from MON 87411 Functional Activity and RNase If Digestion by Northern Blot Analyses. TRR0001178. Bayer CropScience LP

Appendix 16**.** [redacted]. 2021. Amended from TRR0000719: Characterization of DvSnf7.1 Read-through Transcripts in Maize MON 95275. TRR0001021. Bayer CropScience LP. Confidential Business Information

Appendix 17. [redacted]. 2020. Compositional Analyses of Maize Grain and Forage Harvested from MON 95275 Grown in the United States During the 2019 Season. MSL0030998. Monsanto Company.

CHECKLIST

General Requirements (3.1.1)	Reference
A Form of application	
☑ *Application in English*	*Available*
☑ *Executive Summary (separated from main application electronically)*	*Separate document prepared*
☑ *Relevant sections of Part 3 clearly identified*	*Completed*
☑ *Pages sequentially numbered*	*Completed*
☑ *Electronic copy (searcahable)*	*Prepared*
☑ *All references provided*	*Prepared*
B Applicant details	*Page 1*
C Purpose of the application	*Page 1*
D Justification for the application	
☑ *Regulatory impact information*	*Page 2*
☑ *Impact of international trade*	*Page 3*
E Information to support the application	
☑ *Data requirement*	*14*
F Assessment procedure	
☑ *General*	*Page 3*
☐ *Major*	
☐ *Minor*	
☐ *Hight level heath claim variation*	
G Confidential Commercial Information	
☑ *CCI material separated from other application material*	*Completed*
☐ *Formal request including reasons*	
☐ *Non-confidential summary provided*	
H Other confidential information	
☑ *Confidential material separated from other application material*	*Completed*
☑ *Formal request including reasons*	
I Exclusive Capturable Commercial Benefit	

☑ *Justification provided*	*Page 3*
J International and Other National Standards	
☑ *International standards*	*Page 4*
☑ *Other national standards*	*Page 4*
K Statutory Declaration	*Page 183*
L Checklist/s provided with Application	
☑ *3.1.1 Checklist*	*Page xi*
☑ *All page number references from application included*	*Completed*
☑ Any other relevant checklists for Sections 3.2 – 3.7	*Checklist 3.5.1*

Foods Produced using Gene Technology (3.5.1)	
☑ A.1 Nature and identity of the GM food	*Page 5*
☑ A.2 History of use of host and donor organisms	*Page 6*
☑ A.3 Nature of genetic modification	*Page 9*
☑ B.1 Characterisation and safety assessment of new substances	*Page 57*
☑ B.2 New proteins	*Page 104*
☑ B.3 Other (non-protein) new sustances	*Page 131*
☑ B.4 Novel herbicide metabolites in GM herbicide-tolerant plants	*Page 132*
☑ B.5 Compositional assessment	*Page 161*
☑ C Information related to the nutritional impact of the food produced using gene technology	*Page 182*
☑ D Other information	*Page 182*

ABBREVIATIONS AND DEFINITIONS[1]

aadA	Aminoglycoside-modifying enzyme, 3"(9) –*O*–nucleotidyltransferase from the transposon Tn*7*
ACVM	Agricultural Compounds and Veterinary Medicines
ADF	Acid Detergent Fiber
AFSI	Agriculture & Food Systems Institute
APHIS	Animal and Plant Health Inspection Service
aroA	5-enolpyruvylshikimate-3-phosphate synthetase gene from *Agrobacterium* sp. Strain CP4
bp	Basepair
Bt	*Bacillus thuringiensis*
bw	Body Weight
CaMV	Cauliflower Mosaic Virus
COA	Certificate of Analysis
COMPARE	COMprehensive Protein Allergen REsource
CRW	Corn Root Worm
Cry	Crystalline Proteins
CTP	Chloroplast Transit Peptide
d	Day(s)
DaMV	Dalia Mosaic Virus
DNA	Deoxyribonucleic Acid
dw	Dry Weight
E. coli	*Escherichia coli*
ELISA	Enzyme-Linked Immunosorbent Assay
EPA	Environmental Protection Agency
ETS	Excellence Through Stewardship
FA	Fatty Acid
FDA	Food and Drug Administration (U.S.)
fw	Fresh Weight
HESI	Health and Environmental Sciences Institute
ILSI	International Life Science Institute
kb	Kilobase
kDa	Kilodalton
kg	Kilogram
LOQ	Limit of Quantitation
mg	Milligram
mRNA	Messenger RNA
NCR	Northern Corn Rootworm
NDF	Neutral Detergent Fiber
NGS	Next Generation Sequencing
OECD	Organization for Economic Co-operation and Development
OR	Origin of Replication
ORF	Open Reading Frame
OSL	Over Season Leaf
OSR	Over Season Root

[1] Alred, G.J., C.T. Brusaw, and W.E. Oliu. 2003. Handbook of Technical Writing, 7th edn., pp. 2-7. Bedford/St. Martin's, Boston, MA.

PCR	Polymerase Chain Reaction
RNAi	RNA interference
RSR	Regulatory Status Review
SCR	Southern Corn Rootworm
S.E.	Standard Error
TDF	Total Dietary Fiber
T-DNA	Transfer Deoxyribonucleic Acid
µg/g	Microgram per Gram
U.S.	United States
USDA	United States Department of Agriculture
UTR	Untranslated Region
WCR	Western Corn Rootworm

PART 1 GENERAL INFORMATION

1.1 Applicant Details

(a) Applicant's name/s	Nina McCormick, Ph.D.
(b) Company/organisation name	Bayer CropScience Pty Ltd
(c) Address (street and postal)	Level 1, 8 Redfern Road, Hawthorn East, Victoria 3123
(d) Telephone number	+61 429 689 136
(e) Email address	nina.mccormick@bayer.com
(f) Nature of applicant's business	Technology Provider to the Agricultural and Food Industries
(g) Details of other individuals, companies or organisations associated with the application	

1.2 Purpose of the Application

This application is submitted to Food Standards Australia New Zealand by Bayer CropScience Proprietary Limited on behalf of Bayer Group.

The purpose of this submission is to make an application to vary **Standard 1.5.2** – *Food Produced Using Gene Technology* of the *Australia New Zealand Food Standards Code* to seek the addition of maize line MON 95275 and products containing maize line MON 95275 (hereafter referred to as MON 95275) to the Table to Clause 2 (see below).

Food derived from gene technology	Special requirements
Food derived from maize line MON 95275	None

1.3 Justification for the Application

1.3(a) The need for the proposed change

Coleopteran-protected maize MON 95275 was developed to provide growers in North America with new options for protection of maize against the feeding damage from targeted coleopteran pests, including western corn rootworm (WCR; *Diabrotica virgifera virgifera*), and northern corn rootworm (NCR; *Diabrotica barberi*). MON 95275 produces the Mpp75Aa1.1 insecticidal protein derived from *Brevibacillus laterosporus*, the Vpb4Da2[2] insecticidal protein derived from *Bacillus thuringiensis* (*Bt*), and a double-stranded RNA transcript from an inverted repeat sequence designed to match the western corn rootworm (WCR; *Diabrotica virgifera virgifera*) *Snf7* gene (DvSnf7.1). The Mpp75Aa1.1 and Vpb4Da2 proteins combined with DvSnf7.1 RNA provide protection from feeding damage caused by targeted coleopteran insect pests.

1.3(b) The advantages of the proposed change over the status quo, taking into account any disadvantages

MON 95275 was developed to provide growers in North America an additional tool to help control corn rootworm (CRW: *Diabrotica* ssp., Coleoptera; Chrysomelidae) pests, including those that may develop resistance to current *Bt* technologies. MON 95275 will not be offered for commercial use as a stand-alone product, but will be combined through traditional breeding with other deregulated and/or registered traits to provide protection against both above-ground and below-ground maize pests, as well as tolerance to multiple herbicides. These next generation combined-trait maize products will offer broader grower choice, improved production efficiency, and increased pest control durability, and promote a more sustainable agriculture system.

1.4 Regulatory Impact Information

Costs and benefits

If the draft variation to permit the sale and use of food derived from MON 95275 is approved, possible affected parties may include consumers, industry sectors and government. The consumers who may be affected are those that consume food containing ingredients derived from maize. Industry sectors affected may be food importers and exporters, distributors, processors and manufacturers. Lastly, government enforcement agencies may be affected.

A cost/benefit analysis quantified in monetary terms is difficult to determine. In fact, most of the impacts that need to be considered cannot be assigned a dollar value. Criteria would need to be deliberately limited to those involving broad areas such as trade, consumer information and compliance. If the draft variation is approved:

Consumers:

[2] The Mpp75Aa1.1 and Vpb4Da2 proteins expressed in MON 95275 were previously known as Cry75Aa1.1 and Vip4Ba1/Vip4Da2, respectively. The reclassification of these two proteins were based on structural homology. Background information on alias names and current names can be found in the following publication: (Crickmore *et al.*, 2021). Historical names of proteins were used in certain final study reports based on the effective date of name change. Historical and current names are considered equivalent.

There would be benefits in the broader availability of maize products.

There is unlikely to be any significant increase in the prices of foods if manufacturers are able to use comingled maize products.

Consumers wishing to do so will be able to avoid GM maize products as a result of labeling requirements and marketing activities.

Government:

- Benefit that if maize MON 95275 was detected in food products, approval would ensure compliance of those products with the Code. This would ensure no potential for trade disruption on regulatory grounds.
- Approval of maize MON 95275 would ensure no potential conflict with WTO responsibilities.
- In the case of approved GM foods, monitoring is required to ensure compliance with the labeling requirements, and in the case of GM foods that have not been approved, monitoring is required to ensure they are not illegally entering the food supply. The costs of monitoring are thus expected to be comparable, whether a GM food is approved or not.

Industry:

- Sellers of procesed foods containing maize derivatives would benefit as foods derived from maize MON 95275 would be compliant with the Code, allowing broader market access and increased choice in raw materials. Retailers may be able to offer a broader range of maize products or imported foods manufactured using maize derivatives.
- Possible cost to food industry as some food ingredients derived from maize MON 95275 would be required to be labelled

1.5 Impact of International Trade

If the draft variation to permit the sale and use of food derived from MON 95275 was rejected it would result in the requirement for segregation of any maize derived products containing MON 95275 from those containing approved maize, which would be likely to increase the costs of imported maize derived foods.

It is important to note that if the draft variation is approved, maize MON 95275 will not have a mandatory introduction. The consumer will always have the right to choose not to use/consume this product.

1.6 Assessment Procedure

Bayer CropScience is submitting this application in anticipation that it will fall within the General Procedure category.

1.7 Exclusive Capturable Commercial Benefit

This application is likely to result in an amendment to the Code that provides exclusive benefits and therefore Bayer CropScience intends to pay the full cost of processing the application.

1.8 International and Other National Standards

1.8(a) International standards

Bayer CropScience makes all efforts to ensure that safety assessments are aligned, as closely as possible, with relevant international standards such as the Codex Alimentarius Commission's *Principles for the Risk Analysis of Foods Derived from Modern Biotechnology* and supporting *Guideline for the Conduct of Food Safety Assessment of Foods Derived from Recombinant-DNA Plants* (Codex Alimentarius, 2009).

In addition, the composition analysis is conducted in accordance with OECD guidelines and includes the measurement of OECD-defined maize nutrients and anti-nutrients based on conventional commercial maize varieties (OECD, 2002b).

1.8(b) Other national standards or regulations

Bayer CropScience has submitted a food and feed safety and nutritional assessment summary for MON 95275 to the United States Food and Drug Administration (FDA) and has also requested a Regulatory Status Review (RSR) for a determination of plant pest risk potential of MON 95275, including all progenies derived from crosses between MON 95275 and conventional maize, or deregulated biotechnology-derived maize, by the Animal and Plant Health Inspection Service (APHIS) of the U.S. Department of Agriculture (USDA).

Consistent with our commitments to the Excellence Through Stewardship® (ETS)[3] Program, regulatory submissions have been or will be made to countries that import significant maize or food and feed products derived from U.S. maize and have functional regulatory review processes in place.

[3] ® Excellence Through Stewardship is a registered trademark of Excellence Through Stewardship, Washington, DC. http://www.excellencethroughstewardship.org/.

PART 2 SPECIFIC DATA REQUIREMENTS FOR SAFETY ASSESSMENT

A. TECHNICAL INFORMATION ON THE GM FOOD

A.1 Nature and Identity of the Genetically Modified Food

A.1(a) A description of the new GM organism from which the new GM food is derived

Coleopteran-protected maize MON 95275 was developed to provide growers in North America with new options for protection of maize against the feeding damage from targeted coleopteran pests, including western corn rootworm (WCR; *Diabrotica virgifera virgifera*), and northern corn rootworm (NCR; *Diabrotica barberi*). MON 95275 produces two insecticidal proteins, Mpp75Aa1.1 and Vpb4Da2, and the DvSnf7.1 RNA which protect against feeding damage caused by these coleopteran pests. The Mpp75Aa1.1 protein is derived from the full-length precursor form of the insecticidal protein Mpp75Aa1 from Brevibacillus laterosporus, where the native membrane-transiting signal peptide has been removed. Vpb4Da2 is the native protein originally from Bacillus thuringiensis (Bt). The DvSnf7.1 suppression cassette in MON 95275 produces the DvSnf7.1 RNA transcript, which contains the inverted repeat sequences that forms a 240 bp dsRNA (DvSnf7 dsRNA) responsible for an RNAi-based mode of action (MOA). The DNA sequence of the inverted repeat in MON 95275 is identical to that in MON 87411 for which the safety assessment was reviewed and approved by FSANZ in 2015 (A1097) also used to induce the RNAi mechanism in the CRW pests. The only difference between the full length DvSnf7.1 RNA expressed in MON 95275 and the full length DvSnf7 RNA expressed in MON 87411 is the 5′ UTR, which was optimized to increase in planta expression.

A.1(b) Name, line number and OECD Unique Identifier of each of the new lines or strains of GM organism from which the food is derived

In accordance with OECD's "Guidance for the Designation of a Unique Identifier for Transgenic Plants" MON 95275 has been assigned the unique identifier MON-95275-7.

A.1(c) The name the food will be marketed under (if known)

Maize containing the transformation event MON 95275 will be produced in North America. There are currently no plans to produce this product in Australia and New Zealand. A commercial trade name for the product has not been determined at the time of this submission and will be available prior to commercial launch of the product in North America.

A.2 History of Use of the Host and Donor Organisms

A.2(a) For the donor organism(s) from which the genetic elements are derived:

A.2(a)(i) Any known pathogenicity, toxicity or allergenicity relevance to the food

The *mpp75Aa1.1* gene encodes the Mpp75Aa1.1 protein, which is derived from the full-length precursor form of the insecticidal protein Mpp75Aa1 from *Brevibacillus laterosporus*. *B. laterosporus*, formerly classified as *Bacillus laterosporus*, is an endospore-forming insecticidal bacilli and not known for pathogenicity or allergencity in humans or other vertebrates (Laubach, 1916; Shida *et al.*, 1996). *B. laterosporus* shares a similar habitat to *Bt*, and can be isolated from a wide range of environments including soil, rocks, dust, and both fresh and sea waters (Ruiu, 2013; Panda *et al.*, 2014; Nivetha and Jayachandran, 2017). Furthermore, *B. laterosporus* is also found to be present in many food sources such as cheese (Román-Blanco *et al.*, 1999), curd (Panda *et al.*, 2014), beans (Sarkar *et al.*, 2002), and honey (Iurlina and Fritz, 2005), as well as being listed as a probiotic for humans (Hong *et al.*, 2005) and feed additive for birds (Ruiu, 2013). *B. laterosporus* isolate has a characterized broad-spectrum insecticidal activity and was registered for pest control in horticulture and agriculture in New Zealand (NZ EPA, 2022). Taken together, the widespread presence of *B. laterosporus* in the environment provides a documented history of safe exposure and consumption for human and other vertebrates.

The donor organism for the *vpb4Da2* gene, *Bacillus thuringiensis* (*Bt*), has a long history of commercial use in the U.S. to produce microbially-derived products with insecticidal activity. Applications of *Bt* have a documented history of safe use in agriculture, including in organic farming (U.S. EPA, 1988; Cannon, 1993; WHO, 1999). Since the first *Bt* isolate was registered as a pesticide in 1961, over 180 microbial *Bt* products have been registered in the United States (U.S.), with more than 120 microbial products registered in the European Union (EU) (Hammond, 2004). Microbial pesticides containing *Bt* insecticidal proteins have been subjected to extensive toxicity testing showing no adverse effects to human health (Baum *et al.*, 1999; Betz *et al.*, 2000; Mendelsohn *et al.*, 2003; McClintock *et al.*, 1995; U.S. EPA, 2001b; U.S. EPA, 2005). Additionally, there are no confirmed cases of allergic reactions to the insecticidal proteins in microbial-derived *Bt* products during more than 50 years of use (Koch *et al.*, 2015).

Similar to the corn rootworm-protected maize event MON 87411 (approved by FSANZ in 2015, A1097), the sequence present in the *DvSnf7.1* suppression cassette in MON 95275 was designed to match the gene present in western corn rootworm (WCR: *Diabrotica virgifera virgifera*) encoding the SNF7 subunit of the ESCRT-III complex (Babst *et al.*, 2002). The sequence in MON 95275 utilized to induce the RNAi mechanism in CRW is the same sequence present in MON 87411. Based on the ubiquitous nature of RNAi suppression utilizing endogenous dsRNAs in a wide variety of plant species consumed by humans and animals, demonstration of the specificity of *Snf7* suppression in CRW (Bachman *et al.*, 2013; Bachman *et al.*, 2016), the long history of safe consumption of RNA from a range of sources (Rodrigues and Petrick, 2020), and the apparent lack of toxicity or allergenicity of dietary RNA (Petrick *et al.*, 2016), the *DvSnf7.1* RNAi suppression sequence used in MON 95275 poses no observed risks to humans or other vertebrates.

The *mpp75Aa1.1* coding sequence in MON 95275 is under the regulation of the *DaMv-1* enhancer from Dalia mosaic virus (DaMV) promoter region (Kuluev and Chemeris, 2007)

that enhances transcription in plant cells and the *RCc3-Td1* promoter of an *RCc3* gene from *Tripsacum dactyloides* that directs transcription in plant cells (Hernandez-Garcia and Finer, 2014). Additionally, the *mpp75Aa1.1* coding sequence is regulated by the *14-3-3c-Si1* intron for a putative *14-3-3c* gene from *Setaria italica* (foxtail millet) involved in regulating gene expression (Rose, 2008). The *mpp75Aa1.1* coding sequence also utilizes the *HSP-Cl1* 3′ UTR of an *Hsp* gene from *Coix lacryma-jobi* (adlay millet) encoding a heat shock protein that directs polyadenylation of the mRNA (Hunt, 1994).

The *vpb4Da2* coding sequence is under the regulation of the *DaMV-2* enhancer from Dalia mosaic virus (DaMV) promoter region (Kuluev and Chemeris, 2007) that enhances transcription in plant cells and the *Ltp-Zm1* promoter of a lipid transfer protein gene from *Zea mays* (maize) that directs transcription in plant cells (Hernandez-Garcia and Finer, 2014). Additionally, the *vpb4Da2* coding sequence is regulated by the *Act-Si1* intron for an *actin* gene from *Setaria italica* (foxtail millet) that is involved in regulating gene expression (Rose, 2008). The *vpb4Da2* coding sequence also utilizes the *SAM1-Si1* 3′ UTR of an *S-adenosylmethionine synthetase 1* gene from *Setaria italica* (foxtail millet) that directs polyadenylation of the mRNA (Hunt, 1994).

The *DvSnf7* inverted repeat sequence in the MON 95275 is under the regulation of an optimized *pIIG-Zm1* enhancer from the physical impedance induced protein (*pIIg*) gene from *Zea mays* (Huang *et al.*, 1998) that enhances transcription in plant cells and a *35S* promoter from the 35S RNA of cauliflower mosaic virus (CaMV) (Odell *et al.*, 1985) that directs transcription in plant cells. Additionally, the sequence is regulated by the *Hsp70* intron and flanking exon sequence from *Zea mays* (maize) of the *hsp70* gene encoding the heat shock protein 70 (HSP70) (Rochester *et al.*, 1986) and is involved in regulating gene expression (Brown and Santino, 1997). The *DvSnf7.1* suppression cassette also utilizes the 3' UTR sequence of the *E9* gene from *Pisum sativum* (pea) *rbcS* gene family encoding the small subunit of ribulose bisphosphate carboxylase protein (Coruzzi *et al.*, 1984).

The *Isr-1* spacer is positioned between the *DvSnf7.1* suppression cassette and the *mpp75Aa1.1* expression cassette. It is a non-coding intergenic sequence region that minimizes potential effects on gene expression from neighboring cassettes (Casini *et al.*, 2014).

The *cp4 epsps* selectable marker cassette is also part of the originally inserted T-DNA in MON 95275. The *cp4 epsps* coding sequence is under the regulation of the promoter, 5' UTR, intron and 3′ UTR sequences of the *OsTubA* gene family from *Oryza sativa* (rice) encoding α-tubulin (Jeon *et al.*, 2000) that directs transcription and polyadenylation of mRNA in plant cells. The *cp4 epsps* expression cassette was excised from progeny plants using the Cre/*lox* recombination system for marker removal as described in Section A.3(b)(i)(ii) (Hare and Chua, 2002; Zhang *et al.*, 2003).

A.2(a)(ii) History of use of the organism in food supply or history of human exposure to the organism through other than intended food use (e.g. as a normal contaiminant)

As described in Section A.2.(a)(i), *B. laterosporus* has a documented history of safe exposure and consumption for human and other vertebrates as a result of the widespread presence in the environment. The long history of commercial use and the extensive toxicity testing of *Bt* subspecies and *Bt* insecticidal proteins in agriculture, including in organic farming, shows no adverse effects to human health. The long history of safe consumption of RNA from a range of sources (Rodrigues and Petrick, 2020), and the apparent lack of toxicity or allergenicity of

dietary RNA (Petrick *et al.*, 2016), the DvSnf7.1 RNAi suppression sequence used in MON 95275 poses no observed risks to humans or other vertebrates.

A.2(b) For the host organism into which the genes were transferred:

A.2(b)(i) Its history of safe use for food

Maize has been a staple of the human diet for centuries, and its processed fractions are consumed in a multitude of food and animal feed products. For the 2020/2021 market year, values for U.S. domestic maize usage were 40% for feed and residual uses; 35% for alcohol for fuel; 7% for food, seed, and industrial uses other than alcohol for fuel; and 18% for exports (McConnell *et al.*, 2021). Global demand for maize has increased due to greater meat consumption in emerging economic countries including China, and biofuels production (Edgerton, 2009).

Maize is used extensively as a livestock feed for reasons that include its palatability, digestibility, and metabolizable energy (Loy and Lundy, 2019) and its relatively low cost (OECD, 2002b). Maize grain may be fed whole (Watson, 1988), but in many cases it is ground and mixed with other ingredients to provide a balanced ration (Leath and Hill, 1987). As reviewed by Loy and Lundy (2019), animal feed products from the wet milling process include maize gluten feed and maize gluten meal. Animal feed products from the dry milling process include hominy feed (Loy and Lundy, 2019). Ethanol production from dry milled maize provides distillers grains, another source of animal feed (Loy and Lundy, 2019). Maize can also be fed as a whole plant silage.

From 2016/17 to 2020/21, global maize production averaged approximately 1,118 million metric tons (MMT) per marketing year (USDA-FAS, 2022). During this same period, the top maize producers were the United States, China, Brazil, and the European Union (EU), together accounting for approximately 69% of average annual global maize production (USDA-FAS, 2022). Also during this period, global maize production per marketing year ranged from 1,078 MMT to 1,143 MMT (USDA-FAS, 2022).

In the 2020/2021 trade year, the top maize exporters were the United States, Brazil, Argentina, and Ukraine. Together, these countries accounted for approximately 88% of global exports (USDA-FAS, 2022). In the same trade year, the top maize importers were the European Union, Mexico, China and Japan, together accounting for 37% of global imports (USDA-FAS, 2022).

A.2(b)(ii) The part of the organism typically used as food

Maize kernels are typically used as food. The main components of maize kernels are endosperm (83%), germ (11%), and pericarp (bran) (5%) (Watson, 1988). Milling separates the grain into these components, with subsequent products dependent on the milling type (Watson, 1988).

A.2(b)(iii) The types of products likely to include the food or food ingredient

Food uses of maize include processed products from field maize and direct consumption of sweet maize and popcorn. Food products derived from the wet milling process include starch and sweetener products (e.g. high fructose maize syrup) (May, 1987). Food products derived

from the dry milling process include maize grits, maize meal, and maize flour (Watson, 1988). Maize oil may be derived from either milling process (Watson, 1988).

A.2(b)(iv) Whether special processing is required to render food safe to eat

Products from wet milling: As reviewed by (Rausch *et al.*, 2019), the products of the wet milling include starch and sweeteners used in foodstuffs. Native or modified maize starch is used in a wide range of foods, including bakery products, puddings and custards, snack foods, salad dressings, meat products, prepared soups, and many others (Rausch *et al.*, 2019). Starch is also converted into a variety of sweetener products including high fructose maize syrup (Watson, 1988). The various sweeteners are also used in a wide range of foods, including bakery products, breakfast foods, desserts, prepared soups, canned fruits and juices and many others (Rausch *et al.*, 2019). In addition to starch and sweeteners, oil is obtained from the germ fraction that is separated during the wet milling process (Rausch *et al.*, 2019).

Products from dry milling: The products of the dry milling process include maize grits, maize meal, and maize flours, each of which is derived from the endosperm (Watson, 1988). The food uses of these products have been reviewed by (Rooney and Serna-Saldivar, 2003). Maize grits have the largest particles and have less than 1% oil content (Rooney and Serna-Saldivar, 2003). Grits are used in making breakfast cereals and snacks (Rooney and Serna-Saldivar, 2003), and are eaten in the U.S. as side dish (Watson, 1988). Maize meal has smaller particles than maize grits (Rooney and Serna-Saldivar, 2003). It is used in baked products like maize bread and muffins, and may be enriched with vitamins and minerals like thiamine, riboflavin, niacin, and iron (Rooney and Serna-Saldivar, 2003). Maize flour is made up of fine endosperm particles and has many uses as a food ingredient (e.g. in ready to eat snacks or pancake mixes) or binder (e.g. in processed meats) (Rooney and Serna-Saldivar, 2003). In addition to endosperm products, oil is obtained from the germ faction that is separated during the dry milling process (Watson, 1988).

Products from fermentation: Products from the wet and dry milling processes (e.g. corn syrups, grits) can also be used in producing distilled beverages through fermentation (Rooney and Serna-Saldivar, 2003; Watson, 1988).

A.3 The Nature of the Genetic Modification

Characterization of the genetic modification in MON 95275 was conducted using a combination of sequencing, PCR, and bioinformatics. The results of this characterization demonstrate that MON 95275 contains a single copy of the intended T-DNA containing the *DvSnf7.1* suppression cassette and the *mpp75Aa1.1* and *vpb4Da2* expression cassettes that is stably integrated at a single locus and is inherited according to Mendelian principles over multiple generations. These conclusions are based on the following lines of evidence:

- Molecular characterization of MON 95275 by NGS demonstrated that MON 95275 contained a single T-DNA insert. These whole-genome analyses provided a comprehensive assessment of MON 95275 to determine the presence and identity of sequences derived from PV-ZMIR525664 and demonstrated that MON 95275 contains a single T-DNA insert, with no detectable backbone or *cp4 epsps* selectable marker sequences from PV-ZMIR525664 or any sequences from the Cre line transformation vector PV-ZMOO513642.

- Directed sequencing (locus-specific PCR, DNA sequencing and analyses) performed on MON 95275 was used to determine the complete sequence of the single DNA insert from PV-ZMIR525664, the adjacent flanking DNA, and the 5' and 3' insert-to-flank junctions. This analysis confirmed that, other than a single nucleotide difference in a non-coding intervening sequence region, the sequence and organization of the DNA is identical to the corresponding region in the PV-ZMIR525664 T-DNA. Directed sequencing also confirmed that the *cp4 epsps* selectable marker cassette which was excised, along with one *loxP* site, by Cre recombinase, is not present in MON 95275. Furthermore, the genomic organization at the insertion site in MON 95275 was assessed by comparing the sequences flanking the T-DNA insert in MON 95275 to the sequence of the insertion site in conventional maize. This analysis determined that 746 bases were deleted at the insertion site and 6 bases were co-inserted at the 3' flanking region in MON 95275 upon DNA integration.

- Generational stability analysis by NGS demonstrated that the single PV-ZMIR525664 T-DNA insert in MON 95275 has been maintained through five breeding generations, thereby confirming the stability of the T-DNA in MON 95275.

- Segregation data confirm that the inserted T-DNA segregated according to Mendelian inheritance patterns, which corroborates the insert stability demonstrated by NGS and independently establishes the nature of the T-DNA at a single chromosomal locus.

Taken together, the characterization of the genetic modification in MON 95275 demonstrates that a single copy of the T-DNA was stably integrated at a single locus of the maize genome and that no PV-ZMIR525664 plasmid backbone, *cp4 epsps* selectable marker, or PV-ZMOO513642 sequences are present in MON 95275.

A.3(a) A description of the method used to transform the host organism

MON 95275 was developed through *Agrobacterium tumefaciens* mediated transformation of immature maize embryos based on the method described by Sidorov and Duncan (2009) utilizing PV-ZMIR525664. Immature embryos were excised from a post-pollinated maize ear of LH244. After co-culturing the excised immature embryos with *Agrobacterium* carrying the plasmid vector, the immature embryos were placed on selection medium containing glyphosate and carbenicillin disodium salt in order to inhibit the growth of untransformed plant cells and excess *Agrobacterium*, respectively. Once transformed callus developed, the callus was placed on media conducive to shoot and root development. The rooted plants (R0) with normal phenotypic characteristics were selected and transferred to soil for growth and further assessment.

The R0 plants were self-pollinated to produce R1 seed. Subsequently, the R1 population was screened for the presence of T-DNA and absence of vector backbone sequences by construct-level PCR assay and Southern blot analysis. Only plants that were homozygous positive for T-DNA and negative for vector backbone were selected for further development and their progenies were subjected to further molecular and phenotypic assessments. As is typical of a commercial event production and selection process, hundreds of different transformation events (regenerants) were generated in the laboratory using PV-ZMIR525664. Selected R2

events were crossed with a line expressing the Cre recombinase protein and screened for the absence of *cp4 epsps* and the *cre* genes. After careful selection and evaluation of these events in the laboratory, greenhouse and field, MON 95275 was selected as the lead event for commercialization based on superior trait efficacy, agronomic, phenotypic, and molecular characteristics according to the general process described in Prado *et al.* (2014). Studies on MON 95275 were initiated to further characterize the genetic insertion and the expressed product, and to establish the food, feed, and environmental safety relative to conventional maize. The major steps involved in the development of MON 95275 are depicted in Figure 1. The result of this process was the production of MON 95275 maize with the *DvSnf7.1* suppression cassette and the *mpp75Aa1.1* and *vpb4Da2* expression cassettes.

For details, please refer to Appendix 1 ([redacted]., 2021 (TRR0001330)).

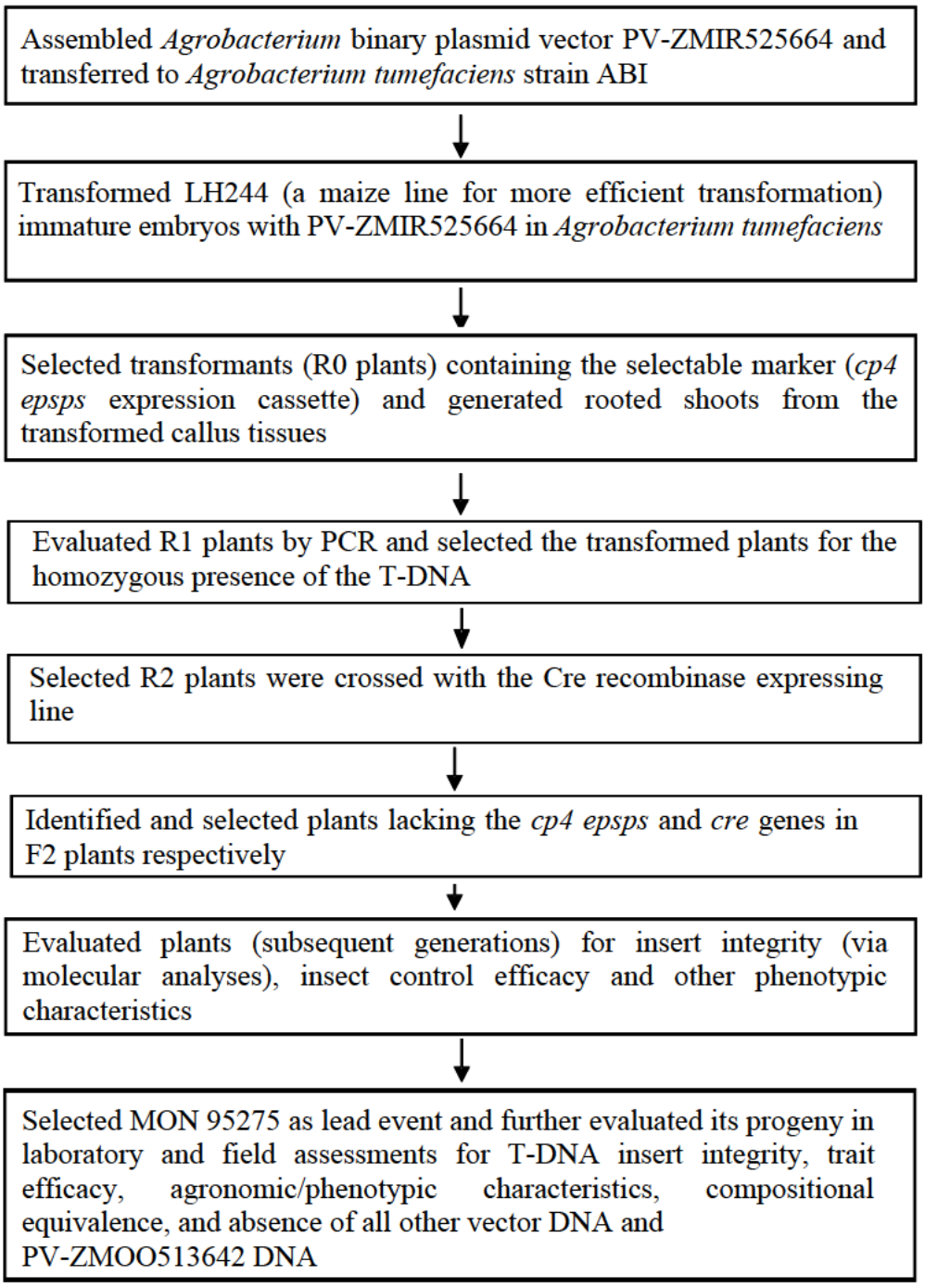

Figure 1. Schematic of the Development of MON 95275

A.3(b) A description of the construct and the transformation vectors used, including:

A.3(b)(i) The size, source and function of all the genetic components including marker genes, regulatory and other elements

A.3(b)(i)(i) Description of Transformation Plasmid PV-ZMIR525664

Plasmid vector PV-ZMIR525664 was used for the transformation of conventional maize to produce MON 95275 and its plasmid map is shown in Figure 2. A description of the genetic elements and their prefixes (e.g. B, T, P, I, E, S, CS, TS and OR) in PV-ZMIR525664 is provided in Table 1. PV-ZMIR525664 is approximately 22.9 kb and contains a single T-DNA (transfer DNA) that is delineated by Left and Right Border regions. The T-DNA, contains the *DvSnf7.1* suppression cassette, the *mpp75Aa1.1* and *vpb4Da2* expression cassettes and the *cp4 epsps* selectable marker cassette. During transformation, the T-DNA was inserted into the maize genome (Section A.3(a)). Following transformation, Cre/*lox* recombination, segregation, molecular screening and selection were used to isolate those plants that contained the *DvSnf7.1* suppression cassette and the *mpp75Aa1.1* and *vpb4Da2* expression cassettes and did not contain the backbone sequences from the transformation vector, the *cp4 epsps* selectable marker cassette or any sequence from the *cre* gene-containing vector PV-ZMOO513642.

The *DvSnf7* inverted repeat sequence in the MON 95275 is under the regulation of an optimized *pIIG-Zm1* enhancer from the physical impedance induced protein (*pIIg*) gene from *Zea mays* (Huang *et al.*, 1998) that enhances transcription in plant cells and a *35S* promoter from the 35S RNA of cauliflower mosaic virus (CaMV) (Odell *et al.*, 1985) that directs transcription in plant cells. Additionally, the sequence is regulated by the *Hsp70* intron and flanking exon sequence from *Zea mays* (maize) of the *hsp70* gene encoding the heat shock protein 70 (HSP70) (Rochester *et al.*, 1986) and is involved in regulating gene expression (Brown and Santino, 1997). The *DvSnf7.1* suppression cassette also utilizes the 3' UTR sequence of the *E9* gene from *Pisum sativum* (pea) *rbcS* gene family encoding the small subunit of ribulose bisphosphate carboxylase protein (Coruzzi *et al.*, 1984).

The *Isr-1* spacer is positioned between the *DvSnf7.1* suppression cassette and the *mpp75Aa1.1* expression cassette. It is a non-coding intergenic sequence region that minimizes potential effects on gene expression from neighboring cassettes (Casini *et al.*, 2014).

The *mpp75Aa1.1* coding sequence in MON 95275 is under the regulation of the *DaMv-1* enhancer from Dalia mosaic virus (DaMV) promoter region (Kuluev and Chemeris, 2007) that enhances transcription in plant cells and the *RCc3-Td1* promoter of an *RCc3* gene from *Tripsacum dactyloides* that directs transcription in plant cells (Hernandez-Garcia and Finer, 2014). Additionally, the *mpp75Aa1.1* coding sequence is regulated by the *14-3-3c-Si1* intron for a putative *14-3-3c* gene from *Setaria italica* (foxtail millet) involved in regulating gene expression (Rose, 2008). The *mpp75Aa1.1* coding sequence also utilizes the *HSP-Cl1* 3′ UTR of an *Hsp* gene from *Coix lacryma-jobi* (adlay millet) encoding a heat shock protein that directs polyadenylation of the mRNA (Hunt, 1994).

The *vpb4Da2* coding sequence is under the regulation of the *DaMV-2* enhancer from Dalia mosaic virus (DaMV) promoter region (Kuluev and Chemeris, 2007) that enhances transcription in plant cells and the *Ltp-Zm1* promoter of a lipid transfer protein gene from *Zea mays* (maize) that directs transcription in plant cells (Hernandez-Garcia and Finer, 2014). Additionally, the

vpb4Da2 coding sequence is regulated by the *Act-Si1* intron for an *actin* gene from *Setaria italica* (foxtail millet) that is involved in regulating gene expression (Rose, 2008). The *vpb4Da2* coding sequence also utilizes the *SAM1-Si1* 3′ UTR of an *S-adenosylmethionine synthetase 1* gene from *Setaria italica* (foxtail millet) that directs polyadenylation of the mRNA (Hunt, 1994).

The *cp4 epsps* selectable marker cassette is also part of the originally inserted T-DNA in MON 95275. The *cp4 epsps* coding sequence is under the regulation of the promoter, 5' UTR, intron and 3′ UTR sequences of the *OsTubA* gene family from *Oryza sativa* (rice) encoding α-tubulin (Jeon *et al.*, 2000) that directs transcription and polyadenylation of mRNA in plant cells. The *cp4 epsps* expression cassette was excised from progeny plants using the Cre/*lox* recombination system for marker removal as described in the following section below (Hare and Chua, 2002; Zhang *et al.*, 2003).

The backbone region of PV-ZMIR525664, located outside of the T-DNA, contains two origins of replication for maintenance of the plasmid vector in bacteria (*oriV, ori-pBR322*) and a bacterial selectable marker gene (*aadA*).

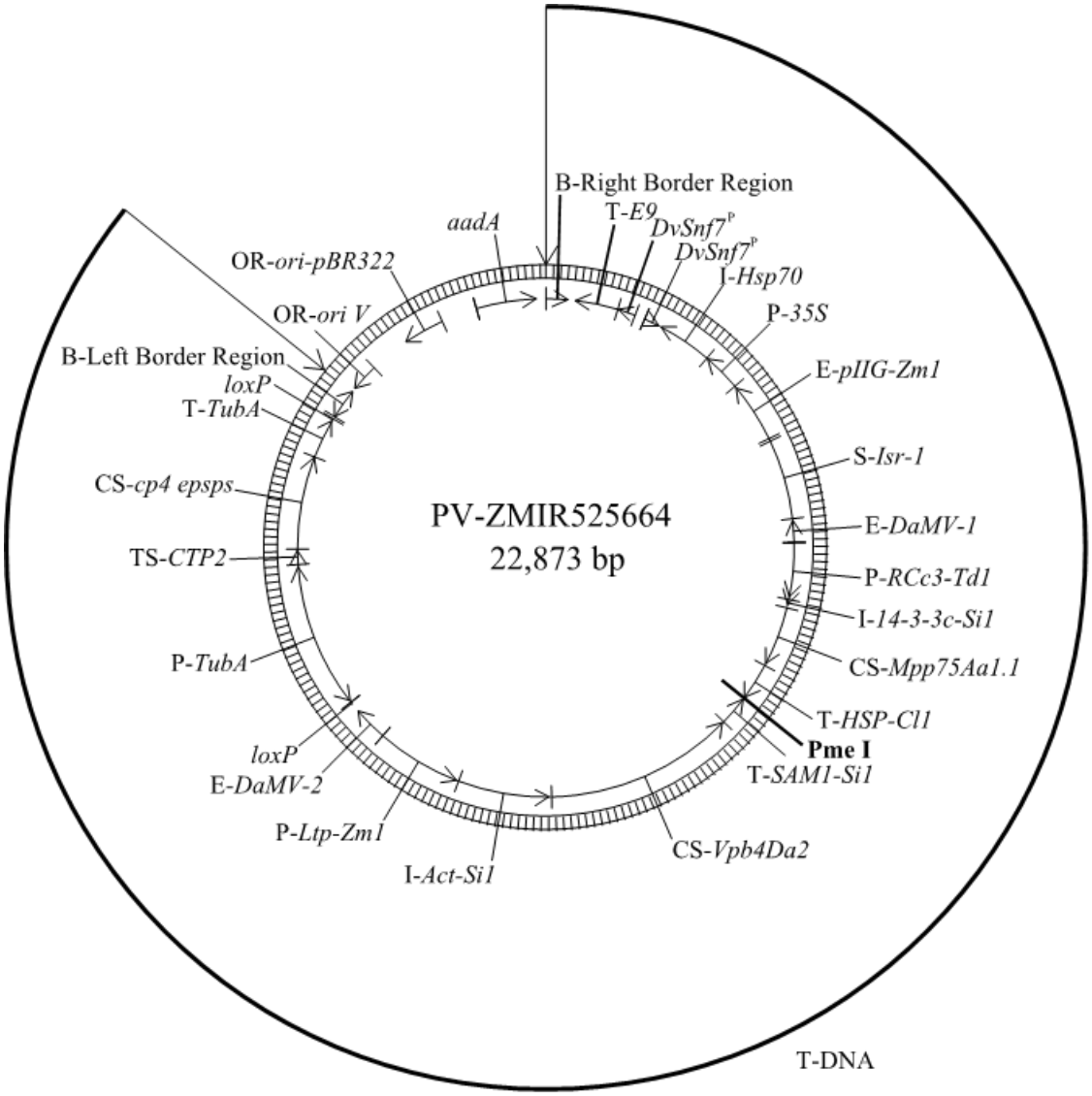

Figure 2. Circular Map of PV-ZMIR525664

A circular map of PV-ZMIR525664 used to develop MON 95275 is shown. PV-ZMIR525664 contains one T–DNA. Genetic elements are shown on the exterior of the map.

A.3(b)(i)(ii) Marker Removal Through Cre/*lox* Recombination System

The use of the Cre/lox recombination system for marker removal has been previously described (Hare and Chua, 2002; Zhang et al., 2003; Russell et al., 1992). The Cre/lox recombination system is derived from the bacteriophage P1 and consists of the Cre recombinase and a stretch of DNA flanked by two copies of the loxP sites. The loxP site is 34 bp in length and consists of two 13 bp inverted repeats and an asymmetrical 8 bp spacer. The 13-bp inverted repeats are the Cre recombinase binding sequence, and the 8 bp spacer is essential for the recombination reaction. Cre recombinase binds to the inverted repeat sequence in the loxP site, catalyzing a crossover in the 8 bp spacer regions of the two loxP sites. The results of this crossover are two-fold: one is the excision of the DNA fragment flanked by the two half loxP sites (in MON 95275 this is the cp4 epsps selectable marker cassette) forming a circular extra-genomic DNA fragment, the other is the recombination of linear DNA between the remaining two half loxP sites within the maize genome (Gilbertson, 2003).

As reviewed by Gilbertson (2003), one of the advantages of the Cre/*lox* system is the specificity of the enzyme for the wild-type *loxP* 34 bp recognition sequence. The frequency of Cre recombinase-mediated DNA recombination can be significantly reduced with even a single nucleotide change in specific regions of the *loxP* sequence (Hartung and Kisters-Woike, 1998; Hoess *et al.*, 1986; Lee and Saito, 1998). Therefore, neither the specific DNA insert nor the usage of the Cre/*lox* system was expected to negatively influence the stability of the T-DNA in MON 95275 across breeding generations, which has been confirmed, and is described in Section A.3(e) of this application. This technology was previously reviewed by FSANZ as part of the Food and Feed Safety Assessment for LY038 maize (A549, 2006). and most recently as part of the review of Lepidopteran Protected Maize MON 95379 (A1226, 2022).

A maize line expressing Cre recombinase (developed with the transformation plasmid vector PV-ZMOO513642) was crossed with lines transformed with PV-ZMIR525664. In the resulting hybrid plants, the cp4 epsps selectable marker cassette that was flanked by the *loxP* sites was excised. The excised *cp4 epsps* selectable marker cassette (circular extra-genomic DNA) was subsequently not maintained during cell division. The *cre* gene and associated genetic elements were subsequently segregated away from the *DvSnf7.1* suppression cassette and the *mpp75Aa1.1* and *vpb4Da2* expression cassettes by conventional breeding to produce the MON 95275 product lacking the *cp4 epsps* gene cassette. The absence of both the *cp4 epsps* gene and *cre* gene were confirmed in the generation prior to the one used to initiate commercial breeding (Figure 3). Since the *cp4 epsps* gene and sequence derived from PV-ZMOO513642 were eliminated through conventional breeding, the resulting progeny only contain the genes of interest (*DvSnf7, mpp75Aa1.1* and *vpb4Da2*) and not the gene used for selection.

For details, please refer to Appendix 1 [redacted]., 2021 (TRR0001330)).

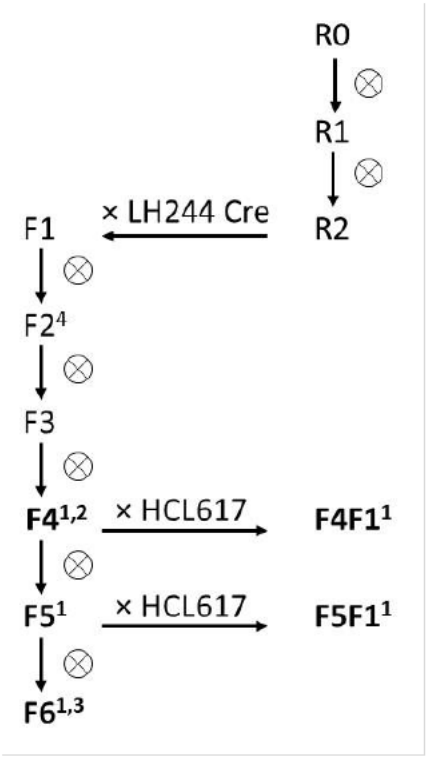

Figure 3. Breeding History of MON 95275

The generations used for molecular characterization and insert stability analyses are indicated in bold text. R0 corresponds to the initial transformed plant, ⊗ designates self-pollination.

[1]Generations used to confirm insert stability
[2] Generation used for molecular characterization
[3] Generation used for commercial development of MON 95275
[4] The F2 generation was screened for plants lacking the *cre* gene. Only those F2 plants lacking the *cre* gene were self-pollinated to create a F3 population of plants lacking the *cre* gene

Table 1. Summary of Genetic Elements in PV-ZMIR525664

Genetic Element	Location in Plasmid Vector	Function (Reference)
T-DNA		
B[1]-Right Border Region	1-331	DNA region from *Agrobacterium tumefaciens* containing the right border sequence used for transfer of the T–DNA (Depicker *et al.*, 1982; Zambryski *et al.*, 1982)
Intervening sequence	332-436	Sequence used in DNA cloning
T[2]-*E9*	437-1069	3' UTR sequence from *Pisum sativum* (pea) *rbcS* gene family encoding the small subunit of ribulose bisphosphate carboxylase protein (Coruzzi *et al.*, 1984) that directs polyadenylation of the mRNA
Intervening sequence	1070-1098	Sequence used in DNA cloning
***DvSnf7*[P]**	1099-1338	Partial coding sequence of the *Snf7* gene from *Diabrotica virgifera* (Baum *et al.*, 2007b; Baum *et al.*, 2007a) encoding the Snf7 subunit of the ESCRT–III complex (Babst *et al.*, 2002) that forms part of the suppression cassette
Intervening sequence	1339-1488	Sequence used in DNA cloning
***DvSnf7*[P]**	1489-1728	Partial coding sequence of the *Snf7* gene from *Diabrotica virgifera* (Baum *et al.*, 2007b; Baum *et al.*, 2007a) encoding the Snf7 subunit of the ESCRT–III complex (Babst *et al.*, 2002) that forms part of the suppression cassette
Intervening sequence	1729-1764	Sequence used in DNA cloning
I[3]-*Hsp70*	1765-2568	Intron and flanking exon sequence from *Zea mays* (maize) of the *hsp70* gene encoding the heat shock protein 70 (HSP70) (Rochester *et al.*, 1986) and is involved in regulating gene expression (Brown and Santino, 1997)
Intervening sequence	2569-2574	Sequence used in DNA cloning
P[4]-*35S*	2575-3150	Promoter and leader from the 35S RNA of cauliflower mosaic virus (CaMV) (Odell *et al.*, 1985) that directs transcription in plant cells

Table 1. Summary of Genetic Elements in PV-ZMIR525664 (Continued)

E[5]-*pIIG-Zm1*	3151-4066	Optimized enhancer sequence of the *pIIG* gene encoding the physical impedance induced protein of *Zea mays* (maize) (Huang *et al.*, 1998) that directs transcription in plant cells
Intervening sequence	4067-4072	Sequence used in DNA cloning
S[6]-*Isr-1*	4073-5291	Non-coding intergenic sequence designed to minimize potential effects of neighboring genes on each other's expression (Casini *et al.*, 2014)
Intervening sequence	5292-5312	Sequence used in DNA cloning
E-*DaMV-1*	5313-5634	Enhancer from a Dalia mosaic virus (DaMV) promoter region (Kuluev and Chemeris, 2007) that enhances transcription in plant cells
Intervening sequence	5635-5647	Sequence used in DNA cloning
P-*RCc3-Td1*	5648-6478	Promoter and leader from *Tripsacum dactyloides* of an *RCc3* gene that directs transcription in plant cells (Hernandez-Garcia and Finer, 2014)
I-*14-3-3c-Si1*	6479-6583	Intron from *Setaria italica* (foxtail millet) for a putative *14-3-3c* gene involved in regulating gene expression (Rose, 2008)
Intervening sequence	6584-6604	Sequence used in DNA cloning
CS[7]- *Mpp75Aa1.1*	6605-7492	Codon optimized coding sequence for Mpp75Aa1.1 protein of *Brevibacillus laterosporus* that provides insect resistance (Bowen *et al.*, 2021)
Intervening sequence	7493-7509	Sequence used in DNA cloning
T-*HSP-Cl1*	7510-8070	3′ UTR sequence from *Coix lacryma-jobi*. (adlay millet) of a *Hsp* gene encoding a heat shock protein that directs polyadenylation of the mRNA (Hunt, 1994)
Intervening sequence	8071-8096	Sequence used in DNA cloning
T-*SAM1-Si1*	8097-8531	3′ UTR sequence from *Setaria italica,* (foxtail millet) of an S-adenosylmethionine synthetase 1 gene that directs polyadenylation of the mRNA (Hunt, 1994)
Intervening sequence	8532-8538	Sequence used in DNA cloning
CS- *Vpb4Da2*	8539-11352	Codon optimized coding sequence for Vpb4Da2 protein of *Bacillus thuringiensis* (*Bt*) that provides insect resistance (Yin *et al.*, 2020)
Intervening sequence	11353-11378	Sequence used in DNA cloning

Table 1. Summary of Genetic Elements in PV-ZMIR525664 (Continued)

I-*Act-Si1*	11379-12743	Intron from foxtail millet (*Setaria italica*) for an *actin* gene and is involved in regulating gene expression (Rose, 2008)
Intervening sequence	12744-12751	Sequence used in DNA cloning
P-*Ltp-Zm1*	12752-14045	Promoter and leader from *Zea mays* (maize) of a lipid transfer protein gene that directs transcription in plant cells (Hernandez-Garcia and Finer, 2014)
E-*DaMV-2*	14046-14541	Enhancer from a Dalia mosaic virus (DaMV) promoter region (Kuluev and Chemeris, 2007) that enhances transcription in plant cells
Intervening sequence	14542-14685	Sequence used in DNA cloning
loxP	14686-14719	Sequence from Bacteriophage P1 for the *loxP* recombination site recognized by the Cre recombinase (Russell *et al.*, 1992)
Intervening sequence	14720-14725	Sequence used in DNA cloning
P-*TubA*	14726-16906	Promoter, 5' UTR leader and intron sequences of the *OsTubA* gene family from *Oryza sativa* (rice) encoding α-tubulin (Jeon *et al.*, 2000) that directs transcription in plant cells.
Intervening sequence	16907-16910	Sequence used in DNA cloning
TS^{8}-*CTP2*	16911-17138	Targeting sequence of the *ShkG* gene from *Arabidopsis thaliana* encoding the EPSPS transit peptide region that directs transport of the protein to the chloroplast (Klee *et al.*, 1987; Herrmann, 1995)
CS-*cp4 epsps*	17139-18506	Coding sequence of the *aroA* gene from *Agrobacterium* sp. strain CP4 encoding the CP4 EPSPS protein that provides herbicide tolerance (Barry *et al.*, 2001; Padgette *et al.*, 1996)
Intervening sequence	18507-18513	Sequence used in DNA cloning
T-*TubA*	18514-19095	3′ UTR sequence of the *OsTubA* gene from *Oryza sativa* (rice) encoding α–tubulin (Jeon *et al.*, 2000) that directs polyadenylation of mRNA
Intervening sequence	19096-19101	Sequence used in DNA cloning
loxP	19102-19135	Sequence from Bacteriophage P1 for the *loxP* recombination site recognized by the Cre recombinase (Russell *et al.*, 1992)
Intervening sequence	19136-19170	Sequence used in DNA cloning

Table 1. Summary of Genetic Elements in PV-ZMIR525664 (Continued)

B-Left Border Region	19171-19612	DNA region from *Agrobacterium tumefaciens* containing the left border sequence used for transfer of the T–DNA (Barker *et al.*, 1983)
Vector Backbone		
Intervening sequence	19613-19698	Sequence used in DNA cloning
OR[9]-*ori V*	19699-20095	Origin of replication from the broad host range plasmid RK2 for maintenance of plasmid in *Agrobacterium* (Stalker *et al.*, 1981)
Intervening sequence	20096-20717	Sequence used in DNA cloning
OR-*ori-pBR322*	20718-21306	Origin of replication from plasmid pBR322 for maintenance of plasmid in *E. coli* (Sutcliffe, 1979)
Intervening sequence	21307-21840	Sequence used in DNA cloning
aadA	21841-22729	Bacterial promoter, coding sequence, and 3' UTR for an aminoglycoside-modifying enzyme, 3"(9) –*O*–nucleotidyltransferase from the transposon *Tn7* (Fling *et al.*, 1985) that confers spectinomycin and streptomycin resistance
Intervening sequence	22730-22873	Sequence used in DNA cloning

[1] B, Border
[2] T, Transcription Termination Sequence
[P] Partial
[3] I, Intron
[4] P, Promoter
[5] E, Enhancer
[6] S, Spacer
[7] CS, Coding Sequence
[8] TS, Targeting Sequence
[9] OR, Origin of Replication

A.3(b)(i)(iii) The *mpp75Aa1.1* Coding Sequence and Mpp75Aa1.1 Protein

The *mpp75Aa1.1* expression cassette in MON 95275 encodes a 35.2 kDa Mpp75Aa1.1 protein consisting of a single polypeptide of 295 amino acids (Figure 4). As is typical for plant-expressed proteins, the lead methionine of the Mpp75Aa1.1 protein is not present. The *mpp75Aa1.1* coding sequence is derived from the full-length precursor form of the insecticidal protein Mpp75Aa1 from *B. laterosporus* where the first 23 amino acids in the N-terminus is a membrane-transiting signal peptide that was removed in the *mpp75Aa1.1* gene. In addition, a starting codon ATG was added in front to enable the proper translation of Mpp75Aa1.1 protein. The presence of the Mpp75Aa1.1 protein in maize provides protection against coleopteran pests.

```
1    MSSTDVQERL RDLAREDEAG TFNEAWNTNF KPSDEQQFSY SPTEGIVFLT

51   PPKNVIGERR ISQYKVNNAW ATLEGSPTEA SGTPLYAGKN VLDNSKGTMD

101  QELLTPEFNY TYTESTSNTT THGLKLGVKT TATMKFPIAQ GSMEASTEYN

151  FQNSSTDTKT KQVSYKSPSQ KIKVPAGKTY RVLAYLNTGS ISGEANLYAN

201  VGGIAWRVSP GYPNGGGVNI GAVLTKCQQK GWGDFRNFQP SGRDVIVKGQ

251  GTFKSNYGTD FILKIEDITD SKLRNNNGSG TVVQEIKVPL IRTEI
```

Figure 4. Deduced Amino Acid Sequence of the Mpp75Aa1.1 Protein

The amino acid sequence of the MON 95275 Mpp75Aa1.1 protein was deduced from the full-length coding nucleotide sequence present in PV-ZMIR525664 (See Table 1 for more details). The lead methionine (boxed with solid line) of the Mpp75Aa1.1 protein produced in MON 95275 is cleaved in vivo. The presence of Mpp75Aa1.1 protein in maize provides protection against targeted coleopteran pests.

A.3(b)(i)(iv) The *vpb4Da2* Coding Sequence and Vpb4Da2 Protein

The *vpb4Da2* expression cassette in MON 95275 encodes a 103.88 kDa Vpb4Da2 protein consisting of a single polypeptide of 937 amino acids (Figure 5). The Vpb4Da2 protein is the full-lenth protein originally from *B. thuringiensis*. The presence of the Vpb4Da2 protein in maize provides protection against targeted coleopteran pests.

```
1   MQNIVSSKSE QATVIGLVGF YFKDSTFKEL MFIQVGEKSN LMNKARINTD

51  AQQIQSIRWM GNLKSPQTGE YRLSTSSDEN VILQINGETV INQASIQKNL

101 KLEANQVYEI KIEYRNTSNT LPDLQLFWSM NNAQKEQIPE KYILSPNFSE

151 KANSLAEKET QSFFPNYNLF DRQQENGEKQ SMSTPVDTDN DCIPDEWEEK

201 GYTFRNQQIV PWNDAYSAEG YKKYVSNPYH ARTVKDPYTD FEKVTGHMPA

251 ATKYEARDPL VAAYPSVGVG MEKLHFSKND TVTEGNADTK SKTTTKTDTT

301 TNTVEIGGSL GFSDKGFSFS ISPKYTHSWS SSTSVADTDS TTWSSQIGIN

351 TAERAYLNAN VRYYNGGTAP IYDLKPTTNF VFQNSGDSIT TITAGPNQIG

401 NSLGAGDTYP QKGQAPISLD KANEAGTVKI AINAEQLDKI QAGTEILNIE

451 TTQNRGQYGI LDEKGQVIPG GEWDPIRTNI DAVSGSLTLN LGTGKDSLER

501 RVAAKNMNDP EDKTPEITIK EAIKKAFNAQ EKDGRLYYTD QGEKDIFIDE

551 PSINLITDEN TKKEIERQLN QMPGKTVYDV KWKRGMKITL HVPIKYYDFE

601 TSENLWYYTY QESGGYTGKK RGRIGTDGHG TAMSNPQLKP YTSYTVRAYV

651 RTASTTGSNE VVFYADNSSG NGQGAKVSGK VTGGKWKIAE FSFNTFNNPE

701 YFKIIGLKNN GNANLHFDDV SVIEWKTNEN LQKKHIFEKW SFGSNDEMVI

751 GATFTRVPSS KIRYQWKING RLGSIIPAPP LDANGKRTVT YGSITAITPM

801 ELYAVDEKND NLKVKVAELG ESEIEKVMID AHKFSGWWYL SENPNLYSGL

851 SLYKLPDIFY NNVSSYKIRV NGKKVQTVSK PSPFLFQITF NLKNPNGGTY

901 PTKDASVELW ATVGGKDLKV LHKWIQKSDV MYSQTNN
```

Figure 5. Deduced Amino Acid Sequence of the Vpb4Da2 Protein

The amino acid sequence of the MON 95275 Vpb4Da2 protein was deduced from the full-length coding nucleotide sequence present in PV-ZMIR525664 (see Table 1 for more details). The presence of Vpb4Da2 protein in maize provides protection against targeted coleopteran pests.

A.3(b)(i)(v) Regulatory Sequences

The T-DNA, contains the *DvSnf7.1* suppression cassette, the *mpp75Aa1.1* and *vpb4Da2* expression cassettes and initially contained the *cp4 epsps* selectable marker cassette, each with their own regulatory sequences. The regulatory sequences associated with each cassette are described in Section A.3(b) and Table 1.

A.3(b)(i)(vi) T-DNA Border Regions

PV-ZMIR525664 contains Left and Right Border regions (Figure 2 and Table 1) that were derived from *A. tumefaciens* plasmid. The border regions each contain a 2425 bp nick site that is the site of DNA exchange during transformation (Barker *et al.*, 1983; Depicker *et al.*, 1982; Zambryski *et al.*, 1982). The border regions separate the T-DNA from the plasmid backbone region and are involved in the efficient transfer of T-DNA into the maize genome.

A.3(b)(i)(vii) Genetic Elements Outside the T-DNA Border Regions

Genetic elements that exist outside of the T-DNA border regions are those that are essential for the maintenance or selection of PV-ZMIR525664 in bacteria and are referred to as plasmid backbone. The origin of replication, *ori-V*, is required for the maintenance of the plasmid in *Agrobacterium* and is derived from the broad host plasmid *RK2* (Stalker *et al.*, 1981). The origin of replication, *ori-pBR322*, is required for the maintenance of the plasmid in *E. coli* and is derived from the plasmid vector pBR322 (Sutcliffe, 1979). The selectable marker *aadA* is the coding sequence for an aminoglycoside-modifying enzyme, 3"(9)–*O*–nucleotidyltransferase from the transposon *Tn7* (Fling *et al.*, 1985) that confers spectinomycin and streptomycin resistance in *E. coli* and *Agrobacterium* during molecular cloning. Because these elements are outside the T-DNA border regions, they are not expected to be transferred into the maize genome. The absence of the backbone and other unintended plasmid sequence in MON 95275 was confirmed by sequencing and bioinformatic analyses (Section A.3(a)).

For details, please refer to Appendix 1 [redacted]., 2021 (TRR0001330)).

A.3(b)(ii) A detailed map of the location and orientation of all genetic elements contained within the construct and vector, including the location of relevant restriction sites

The plasmid map of PV-ZMIR525664 is presented in Figure 2.

A.3(c) A full molecular characterisation of the genetic modification in the new organism, including:

A.3(c)(i) Identification of all transferred genetic material and whether it has undergone any rearrangements

This section describes the methods and results of a comprehensive molecular characterization of the genetic modification present in MON 95275. It provides information on the DNA insertion(s) into the plant genome of MON 95275, and additional information regarding the arrangement and stability of the introduced genetic material. The information provided in this section addresses the relevant factors in Codex Plant Guidelines, Section 4, paragraphs 30, 31, 32, and 33 (Codex Alimentarius, 2009).

A schematic representation of the next generation sequencing (NGS) methodology and the basis of the characterization using NGS and PCR sequencing are illustrated in Figure 6 below.

For details, please refer to Appendix 1 ([redacted]., 2021 (TRR0001330)).

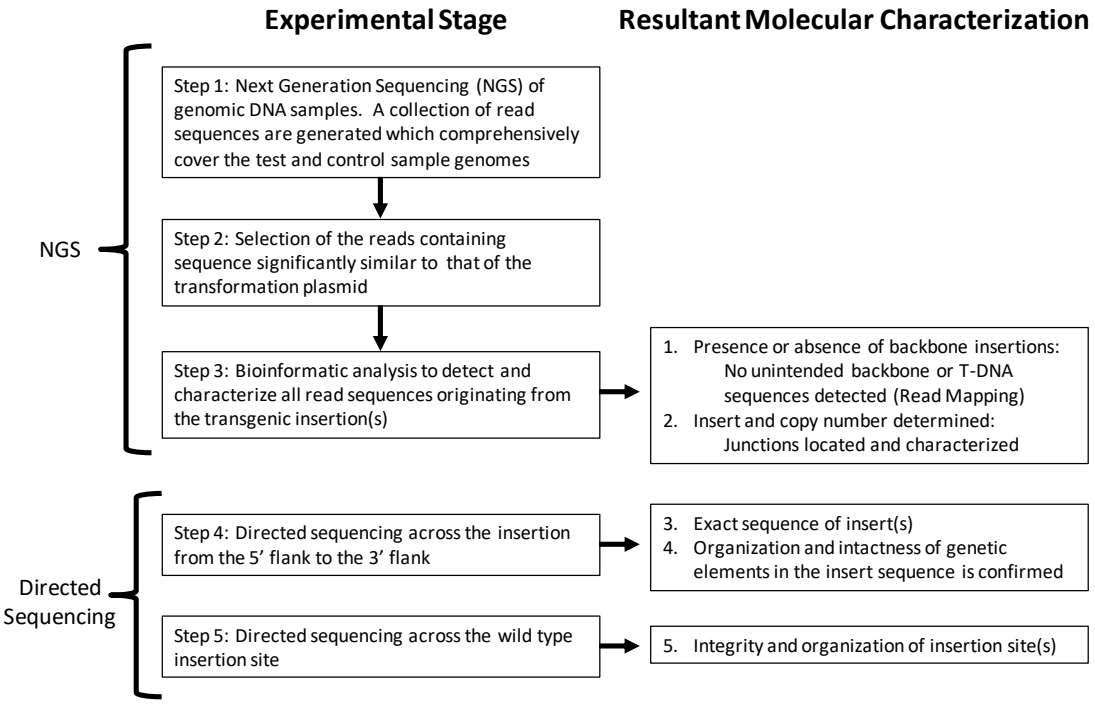

Figure 6. Molecular Characterization using Sequencing and Bioinformatics

Genomic DNA from the MON 95275 test and the conventional control was sequenced using technology that produces a set of short, randomly distributed sequence reads that comprehensively cover test and control genomes (Step 1). Utilizing these genomic sequence reads, bioinformatics searches are conducted to identify all sequence reads that are significantly similar to the transformation plasmid (Step 2). These captured reads are then mapped and analyzed to determine the presence/absence of transformation plasmid backbone sequences, identify insert junctions, and to determine the insert and copy number (Step 3). Overlapping PCR products are also produced which span any insert and their wild type locus (Step 4 and Step 5, respectively); these overlapping PCR products are sequenced to allow for detailed characterization of the inserted DNA and insertion site.

The NGS methods were used to characterize the genomic DNA from MON 95275 and the conventional control by generating short (~150 bp) randomly distributed sequence fragments (sequencing reads) in sufficient number to ensure comprehensive coverage of the sample genomes. It has been previously demonstrated that whole genome sequencing at 75× depth of coverage is adequate to provide comprehensive coverage and ensure detection of inserted DNA (Kovalic *et al.*, 2012). A comprehensive analysis of NGS as a characterization method demonstrated that coverage depth as low as 11× is sufficient to detect both intended transgenes as well as unintended inserted vector-derived fragments as small as 25 bp in length (Cade *et al.*, 2018). Therefore, 75× coverage is a robust level of sequencing for the complete characterization of both homozygous and hemizygous transgenes, and well in excess of the levels which have been demonstrated as sufficient for identifying unintended inserted fragments. To confirm sufficient sequence coverage of the genome, the 150 bp sequence reads are analyzed to determine the coverage of a known single-copy endogenous maize gene. This establishes the depth of coverage (the median number of times each base of the genome is independently sequenced). Furthermore, the sensitivity of the method was assessed by sequencing the transformation plasmid and then sampling the data to represent a single genome equivalent dataset and a 1/10th genome equivalent dataset. This confirms the method's ability

to detect any sequences derived from the transformation plasmid. Bioinformatics analysis was then used to select sequencing reads that contained sequences similar to the transformation plasmid, and these were analyzed in depth to determine the number of DNA inserts. NGS was run on five breeding generations of MON 95275 and the appropriate conventional controls. Results of NGS are shown in Sections A.3(c)(ii).

The DNA inserts of MON 95275 was determined by mapping of sequencing reads relative to the transformation plasmid and identifying junctions and unpaired read mappings adjacent to the junctions. Examples of five types of NGS reads are shown in Figure 7. The junctions of the DNA insert and the flanking DNA are unique for each insertion (Kovalic *et al.*, 2012). Therefore, insertion sites can be recognized by analyzing for sequence reads containing such junctions.

Directed sequencing (locus-specific PCR and DNA sequencing analyses, Figure 6, Step 4) complements the NGS method. Sequencing of the insert and flanking genomic DNA determined the complete sequence of the insert and flanks by evaluating if the sequence of the insert was identical to the corresponding sequence from the T-DNA in PV-ZMIR525664 and if each genetic element in the insert was intact. It also characterizes the flanking sequence beyond the insert corresponding to the genomic DNA of the transformed maize. Results are described in Sections A.3(c)(i) and A.3.(c)(ii) .

For details, please refer to Appendix 1 [redacted]., 2021 (TRR0001330)).

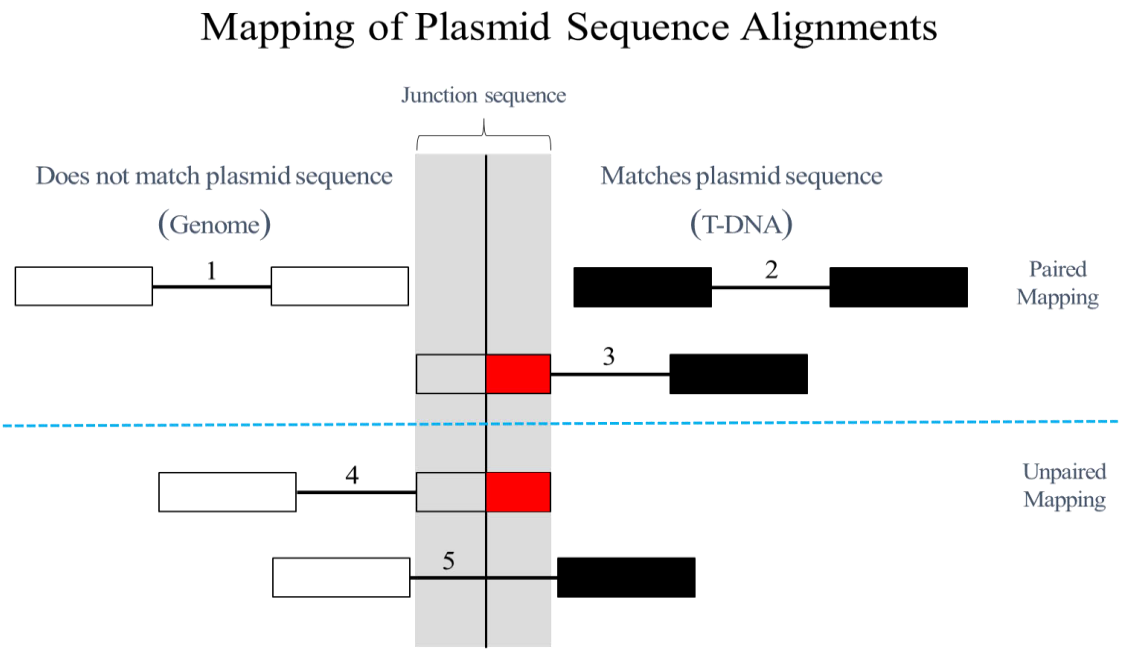

Figure 7. Five Types of NGS Reads

NGS yields data in the form of read pairs where sequence from each end of a size selected DNA fragment is returned. Depicted above are five types of sequencing reads/read pairs generated by NGS which can be found spanning or outside of junction points. Sequence boxes are color-filled if it matches with plasmid sequence, and empty if it matches with genomic sequence. Grey highlighting indicates sequence reads spanning the junction. Junctions are detected by examining the NGS data for reads having portions of plasmid sequences that span less than the full read, as well as reads mapping adjacent to the junction points where their mate pair does not map to the plasmid sequence. The five types of sequencing reads/read pairs being (1) Paired and unpaired reads mapping to genomic sequence outside of the insert, greater than 99.999% of collected reads fall into this category and are not evaluated in this analysis, (2) Paired reads mapping entirely to the transformation plasmid sequence, such reads reveal the presence of transformation sequence *in planta*, (3) Paired reads where one read maps entirely within the inserted DNA and the other read maps partially to the insert (indicating a junction point), (4) Single read mapping partially to the transformation plasmid DNA sequence (indicating a junction point) where its mate maps entirely to genomic flanking sequence and (5) Single read mapping entirely to genomic flanking sequence, such reads are part of the junction signature.

A.3(c)(ii) A determination of number of insertion sites, and the number of copies at each insertion site

A.3(c)(ii)(i) Characterization of the DNA Insert in MON 95275

The number of inserted DNA sequences from PV-ZMIR525664 in MON 95275 was assessed by generating a comprehensive collection of reads via NGS of MON 95275 genomic DNA using the F4 generation (Figure 3). A plasmid map of PV-ZMIR525664 is shown in Figure 2 elements present in MON 95275. Table 2 provides descriptions of the genetic elements present in MON 95275. A schematic representation of the insert and flanking sequences in MON 95275 is shown in Figure 8.

For details, please refer to Appendix 1 ([redacted]., 2021 (TRR0001330)).

A.3(c)(ii)(ii) Next Generation Sequencing for MON 95275 and Conventional Control Genomic DNA

Genomic DNA from five breeding generations of MON 95275 (Figure 3) and conventional controls were isolated from seed and prepared for sequencing. These genomic DNA libraries were used to generate short (~150 bp) randomly distributed sequencing reads of the maize genome (Figure 6, Step 1).

To demonstrate sufficient sequence coverage the 150 bp sequence reads were analyzed by mapping all reads to a known single copy endogenous gene (*Zea mays* pyruvate decarboxylase (*pdc3*), GenBank accession version: AF370006.2) in each of the five distinct breeding generations. The analysis of sequence coverage plots showed that the depth of coverage (*i.e.*, the median number of times any base of the genome is expected to be independently sequenced) was 213× or greater for the five generations of MON 95275 (F4, F4F1, F5, F5F1, and F6) and the conventional control (Appendix 1). It has been previously demonstrated that whole genome sequencing at 75× coverage provides comprehensive coverage and ensures detection of inserted DNA (Cade *et al.*, 2018; Kovalic *et al.*, 2012).

To demonstrate the method's ability to detect any sequences derived from the PV-ZMIR525664 transformation plasmid or the Cre recombinase-containing transformation plasmid vector PV-ZMOO513642, a sample of PV-ZMIR525664 and PV-ZMOO513642, were sequenced by NGS following the same processes outlined for all samples. The resulting PV-ZMIR525664 and PV-ZMOO513642 reads were randomly selected to achieve a depth of one and 1/10th genome equivalent (relative to the median coverage of the LH244 conventional control). In all cases, 100% coverage of the known PV-ZMIR525664 or PV-ZMOO513642 sequences were observed (Appendix 1). This result demonstrates that all nucleotides of PV-ZMIR525664 and PV-ZMOO513642 are detectable by the sequencing and bioinformatic assessments performed and that a detection level of at least 1/10th genome equivalent was achieved for the plasmid DNA sequence assessment.

Table 2. Summary of Genetic Elements in MON 95275

Genetic Element[1]	Location in Sequence[2]	Function (Reference)
5' Flanking DNA	1-1000	DNA sequence flanking the 5' end of the insert
B[3]-Right Border Region	1001-1017	DNA region from *Agrobacterium tumefaciens* containing the right border sequence used for transfer of the T-DNA (Depicker *et al.*, 1982; Zambryski *et al.*, 1982)
Intervening sequence	1018-1122	Sequence used in DNA cloning
T[4]-*E9*	1123-1755	3' UTR sequence from *Pisum sativum* (pea) *rbcS* gene family encoding the small subunit of ribulose bisphosphate carboxylase protein (Coruzzi *et al.*, 1984) that directs polyadenylation of the mRNA
Intervening sequence	1756-1784	Sequence used in DNA cloning
***DvSnf7*[P]**	1785-2024	Partial coding sequence of the *Snf7* gene from *Diabrotica virgifera* (Baum *et al.*, 2007b; Baum *et al.*, 2007a) encoding the Snf7 subunit of the ESCRT–III complex (Babst *et al.*, 2002) that forms part of the suppression cassette
Intervening sequence	2025-2174	Sequence used in DNA cloning
***DvSnf7*[P]**	2175-2414	Partial coding sequence of the *Snf7* gene from *Diabrotica virgifera* (Baum *et al.*, 2007b; Baum *et al.*, 2007a) encoding the Snf7 subunit of the ESCRT–III complex (Babst *et al.*, 2002) that forms part of the suppression cassette
Intervening sequence	2415-2450	Sequence used in DNA cloning
I[5]-*Hsp70*	2451-3254	Intron and flanking exon sequence from *Zea mays* (maize) of the *hsp70* gene encoding the heat shock protein 70 (HSP70) (Rochester *et al.*, 1986) and is involved in regulating gene expression (Brown and Santino, 1997)
Intervening sequence	3255-3260	Sequence used in DNA cloning
P[6]-*35S*	3261-3836	Promoter and leader from the 35S RNA of cauliflower mosaic virus (CaMV) (Odell *et al.*, 1985) that directs transcription in plant cells

Table 2. Summary of Genetic Elements in MON 95275 (Continued)

E[7]-*pIIG-Zm1*	3837-4752	Optimized enhancer sequence of the *pIIG* gene encoding the physical impedance induced protein of *Zea mays* (maize) (Huang *et al.*, 1998) that directs transcription in plant cells
Intervening sequence	4753-2758	Sequence used in DNA cloning
S[8]-*Isr-1*	4759-5977	Non-coding intergenic sequence designed to minimize potential effects of neighboring genes on each other's expression (Casini *et al.*, 2014)
Intervening sequence	5978-5998	Sequence used in DNA cloning
E-*DaMV-1*	5999-6320	Enhancer from a Dalia mosaic virus (DaMV) promoter region (Kuluev and Chemeris, 2007) that enhances transcription in plant cells
Intervening sequence	6321-6333	Sequence used in DNA cloning
P-*RCc3-Td1*	6334-7164	Promoter and leader from *Tripsacum dactyloides* of an *RCc3* gene that directs transcription in plant cells. (Hernandez-Garcia and Finer, 2014)
I-*14-3-3c-Si1*	7165-7269	Intron from *Setaria italica* (foxtail millet) for a putative *14-3-3c* gene involved in regulating gene expression (Rose, 2008)
Intervening sequence	7270-7290	Sequence used in DNA cloning
CS[9]-*Mpp75Aa1.1*	7291-8178	Codon optimized coding sequence for Mpp75Aa1.1 protein of *Brevibacillus laterosporus* that provides insect resistance (Bowen *et al.*, 2021)
Intervening sequence	8179-8195	Sequence used in DNA cloning
T-*HSP-Cl1*	8196-8756	3' UTR sequence from *Coix lacryma-jobi*. (adlay millet) of a *Hsp* gene encoding a heat shock protein that directs polyadenylation of the mRNA (Hunt, 1994)
Intervening sequence	8757-8782	Sequence used in DNA cloning
T-*SAM1-Si1*	8783-9217	3' UTR sequence from *Setaria italica*, (foxtail millet) of an S-adenosylmethionine synthetase 1 gene that directs polyadenylation of the mRNA (Hunt, 1994)
Intervening sequence	9218-9224	Sequence used in DNA cloning
CS-*Vpb4Da2*	9225-12038	Codon optimized coding sequence for Vpb4Da2 protein of *Bacillus thuringiensis* (Bt) that provides insect resistance (Yin *et al.*, 2020)

Table 2. Summary of Genetic Elements in MON 95275 (Continued)

Intervening sequence		Sequence used in DNA cloning
I-*Act-Si1*	12065-13429	Intron from foxtail millet (*Setaria italica*) for an *actin* gene and is involved in regulating gene expression (Rose, 2008)
Intervening sequence	13430-13437	Sequence used in DNA cloning
P-*Ltp-Zm1*	13438-14731	Promoter and leader from *Zea mays* (maize) of a lipid transfer protein gene that directs transcription in plant cells (Hernandez-Garcia and Finer, 2014)
E-*DaMV-2*	14732-15227	Enhancer from a Dalia mosaic virus (DaMV) promoter region (Kuluev and Chemeris, 2007) that enhances transcription in plant cells
Intervening sequence	15228-15371	Sequence used in DNA cloning
loxP	15372-15405	Sequence from Bacteriophage P1 for the *loxP* recombination site recognized by the Cre recombinase (Russell *et al.*, 1992)
Intervening sequence	15406-15440	Sequence used in DNA cloning
B-Left Border Region[r1]	15441-15682	DNA region from *Agrobacterium tumefaciens* containing the left border sequence used for transfer of the T–DNA (Barker *et al.*, 1983)
3' Flanking DNA	15683-16688	6 base pairs of co-inserted DNA followed by 1000 base pairs of genomic DNA flanking the 3' end of the insert

[1] Although flanking sequences and intervening sequences are not functional genetic elements, they comprise a portion of the sequence.
[2] Numbering refers to the sequence of the insert in MON 95275 and adjacent DNA
[3] B, Border
[4] T, Transcription Termination Sequence
[P] Partial
[5] I, Intron
[6] P, Promoter
[7] E, Enhancer
[8] S, Spacer
[9] CS, Coding Sequence
[r1] Superscript in Left and Right Border Regions indicate that the sequence in MON 95275 were truncated compared to the sequences in PV-ZMIR525664

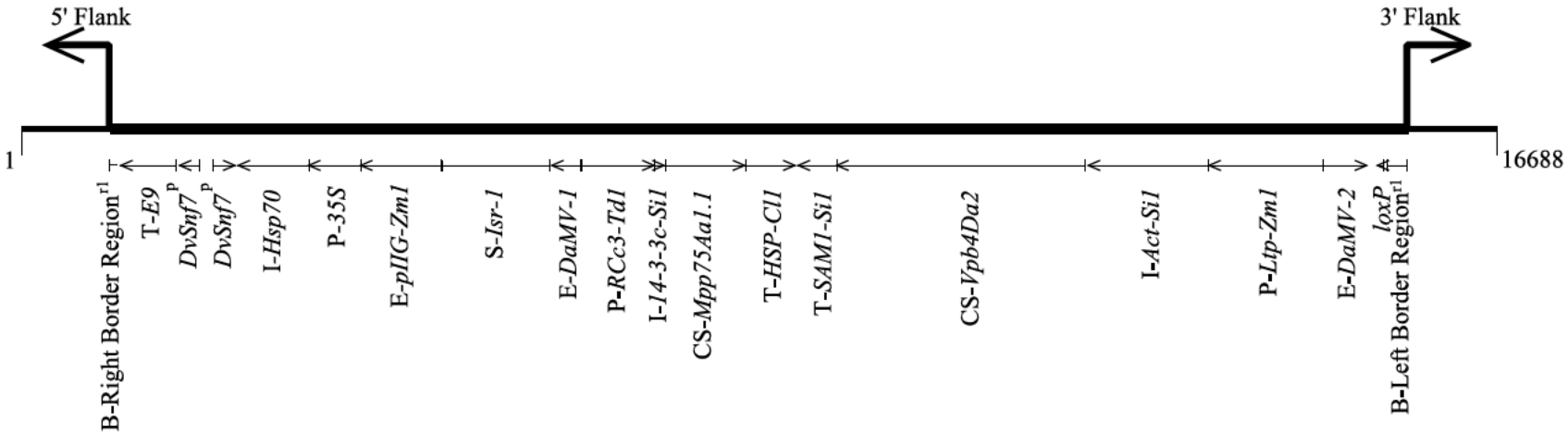

Figure 8. Schematic Representation of the Insert and Flanking Sequences in MON 95275

DNA derived from T-DNA of PV-ZMIR525664 integrated in MON 95275. Right-angled arrows indicate the ends of the integrated T-DNA and the beginning of the flanking sequence. Identified on the map are genetic elements within the insert. This schematic diagram may not be drawn to scale.

r1 Superscript in Left and Right Border Regions indicate that the sequence in MON 95275 was truncated compared to the sequences in PV-ZMIR525664.

P Superscript in DvSnf7 indicates the partial sequence

A.3(c)(ii)(iii) Selection of Sequence Reads Containing Sequence of the PV-ZMIR525664 and PV-ZMOO513642

The transformation plasmid, PV-ZMIR525664, was transformed into the parental variety LH244 to produce MON 95275. Consequently, any DNA inserted into MON 95275 will consist of sequences that are similar to the PV-ZMIR525664 DNA sequence. Therefore, to fully characterize the DNA from PV-ZMIR525664 inserted in MON 95275, it is sufficient to completely analyze only the sequence reads that have similarity to PV-ZMIR525664 (Figure 6, Step 2). Similarly, to confirm the absence of the Cre-containing transformation plasmid vector, PV-ZMOO513642, in MON 95275 it is sufficient to completely analyze only the sequence reads that have similarity to PV-ZMOO513642.

Using established criteria (described in Appendix 1), sequence reads similar to PV-ZMIR525664 and PV-ZMOO513642 were selected from MON 95275 sequence datasets (PV-ZMOO513642 selection was only conducted on the F4 generation) and were then used as input data for bioinformatic junction sequence analysis. PV-ZMIR525664 and PV-ZMOO513642 sequences were also compared against the conventional control sequence datasets.

A.3(c)(ii)(iv) Determination of T-DNA Copy Number and Presence or Absence of Plasmid Vector Backbone

Mapping sequence reads relative to the transformation plasmid allows for the identification of junction signatures, the presence or absence of plasmid backbone sequence and the number of T-DNA insertions. For a single copy T-DNA insert sequence at a single genomic locus and the complete absence of plasmid vector backbone, a single junction signature pair and few if any reads aligning with the transformation plasmid backbone sequences are expected.

When reads from the LH244 dataset were aligned with the transformation plasmid sequence, large numbers of reads mapped to the intended T-DNA sequence elements I-*Hsp70*, E-*pIIG-Zm1* and P-*LtpZm1* sequence (Figure 9). The alignment of these sequence reads is the result of endogenous maize sequences that are homologous to the T-DNA encoded elements I-*Hsp70*, E-*pIIG-Zm1* and P-*Ltp-Zm1* sequence.

When reads from the MON 95275 (F4) dataset were aligned with the transformation plasmid sequence, large numbers of reads mapped to the intended T-DNA sequence (Figure 10), demonstrating that the expected T-DNA is inserted in MON 95275. A few reads were found to map to OR-*ori-pBR322*, OR-*ori V* and sequences used during DNA cloning and a single pair of reads was found to align with P-*TubA* from the *cp4 epsps* selectable marker cassette. These sequence reads do not represent true DNA inserts because they lack the signatures of DNA inserts (junction sequences) and the number of reads is too low for true inserts[4]. The sporadic low-level detection of plasmid sequences such as OR-*ori-pBR322* and OR-ori V has previously been described (Zastrow-Hayes *et al.*, 2015) and reported (see Supplemental Figure S1 in Yang *et al.* (2013)), and is likely due to the presence of environmental bacteria in tissue samples used in the

[4] The depth of coverage (*i.e.*, the median number of times any base of the genome is expected to be independently sequenced) was 213× or greater for the five generations of MON 95275 (F4, F4F1, F5, F5F1, and F6) and the conventional control.

preparation of genomic DNA used for library construction. The presence of this sequence from environmental bacteria does not indicate the presence of backbone sequence in MON 95275. This analysis indicates that MON 95275 does not contain inserted sequence from the transformation plasmid backbone.

The detection of single pair of reads aligned to P-*TubA* is likely due to experimental contamination during library preparation. Other than a single pair of reads aligning to P-*TubA* which is not indicative of the presence of sequences in whole genome sequencing (WGS) dataset, no other reads mapped to the selectable marker cassette (P-*TubA*, TS-*CTP2*, CS-*cp4 epsps*, and T-*TubA*). This lack of reads mapping to the selectable marker cassette is expected as MON 95275 was crossed with a Cre recombinase expressing line that enables the removal of the *cp4 epsps* gene cassette positioned between two excision targeting *lox* sites (Hare and Chua, 2002; Zhang *et al.*, 2003). After excision, a single *lox* site remained, as expected. The absence of the selectable marker cassette results in a gap in reads as illustrated in Figure 10.

To determine the insert number in MON 95275, selected reads mapping to T-DNA as described above were analyzed to identify junctions. This bioinformatic analysis was used to find and classify partially matched reads characteristic of the ends of insertions. The number of unique junctions determined by this analysis are shown in Table 3.

Table 3. Unique Junction Sequence Class Results

Sample	Junctions Detected
MON 95275 (F4)	2
LH244	0

Detailed mapping information of the junction sequences is shown in Figure 10. The location and orientation of the junction sequences relative to the DNA insert in MON 95275 are shown in Figure 10, Panels 1 and 2. As shown in the figure, there are two junctions identified in MON 95275. Both junctions contain the T-DNA border sequence joined to flanking genomic sequence, indicating that they represent the sequences at the junctions of the intended T-DNA insert and the maize genome. As described earlier, no junctions were detected in any of the conventional maize control samples.

Considered together, the absence of plasmid backbone and the presence of two junctions (joining T-DNA borders and flanking sequences) indicate a single intended T-DNA at a single locus in the genome of MON 95275. Both junctions originate from the same locus of the MON 95275 genome and are linked by contiguous, known and expected DNA sequence (with the exception of the selectable marker cassette which was excised as described earlier). This is demonstrated by complete coverage of the sequenced reads spanning the interval between the junctions and the directed sequencing of overlapping PCR products described in Section A.3(c)(iii).

Based on the comprehensive NGS and junction identification it is concluded that MON 95275 contains one copy of the T-DNA inserted into a single locus. This conclusion is confirmed by

the sequencing and analysis of overlapping PCR products from this locus as described Section A.3(c)(iii).

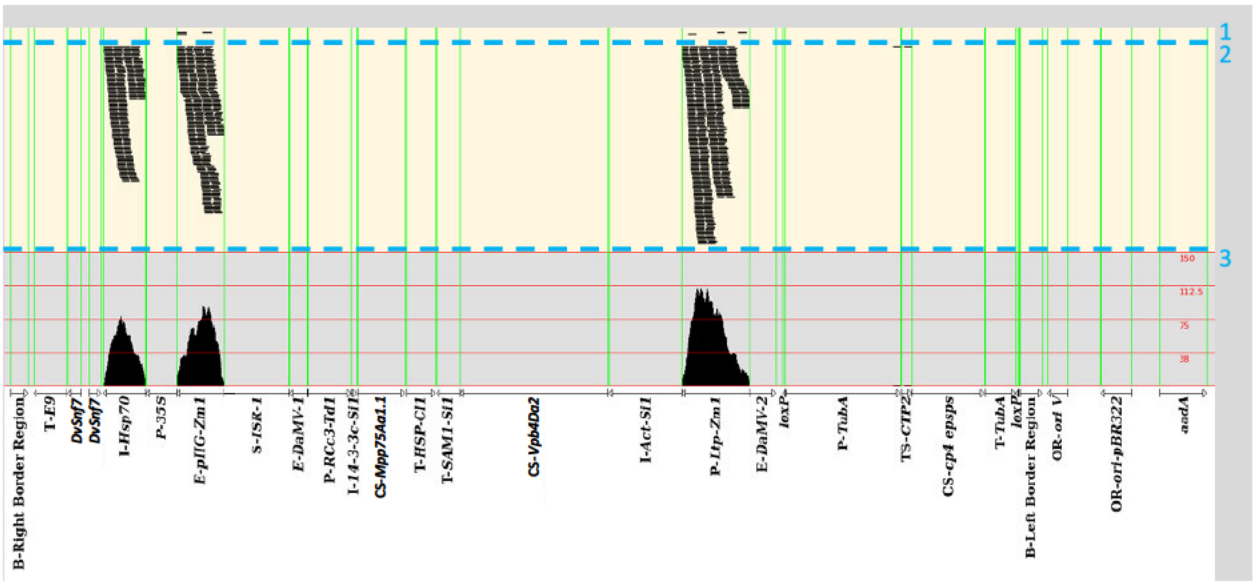

Figure 9. Read Mapping of Conventional Maize LH244 Versus PV-ZMIR525664

Panel 1 shows the location of unpaired mapped reads, Panel 2 shows paired mapped reads, and Panel 3 shows a representation of combined read depth for unpaired and paired reads. Vertical lines show genetic element boundaries.

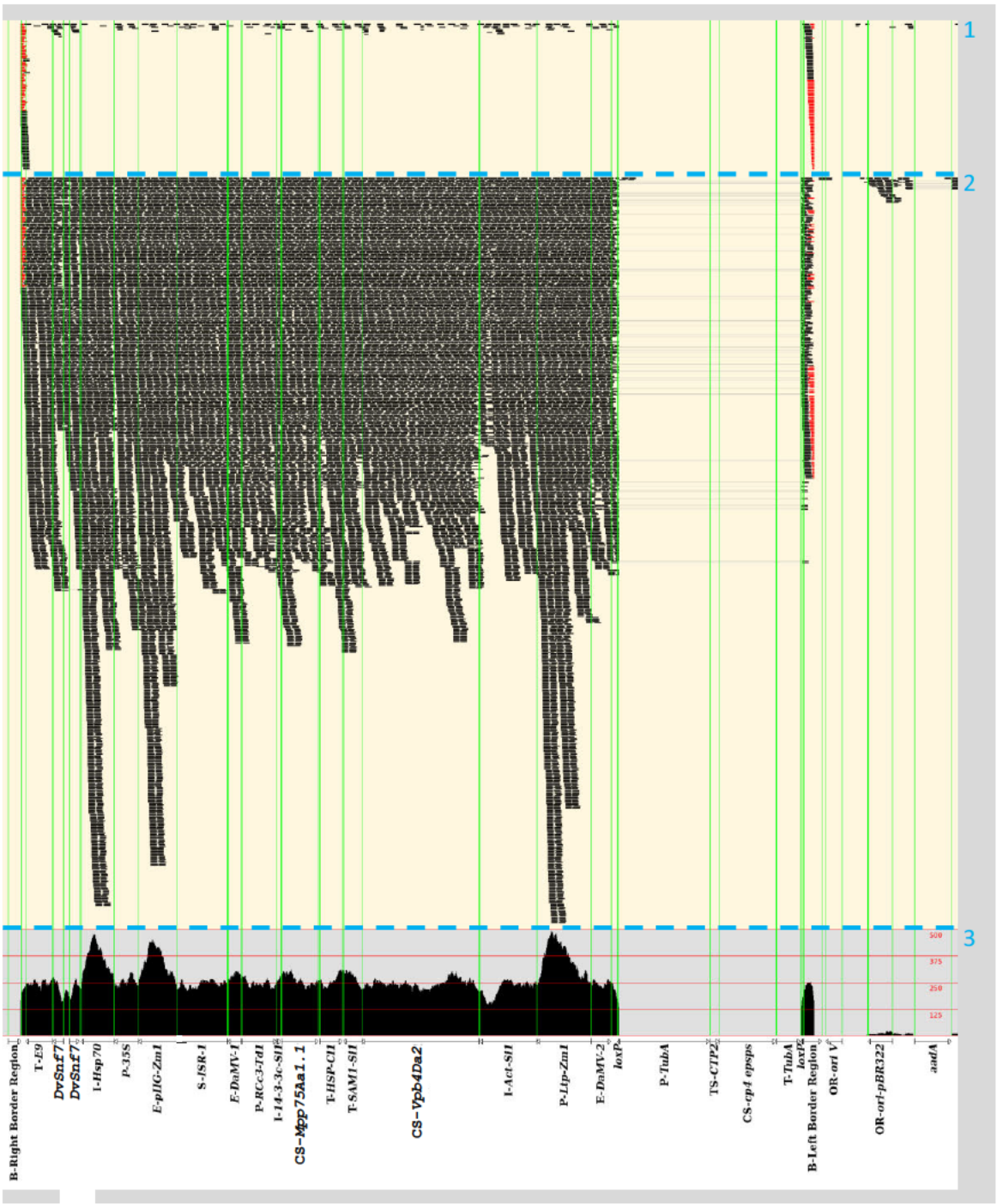

Figure 10. Read Mapping of MON 95275 (F4) Versus PV-ZMIR525664

Panel 1 shows the location of unpaired mapped reads. Panel 2 shows paired mapped reads and Panel 3 shows a representation of combined read depth for unpaired and paired reads. Vertical lines show genetic element boundaries. The region of flank junction sequences that align with the transformation plasmid are shown in red.

A.3(c)(ii)(v) Determination of Absence of Plasmid Vector PV-ZMOO513642

At the R2 generation (Figure 3), MON 95275 was crossed with a Cre recombinase expressing variety. The *Cre/lox* technology enables the removal of the selectable marker cassette (P-*TubA*, TS-*CTP2*, CS-*cp4 epsps*, and T-*TubA*) which was inserted during the transformation as part of the T-DNA insertion that also included the *DvSnf7.1* supression and the *mpp75Aa1.1* and *vpb4Da2* expression cassettes. The resulting F1 progeny were self-pollinated and the F2 generation were screened for the absence of the *cre* gene and associated genetic elements (and other sequences from plasmid PV-ZMOO513642), allowing for selection of lines lacking the Cre recombinase cassette that were used as the progenitor of subsequent generations and the final product.

To confirm the absence of the Cre recombinase cassette and any part of the *cre* gene containing transformation vector, MON 95275 was assessed by generating a comprehensive collection of reads via NGS of MON 95275 genomic DNA and subsequently mapping them to the *cre* gene containing transformation plasmid (PV-ZMOO513642) sequence (Figure 11). In the absence of any PV-ZMOO513642 insertions, there should be zero junction signature pairs and limited reads aligning with the PV-ZMOO531642 sequences.

When reads from the MON 95275 dataset were aligned with the PV-ZMOO513642 sequence, a number of reads aligned to the left border region (B-Left Border Region) and the P-*35S* promoter. No reads other than a small number of un-paired reads mapping to the promoter element *Ract1* mapped to T-DNA, and a few reads mapping to origins of replication *ori-pBR322* and *ori V* and sequences used during DNA cloning were identified which aligned to the PV-ZMOO513642 backbone (Figure 11).

The mapping of a number of reads from the MON 95275 dataset to the left border region and 35S promoter (B-Left Border Region and P-*35S*) is expected since PV-ZMOO513642 and PV-ZMIR525664 share these sequences and PV-ZMIR525664's left border region and *35S* promoter are present in MON 95275 (Figure 11). The small number of reads mapping to the promoter element *Ract1* from rice is consistent with the presence of a homologous maize sequence being present in the LH244 background (Figure 12) and does not indicate the presence of PV-ZMOO513642 T-DNA in MON 95275 because no junction sequences are present. Additionally, very few reads were found to align with OR-*ori-pBR322*, OR-*ori V* and sequences used during DNA cloning (Figure 11). The sporadic low-level detection of plasmid sequences such as OR-*ori-pBR322* has previously been described (Zastrow-Hayes *et al.*, 2015) and reported (see Supplemental Figure S1 in Yang *et al.* (2013)) and is likely due to the presence of environmental bacteria in tissue samples used in the preparation of genomic DNA used for library construction. Considered together, the limited reads aligning with the PV-ZMOO513642 sequences and the absence of junctions (joining T-DNA borders and flanking sequences; Table 4) indicate that MON 95275, does not contain inserted sequence from the *cre* gene containing transformation plasmid, PV-ZMOO513642.

Table 4. Unique Junction Sequence Class Results

Sample	**Junctions Detected**
MON 95275 (F4)	0
LH244	0

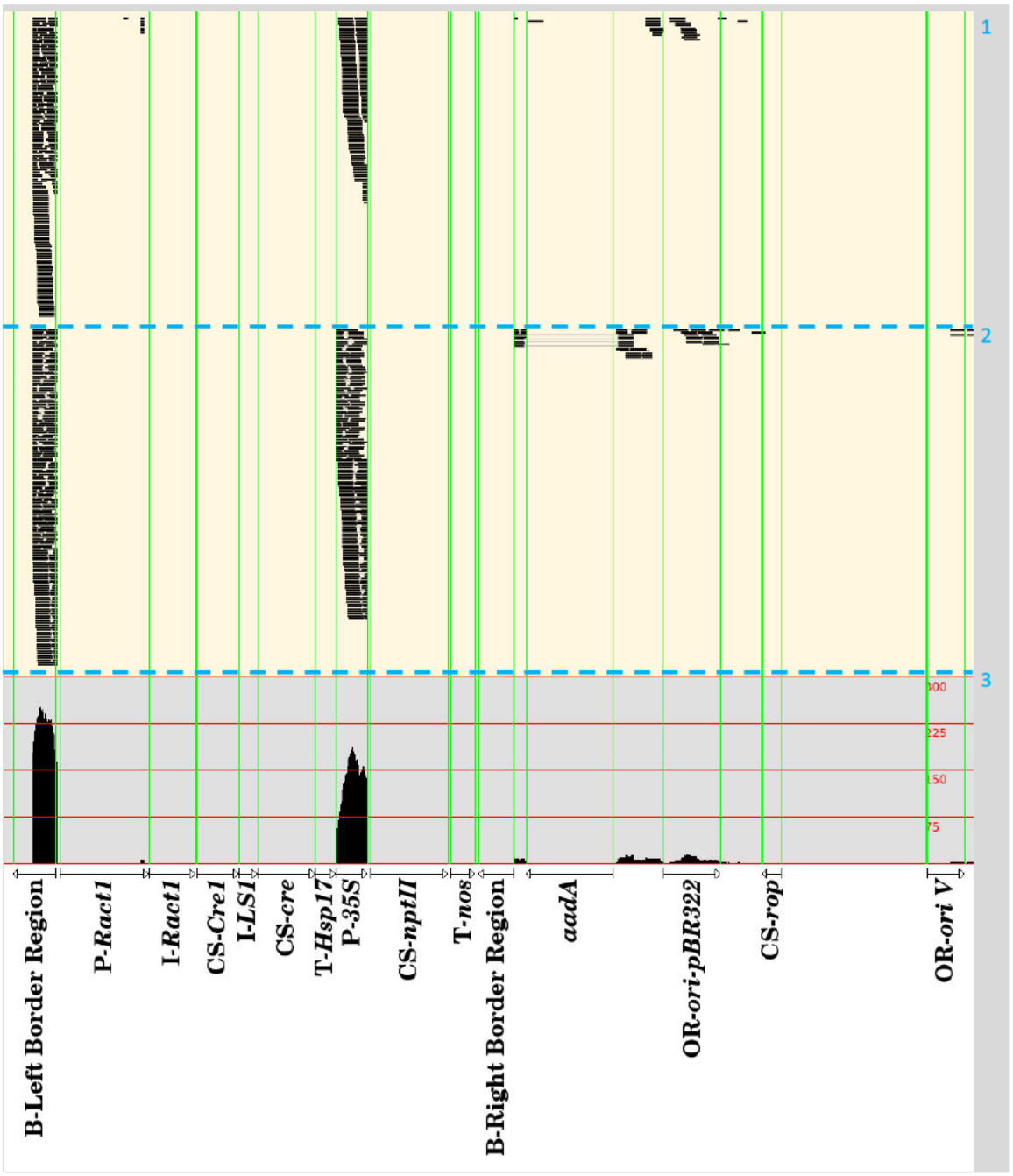

Figure 11. Read Mapping of MON 95275 Versus PV-ZMOO513642

Panel 1 shows the location of unpaired mapped reads. Panel 2 shows paired mapped reads and Panel 3 shows a representation of combined read depth for unpaired and paired reads. Vertical lines show genetic element boundaries.

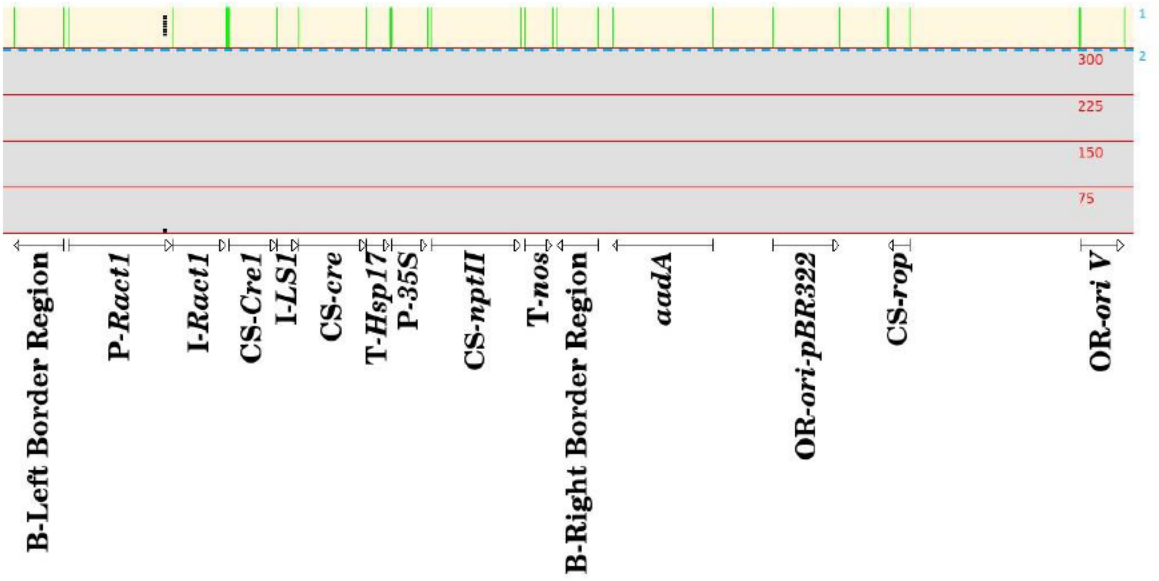

Figure 12. Read Mapping of Conventional Maize LH244 Versus PV-ZMOO513642

Panel 1 shows the location of unpaired mapped reads (there are no paired mapped reads), and Panel 2 shows a representation of combined read depth for unpaired and paired reads. Vertical lines show genetic element boundaries.

A.3(c)(iii) Full DNA sequence of each insertion site, including junction regions with the host DNA

A.3(c)(iii)(i) Organization and Sequence of the Insert and Adjacent DNA in MON 95275

The organization of the elements within the DNA insert and the adjacent genomic DNA was assessed using directed DNA sequence analysis (refer Figure 6, Step 4). PCR primers were designed to amplify two overlapping regions of the MON 95275 genomic DNA that span the entire length of the insert (Figure 13). The amplified PCR products were subjected to DNA sequencing analyses. The results of this analysis confirm that the MON 95275 insert is 14,682 bp and that each genetic element within the T-DNA is intact compared to PV-ZMIR525664, with the exception of the border regions and a single nucleotide difference, between MON 95275 and PV-ZMIR525664. This single nucleotide difference has no functional impact on MON 95275 as it is found within non-coding intervening sequence between elements S-*Isr-1* and E-*DaMV-1*. The sequence of both border regions are truncated with the remainder of the inserted border regions being identical to the sequence in PV-ZMIR525664. With the exception of the previously noted single nucleotide difference, the sequence and organization of the insert was shown to be identical to the corresponding T-DNA of PV-ZMIR525664. As noted, in Section A.3(c)(ii)(iv), the selectable marker cassette (P-*TubA*, TS-*CTP2*, CS-*cp4 epsps*, and T-*TubA*) and one of the two *loxP* sites (bases 14720 through 19135 of the PVZMIR525664 sequence) were excised by Cre recombinase, and as expected, are not present in the MON 95275 sequence. This analysis also shows that only T-DNA elements (described in Table 1) were present. In addition, 1,000 bp flanking the 5′ end of the MON 95275 insert (Table 2, bases 1-1,000) and 1,006 bp flanking the 3′ end of the MON 95275 insert (Table 2, bases 15,683-16,688) were determined.

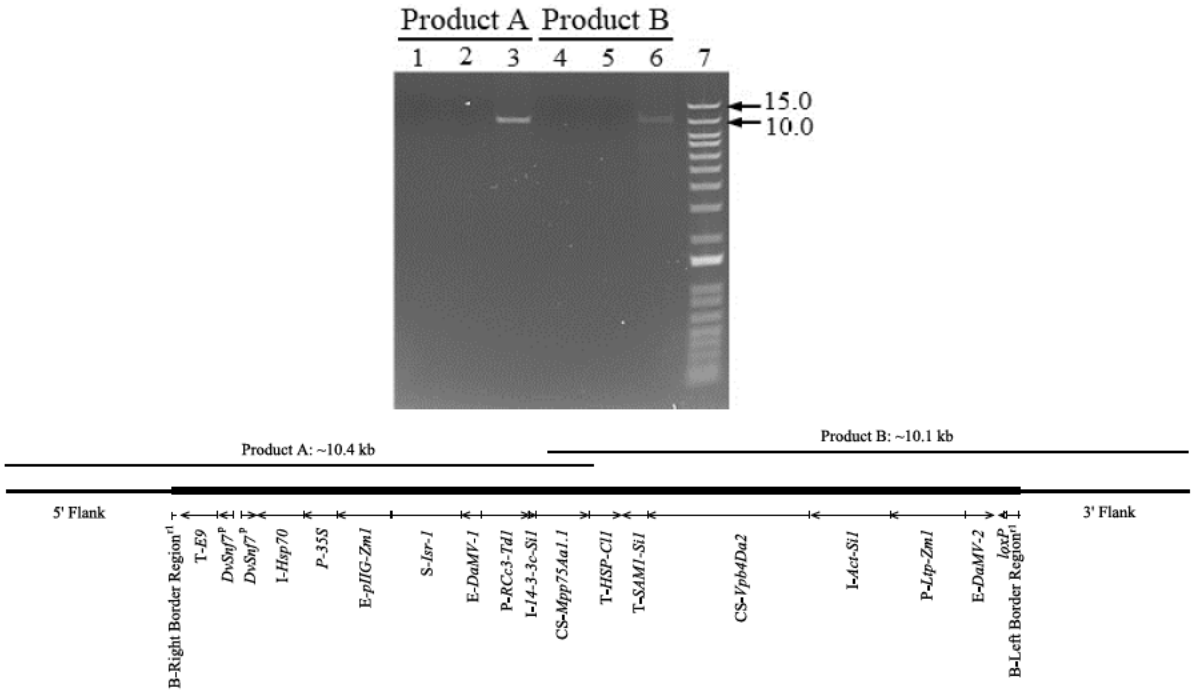

Figure 13. Overlapping PCR Analysis Across the Insert in MON 95275

PCR was performed on both conventional control genomic DNA and genomic DNA of the F4 generation of MON 95275 using two pairs of primers to generate overlapping PCR fragments from MON 95275 for sequencing analysis. To verify the PCR products, 2-4 µl of each of the PCR reactions was loaded on the gel. The expected product size for each amplicon is provided in the illustration of the insert in MON 95275 that appears at the bottom of the figure. This figure is a representative of the data generated in the study. Lane designations are as follows:

Lane	
1	No template control
2	LH244 Conventional Control
3	MON 95275
4	No template control
5	LH244 Conventional Control
6	MON 95275
7	1 Kb Plus DNA Ladder

Arrows on the agarose gel photograph denote the size of the DNA, in kilobase pairs, obtained from the 1 Kb Plus DNA Ladder (Invitrogen) on the ethidium bromide stained gel.

[r1] Superscript in Left and Right Border Regions indicate that the sequence in MON 95275 was truncated compared to the sequences in PV-ZMIR525664.

[P] Superscript in DvSnf7 indicates the partial sequence

A.3(c)(iii)(ii) Sequencing of the MON 95275 Insertion Site

PCR and sequence analysis were performed on genomic DNA extracted from the conventional control to examine the insertion site in conventional maize (see Figure 6, Step 5). The PCR was performed with one primer specific to the genomic DNA sequence flanking the 5′ end of the MON 95275 insert paired with a second primer specific to the genomic DNA sequence flanking the 3′ end of the insert (Figure 14). A sequence comparison between the PCR product generated from the conventional control and the sequence generated from the 5′ and 3′ flanking sequences of MON 95275 indicates that 746 bases of maize genomic DNA were deleted during integration of the T-DNA. There is also a co-insertion of 6 bases, (bases 15,683-15,688 Table 2) in the MON 95275 3′ flanking sequence. Such changes are common during plant transformation (Anderson *et al*., 2016) and these changes presumably resulted from double stranded break repair mechanisms in the plant during *Agrobacterium*-mediated transformation process (Salomon and Puchta, 1998). The remainder of the maize genomic DNA sequences flanking the insert in MON 95275 that were evaluated are identical to the conventional control.

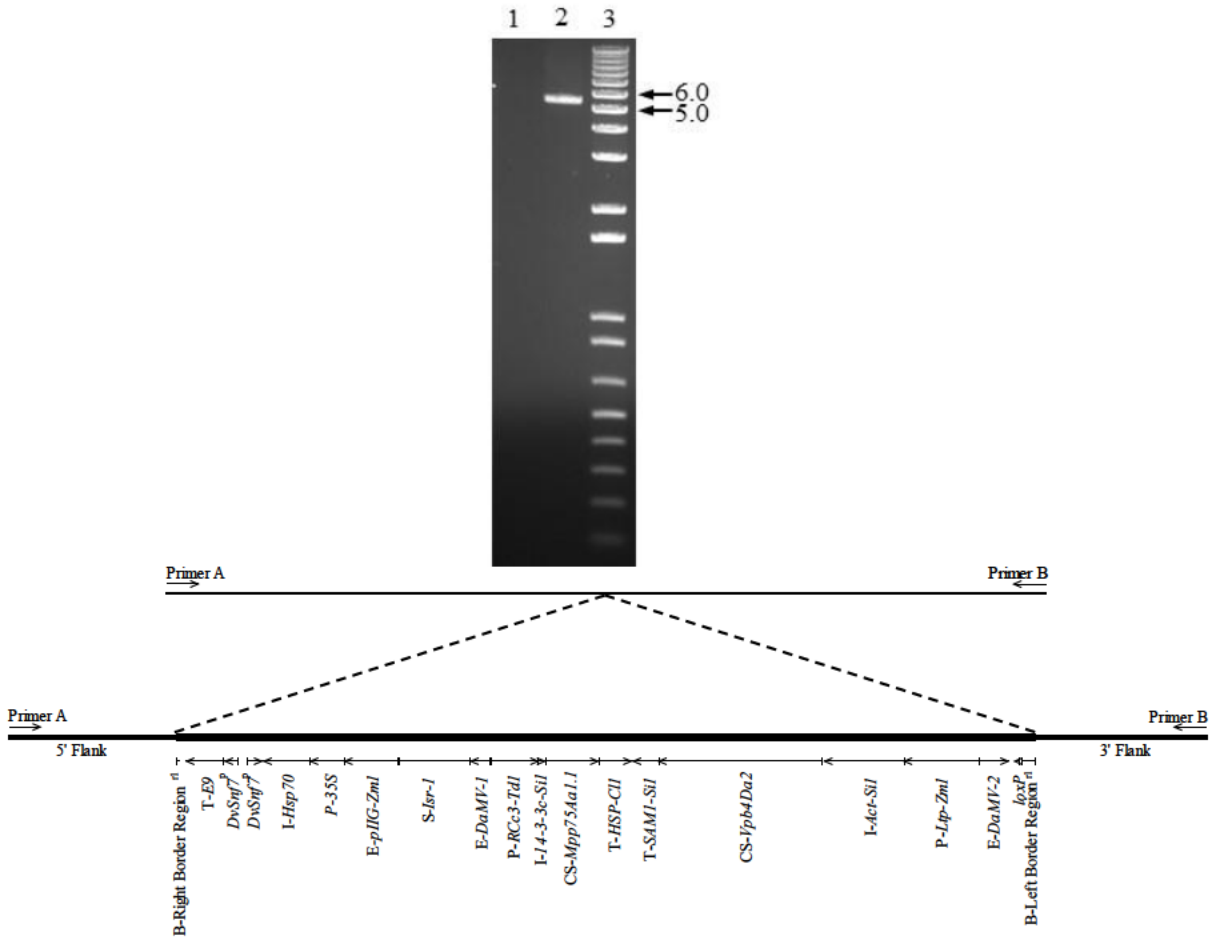

Figure 14. PCR Amplification of the MON 95275 Insertion Site

PCR analysis was performed to evaluate the insertion site. PCR was performed on conventional control DNA using Primer A, specific to the 5′ flanking sequence, and Primer B, specific to the 3′ flanking sequence of the insert in MON 95275. The DNA generated from the conventional control PCR was used for sequencing analysis. This illustration depicts the MON 95275 insertion site in the conventional control (upper panel) and the MON 95725 insert (lower panel). Approximately 2 µl of each of the PCR reactions were loaded on the gel. This figure is representative of the data generated in the study. Lane designations are as follows:

Lane	
1	No template control
2	LH244 Conventional Control
3	1 Kb Plus DNA Ladder

Arrows on the agarose gel photograph denote the size of the DNA, in kilobase pairs, obtained from the 1 Kb Plus DNA Ladder (Invitrogen) on the ethidium bromide stained gel.

[r1] Superscript in Left and Right Border Regions indicate that the sequence in MON 95275 was truncated compared to the sequences in PV-ZMIR525664.

[P] Superscript in DvSnf7 indicates the partial sequence.

A.3(c)(iv) A map depicting the organisation of the inserted genetic material at each insertion site

PCR and DNA sequence analyses performed on MON 95275 and the conventional control determined the organisation of the genetic elements within the insert as given in Figure 14.

A.3(c)(v) Details of an analysis of the insert and junction regions for the occurrence of any open reading frames (ORFs)

A.3(c)(v)(i) Bioinformatics Assessment of Putative Open Reading Frames (ORFs) of MON 95275 Insert and Flanking Sequences

In addition to the bioinformatic analyses conducted on MON 95275 Mpp75Aa1.1 and Vpb4Da2 protein sequences (Section B.2(a)(i)), bioinformatic analyses were also performed on the MON 95275 insert to assess the potential for allergenicity, toxicity, or biological activity of putative polypeptides encoded by all six reading frames present in the MON 95275 insert DNA, as well as ORFs present in the 5' and 3' flanking sequence junctions. These various bioinformatic evaluations are depicted in Figure 15. ORFs spanning the 5' and 3' maize genomic DNA-inserted DNA junctions were translated from stop codon to stop codon in all six reading frames (three forward reading frames and three reading frames in reverse orientation)[5]. Polypeptides of eight amino acids or greater from each reading frame were then compared to toxin, allergen and all proteins databases using bioinformatic tools. Similarly, the entire T-DNA sequence was translated in all six reading frames and the resulting deduced amino acid sequence was subjected to bioinformatic analyses. The data generated from these analyses confirm that even in the highly unlikely occurrence that a translation product other than MON 95275 Mpp75Aa1.1 and Vpb4Da2 proteins were derived from frames one to six of the insert DNA or the ORFs spanning the insert junctions, they would not share significant similarity or identity to known allergens, toxins, or other biologically active proteins that could affect human or animal health. Therefore, there is no evidence for concern regarding the relatedness of the putative polypeptides for MON 95275 to known toxins, allergens, or biologically active putative peptides.

For details, please refer to Appendix 2 [redacted], 2021 (TRR0001435)) and Appendix 3 ([redacted], 2021 (TRR0001434)).

[5] An evaluation of sequence translated from stop codon to stop codon represents the most conservative approach possible for flank junction analysis as it does not take into consideration that a start codon is necessary for the production of a protein sequence.

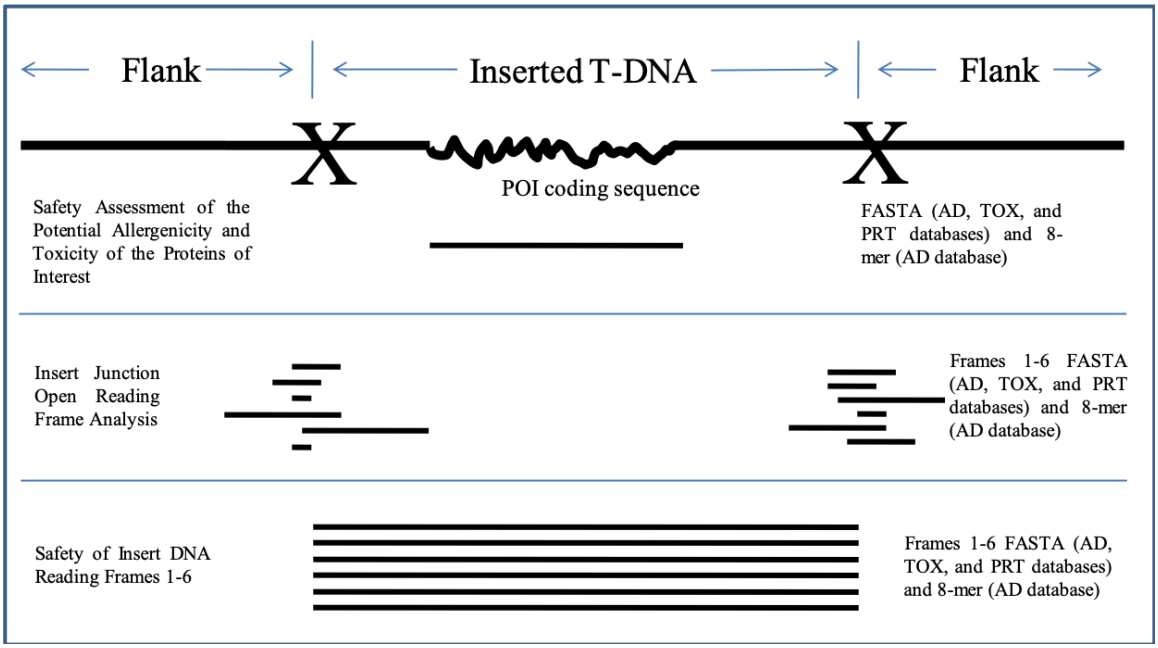

Figure 15. Schematic Summary of MON 95275 Bioinformatic Analyses

AD: AD_2021, TOX: TOX_2021, PRT: PRT_2021; 8-mer represents the eight amino acid sliding window search.

A.3(c)(v)(ii) Bioinformatics Evaluation of the T-DNA Insert in MON 95275

Bioinformatic analyses were performed to assess the potential of toxicity, allergenicity or biological activity of any putative peptides encoded by translation of reading frames 1 through 6 of the inserted DNA in MON 95275 (Figure 15).

The FASTA sequence alignment tool was used to assess structural relatedness between the query sequences and any protein sequences in the AD_2021, TOX_2021, and PRT_2021 databases. Structural similarities shared between each putative polypeptide with each sequence in the database were examined. The extent of structural relatedness was evaluated by detailed visual inspection of the alignment, the calculated percent identity and alignment length to ascertain if alignments exceeded Codex (Codex Alimentarius, 2009) thresholds for FASTA searches of the AD_2021 database, and the *E*-score. Alignments having an *E*-score-less than 1×10^{-5} are deemed significant because they may reflect shared structure and function among sequences. In addition to structural similarity, each putative polypeptide was screened for short polypeptide matches using a pair-wise comparison algorithm. In these analyses, eight contiguous and identical amino acids were defined as immunologically relevant, where eight represents the typical minimum sequence length likely to represent an immunological epitope (Silvanovich *et al.*, 2006) and evaluated against the AD_2021 database.

A.3(c)(v)(iii) Bioinformatics Evaluation of the DNA Sequences Flanking the 5′ and 3′ Junctions of the MON 95275 Insert: Assessment of Putative Peptides

Analyses of putative polypeptides encoded by DNA spanning the 5' and 3' genomic junctions of the MON 95275 inserted DNA were performed using a bioinformatic comparison strategy. The purpose of the assessment is to evaluate the potential for novel open reading frames (ORFs) that may have homology to known allergens, toxins, or proteins that display adverse biological activity. Sequences spanning the 5' and 3' genomic DNA-insert DNA junctions, (Figure 15) were translated from stop codon (TGA, TAG, TAA) to stop codon in all six reading frames. Putative polypeptides from each reading frame, that were eight amino acids or greater in length, were compared to AD_2021, TOX_2021, and PRT_2021 databases using FASTA and to the AD_2021 database using an eight amino acid sliding window search. A total of 10 putative peptides were compared to allergen (AD_2021), toxin (TOX_2021), and all protein (PRT_2021) databases using bioinformatic tools.

The FASTA sequence alignment tool was used to assess the relatedness between the query sequences and any protein sequence in the AD_2021, TOX_2021, and PRT_2021 databases. Similarities shared between the sequence with each sequence in the database were examined. The extent of relatedness was evaluated by detailed visual inspection of the alignment, the calculated percent identity, and the *E*-score. Alignments having *E*-scores of ≤1e-5 (1×10^{-5}) are deemed significant because they may reflect shared structure and function among sequences. In addition to sequence similarity, sequences were screened for short peptide matches using a pair-wise comparison algorithm. In these analyses, eight contiguous and identical amino acids were defined as immunologically relevant, where eight represents the typical minimum sequence length likely to represent an immunological epitope (Silvanovich *et al.*, 2006).

The bioinformatic analysis performed using the 10 putative peptide sequences translated from junctions is theoretical as there is no reason to suspect, or evidence to indicate, the presence of transcripts spanning the flank junctions. The results of these bioinformatic analyses indicate that no structurally relevant sequence similarities were observed between the 10 putative flank junction derived sequences and allergens, toxins, or biologically active proteins. As a result, in the unlikely occurrence that any of the 10 peptides analyzed herein is found *in planta*, none would share significant similarity or identity to known allergens, toxins, or other biologically active proteins that could affect human or animal health.

A.3(c)(v)(iv) Bioinformatics Evaluation of Putative Open Reading Frames of MON 95275 Insert and Flanking Sequences Summary and Conclusions

A conservative bioinformatics assessment of potential allergenicity, toxicity and adverse biological activity for putative polypeptides derived from different reading frames of the entire insert MON 95275 or that span the 5' and 3' insert junctions was conducted. There are no analytical data that indicate any putative polypeptides subjected to bioinformatics evaluation are produced by MON 95275. Moreover, the data generated from these analyses confirm that even in the highly unlikely occurrence that a translation product other than Mpp75Aa1.1 and Vpb4Da2 proteins was derived from frames 1 to 6 of the insert DNA, or the ORFs spanning the insert junctions; they would not share a sufficient degree of sequence similarity with other proteins to

indicate they would be potentially allergenic, toxic, or have other safety implications. Therefore, there is no evidence for concern regarding the putative polypeptides for MON 95275 relatedness to known toxins, allergens, or biologically active putative peptides.

For details, please refer to Appendix 3 [redacted], 2021 (TRR0001434)).

A.3(d) A description of how the line or strain from which food is derived was obtained from the original tranformant (i.e. provide a family tree or describe the breeding process) including which generations have been used for each study

The MON 95275 transformation was conducted with inbred maize line LH244, a maize line assigned to Holden's Foundation Seeds, LLC in 2001 (U.S. Patent #6,252,148). LH244 is a medium season yellow dent maize line of Stiff Stalk background that is best adapted to the central regions of the U.S. corn belt.

Following transformation of immature LH244 embryos, selected transformants were self-pollinated to increase seed supplies. A Cre recombination system was used to remove the *cp4 epsp* selectable marker starting with the selected events at the R2 generation. A selected inbred line homozygous for the presence of the T-DNA and lacking the selectable marker cassette was used to produce other MON 95275 materials for product testing, safety assessment studies, and commercial hybrid development. The non-transformed LH244 was used to produce conventional maize comparators (hereafter referred to as conventional controls) in the safety assessment of MON 95275.

For more details, see MON 95275 breeding history, Figure 3.

Please also refer to Section A.3(a).

A.3(e) Evidence of the stability of the genetic changes, including:

A.3(e)(i) The pattern of inheritance of the transferred gene(s) and the number of generations over which this has been monitored

In order to demonstrate the stability of the T-DNA present in MON 95275 through multiple breeding generations, NGS was performed using DNA obtained from five breeding generations of MON 95275. The breeding history of MON 95275 is presented in Figure 3, and the specific generations tested are indicated in the figure legend. The MON 95275 generation was used for the molecular characterization analyses discussed in Sections A.3(c)(i) and A.3(c)(iii) shown in Figure 3. To assess stability, four additional generations were evaluated by NGS as previously described in Section A.3(c)(i), and compared to the fully characterized F4 generation. The conventional controls used for the generational stability analysis included LH244, with similar background genetics to the F4, F5 and F6 generations and represents the original transformation line; and LH244 + HCL617, a conventional hybrid with similar background genetics to the F4F1 and F5F1 hybrids. Genomic DNA isolated from each of the selected generations of MON 95275 and conventional control was used for NGS mapping, and subsequent junction identification (Table 5).

Table 5. Junction Sequence Classes Detected

Sample	Junction Sequence Classes Detected
MON 95275 (F4)	2
MON 95275 (F4F1)	2
MON 95275 (F5)	2
MON 95275 (F5F1)	2
MON 95275 (F6)	2
LH244	0
LH244 + HCL617	0

As shown by alignment to the full flank/insert sequence obtained from directed sequencing, a single conserved pair of junctions linked by contiguous known and expected DNA sequence is present in MON 95275 F4. Two identical junctions are found in each of the breeding generations (F4F1, F5, F5F1 and F6), confirming the insertion of a single copy of PVZMIR525664 T-DNA at a single locus in the genome of MON 95275, and the consistency of these junctions in the mapping data across all generations tested demonstrates that this single locus is stably maintained throughout the MON 95275 breeding process.

These results demonstrate that the single locus of integration characterized in the F4 generation of MON 95275 is found in five breeding generations of MON 95275, confirming the stability of the insert. This comprehensive NGS and bioinformatic analysis of NGS data from multiple generations supports the conclusion that MON 95275 contains a single, stable insert T-DNA.

A.3(e)(ii) The pattern of inheritance and expression of the phenotype over several generations and, where appropriate, across different environments

A.3.(3)(ii)(i) In heritance of the Genetic Insert in MON 95275

The MON 95275 T-DNA resides at a single locus within the MON 95275 genome and therefore should be inherited according to Mendelian principles of inheritance. During development of lines containing MON 95275 genotypic segregation data were recorded to assess the inheritance and stability of the MON 95275 T-DNA using Chi square (χ^2) analysis over several generations. The χ^2 analysis is based on comparing the observed segregation ratio to the expected segregation ratio according to Mendelian principles.

The MON 95275 breeding path for generating segregation data is described in Figure 16. The transformed R0 plant was self-pollinated to generate R1 seed. An individual plant homozygous for the MON 95275 T-DNA (homozygous positive) was identified in the R1 segregating population via a RealTime -TaqMan® PCR assay.

The homozygous positive R1 plant was self-pollinated to give rise to R2 seed. At the R2 generation, plants were crossed with a Cre recombinase expressing line (Hare and Chua, 2002; Zhang *et al.*, 2003). After excision of the *cp4 epsps* selectable marker cassette, a single *lox* site remains in the F1 generation. The resulting F1 progeny were self-pollinated and the F2 generation were screened for the absence of the *cre* gene (and other sequences from plasmid PV-

ZMOO513642), allowing for selection of lines lacking the Cre recombinase cassette from subsequent generations and the final product. The F2 plants lacking the *cre* gene were self-pollinated to produce F3 seed. The homozygous positive F3 plant was self-pollinated to give rise to F4 seed. The homozygous positive F4 plants were crossed via traditional breeding techniques to a proprietary elite inbred parent that does not contain the *mpp75Aa1.1* coding sequences to produce hemizygous F4F1 seed. The hemizygous F4F1 plants were self-pollinated to produce F4F2 seed. The F4F2 generation was tested for the presence of MON 95275 T-DNA by Real Time TaqMan® PCR assay for *mpp75Aa1.1*. Hemizygous positive F4F2 plants were self-pollinated to produce F4F3 seed. The F4F3 generation was tested for the presence of the T-DNA by Real Time TaqMan® PCR assay for *mpp75Aa1.1*. Hemizygous positive F4F3 plants were self-pollinated to produce F4F4 seed. The F4F4 generation was tested for the presence of the T-DNA by Real Time TaqMan® PCR assay for *mpp75Aa1.1*.

The inheritance of the MON 95275 T-DNA was assessed in the F4F2, F4F3, and F4F4 generations. At all generations, the MON 95275 T-DNA was predicted to segregate at a 1:2:1 ratio (homozygous positive: hemizygous positive: homozygous negative) according to Mendelian inheritance principles.

A Pearson's chi square (χ^2) analysis was used to compare the observed segregation ratios of the MON 95275 T-DNA coding sequence to the expected ratios.

The Chi square was calculated as:

$$\chi^2 = \sum [(| o - e |)^2 / e]$$

where o = observed frequency of the genotype or phenotype and e = expected frequency of the genotype or phenotype. The level of statistical significance was predetermined to be 5% ($\alpha = 0.05$).

The results of the χ^2 analysis of the segregating progeny of MON 95275 are presented in Table 6. The χ^2 value in the F4F2, F4F3, and F4F4 generations indicated no statistically significant difference between the observed and expected segregation ratios of MON 95275 T-DNA. These results support the conclusion that the MON 95275 T-DNA resides at a single locus within the maize genome and is inherited according to Mendelian principles of inheritance. These results are also consistent with the molecular characterization data indicating that
MON 95275 contains a single intact copy of the T-DNA inserted at a single locus in the maize genome (Sections A.3(c)(ii) and A.3(c)(iii)).

For details, please also refer to Appendix 4 ([redacted], 2022 (TRR0001419)).

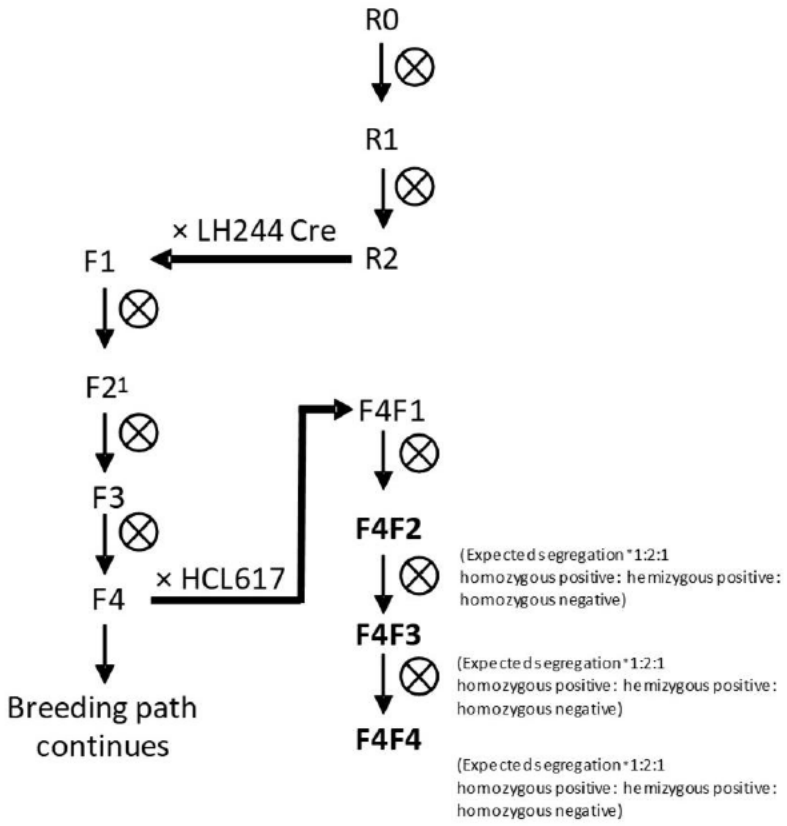

Figure 16. Breeding Path for Generating Segregation Data for MON 95275

*Chi-square analysis was conducted on segregation data from F4F2, F4F3, and F4F4 generations (bolded text).

⊗: Self-Pollinated

[1] The F2 generation was screened for plants lacking the *cre* gene. Only those plants lacking the *cre* gene cassette were self-pollinated to create a F3 generation lacking the *cre* gene cassette.

Table 6. Segregation of the T-DNA During the Development of MON 95275

					1:2:1 Segregation				
Generation	Total Plants	Observed # Plant Homozygous Positive	Observed # Plant Hemizygous Positive	Observed # Plant Homozygous Negative	Expected # Plant Homozygous Positive	Expected # Plant Hemizygous Positive	Expected # Plant Homozygous Negative	$\chi 2$	Probability
F4F2	350	87	169	94	87.50	175	87.50	0.69	0.708
F4F3	293	63	152	78	73.25	146.50	73.25	1.95	0.377
F4F4	302	75	147	80	75.50	151	75.50	0.38	0.828

A.3.(3)(ii)(i) Expression of the Genetic Insert

In order to assess the presence of the Mpp75Aa1.1 and Vpb4Da2 proteins in MON 95275 across multiple breeding generations, western blot analysis of MON 95275 was conducted on grain tissues collected from generations F4, F4F1, F5, F5F1, and F6 of MON 95275, using grain tissues of conventional maize lines (LH244 and LH244 + HCL617) as negative controls.

The presence of the Mpp75Aa1.1 protein was demonstrated in five breeding generations of MON 95275 using western blot analysis. The *E. coli*-produced Mpp75Aa1.1 protein reference standard (2 ng) was used as a reference for the positive identification of the Mpp75Aa1.1 protein (Figure 17, lane 3). The presence of the Mpp75Aa1.1 protein in grain tissue samples of MON 95275 was determined by visual comparison of the bands detected in five breeding generations (Figure 17, lanes 6-10) to the *E. coli*-produced Mpp75Aa1.1 protein reference standard. The MON 95275-produced Mpp75Aa1.1 protein migrated indistinguishably from that of the *E. coli*-produced Mpp75Aa1.1 protein analyzed on the same western blot. As expected, the Mpp75Aa1.1 protein was not detected in the conventional control grain extracts (Figure 17, lanes 4 & 5).

The presence of the Vpb4Da2 protein was demonstrated in five breeding generations of MON 95275 using western blot analysis. The *E. coli*-produced Vpb4Da2 protein reference standard (2 ng) was used as a reference for the positive identification of the Vpb4Da2 protein (Figure 18 lane 3). The presence of the Vpb4Da2 protein in grain tissue samples of MON 95275 was determined by visual comparison of the bands detected in five breeding generations (Figure 18, lanes 6-10) to the *E. coli*-produced Vpb4Da2 protein reference standard. The MON 95275-produced Vpb4Da2 protein migrated indistinguishably from that of the *E. coli*-produced protein standard analyzed on the same western blot. As expected, the Vpb4Da2 protein was not detected in the conventional control grain extracts (Figure 18, lanes 4 & 5).

For details, please refer to Appendix 5 ([redacted], 2021 (TRR0000780)).

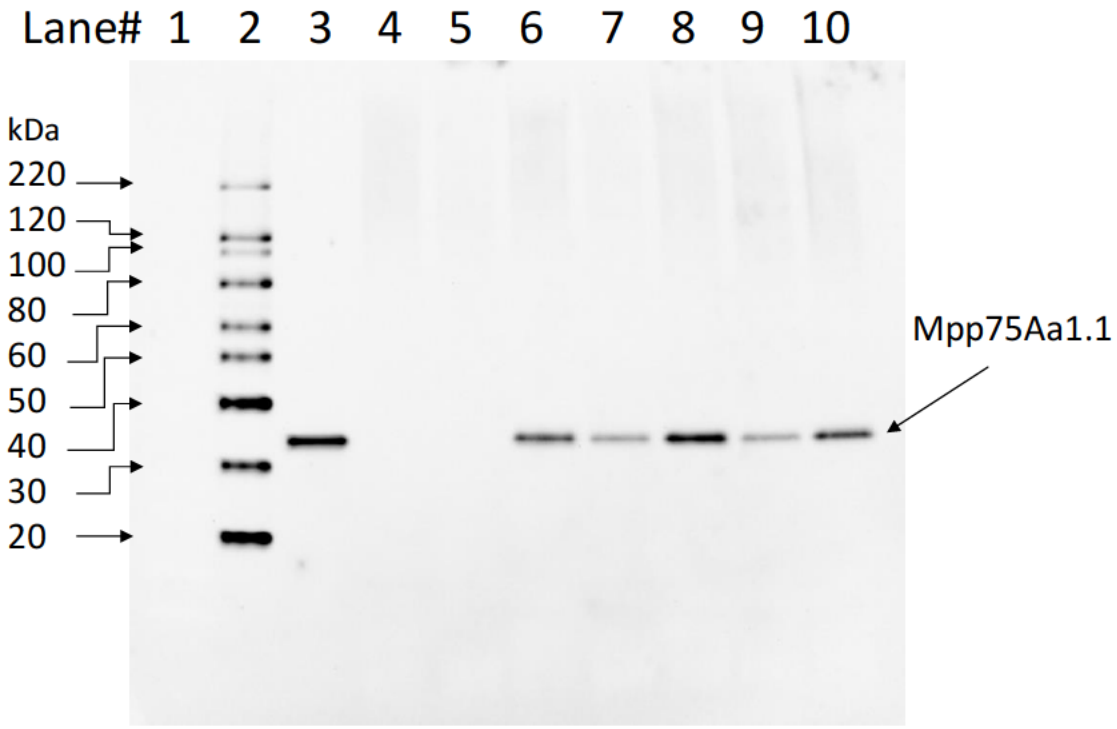

Figure 17. Presence of Mpp75Aa1.1 Protein in Multiple Generations of MON 95275
Western blot probed with a monoclonal anti-Mpp75Aa1.1 primary antibody and an HRP-conjugated anti-mouse IgG secondary antibody. The 30-second exposure image is shown. The approximate MWs (kDa) of the MagicMark™ Protein Standards were shown on the left. Lane designations are as follows.

Lane	Sample	Amount
1	Precision Plus™ Protein Standards	5 µl
2	MagicMark™ Protein Standards (diluted)	1 µl
3	*E. coli*-produced Mpp75Aa1.1 protein	2 ng
4	Conventional LH244, 11464930	8 µl
5	Conventional LH244 + HCL617, 11494212	8 µl
6	Test Substance, F4, 11510458	8 µl
7	Test Substance, F4F1, 11493836	8 µl
8	Test Substance, F5, 11510459	8 µl
9	Test Substance, F5F1, 11494213	8 µl
10	Test Substance, F6, 11494208	8 µl

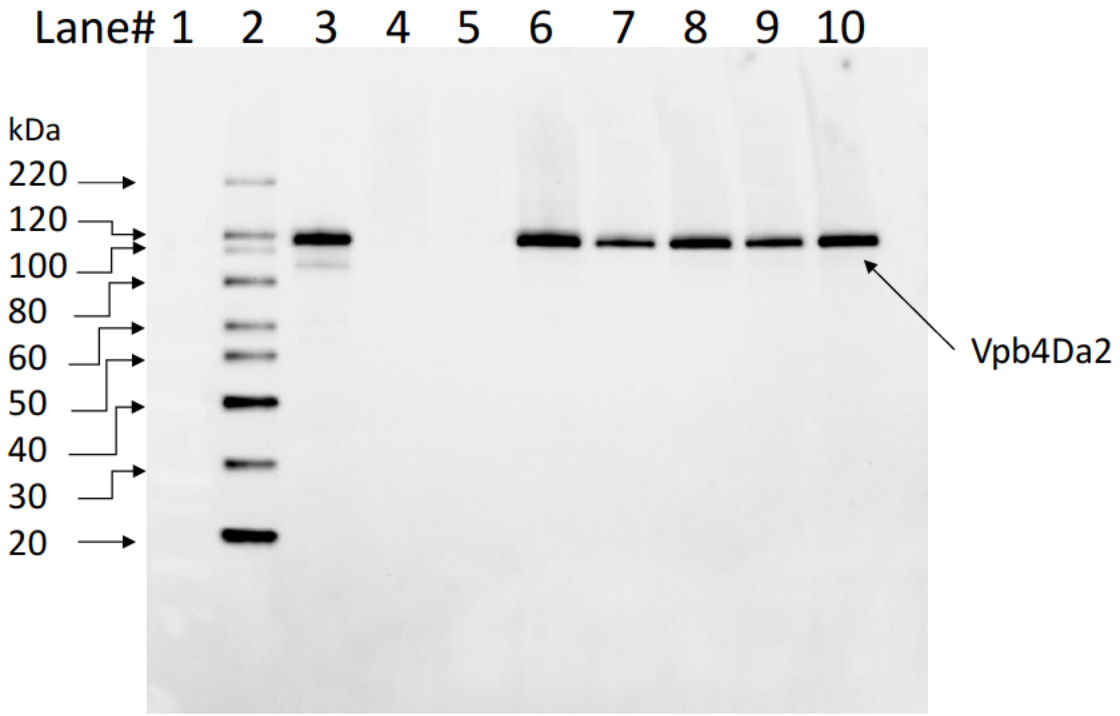

Figure 18. Presence of Vpb4Da2 Protein in Multiple Generations of MON 95275
Western blot probed with a monoclonal anti-Vpb4Da2 primary antibody and an HRP-conjugated anti-mouse IgG secondary antibody. The 15-second exposure image is shown. The approximate MWs (kDa) of the MagicMark™ Protein Standards were shown on the left. Lane designations are as follows.

Lane	Sample	Amount
1	Precision Plus™ Protein Standards	5 µl
2	MagicMark™ Protein Standards (diluted)	1 µl
3	*E. coli*-produced Vpb4Da2 protein	2 ng
4	Conventional LH244, 11464930	8 µl
5	Conventional LH244+ HCL617, 11494212	8 µl
6	Test Substance, F4, 11510458	8 µl
7	Test Substance, F4F1, 11493836	8 µl
8	Test Substance, F5, 11510459	8 µl
9	Test Substance, F5F1, 11494213	8 µl
10	Test Substance, F6, 11494208	8 µl

A.3(f) An analysis of the expressed RNA transcripts, where RNA interference has been used

The *DvSnf7.1* suppression cassette in MON 95275 produces the DvSnf7.1 RNA transcript, which contains the inverted repeat sequences that forms a 240 bp dsRNA (DvSnf7 dsRNA) responsible for an RNAi-based mode of action (MOA). The DNA sequence of the inverted repeat in MON 95275 is identical to that in MON 87411 (approved by FSANZ in 2015, A1097) also used to induce the RNAi mechanism in the CRW pests. The only difference between the full length DvSnf7.1 RNA expressed in MON 95275 and the full length DvSnf7 RNA expressed in MON 87411 is the 5′ UTR, which was optimized to increase in planta expression. The detailed results of characterization of *DvSnf7.1* in MON 95275 are described in Section B.3.

B. CHARACTERISATION AND SAFETY ASSESSMENT OF NEW SUBSTANCES

B.1 Characterisation and Safety Assessment of New Substances

B.1(a) Full description of the biochemical and phenotypic effects of all new substances (e.g. a protein or an untranslated RNA) that are expressed in the new GM organism, including their levels and site of accumulation, particularly in edible portions

Insecticidal proteins from *Bacillus thuringiensis* (*Bt*) have been historically classified as members of Cry (Crystal), Cyt (Cytolytic), and Vip (Vegetative Insecticidal Protein) protein groups based on the homology between their primary sequences (Crickmore *et al.*, 1998). As new insecticidal proteins have been identified and characterized from a wider range of bacteria (including non-*Bt* bacteria), limitations in this classification system were realized due to the increased diversity of the protein structures observed. In July of 2020, a revised nomenclature system was published (Crickmore *et al.*, 2021) and a new database created (https://camtech-bpp.ifas.ufl.edu/). This revised nomenclature system maintains the basic principles of the previous nomenclature system while accounting for the increased diversity in observed protein structures.

Historically, the "Cry" protein class was so named because members of this class formed protein crystals during *Bt* sporulation. Many Cry proteins are categorized biochemically as α-pore forming proteins (α-PFPs) for the α-helical transmembrane pores they form on the insect gut epithelium, which is one of the key events leading to target pest mortality. Familiar examples of such α-PFPs include the Cry1 and Cry2 proteins that have been used in biotechnology-derived crops against lepidopteran insects, and Cry3 proteins against coleopteran pests. These α-pore forming insecticidal proteins share a conserved structural fold, and thus continue to be classified as members of the "Cry" protein class in the newly revised nomenclature, regardless of what bacterial species the genes/proteins are derived from. In contrast, insecticidal proteins from the β-PFP class, so named because they form β-barrel transmembrane pores, have been reclassified to distinguish their unique structure from α-PFP Cry proteins. The Mpp75Aa1.1 protein in MON 95275 was previously designated as Cry75Aa1.1, however based on its unique structure compared to other Cry proteins it has been reclassified as an "Mpp" protein (Crickmore *et al.*, 2021). The Mpp protein class is comprised of β-PFPs from the ETX_MTX2 family, such as the Mpp51Aa2 protein (formerly classified as Cry51Aa2) expressed in MON 88702[6]. Similar to Cry proteins, the Vip protein class in the previous nomenclature was so named because this class of proteins was secreted into the *Bt* culture media during the vegetative phase of growth. The Vpb4Da2 protein expressed in MON 95275 was previously designated as Vip4Da2 as a member of the Vip4 insecticidal protein family under the previous nomenclature, however based on its unique structure compared to other Vip proteins it has been reclassified as a "Vpb" protein. The Vpb protein class is comprised of proteins related to the binding component of binary toxins, or AB toxins (Crickmore *et al.*, 2021).

Despite their reclassification, the insecticidal modes of action (MOA) of the Mpp75Aa1.1 and Vpb4Da2 proteins has been well-characterized and both proteins follow the same general MOA steps as other *Bt* insecticidal proteins currently in commercial use for insect crop protection

[6] The safety of Mpp51Aa2 and MON 88702 has been evaluated and approved in numerous countries.

(Kouadio *et al.*, 2021a). These steps include insect uptake (ingestion), proteolytic activation (which converts the inactive protoxin form of the *Bt* protein to the active toxin form), receptor binding in the insect midgut, oligomerization at the membrane interface, and membrane pore formation in the midgut cells, which in turn leads to insect death (Gill *et al.*, 1992; Pigott and Ellar, 2007; Schnepf *et al.*, 1998).

The *mpp75Aa1.1* gene encodes the Mpp75Aa1.1 protein, which is derived from the full-length precursor of the insecticidal protein Mpp75Aa1 from *B. laterosporus*. The first 23 N-terminal amino acids of the precursor Mpp75Aa1 protein constitutes a membrane-transiting signal peptide that is naturally removed in bacteria during protein translocation and activation after its synthesis (Bowen *et al.*, 2021). The nucleotide sequence encoding this signal peptide was therefore removed in the *mpp75Aa1.1* gene present in MON 95275 to express the mature form of Mpp75Aa1. In addition, a starting codon, or ATG, was added in the 5' end to enable proper translation of the Mpp75Aa1.1 protein. The Mpp75Aa1.1 protein is comprised of a single polypeptide chain of 295 amino acids with a molecular weight of 34 kDa and belongs to the ETX_MTX2 β PFP family. Structurally, the Mpp75Aa1.1 protein is composed of three domains (Kouadio *et al.*, 2021a). Domain I is the receptor binding region, and Domain II and III are responsible for pore formation. The insecticidal specificity of Mpp75Aa1.1 is mediated by processing at its carboxyl-terminus by WCR midgut proteases, forming an oligomer, and specifically interacting with putative membrane-associated receptors on the midgut apical microvilli to cause cellular tissue damage (Kouadio *et al.*, 2021a).

The *vpb4Da2* gene encodes the Vpb4Da2 protein, which is derived from *Bt*. The MON 95275 Vpb4Da2 protein is a native protein without any modification. It is comprised of a single polypeptide chain of 937 amino acids with a molecular weight of 103.8 kDa and belongs to bacterial exotoxin B class of β-PFPs. Structurally, the Vpb4Da2 protein is composed of 6 domains (Kouadio *et al.*, 2021b). The amino-terminal domains 1-3 of the Vpb4Da2 protein display β-barrel architectures that are structurally homologous to domains found in a wide variety of bacterial and eukayotic proteins including glycosyltransferases, proteases, amidases, adhesins and bacterial toxins such as the protective antigen (PA) protein from *Bacillus anthracis* (*B.* anthracis) (Rigden *et al.*, 2004). This commonly observed stuctural domain is named "PA14" after its location in the crystal structure of the PA protein. Sequence allignment across proteins possessing homologous domains indicate that it is typically combined in a mosaic manner with other domains involved in carbohydrate binding. Additionally, domains 1-3 of Vpb4Da2 protein encompass a long β-pore forming loop constituent of the clostridial binary-toxB module (Kouadio *et al.*, 2021b). The carboxyl-terminal half of Vpb4Da2 protein includes a unique set of domains 4 to 6 that adopt specific carbohydrate-binding module topologies. Upon exposure to the midgut of WCR, the Vpb4Da2 protein is processed to a stable core by WCR gut proteases, where the core protein utilizes its structurally distinct carboxyl-terminal domains to bind putative receptors on the insect epithelium cells thereby conferring WCR specificity (Kouadio *et al.*, 2021b).

B.1(a)(i) Characterisation of the MON 95275 Mpp75Aa1.1 Protein

B.1(a)(i)(i) Mpp75Aa1.1 Protein Identity and Equivalence

The safety assessment of crops derived through biotechnology includes characterization of the physicochemical and functional properties and confirmation of the safety of the introduced

protein(s). For the safety data generated using the *E. coli*-produced Mpp75Aa1.1 protein to be applied to the MON 95275-produced Mpp75Aa1.1 protein (plant-produced Mpp75Aa1.1), the equivalence of the plant- and *E. coli*-produced proteins must first be demonstrated. To assess the equivalence between the MON 95275-produced and *E. coli*-produced Mpp75Aa1.1 proteins, a small quantity of the MON 95275-produced Mpp75Aa1.1 protein was purified from MON 95275 grain. The MON 95275-produced Mpp75Aa1.1 protein was characterized and the equivalence of the physicochemical characteristics and functional activity between the MON 95275-produced and *E. coli*-produced Mpp75Aa1.1 proteins was assessed using a panel of analytical tests; as shown in Table 7. Taken together, these data provide a detailed characterization of the MON 95275-produced Mpp75Aa1.1 protein and demonstrate that the *E. coli*-produced Mpp75Aa1.1 protein is a suitable surrogate to the MON 95275-produced Mpp75Aa1.1 protein. Based on these assessments, conclusions derived from digestibility, heat susceptibility, acute oral toxicology study and non-target organism studies conducted with the *E. coli*-produced Mpp75Aa1.1 protein are applicable to MON 95275-produced Mpp75Aa1.1 protein.

Table 7. Summary of MON 95275 Mpp75Aa1.1 Protein Identity and Equivalence

Analytical Test	Assessment	Analytical Test Outcome
N-terminal sequence	Identity	The expected N-terminal sequence for MON 95275-produced Mpp75Aa1.1 protein was observed by LC-MS/MS[1]
LC-MS/MS[1]	Identity	LC-MS/MS[1] analysis of trypsin digested peptides from MON 95275-produced Mpp75Aa1.1 protein yielded peptide masses consistent with expected peptide masses from the theoretical trypsin digest of the amino acid sequence
Western blot analysis	Identity and Equivalence	MON 95275-produced Mpp75Aa1.1 protein identity was confirmed using a western blot probed with polyclonal antibodies specific for Mpp75Aa1.1 protein Immunoreactive properties of the MON 95275-produced Mpp75Aa1.1 and the *E. coli*-produced Mpp75Aa1.1 proteins were shown to be equivalent
Apparent molecular weight (MW)	Equivalence	Electrophoretic mobility and apparent molecular weight of the MON 95275-produced Mpp75Aa1.1 and the *E. coli*-produced Mpp75Aa1.1 proteins were shown to be equivalent
Glycosylation analysis	Equivalence	Glycosylation status of MON 95275-produced Mpp75Aa1.1 and *E. coli*-produced Mpp75Aa1.1 proteins were shown to be equivalent and non glycosylated
Functional activity	Equivalence	Functional activity of the MON 95275-produced Mpp75Aa1.1 and the *E. coli*-produced Mpp75Aa1.1 proteins were shown to be equivalent by insect bioassay

[1] LC-MS/MS = liquid chromatography-tandem mass spectrometry

The details of the materials and methods for the panel of analytical tests used to evaluate and compare the properties of the MON 95275-produced Mpp75Aa1.1 and *E. coli*-produced Mpp75Aa1.1 proteins are described at the end of Appendix 6. A summary of the data obtained to support a conclusion of protein equivalence is provided below.

B.1(a)(i)(ii) Results of the N-Terminal Sequencing Analysis

The expected N-terminal sequence for the Mpp75Aa1.1 protein deduced from the *mpp75Aa1.1* gene present in maize of MON 95275 was observed by LC-MS/MS, except that the N-terminal methionine was cleaved *in vivo* from MON 95275-produced Mpp75Aa1.1 by methionine aminopeptidase or other aminopeptidases (Table 7). The cleavage of the N-terminal methionine from proteins *in vivo* by methionine aminopeptidase is common in many organisms (Bradshaw *et al.*, 1998; Wang *et al.*, 2016). The N-terminal sequence for MON 95275-produced Mpp75Aa1.1 protein was consistent with the N-terminal sequence for the *E. coli*-produced Mpp75Aa1.1 protein observed by LC-MS/MS (Figure 19). Hence, the sequence information confirms the identity of the Mpp75Aa1.1 protein isolated from the grain of MON 95275.

Amino Acids Residue # from the N-terminus	→	1	2	3	4	5	6	7	8	9	10	11	12	13	14	15	16
E.coli-produced Mpp75Aa1.1 sequence	→	X	S	S	T	D	V	Q	E	R	L	R	D	L	A	R	E
		|	|	|	|	|	|	|	|	|	|	|	|	|	|	|	|
Expected Mpp75Aa1.1 Sequence	→	M	S	S	T	D	V	Q	E	R	L	R	D	L	A	R	E
		|	|	|	|	|	|	|	|	|	|	|	|	|	|	|	|
MON 95275 Experimental Sequence	→	X	S	S	T	D	V	Q	E	R	L	R	D	L	A	R	E

Figure 19. N-terminal Sequence of the MON 95275-Produced Mpp75Aa1.1 Protein

The experimental sequence obtained from the MON 95275-produced Mpp75Aa1.1 was compared to the expected sequence deduced from the *mpp75Aa1.1* gene present in MON 95275. *E. coli*-produced Mpp75Aa1.1 protein sequence above was derived from the reference substance Certificate of Analysis (COA) (lot 7536). The single letter International Union of Pure and Applied Chemistry - International Union of Biochemistry (IUPAC-IUB) amino acid code is M, Methionine; S, Serine; T, Threonine; D, Aspartic Acid; V, Valine; Q, Glutamine; E, Glutamic acid; R, Arginine; L, Leucine; A, Alanine. 'X' indicates the residue was not observed.

B.1(a)(i)(iii) Results of Mass Fingerprint Analysis

Peptide mass fingerprint analysis is a standard technique used for confirming the identity of proteins. The ability to identify a protein using this method is dependent upon matching a sufficient number of observed tryptic peptide fragment masses with predicted tryptic peptide fragment masses. In general, protein identification made by peptide mapping is considered to be reliable if ≥ 40% of the protein sequence was identified by matching experimental masses observed for the tryptic peptide fragments to the expected masses for the fragments (Krause *et al.*, 1999; Biron *et al.*, 2006). The identity of the MON 95275-produced Mpp75Aa1.1 protein was confirmed by LC-MS/MS analysis of peptide fragments produced by the trypsin digestion of the MON 95275-produced Mpp75Aa1.1 protein.

There were 41 unique peptides identified that corresponded to the masses expected to be produced by trypsin digestion of the MON 95275-produced Mpp75Aa1.1 protein (Table 8). The identified masses were used to assemble a coverage map of the entire Mpp75Aa1.1 protein (Figure 20, Panel A). The experimentally determined coverage of the MON 95275-produced Mpp75Aa1.1 protein was 96% (Figure 20, Panel A, 283 out of 295 amino acids). This analysis further confirms the identity of MON 95275-produced Mpp75Aa1.1 protein.

There were 61 unique peptides identified that corresponded to the masses expected to be produced by trypsin digestion of the *E. coli*-produced Mpp75Aa1.1 protein (Table 9) by LC-MS/MS analysis during the protein characterization. The identified masses were used to assemble a coverage map of the entire Mpp75Aa1.1 protein (Figure 20, Panel B). The experimentally determined coverage

of the *E. coli*-produced Mpp75Aa1.1 protein was 99.7% (Figure 20, Panel B, 294 out of 295 amino acids). An additional minor population of the Mpp75Aa1.1 protein with an intact N-terminal methionine was also observed from LC- MS/MS and Edman sequencing. This analysis further confirms the identity of *E. coli*-produced Mpp75Aa1.1 protein.

Table 8. Summary of the Tryptic Masses Identified for the MON 95275-Produced Mpp75Aa1.1 Using LC-MS/MS[1]

Experimental Mass[2]	Calculated Mass[3]	Difference[4]	Fragment[5]	Sequence[6]
962.4311	962.4305	0.0006	2 - 9	SSTDVQER
742.4449	742.4449	0.0000	10 - 15	LRDLAR
5044.4177	5044.4155	0.0022	10 - 53	LRDL...TPPK
473.2599	473.2598	0.0001	12 - 15	DLAR
4775.2272	4775.2303	-0.0031	12 - 53	DLAR...TPPK
4319.9767	4319.9811	-0.0044	16 - 53	EDEA...TPPK
4988.3395	4988.3417	-0.0022	16 - 59	EDEA...IGER
686.3711	686.3711	0.0000	54 - 59	NVIGER
842.4723	842.4722	0.0001	54 - 60	NVIGERR
793.4444	793.4446	-0.0002	60 - 65	RISQYK
3208.6152	3208.6152	0.0000	60 - 89	RISQ...YAGK
637.3434	637.3435	-0.0001	61 - 65	ISQYK
3052.5130	3052.5141	-0.0011	61 - 89	ISQY...YAGK
2433.1820	2433.1812	0.0008	66 - 89	VNNA...YAGK
3203.5706	3203.5735	-0.0029	66 - 96	VNNA...DNSK
788.4028	788.4028	0.0000	90 - 96	NVLDNSK
3278.4958	3278.4925	0.0033	97 - 125	GTMD...HGLK
415.2795	415.2795	0.0000	126 - 129	LGVK
3285.4667	3285.4806	-0.0139	130 - 159	TTAT...TDTK
2652.1781	2652.1650	0.0131	136 - 159	FPIA...TDTK
545.2808	545.2809	-0.0001	167 - 171	SPSQK
711.4645	711.4643	0.0002	172 - 178	IKVPAGK
2708.3875	2708.3922	-0.0047	182 - 207	VLAY...IAWR
1798.9593	1798.9578	0.0015	208 - 226	VSPG...VLTK
736.3291	736.3293	-0.0002	231 - 236	GWGDFR
804.3881	804.3878	0.0003	237 - 243	NFQPSGR
1358.7314	1358.7307	0.0007	237 - 248	NFQP...VIVK
1977.0424	1977.0432	-0.0008	237 - 254	NFQP...GTFK
572.3537	572.3534	0.0003	244 - 248	DVIVK
1190.6655	1190.6659	-0.0004	244 - 254	DVIV...GTFK
636.3230	636.3231	-0.0001	249 - 254	GQGTFK
2676.3255	2676.3283	-0.0028	249 - 272	GQGT...TDSK
1156.5770	1156.5764	0.0006	255 - 264	SNYG...FILK
2058.0169	2058.0157	0.0012	255 - 272	SNYG...TDSK

Experimental Mass[2]	Calculated Mass[3]	Difference[4]	Fragment[5]	Sequence[6]
2327.2011	2327.2009	0.0002	255 - 274	SNYG...SKLR
919.4501	919.4498	0.0003	265 - 272	IEDITDSK
1188.6356	1188.6350	0.0006	265 - 274	IEDI...SKLR
1627.8662	1627.8642	0.0020	273 - 287	LRNN...QEIK
1358.6793	1358.6790	0.0003	275 - 287	NNNG...QEIK
1937.0700	1937.0694	0.0006	275 - 292	NNNG...PLIR
596.4009	596.4010	-0.0001	288 - 292	VPLIR

[1] All imported values were rounded to 4 decimal places.
[2] Only experimental masses that matched calculated masses with the highest scores are listed in the table.
[3] The calculated mass is the exact molecular mass calculated from the matched peptide sequence.
[4] The calculated difference = experimental mass – calculated mass.
[5] Position refers to amino acid residues within the predicted MON 95275-produced Mpp75Aa1.1 sequence as depicted in Figure 20 (A).
[6] For peptide matches greater than nine amino acids in length, the first 4 residues and last 4 residues are show separated by three dots (...).

Table 9. Summary of the Tryptic Masses Identified for the *E. coli*-produced Mpp75Aa1.1 Using LC-MS/MS1

Experimental Mass[2]	Calculated Mass[3]	Difference[4]	Fragment[5]	Sequence[6]
1051.4604	1051.4604	0.0000	1 - 9	MSST...VQER
920.4202	920.4199	0.0003	2 - 9	SSTDVQER
1189.6065	1189.6051	0.0014	2 - 11	SSTD...ERLR
742.4455	742.4449	0.0006	10 - 15	LRDLAR
5044.4152	5044.4155	-0.0003	10 - 53	LRDL...TPPK
4775.2336	4775.2303	0.0033	12 - 53	DLAR...TPPK
4319.9727	4319.9811	-0.0084	16 - 53	EDEA...TPPK
4988.3425	4988.3417	0.0008	16 - 59	EDEA...IGER
5144.4392	5144.4428	-0.0036	16 - 60	EDEA...GERR
686.3711	686.3711	0.0000	54 - 59	NVIGER
842.4719	842.4722	-0.0003	54 - 60	NVIGERR
793.4449	793.4446	0.0003	60 - 65	RISQYK
3208.6137	3208.6152	-0.0015	60 - 89	RISQ...YAGK
3052.5168	3052.5141	0.0027	61 - 89	ISQY...YAGK
2433.1812	2433.1812	0.0000	66 - 89	VNNA...YAGK
3203.5709	3203.5735	-0.0026	66 - 96	VNNA...DNSK
788.4031	788.4028	0.0003	90 - 96	NVLDNSK
4048.8887	4048.8848	0.0039	90 - 125	NVLD...HGLK
3278.4922	3278.4925	-0.0003	97 - 125	GTMD...HGLK
3675.7575	3675.7614	-0.0039	97 - 129	GTMD...LGVK
4309.0788	4309.077	0.0018	97 - 135	GTMD...ATMK
1048.5967	1048.5951	0.0016	126 - 135	LGVK...ATMK
651.3262	651.3262	0.0000	130 - 135	TTATMK
3285.4791	3285.4806	-0.0015	130 - 159	TTAT...TDTK
3514.6265	3514.6232	0.0033	130 - 161	TTAT...TKTK
2652.1639	2652.165	-0.0011	136 - 159	FPIA...TDTK
2881.3153	2881.3076	0.0077	136 - 161	FPIA...TKTK
3486.6249	3486.6249	0.0000	136 - 166	FPIA...VSYK
852.4707	852.4705	0.0002	160 - 166	TKQVSYK
1379.7414	1379.7409	0.0005	160 - 171	TKQV...PSQK
1150.5978	1150.5982	-0.0004	162 - 171	QVSY...PSQK
1238.7356	1238.7347	0.0009	167 - 178	SPSQ...PAGK
711.4646	711.4643	0.0003	172 - 178	IKVPAGK

Experimental Mass[2]	Calculated Mass[3]	Difference[4]	Fragment[5]	Sequence[6]
1131.6762	1131.6764	-0.0002	172 - 181	IKVP...KTYR
3580.8913	3580.879	0.0123	174 - 207	VPAG...IAWR
3128.6043	3128.6043	0.0000	179 - 207	TYRV...IAWR
4909.5505	4909.5515	-0.0010	179 - 226	TYRV...VLTK
2708.3922	2708.3922	0.0000	182 - 207	VLAY...IAWR
4489.3397	4489.3394	0.0003	182 - 226	VLAY...VLTK
1798.9566	1798.9578	-0.0012	208 - 226	VSPG...VLTK
2343.1992	2343.2005	-0.0013	208 - 230	VSPG...CQQK
1280.5731	1280.5721	0.0010	227 - 236	CQQK...GDFR
736.3305	736.3293	0.0012	231 - 236	GWGDFR
1522.7057	1522.7066	-0.0009	231 - 243	GWGD...PSGR
804.3882	804.3878	0.0004	237 - 243	NFQPSGR
1358.73	1358.7307	-0.0007	237 - 248	NFQP...VIVK
1977.044	1977.0432	0.0008	237 - 254	NFQP...GTFK
1190.6672	1190.6659	0.0013	244 - 254	DVIV...GTFK
636.3234	636.3231	0.0003	249 - 254	GQGTFK
2676.3305	2676.3283	0.0022	249 - 272	GQGT...TDSK
1156.5775	1156.5764	0.0011	255 - 264	SNYG...FILK
2058.016	2058.0157	0.0003	255 - 272	SNYG...TDSK
2327.2005	2327.2009	-0.0004	255 - 274	SNYG...SKLR
919.4502	919.4498	0.0004	265 - 272	IEDITDSK
1188.6353	1188.635	0.0003	265 - 274	IEDI...SKLR
2529.3014	2529.3034	-0.0020	265 - 287	IEDI...QEIK
1627.8635	1627.8642	-0.0007	273 - 287	LRNN...QEIK
2206.2619	2206.2546	0.0073	273 - 292	LRNN...PLIR
1358.6801	1358.679	0.0011	275 - 287	NNNG...QEIK
1937.0707	1937.0694	0.0013	275 - 292	NNNG...PLIR
939.5753	939.5753	0.0000	288 - 295	VPLIRTEI

[1] All imported values were rounded to 4 decimal places.
[2] Only experimental masses that matched calculated masses with the highest scores are listed in table.
[3] The calculated mass is the exact molecular mass calculated from the matched peptide sequence.
[4] The calculated difference = experimental mass – calculated mass.
[5] Position refers to amino acid residues within the predicted *E. coli*-produced Mpp75Aa1.1 sequence as depicted in Figure 20 (B).
[6] For peptide matches greater than nine amino acids in length the first 4 residues and last 4 residues are shown separated by dots (…).

(A)

1 MSSTDVQERL RDLAREDEAG TFNEAWNTNF KPSDEQQFSY SPTEGIVFLT

51 PPKNVIGERR ISQYKVNNAW ATLEGSPTEA SGTPLYAGKN VLDNSKGTMD

101 QELLTPEFNY TYTESTSNTT THGLKLGVKT TATMKFPIAQ GSMEASTEYN

151 FQNSSTDTKT KQVSYKSPSQ KIKVPAGKTY RVLAYLNTGS ISGEANLYAN

201 VGGIAWRVSP GYPNGGGVNI GAVLTKCQQK GWGDFRNFQP SGRDVIVKGQ

251 GTFKSNYGTD FILKIEDITD SKLRNNNGSG TVVQEIKVPL IRTEI

(B)

1 MSSTDVQERL RDLAREDEAG TFNEAWNTNF KPSDEQQFSY SPTEGIVFLT

51 PPKNVIGERR ISQYKVNNAW ATLEGSPTEA SGTPLYAGKN VLDNSKGTMD

101 QELLTPEFNY TYTESTSNTT THGLKLGVKT TATMKFPIAQ GSMEASTEYN

151 FQNSSTDTKT KQVSYKSPSQ KIKVPAGKTY RVLAYLNTGS ISGEANLYAN

201 VGGIAWRVSP GYPNGGGVNI GAVLTKCQQK GWGDFRNFQP SGRDVIVKGQ

251 GTFKSNYGTD FILKIEDITD SKLRNNNGSG TVVQEIKVPL IRTEI

Figure 20. Peptide Map of the MON 95275-Produced Mpp75Aa1.1 and *E. coli*-Produced Mpp75Aa1.1

(A). The amino acid sequence of the MON 95275-produced Mpp75Aa1.1 protein was deduced from the *mpp75Aa1.1* gene present in MON 95275. Boxed regions correspond to peptides that were identified from the MON 95275-produced Mpp75Aa1.1 protein sample using LC-MS/MS. In total, 96% coverage (283 out of 295 amino acids) of the expected protein sequence was covered by the identified peptides.

(B). The amino acid sequence of the *E. coli*-produced Mpp75Aa1.1 protein was deduced from the *mpp75Aa1.1* gene that is contained on the expression plasmid pMON403758. Boxed regions correspond to peptides that were identified from the *E. coli*-produced Mpp75Aa1.1 protein sample using LC-MS/MS. In total, 99.7% coverage (294 out of 295 amino acids) of the expected protein sequence was covered by the identified peptides.

B.1(a)(i)(iv) Results of Western Blot Analysis of the Mpp75Aa1.1 Protein Isolated from the Grain of MON 95275 and Immunoreactivity Comparison to *Bt*-produced Mpp75Aa1.1 Protein

Western blot analysis was conducted using rabbit anti-Mpp75Aa1.1 polyclonal antibody as additional means to confirm the identity of the Mpp75Aa1.1 protein isolated from the grain of MON 95275 and to assess the equivalence of the immunoreactivity of the MON 95275-produced and *E. coli*-produced Mpp75Aa1.1 proteins.

The results showed that immunoreactive bands with the same electrophoretic mobility were present in all lanes loaded with the MON 95275-produced and *E. coli*-produced Mpp75Aa1.1 proteins Figure 21. For each amount loaded, comparable signal intensity was observed between the MON 95275-produced and *E. coli*-produced Mpp75Aa1.1 protein bands. As expected, the signal intensity increased with increasing load amounts of the MON 95275-produced and *E. coli*-produced Mpp75Aa1.1 proteins, thus supporting identification of MON 95275 -produced Mpp75Aa1.1 protein.

To compare the immunoreactivity of the MON 95275-produced and *E. coli*-produced Mpp75Aa1.1 proteins, densitometric analysis was conducted on the bands that migrated at the expected apparent MW for Mpp75Aa1.1 proteins (~ 35 kDa). The signal intensity (reported in OD) of the band of interest in lanes loaded with MON 95275-produced and *E. coli*-produced Mpp75Aa1.1 proteins was measured Table 10. Because the mean signal intensity of the MON 95275-produced Mpp75Aa1.1 protein was within 35% of the mean signal intensity of the *E. coli*-produced Mpp75Aa1.1 protein, the MON 95275-produced Mpp75Aa1.1 and *E. coli*-produced Mpp75Aa1.1 proteins were determined to have equivalent immunoreactivity.

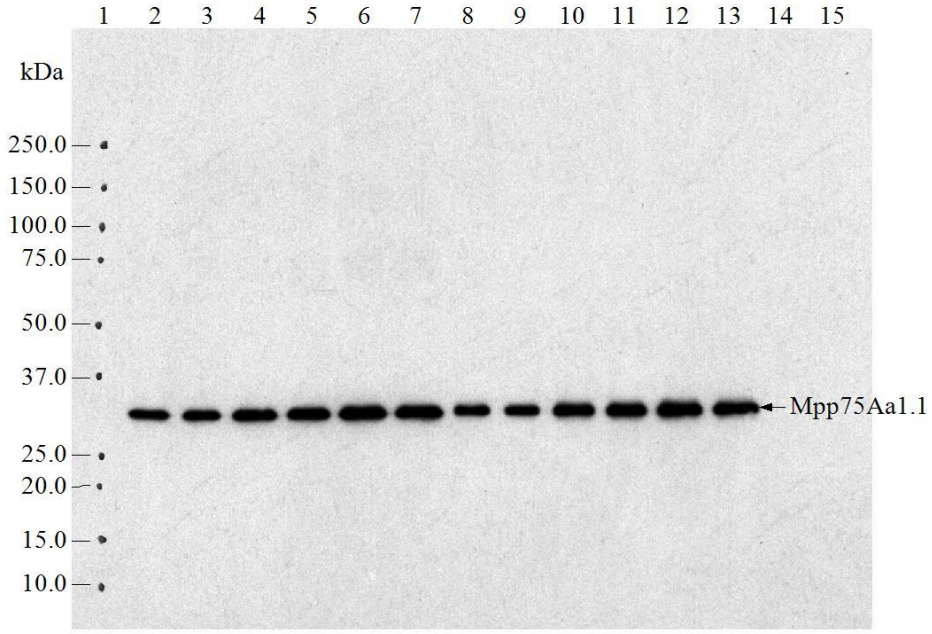

Figure 21. Western Blot Analysis and Immunoreactivity of MON 95275-Produced and *E. coli*-Produced Mpp75Aa1.1 Proteins

Aliquots of the MON 95275-produced and *E. coli*-produced Mpp75Aa1.1 proteins were subjected to SDS-PAGE and electrotransferred to a nitrocellulose membrane. Proteins were detected using rabbit anti-Mpp75Aa1.1 polyclonal antibodies as the primary antibodies. Immunoreactive bands were visualized using HRP-conjugated secondary antibodies and an ECL system. The 10-second exposure is shown. The approximate MW (kDa) of the standards are shown on the left. Lane designations are as follows:

Lane	Sample	Amount (ng)
1	Precision Plus Protein™ Standards	-
2	*E. coli*-produced Mpp75Aa1.1	1
3	*E. coli*-produced Mpp75Aa1.1	1
4	*E. coli*-produced Mpp75Aa1.1	2
5	*E. coli*-produced Mpp75Aa1.1	2
6	*E. coli*-produced Mpp75Aa1.1	3
7	*E. coli*-produced Mpp75Aa1.1	3
8	MON 95275-produced Mpp75Aa1.1	1
9	MON 95275-produced Mpp75Aa1.1	1
10	MON 95275-produced Mpp75Aa1.1	2
11	MON 95275-produced Mpp75Aa1.1	2
12	MON 95275-produced Mpp75Aa1.1	3
13	MON 95275-produced Mpp75Aa1.1	3
14	Blank	-
15	Blank	-

Table 10. Immunoreactivity of the MON 95275-Produced and *E. coli*-Produced Mpp75Aa1.1 Proteins

Mean Signal Intensity from MON 95275-Produced Mpp75Aa1.1 [1] (OD)	Mean Signal Intensity from *E. coli*-Produced Mpp75Aa1.1 [1] (OD)	Acceptance Limits[2] (OD)
1,896.14	2,033.35	1321.68 – 2745.02

[1] Each value represents the mean of six values (n = 6).

[2] The acceptance limits are for the MON 95275-produced Mpp75Aa1.1 protein and are based on the interval between -35% (2033.35 x 0.65 = 1321.68) and +35 % (2033.35 x 1.35 = 2745.02) of the mean of the *E. coli*-produced Mpp75Aa1.1 signal intensity across all loads.

B.1(a)(i)(v) Results of the Mpp75Aa1.1 Protein Molecular Weight and Purity Analysis

For apparent MW and purity determination, the MON 95275-produced Mpp75Aa1.1 and the *E. coli*-produced Mpp75Aa1.1 proteins were subjected to SDS-PAGE. Following electrophoresis, the gel was stained with Brilliant Blue G-Colloidal stain and analyzed by densitometry. The MON 95275-produced Mpp75Aa1.1 protein (Figure 22, lanes 3-8) migrated to the same position on the gel as the *E. coli*-produced Mpp75Aa1.1 protein (Figure 22, lane 2) and the apparent MW was calculated to be 35.2 kDa (Table 11). Because the experimentally determined apparent MW of the MON 95275-produced Mpp75Aa1.1 protein was within the acceptance limits for equivalence (Table 12), the MON 95275-produced Mpp75Aa1.1 and *E. coli*-produced Mpp75Aa1.1 proteins were determined to have equivalent apparent molecular weights.

The purity of the MON 95275-produced Mpp75Aa1.1 protein was calculated based on the six lanes loaded on the gel (Figure 22, lanes 3-8). The average purity was determined to be 70% (Table 11).

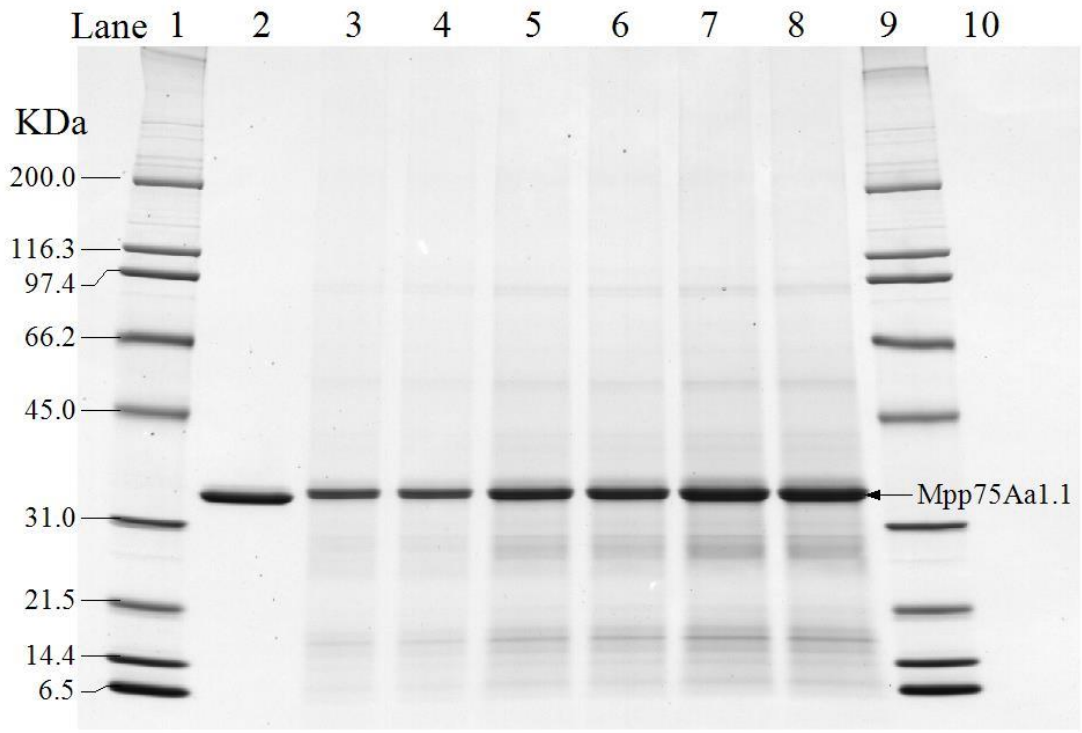

Figure 22. Purity and Apparent Molecular Weight Analysis of the MON 95275- Produced Mpp75Aa1.1 Protein

Aliquots of the MON 95275-produced and the *E. coli*-produced Mpp75Aa1.1 proteins were subjected to SDS-PAGE and the gel was stained with Brilliant Blue G-Colloidal stain. The MWs (kDa) are shown on the left and correspond to the standards loaded in lanes 1 and 9. The Mpp75Aa1.1 protein is indicated with an arrow in the image. Lane designations are as follows:

Lane	Sample	Amount (µg)
1	Broad Range MW Standard	5.0
2	*E. coli*-produced Mpp75Aa1.1	1.0
3	MON 95275-produced Mpp75Aa1.1	1.0
4	MON 95275-produced Mpp75Aa1.1	1.0
5	MON 95275-produced Mpp75Aa1.1	2.0
6	MON 95275-produced Mpp75Aa1.1	2.0
7	MON 95275-produced Mpp75Aa1.1	3.0
8	MON 95275-produced Mpp75Aa1.1	3.0
9	Broad Range MW Standard	5.0
10	Blank	

Table 11. Apparent Molecular Weight and Purity Analysis of the MON 95275-Produced Mpp75Aa1.1 Protein

	Apparent MW[1] (kDa)	Purity[2] (%)
Average (n=6)	35.2	70

[1]Final MW was rounded to one decimal place.
[2]Average % purity was rounded to the nearest whole number.

Table 12. Apparent Molecular Weight Comparison Between the MON 95275-Produced Mpp75Aa1.1 and *E. coli*-Produced Mpp75Aa1.1 Proteins

Apparent MW of MON 95275-Produced Mpp75Aa1.1 Protein (kDa)	Apparent MW of *E. coli*-Produced Mpp75Aa1.1 Protein[1] (kDa)	Acceptance Limits[2] (kDa)
35.2	34.0	31.0 – 36.3

[1] As reported on COA of the *E. coli*-produced Mpp75Aa1.1 protein.
[2] Data obtained for the *E. coli*-produced Mpp75Aa1.1 protein was used to generate the prediction interval (Appendix 6).

B.1(a)(i)(vi) Mpp75Aa1.1 Glycosylation Analysis

Some eukaryotic proteins are post-translationally modified by the addition of carbohydrate moieties (Rademacher *et al.*, 1988). To test whether the Mpp75Aa1.1 protein was glycosylated when expressed in the maize grain of MON 95275, the MON 95275-produced Mpp75Aa1.1 protein was analyzed using an ECL™ glycoprotein detection method. Transferrin, a glycosylated protein, was used as a positive control in the assay. To assess equivalence of the MON 95275-produced and *E. coli*-produced Mpp75Aa1.1 proteins, the *E. coli*-produced Mpp75Aa1.1 protein was also analyzed.

A clear glycosylation signal was observed at the expected molecular weight (~80 kDa) in the lanes containing the positive control (transferrin) and the band intensity increased with increasing concentration (Figure 23, Panel A). In contrast, no glycosylation signal was observed in the lanes containing the *E. coli*-produced Mpp75Aa1.1 protein or MON 95275-produced Mpp75Aa1.1 protein (Figure 23, Panel A).

To confirm that MON 95275-produced Mpp75Aa1.1 and *E. coli*-produced Mpp75Aa1.1 proteins were appropriately loaded for glycosylation analysis, a second membrane with identical loadings and transfer time was stained with Coomassie Blue R250 for protein detection. Both the MON 95275-produced and *E. coli*-produced Mpp75Aa1.1 proteins were detected (Figure 23, Panel B). These data indicate that the glycosylation status of MON 95275-produced Mpp75Aa1.1 protein is equivalent to that of the *E. coli*-produced Mpp75Aa1.1 protein and that neither is glycosylated.

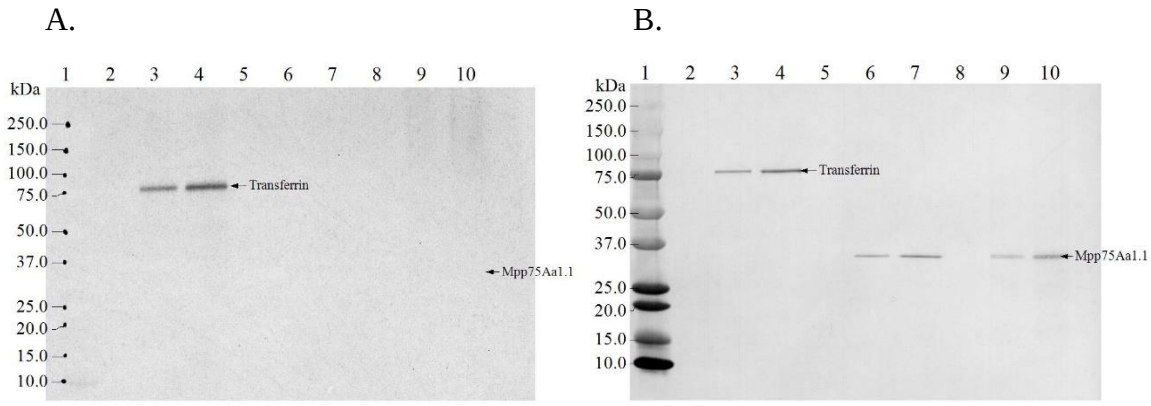

Figure 23. Glycosylation Analysis of the MON 95275-Produced and *E. coli*-Produced Mpp75Aa1.1 Proteins

Aliquots of the transferrin (positive control), *E. coli*-produced Mpp75Aa1.1 and MON 95275-produced Mpp75Aa1.1 proteins were subjected to SDS-PAGE and electrotransferred to a PVDF membrane. The MWs (kDa) correspond to the Precision Plus Protein™ Standards. The arrows show the expected migration of the MON 95275 -produced and *E. coli*-produced Mpp75Aa1.1 proteins and transferrin. (A) Where present, the labeled carbohydrate moieties were detected by using ECL reagents and exposure to Hyperfilm®. The 20-minute exposure is shown. (B) An equivalent blot was stained with Coomassie Blue R250 to confirm the presence of proteins. Lane designations are as follows:

Lane	Sample	Amount (ng)
1	Precision Plus Protein™ Standards	-
2	Blank	-
3	Transferrin (positive control)	100
4	Transferrin (positive control)	200
5	Blank	-
6	*E. coli*-produced Mpp75Aa1.1	100
7	*E. coli*-produced Mpp75Aa1.1	200
8	Blank	-
9	MON 95275-produced Mpp75Aa1.1	100
10	MON 95275-produced Mpp75Aa1.1	200

B.1(a)(i)(vii) Mpp75Aa1.1 Functional Activity

The MON 95275-produced Mpp75Aa1.1 and *E. coli*-produced Mpp75Aa1.1 proteins will be considered to have equivalent functional activity if the biological activity of both proteins (EC_{50}) meets one of criteria[7].

The experimentally determined functional activity for the MON 95275-produced and *E. coli*-produced Mpp75Aa1.1 proteins are presented in Figure 20. The mean EC_{50} values based upon the purity correct concentrations of the MON 95275-produced and *E. coli*-produced Mpp75Aa1.1 proteins were 9.4 and 6.8 µg of Mpp75Aa1.1 protein/ml diet, respectively. Because no significant difference on the EC_{50} of both proteins was observed by t-test (two-sided, $p > 0.05$) (Table 13), the MON 95275-produced Mpp75Aa1.1 protein was considered to have equivalent functional activity to that of the *E. coli*-produced Mpp75Aa1.1 protein.

Table 13. Functional Activity (EC_{50}) of MON 95275-Produced and *E. coli*-Produced Mpp75Aa1.1 Proteins

Replicates	MON 95275-Produced Mpp75Aa1.1 [1, 6] (µg protein/ml diet)	*E. coli*-produced Mpp75Aa1.1 [1, 6] (µg protein/ml diet)	t-test[2] (p-value)	95% Prediction Intervals[3,4] (µg protein/ml diet)	99% Prediction Intervals[3,5] (µg protein/ml diet)
1	8.8	4.1	0.1541	2.43-5.60	1.98-6.85
2	11	8.6			
3	8.3	7.6			
Mean	9.4	6.8	-	-	-

[1] Value refers to mean calculated based on three independent assays (n=3).
[2] No significant difference is based on two sided t-test and α=0.05.
[3] Data obtained for the *E. coli*-produced Mpp75Aa1.1 protein were used to generate a prediction interval to set the acceptance limits for EC50 values of 3 future independent assays (Appendix 6).
[4] Lower and upper acceptance limits for 95% prediction interval.
[5] Lower and upper acceptance limits for 99% prediction interval.
[6] the purity-corrected *E.coli*-produced and MON 95275-prodcued proteins were used for functional activity measurement.

B.1(a)(i)(viii) MON 95275 Mpp75Aa1.1 Identity and Equivalence Conclusion

The MON 95275-produced Mpp75Aa1.1 protein purified from MON 95275 grain was characterized, and a comparison of the physicochemical and functional properties between the MON 95275-produced and the E. coli-produced Mpp75Aa1.1 proteins was conducted following a panel of analytical tests: 1) N-terminal sequence analysis established the same identity for the MON 95275-produced and the E. coli-produced Mpp75Aa1.1 proteins; 2) LC-MS/MS analysis yielded peptide masses consistent with the expected peptide masses from the theoretical trypsin

[7] The equivalence of the test and reference substances will be determined by a stepwise procedure. 1) the biological activity (EC50) from the test and reference substances will be compared using a t-test and to evaluate if a significant difference in activity is observed. 2) the biological activity of the test substance is within the upper and lower limits of the 95% prediction interval derived from data of the reference substance. 3) the biological activity of the test substance is within the upper and lower limits of the 99% prediction interval derived from data of the reference substance.

digest of the mpp75Aa1.1 gene product present in MON 95275; 3) the MON 95275-produced and the *E. coli*-produced Mpp75Aa1.1 proteins were both detected on a western blot probed with antibodies specific for Mpp75Aa1.1 protein and the immunoreactive properties of both proteins was shown to be equivalent; 4) the electrophoretic mobility and apparent molecular weight of the MON 95275-produced and the *E. coli-produced* Mpp75Aa1.1 proteins were shown to be equivalent; 5) the glycosylation status of MON 95275-produced and the *E. coli*-produced Mpp75Aa1.1 proteins was determined to be equivalent and not glycosylated; and 6) the functional activity of the MON 95275-produced and *E. coli*-produced Mpp75Aa1.1 proteins was demonstrated to be equivalent. These results demonstrate that the MON 95275-produced and the *E. coli*-produced Mpp75Aa1.1 proteins are equivalent.

The ability of the Mpp75Aa1.1 to bind to its target receptor is dependent on the conformation of the Mpp75Aa1.1 receptor binding domain. Protein structure, or conformation, is determined by the primary amino acid sequence that comprises the different structural and functional motifs. It can be inferred that once properly folded, proteins that possess the same amino acid sequences would have equivalent functional activity or receptor binding. The MON 95275- and *E. coli*-produced Mpp75Aa1.1 proteins possess the same amino sequences, and thereby equivalent receptor binding domains, as evidenced by the amino acid sequence identity seen by mass fingerprint analysis where >96% coverage was detected. The identity of the protein sequences was also confirmed through sequencing the genes of the expressed MON 95275- and *E. coli*-produced Mpp75Aa1.1 proteins. Finally, the equivalent biological activity of the protein isolated from both sources indicates that the functional structure of the receptor binding domains in both proteins is equivalent.

Taken together, the equivalency data provided in support of the MON 95275 Mpp75Aa1.1 protein confirms that the *E. coli*-produced Mpp75Aa1.1 protein is appropriate surrogate for use in the evaluation of the safety of the MON 95275-produced Mpp75Aa1.1 protein.

For details please refer to Appendix 6 [redacted]., 2021 (TRR0001571)).

B.1(a)(ii) Characterization of the Vpb4Da2 Protein

B.1(a)(ii)(i) Vpb4Da2 Protein Identity and Equivalence

The safety assessment of crops derived through biotechnology includes characterization of the physicochemical and functional properties and confirmation of the safety of the introduced protein(s). For the safety data generated using the *E. coli*-produced Vpb4Da2 protein to be applied to the MON 95275-produced Vpb4Da2 protein (plant-produced Vpb4Da2), the equivalence of the plant- and *E. coli*-produced proteins must first be evaluated. To assess the equivalence between the MON 95275-produced and *E. coli*-produced Vpb4Da2 proteins, a small quantity of the MON 95275-produced Vpb4Da2 protein was purified from MON 95275 grain. The MON 95275-produced Vpb4Da2 protein was characterized and the equivalence of the physicochemical characteristics and functional activity between the MON 95275-produced and *E. coli*-produced Vpb4Da2 proteins was assessed using a panel of analytical tests. These data provide a detailed characterization of the MON 95275-produced Vpb4Da2 protein and demonstrate that the *E. coli*-produced Vpb4Da2 protein is a suitable surrogate to the MON 95275-produced Vpb4Da2 as shown in Table 14. Based on these assessments , conclusions derived from digestibility, heat

susceptibility, acute toxicology, and non-target organism studies conducted with the *E. coli*-produced Vpb4Da2 protein are applicable to MON 95275-produced Vpb4Da2 protein.

For details please refer to Appendix 7 [redacted]., 2021 (TRR0001572)).

Table 14. Summary of MON 95275 Vpb4Da2 Protein Identity and Equivalence

Analytical Test	Assessment	Analytical Test Outcome
N-terminal sequence	Identity	The expected N-terminal sequence for MON 95275-produced Vpb4Da2 protein was observed by LC-MS/MS[1]
LC-MS/MS[1]	Identity	LC-MS/MS[1] analysis of trypsin digested peptides from MON 95275-produced Vpb4Da2 protein yielded peptide masses consistent with expected peptide masses from the theoretical trypsin digest of the amino acid sequence
Western blot analysis	Identity and Equivalence	MON 95275-produced Vpb4Da2 protein identity was confirmed using a western blot probed with an antibody specific for Vpb4Da2 protein Immunoreactive properties of the MON 95275-produced Vpb4Da2 and the *E. coli*-produced Vpb4Da2 proteins were shown to be equivalent
Apparent molecular weight (MW)	Equivalence	Electrophoretic mobility and apparent molecular weight of the MON 95275-produced Vpb4Da2 and the *E. coli*-produced Vpb4Da2 proteins were shown to be equivalent
Glycosylation analysis	Equivalence	Glycosylation status of MON 95275-produced Vpb4Da2 and *E. coli*-produced Vpb4Da2 proteins were shown to be equivalent
Functional activity	Equivalence	Functional activity was shown that the *E. coli*-produced Vpb4Da2 protein is a suitable surrogate for evaluating the safety of the Vpb4Da2 protein expressed in MON 95275

[1] LC-MS/MS = liquid chromatography-tandem mass spectrometry

The details of the materials and methods for the panel of analytical tests used to evaluate and compare the properties of the MON 95275-produced Vpb4Da2 and *E. coli*-produced Vpb4Da2 proteins are described at the end of Appendix 7. A summary of the data obtained to support a conclusion of protein equivalence is provided below.

B.1(a)(ii)(ii) Results of the N-Terminal Sequencing Analysis

The expected N-terminal sequence for the Vpb4Da2 protein deduced from the *Vpb4Da2* gene present in maize of MON 95275 was observed by LC-MS/MS. The N-terminal sequence for MON 95275-produced Vpb4Da2 protein was identical with the N-terminal sequence for the *E. coli*-produced Vpb4Da2 protein observed by LC-MS/MS (Figure 24). Hence, the sequence information confirms the identity of the Vpb4Da2 protein isolated from the grain of MON 95275.

Amino Acids Residue # from the N-terminus	→	1	2	3	4	5	6	7	8	9	10	11	12	13	14	15
E.coli-produced Vpb4Da2 sequence	→	M	Q	N	I	V	S	S	K	S	E	Q	A	T	V	I
		|	|	|	|	|	|	|	|	|	|	|	|	|	|	|
Expected Vpb4Da2 Sequence	→	M	Q	N	I	V	S	S	K	S	E	Q	A	T	V	I
		|	|	|	|	|	|	|	|	|	|	|	|	|	|	|
MON 95275 Experimental Sequence	→	M	Q	N	I	V	S	S	K	S	E	Q	A	T	V	I

Figure 24. N-Terminal Sequence of the MON 95275-Produced Vpb4Da2 Protein

The experimental sequence obtained from the MON 95275-produced Vpb4Da2 was compared to the expected sequence deduced from the *vpb4Da2* gene present in MON 95275. *E. coli*-produced Vpb4Da2 protein sequence above was derived from the reference substance COA (lot 7941). The single letter International Union of Pure and Applied Chemistry - International Union of Biochemistry (IUPAC-IUB) amino acid code is M, Methionine; Q, Glutamine; N, Asparagine; I, Isoleucine; V, Valine; S, Serine; K, Lysine; E, Glutamic acid; A, Alanine; and T, Threonine;.

B.1(a)(ii)(iii) Results of Mass Fingerprint Analysis

Peptide mass fingerprint analysis is a standard technique used for confirming the identity of proteins. The identity of the MON 95275-produced Vpb4Da2 protein was confirmed by LC-MS/MS analysis of peptide fragments produced by the trypsin digestion of the MON 95275-produced Vpb4Da2 protein.

There were 121 unique peptides identified that corresponded to the masses expected to be produced by trypsin digestion of the MON 95275-produced Vpb4Da2 protein (Table 15). The identified masses were used to assemble a coverage map of the entire Vpb4Da2 protein (Figure 25, Panel A). The experimentally determined coverage of the MON 95275-produced Vpb4Da2 protein was 98% (Figure 25, Panel A, 914 out of 937 amino acids). This analysis further confirms the identity of MON 95275-produced Vpb4Da2 protein.

There were 182 unique peptides identified that corresponded to the masses expected to be produced by trypsin digestion of the *E. coli*-produced Vpb4Da2 protein (Table 16) by LC-MS/MS analysis during the protein characterization. The identified masses were used to assemble a coverage map of the entire Vpb4Da2 protein (Figure 25, Panel B). The experimentally determined coverage of

the *E. coli*-produced Vpb4Da2 protein was 99% (Figure 25, Panel B, 929 out of 937 amino acids). This analysis further confirms the identity of *E. coli*-produced Vpb4Da2 protein.

Table 15. Summary of the Tryptic Masses Identified for the MON 95275-Produced Vpb4Da2 Using LC-MS/MS[1]

Experimental Mass[2]	Calculated Mass[3]	Difference[4]	Fragment[5]	Sequence[6]
947.4754	947.4746	0.0008	1 - 8	MQNIVSSK
774.4234	774.4236	-0.0002	2 - 8	QNIVSSK
1657.8731	1657.8716	0.0015	9 - 23	SEQA...FYFK
2236.1458	2236.1416	0.0042	9 - 28	SEQA...STFK
596.2805	596.2806	-0.0001	24 - 28	DSTFK
1770.8871	1770.8862	0.0009	24 - 38	DSTF...VGEK
1192.6180	1192.6162	0.0018	29 - 38	ELMF...VGEK
705.3477	705.3479	-0.0002	39 - 44	SNLMNK
1385.7262	1385.7263	-0.0001	47 - 58	INTD...QSIR
747.3723	747.3738	-0.0015	59 - 64	WMGNLK
936.4303	936.4301	0.0002	65 - 72	SPQTGEYR
2800.4466	2800.4454	0.0012	73 - 98	LSTS...SIQK
1560.8517	1560.8511	0.0006	99 - 111	NLKL...YEIK
2122.1455	2122.1422	0.0033	99 - 115	NLKL...IEYR
1205.6292	1205.6292	0.0000	102 - 111	LEAN...YEIK
579.3021	579.3016	0.0005	112 - 115	IEYR
2321.1168	2321.1110	0.0058	116 - 135	NTSN...NAQK
742.3869	742.3861	0.0008	136 - 141	EQIPEK
1920.9905	1920.9832	0.0073	136 - 151	EQIP...FSEK
1196.6026	1196.6077	-0.0051	142 - 151	YILS...FSEK
731.3813	731.3813	0.0000	152 - 158	ANSLAEK
2490.1842	2490.1815	0.0027	152 - 172	ANSL...LFDR
3303.5505	3303.5432	0.0073	152 - 179	ANSL...NGEK
1776.8122	1776.8107	0.0015	159 - 172	ETQS...LFDR
2495.0211	2495.0105	0.0106	180 - 200	QSMS...WEEK
3119.3175	3119.3125	0.0050	180 - 205	QSMS...YTFR
1981.9204	1981.9170	0.0034	206 - 222	NQQI...EGYK
2110.0143	2110.0119	0.0024	206 - 223	NQQI...GYKK
1233.6253	1233.6254	-0.0001	223 - 232	KYVS...YHAR
1105.5304	1105.5305	-0.0001	224 - 232	YVSN...YHAR
1341.6421	1341.6452	-0.0031	233 - 243	TVKD...DFEK
2335.1459	2335.1518	-0.0059	233 - 253	TVKD...AATK
1013.4344	1013.4342	0.0002	236 - 243	DPYTDFEK
1011.5174	1011.5172	0.0002	244 - 253	VTGH...AATK
1530.7598	1530.7613	-0.0015	244 - 257	VTGH...YEAR
537.2545	537.2547	-0.0002	254 - 257	YEAR
2151.0753	2151.0670	0.0083	254 - 273	YEAR...GMEK
1631.8236	1631.8229	0.0007	258 - 273	DPLV...GMEK

Experimental Mass[2]	Calculated Mass[3]	Difference[4]	Fragment[5]	Sequence[6]
630.3487	630.3489	-0.0002	274 - 278	LHFSK
1875.8991	1875.8963	0.0028	274 - 290	LHFS...ADTK
1263.5581	1263.5579	0.0002	279 - 290	NDTV...ADTK
1909.9253	1909.9229	0.0024	279 - 296	NDTV...TTTK
449.2485	449.2486	-0.0001	293 - 296	TTTK
1941.9146	1941.9168	-0.0022	297 - 315	TDTT...FSDK
968.4961	968.4967	-0.0006	316 - 324	GFSF...ISPK
3274.4661	3274.4651	0.0010	325 - 354	YTHS...TAER
919.4870	919.4875	-0.0005	355 - 362	AYLNANVR
5266.5446	5266.5371	0.0075	363 - 412	YYNG...YPQK
927.5023	927.5025	-0.0002	413 - 421	GQAP...SLDK
1697.8941	1697.8948	-0.0007	413 - 429	GQAP...GTVK
788.4026	788.4028	-0.0002	422 - 429	ANEAGTVK
1113.6028	1113.6030	-0.0002	430 - 439	IAIN...QLDK
2895.5357	2895.5301	0.0056	430 - 455	IAIN...TQNR
1799.9397	1799.9377	0.0020	440 - 455	IQAG...TQNR
2803.4357	2803.4352	0.0005	440 - 464	IQAG...LDEK
1021.5069	1021.5080	-0.0011	456 - 464	GQYG...LDEK
2426.2196	2426.2230	-0.0034	456 - 477	GQYG...DPIR
1422.7191	1422.7256	-0.0065	465 - 477	GQVI...DPIR
3164.6500	3164.6466	0.0034	465 - 495	GQVI...GTGK
3764.9467	3764.9333	0.0134	465 - 500	GQVI...SLER
1759.9367	1759.9316	0.0051	478 - 495	TNID...GTGK
2360.2198	2360.2183	0.0015	478 - 500	TNID...SLER
618.2973	618.2973	0.0000	496 - 500	DSLER
774.3986	774.3984	0.0002	496 - 501	DSLERR
543.3492	543.3493	-0.0001	501 - 505	RVAAK
1743.8362	1743.8349	0.0013	506 - 520	NMND...ITIK
800.4643	800.4644	-0.0001	514 - 520	TPEITIK
587.3641	587.3642	-0.0001	521 - 525	EAIKK
934.4875	934.4872	0.0003	525 - 532	KAFNAQEK
1262.6377	1262.6367	0.0010	525 - 535	KAFN...KDGR
806.3933	806.3922	0.0011	526 - 532	AFNAQEK
1134.5422	1134.5418	0.0004	526 - 535	AFNA...KDGR
1115.5136	1115.5135	0.0001	536 - 544	LYYT...QGEK
3173.5329	3173.5292	0.0037	536 - 562	LYYT...ENTK
3301.6276	3301.6241	0.0035	536 - 563	LYYT...NTKK
2076.0301	2076.0263	0.0038	545 - 562	DIFI...ENTK
2204.1239	2204.1212	0.0027	545 - 563	DIFI...NTKK
673.3756	673.3759	-0.0003	563 - 567	KEIER

Experimental Mass[2]	Calculated Mass[3]	Difference[4]	Fragment[5]	Sequence[6]
545.2809	545.2809	0.0000	564 - 567	EIER
914.4639	914.4644	-0.0005	568 - 575	QLNQMPGK
723.3807	723.3803	0.0004	576 - 581	TVYDVK
919.5857	919.5855	0.0002	588 - 595	ITLHVPIK
2963.2454	2963.2450	0.0004	596 - 619	YYDF...YTGK
3091.3412	3091.3399	0.0013	596 - 620	YYDF...TGKK
2593.2603	2593.2595	0.0008	624 - 647	IGTD...YTVR
507.2806	507.2805	0.0001	648 - 651	AYVR
2461.0978	2461.0994	-0.0016	652 - 676	TAST...QGAK
460.2644	460.2646	-0.0002	681 - 685	VTGGK
774.4381	774.4388	-0.0007	681 - 687	VTGGKWK
1966.9115	1966.9101	0.0014	688 - 703	IAEF...EYFK
542.3791	542.3792	-0.0001	704 - 708	IIGLK
2070.9833	2070.9759	0.0074	709 - 726	NNGN...IEWK
845.4244	845.4243	0.0001	727 - 733	TNENLQK
973.5190	973.5192	-0.0002	727 - 734	TNENLQKK
800.4544	800.4545	-0.0001	734 - 739	KHIFEK
672.3596	672.3595	0.0001	735 - 739	HIFEK
1916.8729	1916.8727	0.0002	740 - 756	WSFG...TFTR
516.2907	516.2908	-0.0001	757 - 761	VPSSK
892.4922	892.4919	0.0003	762 - 767	IRYQWK
623.3063	623.3067	-0.0004	764 - 767	YQWK
1461.8203	1461.8191	0.0012	772 - 786	LGSI...ANGK
1617.9270	1617.9202	0.0068	772 - 787	LGSI...NGKR
2301.1510	2301.1450	0.0060	788 - 808	TVTY...VDEK
2885.4408	2885.4368	0.0040	788 - 813	TVTY...DNLK
1429.7652	1429.7664	-0.0012	814 - 826	VKVA...EIEK
1202.6019	1202.6030	-0.0011	816 - 826	VAEL...EIEK
1997.0164	1997.0139	0.0025	816 - 833	VAEL...DAHK
812.4215	812.4214	0.0001	827 - 833	VMIDAHK
2523.2152	2523.2110	0.0042	834 - 854	FSGW...SLYK
1558.7694	1558.7667	0.0027	855 - 867	LPDI...SSYK
1827.9523	1827.9519	0.0004	855 - 869	LPDI...YKIR
2321.3172	2321.3147	0.0025	874 - 893	KVQT...FNLK
2193.2195	2193.2198	-0.0003	875 - 893	VQTV...FNLK
3222.7155	3222.7077	0.0078	875 - 903	VQTV...YPTK
1047.4990	1047.4985	0.0005	894 - 903	NPNG...YPTK
2361.1598	2361.1601	-0.0003	894 - 916	NPNG...VGGK
1331.6725	1331.6721	0.0004	904 - 916	DASV...VGGK
1687.8794	1687.8781	0.0013	904 - 919	DASV...KDLK

Experimental Mass[2]	Calculated Mass[3]	Difference[4]	Fragment[5]	Sequence[6]
495.3167	495.3169	-0.0002	920 - 923	VLHK
573.3278	573.3275	0.0003	924 - 927	WIQK
1157.4680	1157.4659	0.0021	928 - 937	SDVM...QTNN

[1] All imported values were rounded to 4 decimal places.
[2] Only experimental masses that matched calculated masses with the highest scores are listed in the table.
[3] The calculated mass is the exact molecular mass calculated from the matched peptide sequence.
[4] The calculated difference = experimental mass – calculated mass.
[5] Position refers to amino acid residues within the predicted MON 95275-produced Vpb4Da2 sequence as depicted in Figure 25 panel A.
[6] For peptide matches greater than nine amino acids in length, the first 4 residues and last 4 residues are show separated by three dots (...).

Table 16. Summary of the Tryptic Masses Identified for the *E. coli*-produced Vpb4Da2 Using LC-MS/MS[1]

Experimental Mass[2]	Calculated Mass[3]	Difference[4]	Fragment[5]	Sequence[6]
905.4640	905.464	0.0000	1 - 8	MQNIVSSK
2545.3267	2545.325	0.0017	1 - 23	MQNI...FYFK
3123.6005	3123.5951	0.0054	1 - 28	MQNI...STFK
1657.8724	1657.8716	0.0008	9 - 23	SEQA...FYFK
2236.1446	2236.1416	0.0030	9 - 28	SEQA...STFK
3410.7460	3410.7472	-0.0012	9 - 38	SEQA...VGEK
596.2802	596.2806	-0.0004	24 - 28	DSTFK
1770.8868	1770.8862	0.0006	24 - 38	DSTF...VGEK
1192.6169	1192.6162	0.0007	29 - 38	ELMF...VGEK
705.3474	705.3479	-0.0005	39 - 44	SNLMNK
1612.8659	1612.8645	0.0014	45 - 58	ARIN...QSIR
1385.7268	1385.7263	0.0005	47 - 58	INTD...QSIR
2115.0895	2115.0895	0.0000	47 - 64	INTD...GNLK
3033.5075	3033.509	-0.0015	47 - 72	INTD...GEYR
747.3717	747.3738	-0.0021	59 - 64	WMGNLK
1665.7897	1665.7933	-0.0036	59 - 72	WMGN...GEYR
936.4286	936.4301	-0.0015	65 - 72	SPQTGEYR
3718.8539	3718.8649	-0.0110	65 - 98	SPQT...SIQK
2800.4432	2800.4454	-0.0022	73 - 98	LSTS...SIQK
3155.6764	3155.6673	0.0091	73 - 101	LSTS...KNLK
1560.8519	1560.8511	0.0008	99 - 111	NLKL...YEIK
2122.1425	2122.1422	0.0003	99 - 115	NLKL...IEYR
1205.6303	1205.6292	0.0011	102 - 111	LEAN...YEIK
1766.9154	1766.9202	-0.0048	102 - 115	LEAN...IEYR
579.2992	579.3016	-0.0024	112 - 115	IEYR
2321.1092	2321.111	-0.0018	116 - 135	NTSN...NAQK
3045.4837	3045.4865	-0.0028	116 - 141	NTSN...IPEK
742.3863	742.3861	0.0002	136 - 141	EQIPEK
1920.9825	1920.9832	-0.0007	136 - 151	EQIP...FSEK
1196.6090	1196.6077	0.0013	142 - 151	YILS...FSEK
3668.7834	3668.7787	0.0047	142 - 172	YILS...LFDR
731.3811	731.3813	-0.0002	152 - 158	ANSLAEK
2490.1820	2490.1815	0.0005	152 - 172	ANSL...LFDR
1776.8128	1776.8107	0.0021	159 - 172	ETQS...LFDR
2590.1639	2590.1724	-0.0085	159 - 179	ETQS...NGEK
831.3722	831.3722	0.0000	173 - 179	QQENGEK
3309.3528	3309.3561	-0.0033	173 - 200	QQEN...WEEK
3933.6506	3933.6581	-0.0075	173 - 205	QQEN...YTFR
2495.9923	2495.9945	-0.0022	180 - 200	QSMS...WEEK

Experimental Mass[2]	Calculated Mass[3]	Difference[4]	Fragment[5]	Sequence[6]
3120.2990	3120.2965	0.0025	180 - 205	QSMS...YTFR
642.3125	642.3126	-0.0001	201 - 205	GYTFR
1981.9203	1981.917	0.0033	206 - 222	NQQI...EGYK
2110.0113	2110.0119	-0.0006	206 - 223	NQQI...GYKK
3197.5241	3197.5318	-0.0077	206 - 232	NQQI...YHAR
1233.6251	1233.6254	-0.0003	223 - 232	KYVS...YHAR
1105.5321	1105.5305	0.0016	224 - 232	YVSN...YHAR
1433.7406	1433.7415	-0.0009	224 - 235	YVSN...RTVK
1341.6463	1341.6452	0.0011	233 - 243	TVKD...DFEK
2335.1538	2335.1518	0.0020	233 - 253	TVKD...AATK
1013.4334	1013.4342	-0.0008	236 - 243	DPYTDFEK
2006.9447	2006.9408	0.0039	236 - 253	DPYT...AATK
1011.5161	1011.5172	-0.0011	244 - 253	VTGH...AATK
1530.7597	1530.7613	-0.0016	244 - 257	VTGH...YEAR
3144.5734	3144.5736	-0.0002	244 - 273	VTGH...GMEK
537.2547	537.2547	0.0000	254 - 257	YEAR
2151.0667	2151.067	-0.0003	254 - 273	YEAR...GMEK
1631.8227	1631.8229	-0.0002	258 - 273	DPLV...GMEK
3489.7252	3489.7086	0.0166	258 - 290	DPLV...ADTK
630.3487	630.3489	-0.0002	274 - 278	LHFSK
1875.8952	1875.8963	-0.0011	274 - 290	LHFS...ADTK
2091.0216	2091.0233	-0.0017	274 - 292	LHFS...TKSK
1263.5586	1263.5579	0.0007	279 - 290	NDTV...ADTK
449.2488	449.2486	0.0002	293 - 296	TTTK
1941.9149	1941.9168	-0.0019	297 - 315	TDTT...FSDK
2892.4061	2892.4029	0.0032	297 - 324	TDTT...ISPK
968.4965	968.4967	-0.0002	316 - 324	GFSF...ISPK
3274.4542	3274.4651	-0.0109	325 - 354	YTHS...TAER
919.4886	919.4875	0.0011	355 - 362	AYLNANVR
5266.5324	5266.5371	-0.0047	363 - 412	YYNG...YPQK
6176.0310	6176.0291	0.0019	363 - 421	YYNG...SLDK
927.5011	927.5025	-0.0014	413 - 421	GQAP...SLDK
1697.8911	1697.8948	-0.0037	413 - 429	GQAP...GTVK
2793.4821	2793.4872	-0.0051	413 - 439	GQAP...QLDK
788.4031	788.4028	0.0003	422 - 429	ANEAGTVK
3665.9174	3665.9224	-0.0050	422 - 455	ANEA...TQNR
1113.5979	1113.603	-0.0051	430 - 439	IAIN...QLDK
2895.5299	2895.5301	-0.0002	430 - 455	IAIN...TQNR
3899.0275	3899.0276	-0.0001	430 - 464	IAIN...LDEK
1799.9387	1799.9377	0.0010	440 - 455	IQAG...TQNR

Experimental Mass[2]	Calculated Mass[3]	Difference[4]	Fragment[5]	Sequence[6]
4208.1403	4208.1502	-0.0099	440 - 477	IQAG...DPIR
1021.5086	1021.508	0.0006	456 - 464	GQYG...LDEK
2426.2220	2426.223	-0.0010	456 - 477	GQYG...DPIR
4168.1496	4168.1441	0.0055	456 - 495	GQYG...GTGK
1422.7276	1422.7256	0.0020	465 - 477	GQVI...DPIR
3164.6431	3164.6466	-0.0035	465 - 495	GQVI...GTGK
3764.9386	3764.9333	0.0053	465 - 500	GQVI...SLER
1759.9331	1759.9316	0.0015	478 - 495	TNID...GTGK
2360.2212	2360.2183	0.0029	478 - 500	TNID...SLER
2516.3085	2516.3194	-0.0109	478 - 501	TNID...LERR
618.2970	618.2973	-0.0003	496 - 500	DSLER
543.3494	543.3493	0.0001	501 - 505	RVAAK
961.3802	961.3811	-0.0009	506 - 513	NMNDPEDK
1743.8336	1743.8349	-0.0013	506 - 520	NMND...ITIK
2185.0942	2185.0936	0.0006	506 - 524	NMND...EAIK
800.4640	800.4644	-0.0004	514 - 520	TPEITIK
587.3642	587.3642	0.0000	521 - 525	EAIKK
934.4871	934.4872	-0.0001	525 - 532	KAFNAQEK
1262.6369	1262.6367	0.0002	525 - 535	KAFN...KDGR
806.3908	806.3922	-0.0014	526 - 532	AFNAQEK
1134.5426	1134.5418	0.0008	526 - 535	AFNA...KDGR
1443.6607	1443.663	-0.0023	533 - 544	DGRL...QGEK
1115.5139	1115.5135	0.0004	536 - 544	LYYT...QGEK
3173.5233	3173.5292	-0.0059	536 - 562	LYYT...ENTK
3301.6206	3301.6241	-0.0035	536 - 563	LYYT...NTKK
2076.0257	2076.0263	-0.0006	545 - 562	DIFI...ENTK
2204.1214	2204.1212	0.0002	545 - 563	DIFI...NTKK
2731.3899	2731.3916	-0.0017	545 - 567	DIFI...EIER
673.3759	673.3759	0.0000	563 - 567	KEIER
545.2809	545.2809	0.0000	564 - 567	EIER
1441.7350	1441.7347	0.0003	564 - 575	EIER...MPGK
914.4641	914.4644	-0.0003	568 - 575	QLNQMPGK
1619.8333	1619.8341	-0.0008	568 - 581	QLNQ...YDVK
723.3805	723.3803	0.0002	576 - 581	TVYDVK
490.2686	490.2686	0.0000	584 - 587	RGMK
919.5838	919.5855	-0.0017	588 - 595	ITLHVPIK
3864.8183	3864.8199	-0.0016	588 - 619	ITLH...YTGK
3992.9217	3992.9149	0.0068	588 - 620	ITLH...TGKK
2963.2459	2963.245	0.0009	596 - 619	YYDF...YTGK

Experimental Mass[2]	Calculated Mass[3]	Difference[4]	Fragment[5]	Sequence[6]
3247.4372	3247.441	-0.0038	596 - 621	YYDF...GKKR
2593.2595	2593.2595	0.0000	624 - 647	IGTD...YTVR
3082.5332	3082.5294	0.0038	624 - 651	IGTD...AYVR
5525.6103	5525.6182	-0.0079	624 - 676	IGTD...QGAK
507.2805	507.2805	0.0000	648 - 651	AYVR
2950.3659	2950.3693	-0.0034	648 - 676	AYVR...QGAK
2461.0990	2461.0994	-0.0004	652 - 676	TAST...QGAK
460.2646	460.2646	0.0000	681 - 685	VTGGK
2723.3454	2723.3384	0.0070	681 - 703	VTGG...EYFK
2805.4497	2805.453	-0.0033	686 - 708	WKIA...IGLK
1966.9106	1966.9101	0.0005	688 - 703	IAEF...EYFK
4544.2404	4544.2441	-0.0037	688 - 726	IAEF...IEWK
542.3794	542.3792	0.0002	704 - 708	IIGLK
2070.9725	2070.9759	-0.0034	709 - 726	NNGN...IEWK
2898.3874	2898.3896	-0.0022	709 - 733	NNGN...NLQK
845.4244	845.4243	0.0001	727 - 733	TNENLQK
973.5193	973.5192	0.0001	727 - 734	TNENLQKK
800.4541	800.4545	-0.0004	734 - 739	KHIFEK
672.3592	672.3595	-0.0003	735 - 739	HIFEK
2571.2206	2571.2216	-0.0010	735 - 756	HIFE...TFTR
3069.4945	3069.5018	-0.0073	735 - 761	HIFE...PSSK
1916.8727	1916.8727	0.0000	740 - 756	WSFG...TFTR
2415.1514	2415.1529	-0.0015	740 - 761	WSFG...PSSK
2684.3349	2684.3381	-0.0032	740 - 763	WSFG...SKIR
516.2909	516.2908	0.0001	757 - 761	VPSSK
892.4929	892.4919	0.0010	762 - 767	IRYQWK
623.3066	623.3067	-0.0001	764 - 767	YQWK
1902.0661	1902.0687	-0.0026	768 - 786	INGR...ANGK
1461.8144	1461.8191	-0.0047	772 - 786	LGSI...ANGK
1617.9233	1617.9202	0.0031	772 - 787	LGSI...NGKR
3901.0549	3901.0547	0.0002	772 - 808	LGSI...VDEK
2457.2569	2457.2461	0.0108	787 - 808	RTVT...VDEK
3041.5318	3041.5379	-0.0061	787 - 813	RTVT...DNLK
2301.1461	2301.145	0.0011	788 - 808	TVTY...VDEK
2885.4369	2885.4368	0.0001	788 - 813	TVTY...DNLK
3112.6001	3112.6002	-0.0001	788 - 815	TVTY...LKVK
602.3030	602.3024	0.0006	809 - 813	NDNLK
1429.7672	1429.7664	0.0008	814 - 826	VKVA...EIEK
1202.6043	1202.603	0.0013	816 - 826	VAEL...EIEK

Experimental Mass[2]	Calculated Mass[3]	Difference[4]	Fragment[5]	Sequence[6]
1997.0152	1997.0139	0.0013	816 - 833	VAEL...DAHK
4502.2179	4502.2144	0.0035	816 - 854	VAEL...SLYK
812.4210	812.4214	-0.0004	827 - 833	VMIDAHK
3317.6204	3317.6219	-0.0015	827 - 854	VMID...SLYK
4858.3785	4858.3781	0.0004	827 - 867	VMID...SSYK
2523.2066	2523.211	-0.0044	834 - 854	FSGW...SLYK
4063.9693	4063.9672	0.0021	834 - 867	FSGW...SSYK
1558.7672	1558.7667	0.0005	855 - 867	LPDI...SSYK
1827.9525	1827.9519	0.0006	855 - 869	LPDI...YKIR
416.2384	416.2383	0.0001	870 - 873	VNGK
2321.3192	2321.3147	0.0045	874 - 893	KVQT...FNLK
3350.7861	3350.8027	-0.0166	874 - 903	KVQT...YPTK
2193.2242	2193.2198	0.0044	875 - 893	VQTV...FNLK
3222.7150	3222.7077	0.0073	875 - 903	VQTV...YPTK
1047.4979	1047.4985	-0.0006	894 - 903	NPNG...YPTK
2361.1596	2361.1601	-0.0005	894 - 916	NPNG...VGGK
1331.6731	1331.6721	0.0010	904 - 916	DASV...VGGK
1687.8805	1687.8781	0.0024	904 - 919	DASV...KDLK
2165.1883	2165.1844	0.0039	904 - 923	DASV...VLHK
851.5224	851.5229	-0.0005	917 - 923	DLKVLHK
495.3170	495.3169	0.0001	920 - 923	VLHK
2190.0891	2190.0892	-0.0001	920 - 937	VLHK...QTNN
573.3277	573.3275	0.0002	924 - 927	WIQK
1712.7827	1712.7828	-0.0001	924 - 937	WIQK...QTNN
1157.4656	1157.4659	-0.0003	928 - 937	SDVM...QTNN

[1] All imported values were rounded to 4 decimal places.
[2] Only experimental masses that matched calculated masses with the highest scores are listed in table.
[3] The calculated mass is the exact molecular mass calculated from the matched peptide sequence.
[4] The calculated difference = experimental mass – calculated mass.
[5] Position refers to amino acid residues within the predicted *E. coli*-produced Vpb4Da2 sequence as depicted in Figure 25, panel B.
[6] For peptide matches greater than nine amino acids in length the first 4 residues and last 4 residues are shown separated by dots (…).

(A)

```
1    MQNIVSSKSE QATVIGLVGF YFKDSTFKEL MFIQVGEKSN LMNKARINTD

51   AQQIQSIRWM GNLKSPQTGE YRLSTSSDEN VILQINGETV INQASIQKNL

101  KLEANQVYEI KIEYRNTSNT LPDLQLFWSM NNAQKEQIPE KYILSPNFSE

151  KANSLAEKET QSFFPNYNLF DRQQENGEKQ SMSTPVDTDN DCIPDEWEEK

201  GYTFRNQQIV PWNDAYSAEG YKKYVSNPYH ARTVKDPYTD FEKVTGHMPA

251  ATKYEARDPL VAAYPSVGVG MEKLHFSKND TVTEGNADTK SKTTTKTDTT

301  TNTVEIGGSL GFSDKGFSFS ISPKYTHSWS SSTSVADTDS TTWSSQIGIN

351  TAERAYLNAN VRYYNGGTAP IYDLKPTTNF VFQNSGDSIT TITAGPNQIG

401  NSLGAGDTYP QKGQAPISLD KANEAGTVKI AINAEQLDKI QAGTEILNIE

451  TTQNRGQYGI LDEKGQVIPG GEWDPIRTNI DAVSGSLTLN LGTGKDSLER

501  RVAAKNMNDP EDKTPEITIK EAIKKAFNAQ EKDGRLYYTD QGEKDIFIDE

551  PSINLITDEN TKKEIERQLN QMPGKTVYDV KWKRGMKITL HVPIKYYDFE

601  TSENLWYYTY QESGGYTGKK RGRIGTDGHG TAMSNPQLKP YTSYTVRAYV

651  RTASTTGSNE VVFYADNSSG NGQGAKVSGK VTGGKWKIAE FSFNTFNNPE

701  YFKIIGLKNN GNANLHFDDV SVIEWKTNEN LQKKHIFEKW SFGSNDEMVI

751  GATFTRVPSS KIRYQWKING RLGSIIPAPP LDANGKRTVT YGSITAITPM

801  ELYAVDEKND NLKVKVAELG ESEIEKVMID AHKFSGWWYL SENPNLYSGL

851  SLYKLPDIFY NNVSSYKIRV NGKKVQTVSK PSPFLFQITF NLKNPNGGTY

901  PTKDASVELW ATVGGKDLKV LHKWIQKSDV MYSQTNN
```

(B)

1 MQNIVSSKSE QATVIGLVGF YFKDSTFKEL MFIQVGEKSN LMNKARINTD

51 AQQIQSIRWM GNLKSPQTGE YRLSTSSDEN VILQINGETV INQASIQKNL

101 KLEANQVYEI KIEYRNTSNT LPDLQLFWSM NNAQKEQIPE KYILSPNFSE

151 KANSLAEKET QSFFPNYNLF DRQQENGEKQ SMSTPVDTDN DCIPDEWEEK

201 GYTFRNQQIV PWNDAYSAEG YKKYVSNPYH ARTVKDPYTD FEKVTGHMPA

251 ATKYEARDPL VAAYPSVGVG MEKLHFSKND TVTEGNADTK SKTTTKTDTT

301 TNTVEIGGSL GFSDKGFSFS ISPKYTHSWS SSTSVADTDS TTWSSQIGIN

351 TAERAYLNAN VRYYNGGTAP IYDLKPTTNF VFQNSGDSIT TITAGPNQIG

401 NSLGAGDTYP QKGQAPISLD KANEAGTVKI AINAEQLDKI QAGTEILNIE

451 TTQNRGQYGI LDEKGQVIPG GEWDPIRTNI DAVSGSLTLN LGTGKDSLER

501 RVAAKNMNDP EDKTPEITIK EAIKKAFNAQ EKDGRLYYTD QGEKDIFIDE

551 PSINLITDEN TKKEIERQLN QMPGKTVYDV KWKRGMKITL HVPIKYYDFE

601 TSENLWYYTY QESGGYTGKK RGRIGTDGHG TAMSNPQLKP YTSYTVRAYV

651 RTASTTGSNE VVFYADNSSG NGQGAKVSGK VTGGKWKIAE FSFNTFNNPE

701 YFKIIGLKNN GNANLHFDDV SVIEWKTNEN LQKKHIFEKW SFGSNDEMVI

751 GATFTRVPSS KIRYQWKING RLGSIIPAPP LDANGKRTVT YGSITAITPM

801 ELYAVDEKND NLKVKVAELG ESEIEKVMID AHKFSGWWYL SENPNLYSGL

851 SLYKLPDIFY NNVSSYKIRV NGKKVQTVSK PSPFLFQITF NLKNPNGGTY

901 PTKDASVELW ATVGGKDLKV LHKWIQKSDV MYSQTNN

Figure 25. Peptide Map of the MON 95275-Produced Vpb4Da2 and *E. coli*-Produced Vpb4Da2

(A). The amino acid sequence of the MON 95275-produced Vpb4Da2 protein was deduced from the *vpb4Da2* gene present in MON 95275. Boxed regions correspond to peptides that were identified from the MON 95275-produced Vpb4Da2 protein sample using LC-MS/MS. In total, 98% coverage (914 out of 937 amino acids) of the expected protein sequence was covered by the identified peptides.

(B). The amino acid sequence of the *E. coli*-produced Vpb4Da2 protein was deduced from the *vpb4Da2* gene that is contained on the expression plasmid pMON420664. Boxed regions correspond to peptides that were identified from the *E. coli*-produced Vpb4Da2 protein sample using LC-MS/MS. In total, 99% coverage (929 out of 937 amino acids) of the expected protein sequence was covered by the identified peptides.

B.1(a)(ii)(iv) Results of Western Blot Analysis of the Vpb4Da2 Protein Isolated from the Grain of MON 95275 and Immunoreactivity Comparison to *E. coli*-produced Vpb4Da2 Protein

Western blot analysis was conducted using mouse anti-Vpb4Da2 monoclonal antibody as additional means to confirm the identity of the Vpb4Da2 protein isolated from the grain of MON 95275 and to assess the equivalence of the immunoreactivity of the MON 95275-produced and *E. coli*-produced Vpb4Da2 proteins.

The results showed that immunoreactive bands with the same electrophoretic mobility were present in all lanes loaded with the MON 95275-produced and *E. coli*-produced Vpb4Da2 proteins (Figure 26). For each amount loaded, comparable signal intensity was observed between the MON 95275-produced and *E. coli*-produced Vpb4Da2 protein bands. As expected, the signal intensity increased with increasing load amounts of the MON 95275-produced and *E. coli*-produced Vpb4Da2 proteins, thus supporting identification of MON 95275-produced Vpb4Da2 protein.

To compare the immunoreactivity of the MON 95275-produced and *E. coli*-produced Vpb4Da2 proteins, densitometric analysis was conducted on the bands that migrated at the expected apparent MW for the intact Vpb4Da2 protein (~ 103.8 kDa) in the test substance and for both the intact Vpb4Da2 protein (~ 103.8 kDa) and a minor band (~90 kDa) for reference substance. The additional minor immunoreactive band observed (~90 kDa) in the reference substance was included in the immunoreactivity analysis because it likely represents a minor amount of degraded Vpb4Da2 protein that resulted from exposure to proteases present in *E. coli* during expression and purification. The signal intensity (reported in OD) of the expected bands(s) at ~103.8 kDa in lanes loaded with MON 95275-produced and at ~103.8 and ~90 kDa in lanes loaded with *E. coli*-produced Vpb4Da2 proteins were measured (Table 17). Because the mean signal intensity of the MON 95275-produced Vpb4Da2 protein was within 35% of the mean signal intensity of the *E. coli*-produced Vpb4Da2 protein, the MON 95275-produced Vpb4Da2 and *E. coli*-produced Vpb4Da2 proteins were determined to have equivalent immunoreactivity.

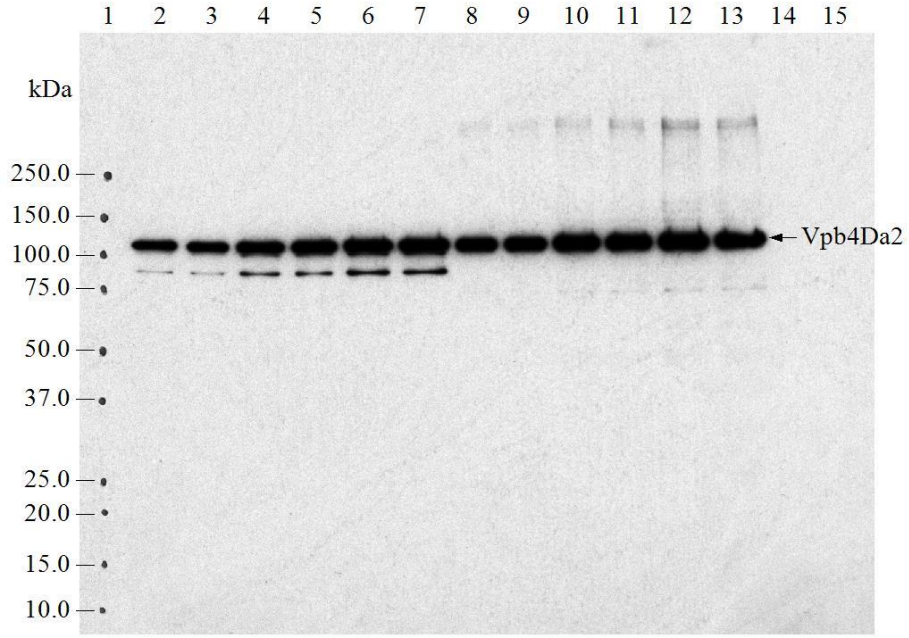

Figure 26. Western Blot Analysis and Immunoreactivity of MON 95275-Produced and *E. coli*-Produced Vpb4Da2 Proteins

Aliquots of the MON 95275-produced and *E. coli*-produced Vpb4Da2 proteins were subjected to SDS-PAGE and electrotransferred to a nitrocellulose membrane. Proteins were detected using mouse anti-Vpb4Da2 monoclonal antibodies as the primary antibodies. Immunoreactive bands were visualized using HRP-conjugated secondary antibodies and an ECL system. The 20-second exposure is shown. The approximate MW (kDa) of the standards are shown on the left. Lane designations are as follows:

Lane	Sample	Amount (ng)
1	Precision Plus Protein™ Standards	-
2	*E. coli*-produced Vpb4Da2	5
3	*E. coli*-produced Vpb4Da2	5
4	*E. coli*-produced Vpb4Da2	10
5	*E. coli*-produced Vpb4Da2	10
6	*E. coli*-produced Vpb4Da2	15
7	*E. coli*-produced Vpb4Da2	15
8	MON 95275-produced Vpb4Da2	5
9	MON 95275-produced Vpb4Da2	5
10	MON 95275-produced Vpb4Da2	10
11	MON 95275-produced Vpb4Da2	10
12	MON 95275-produced Vpb4Da2	15
13	MON 95275-produced Vpb4Da2	15
14	Blank	-
15	Blank	-

Table 17. Immunoreactivity of the MON 95275-Produced and *E. coli*-Produced Vpb4Da2 Proteins

Mean Signal Intensity from MON 95275-Produced Vpb4Da2 [1] (OD)	Mean Signal Intensity from *E. coli*-Produced Vpb4Da2 [1] (OD)	Acceptance Limits[2] (OD)
11,593.20	9,685.78	6,295.76 – 13,075.80

[1] Each value represents the mean of six values (n = 6).

[2] The acceptance limits are for the MON 95275-produced Vpb4Da2 protein and are based on the interval between -35% (9685.78 x 0.65 = 6295.76) and +35 % (9685.78 x 1.35 = 13075.80) of the mean of the *E. coli*-produced Vpb4Da2 signal intensity across all loads.

B.1(a)(ii)(v) Results of the Vpb4Da2 Protein Molecular Weights and Purity Analysis

For apparent MW and purity determination, the MON 95275-produced Vpb4Da2 and the *E. coli*-produced Vpb4Da2 proteins were subjected to SDS-PAGE. Following electrophoresis, the gel was stained with Brilliant Blue G-Colloidal stain and analyzed by densitometry. The MON 95275-produced Vpb4Da2 protein (Figure 27, lanes 3-8) migrated to the same position on the gel as the *E. coli*-produced Vpb4Da2 protein (Figure 27, lane 2) and the apparent MW was calculated to be 104.9 kDa (Table 18). Because the experimentally determined apparent MW of the MON 95275-produced Vpb4Da2 protein was within the acceptance limits for equivalence (Table 18), the MON 95275-produced Vpb4Da2 and *E. coli*-produced Vpb4Da2 proteins were determined to have equivalent apparent molecular weights (Table 19).

The purity of the MON 95275-produced Vpb4Da2 protein was calculated based on the six lanes loaded on the gel (Figure 27, lanes 3-8). The average purity was determined to be 26% (Table 18).

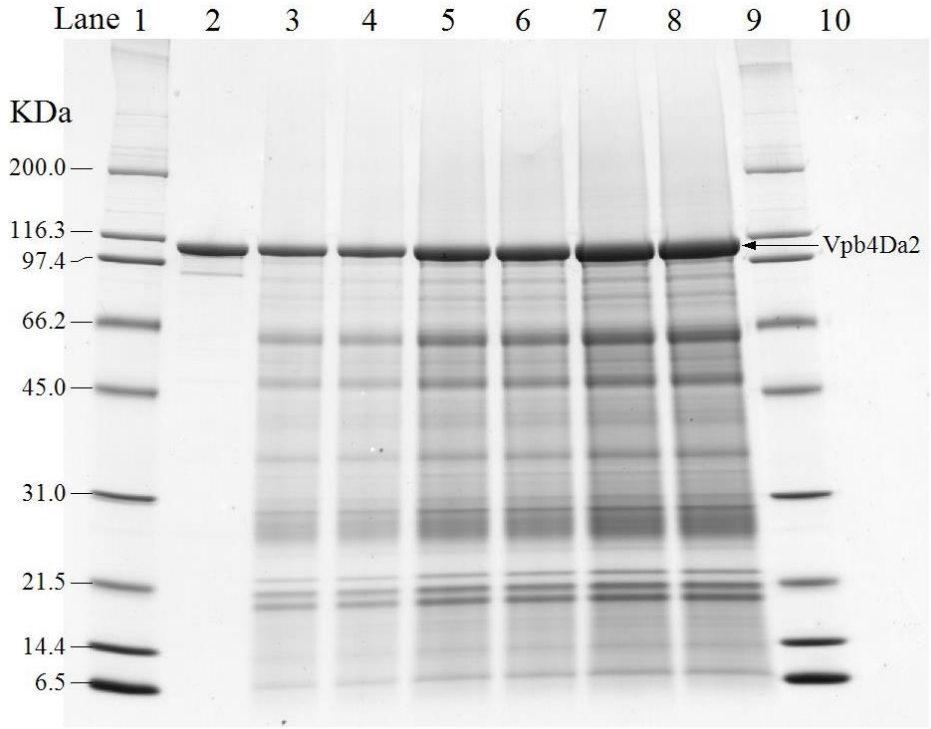

Figure 27. Purity and Apparent Molecular Weight Analysis of the MON 95275-Produced Vpb4Da2 Protein

Aliquots of the MON 95275-produced and the *E. coli*-produced Vpb4Da2 proteins were subjected to SDS-PAGE and the gel was stained with Brilliant Blue G-Colloidal stain. The MWs (kDa) are shown on the left and correspond to the standards loaded in lanes 1 and 9. The Vpb4Da2 protein is indicated with an arrow in the image. Lane designations are as follows:

Lane	Sample	Amount* (µg)
1	Broad Range MW Standard	5.0
2	*E. coli*-produced Vpb4Da2	1.0
3	MON 95275-produced Vpb4Da2	0.35
4	MON 95275-produced Vpb4Da2	0.35
5	MON 95275-produced Vpb4Da2	0.70
6	MON 95275-produced Vpb4Da2	0.70
7	MON 95275-produced Vpb4Da2	1.05
8	MON 95275-produced Vpb4Da2	1.05
9	Broad Range MW Standard	5.0
10	Blank	-

*Amounts of proteins loaded for Broad Range MW standard and *E. coli*-produced Vpb4Da2 are total protein and amount of proteins loaded for MON 95275-produced Vpb4Da2 is purity-corrected protein.

Table 18. Apparent Molecular Weight and Purity Analysis of the MON 95275-Produced Vpb4Da2 Protein

	Apparent MW[1] (kDa)	Purity[2] (%)
Average (n=6)	104.9	26

[1]Final MW was rounded to one decimal place.
[2]Average % purity was rounded to the nearest whole number.

Table 19. Apparent Molecular Weight Comparison Between the MON 95275-Produced Vpb4Da2 and *E. coli*-Produced Vpb4Da2 Proteins

Apparent MW of MON 95275-Produced Vpb4Da2 Protein (kDa)	Apparent MW of *E. coli*-Produced Vpb4Da2 Protein[1] (kDa)	Acceptance Limits[2] (kDa)
104.9	103.8	97.9 – 108.6

[1] As report on COA of the *E. coli*-produced Vpb4Da2 protein.
[2] Data obtained for the *E. coli*-produced Vpb4Da2 protein was used to generate the prediction interval (Appendix 7).

B.1(a)(ii)(vi) Vpb4Da2 Glycosylation Analysis

Some eukaryotic proteins are post-translationally modified by the addition of carbohydrate moieties (Rademacher *et al.*, 1988). To test whether the Vpb4Da2 protein was glycosylated when expressed in the maize grain of MON 95275, the MON 95275-produced Vpb4Da2 protein was analyzed using an ECL™ glycoprotein detection method. Transferrin, a glycosylated protein, was used as a positive control in the assay. To assess equivalence of the MON 95275-produced and *E. coli*-produced Vpb4Da2 proteins, the *E. coli*-produced Vpb4Da2 protein was also analyzed.

A clear glycosylation signal was observed at the expected molecular weight (~80 kDa) in the lanes containing the positive control (transferrin) and the band intensity increased with increasing concentration (Figure 28, Panel A). In contrast, no glycosylation signal was observed at the expected molecular weight in the lanes containing the *E. coli*-produced Vpb4Da2 protein or MON 95275-produced Vpb4Da2 protein (Figure 28, Panel A).

To confirm that MON 95275-produced Vpb4Da2 and *E. coli*-produced Vpb4Da2 proteins were appropriately loaded for glycosylation analysis, a second membrane with identical loadings and transfer time was stained with Coomassie Blue R250 for protein detection. Both the MON 95275-produced and *E. coli*-produced Vpb4Da2 proteins were detected (Figure 28, Panel B). These data indicate that the glycosylation status of MON 95275-produced Vpb4Da2 protein is equivalent to that of the *E. coli*-produced Vpb4Da2 protein and that neither is glycosylated.

A. B.

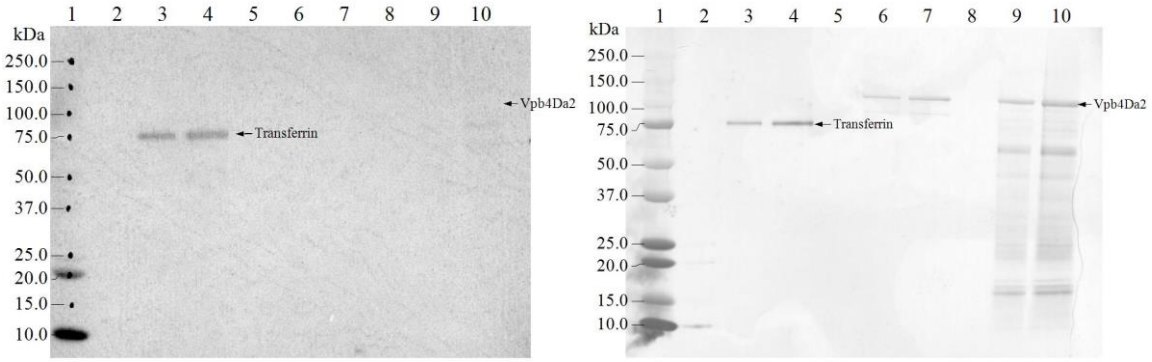

Figure 28. Glycosylation Analysis of the MON 95275-Produced and *E. coli*-Produced Vpb4Da2 Proteins

Aliquots of the transferrin (positive control), *E. coli*-produced Vpb4Da2 and MON 95275-produced Vpb4Da2 proteins were subjected to SDS-PAGE and electrotransferred to a PVDF membrane. The MWs (kDa) correspond to the Precision Plus Protein™ Standards. The arrows show the expected migration of the MON 95275 -produced and *E. coli*-produced Vpb4Da2 proteins and transferrin. (A) Where present, the labeled carbohydrate moieties were detected by using ECL reagents and exposure to Hyperfilm®. The 20-minute exposure is shown. (B) An equivalent blot was stained with Coomassie Blue R250 to confirm the presence of proteins. Lane designations are as follows:

Lane	Sample	Amount (ng)
1	Precision Plus Protein™ Standards	-
2	Blank	-
3	Transferrin (positive control)	100
4	Transferrin (positive control)	200
5	Blank	-
6	*E. coli*-produced Vpb4Da2	100
7	*E. coli*-produced Vpb4Da2	200
8	Blank	-
9	MON 95275-produced Vpb4Da2	100
10	MON 95275-produced Vpb4Da2	200

B.1(a)(ii)(vii) Vpb4Da2 Functional Activity

The MON 95275-produced Vpb4Da2 and *E. coli*-produced Vpb4Da2 proteins were considered to have equivalent functional activity if the biological activity of both proteins (EC_{50}) meets one of criteria[8].

The mean EC_{50} values based upon the purity-correct concentrations of MON 95275-produced and *E. coli*-produced Vpb4Da2 proteins were 12.3 and 6.1 µg of Vpb4Da2 protein/ml diet, respectively (Table 20). The functional activity of MON 95275-produced Vpb4Da2 protein was significantly different from the *E. coli*-produced Vpb4Da2 protein (two-sided t-test p=0.0024 at a=0.05). In addition, the functional activity of the MON 95275-produced Vpb4Da2 protein did not fall within the 95% and 99% prediction intervals derived from the reference substance (Table 20). These results indicate that the test substance, MON 95275 produced Vpb4Da2 has lower functional activity (i.e., higher EC_{50} value) than the *E. coli*-produced Vpb4Da2 protein. The lower functional activity of the MON 95275-produced Vpb4Da2 as compared to the *E. coli*-produced Vpb4Da2 observed in this assessment is likely due to a combination of effects including differences in the matrices each protein was purified from and differences in the methods required to isolate or purify each protein (Raybould *et al.*, 2013).

Table 20. Functional Activity (EC_{50}) of MON 95275-Produced and *E. coli*-Produced Vpb4Da2 Proteins

Replicates	MON 95275-Produced Vpb4Da2 [1, 6] (µg protein/mL diet)	*E. coli*-Produced Vpb4Da2 [1, 6] (µg protein/ml diet)	t-test[2] (p-value)	95% Prediction Intervals[3,4] (µg protein/ml diet)	99% Prediction Intervals[3,5] (µg protein/ml diet)
1	14	5.6	0.0024	2.65 to 8.53	2.00 to 11.29
2	11	6.4			
3	12	6.3			
Mean	12.3	6.1	-	-	-

[1] Value refers to mean calculated based on three independent assays (n=3).
[2] Significant difference is based on two sided t-test α=0.05.
[3] Data obtained for the *E. coli*-produced Vpb4Da2 protein were used to generate a prediction interval for setting the acceptance limits for EC50 values of 3 future independent assays (Appendix 7).
[4] Lower and upper acceptance limits for 95% prediction interval.
[5] Lower and upper acceptance limits for 99% prediction interval.
[6] the purity-corrected *E.coli*-produced and MON 95275-prodcued proteins were used for functional activity measurement.

[8] The equivalence of the test and reference substances will be determined by a stepwise procedure. 1) the biological activity (EC50) from the test and reference substances will be compared using a t-test and to evaluate if a significant difference in activity is observed. 2) the biological activity of the test substance is within the upper and lower limits of the 95% prediction interval derived from data of the reference substance. 3) the biological activity of the test substance is within the upper and lower limits of the 99% prediction interval derived from data of the reference substance.

B.1(a)(ii)(viii) Vpb4Da2 Protein Identity and Equivalence Conclusion

The MON 95275-produced Vpb4Da2 protein purified from MON 95275 grain was characterized, and a comparison of the physicochemical and functional properties between the MON 95275-produced and the *E. coli*-produced Vpb4Da2 proteins was conducted following a panel of analytical tests: 1) N-terminal sequence analysis established the same identity for the MON 95275-produced and the *E. coli*-produced Vpb4Da2 proteins; 2) LC-MS/MS analysis yielded peptide masses consistent with the expected peptide masses from the theoretical trypsin digest of the *vpb4Da2* gene product present in MON 95275; 3) the MON 95275-produced and the *E. coli*-produced Vpb4Da2 proteins were both detected on a western blot probed with an antibody specific for Vpb4Da2 protein and the immunoreactive properties of both proteins was shown to be equivalent; 4) the electrophoretic mobility and apparent molecular weight of the MON 95275-produced and the *E. coli*-produced Vpb4Da2 proteins were shown to be equivalent; 5) the glycosylation status of MON 95275-produced and the *E. coli*-produced Vpb4Da2 proteins was determined to be equivalent and not glycosylated; and 6) the functional activity of the MON 95275-produced and the *E. coli-produced* Vpb4Da2 proteins was determined and the results indicate they are not equivalent, with the *E. coli-produced* Vpb4Da2 protein displaying a high potency than the MON 95275-produced Vpb4Da2 protein. However, because the overall weight of evidence supports equivalency between the MON 95275-produced and the *E. coli*-produced Vpb4Da2 proteins, and because the *E. coli*-produced Vpb4Da2 protein represents a more conservative test substance for evaluating protein safety due to its increased biological potency relative to the MON 95275-produced Vpb4Da2 protein, the *E. coli*-produced Vpb4Da2 protein was determined to be a suitable surrogate for evaluating the safety of the Vpb4Da2 protein expressed in MON 95275. These results support the use of the *E. coli*-produced MON 95275 protein to evaluate the safety of the Vpb4Da2 protein expressed in MON 95275.

The ability of the Vpb4Da2 to bind to its target receptor is dependent on the conformation of the Vpb4Da2 receptor binding domain. Protein structure, or conformation, is determined by the primary amino acid sequence that comprises the different structural and functional motifs. It can be inferred that once properly folded, proteins that possess the same amino acid sequences would have equivalent functional activity or receptor binding. The MON 95275- and *E. coli*-produced Vpb4Da2 proteins possess the same amino sequences, and thereby equivalent receptor binding domains, as evidenced by the amino acid sequence identity seen by mass fingerprint analysis where >98% coverage was detected. The identity of the protein sequences was also confirmed through sequencing the genes of the expressed MON 95275- and *E. coli*-produced Vpb4Da2 proteins. Finally, although a difference in biological potency was observed between the MON 95275- and *E. coli*-produced Vpb4Da2 proteins, the observed functional activity of each indicates that the functional structure of the receptor binding domains in both proteins is similar.

Taken together, the characterization data provided in support of MON 95275 Vpb4Da2 confirms that the *E. coli*-produced Vpb4Da2 protein is a suitable surrogate for use in the evaluation of the safety of the MON 95275-produced Vpb4Da2 protein.

B.1(a)(iii) Expression Levels of Mpp75Aa1.1 and Vpb4Da2 Proteins in MON 95275

Mpp75Aa1.1 and Vpb4Da2 protein levels determined in MON 95275 are used to assess potential exposure to the introduced proteins via food or feed ingestion or potential environmental exposure. To support environmental exposure scenarios, the most appropriate tissues to evaluate Mpp75Aa1.1 and Vpb4Da2 protein levels are leaf [over season leaf], root [over season root], pollen, forage and grain tissue samples. Expression levels of the introduced proteins were determined in forage and grain tissue to evaluate food and feed exposure of each protein to humans and mammals. The expression levels of the Mpp75Aa1.1 and Vpb4Da2 proteins in various tissues of MON 95275 relevant to the characterization and environmental assessment were determined by a validated enzyme-linked immunosorbent assay (ELISA) as part of the characterization of MON 95275 (Appendix 8).

Tissues of MON 95275 were collected from four replicate plots planted in a randomized complete block design during the 2019 growing season from five field sites in the United States that were representative of maize-producing regions.

B.1(a)(iii)(i) Expression Levels of Mpp75Aa1.1 Protein

The expression levels of Mpp75Aa1.1 in MON 95275 maize were determined and reported on a dry weight basis and are summarized in Table 21. Dry weight (dw) values were converted to a µg/g fresh weight (fw) using a moisture conversion factor. The mean Mpp75Aa1.1 protein expression level in MON 95275 across all sites was highest in leaf at 100 µg/g dw and lowest in pollen at <LOQ (0.125 µg/g dw). The mean Mpp75Aa1.1 protein level in MON 95275 was 1.3 µg/g dw in grain.

For details please refer to Appendix 8 ([redacted]2021(TRR0000722)).

Table 21. Summary of Mpp75Aa1.1 Protein Levels in Maize Tissues Collected from MON 95275 Produced from Five U.S Field Trial sites in 2019

Tissue Type[1]	Development Stage[2]	Mean (SE) Range (µg/g fw) [3]	Mean (SE) Range (µg/g dw)[4]	LOQ/LOD (µg/g dw)[5]
OSL	V2-V4	15 (1.1) 6.5 – 31	100 (7.0) 43 – 200	0.125/0.023
OSR	V2-V4	3.8 (0.48) 1.2 – 9.3	35 (4.3) 11 – 84	0.125/0.053
Forage	R5	4.9 (0.23) 3.5 – 7.5	16 (0.76) 12 – 25	0.125/0.039
Grain	R6	1.1 (0.076) 0.59 – 1.7	1.3 (0.086) 0.67 – 1.9	0.125/0.065
Pollen	VT-R1	<LOQ (NA[6]) NA – NA	<LOQ (NA) NA – NA	0.125/0.043

[1] OSL = over season leaf, OSR = over season root

[2] The crop development stage at which each tissue was collected.

[3] Protein levels are expressed as the arithmetic mean and standard error (SE) as microgram (µg) of protein per gram (g) of tissue converted from a dry weight (dw) to a fresh weight basis (fw). The means, SE, and ranges (minimum and maximum values) were calculated for each tissue across all five sites (n=20).

[4] Protein levels are expressed as the arithmetic mean and standard error (SE) as microgram (µg) of protein per gram (g) of tissue on a dry weight basis (dw).

[5] LOQ=limit of quantitation. LOD=limit of detection.

[6] NA=Not Applicable.

B.1(a)(iii)(ii) Expression levels of Vpb4Da2 Protein

The results obtained from the ELISA are summarized in Table 22 and the details of the materials and methods are described in Appendix 8. The expression levels of Vpb4Da2 in MON 95275 maize were determined and reported on a dry weight basis. Dry weight (dw) values were converted to a µg/g fresh weight (fw) using a moisture conversion factor. The mean Vpb4Da2 protein expression level in MON 95275 across all sites was highest in leaf at 39 µg/g dw and lowest in pollen at <LOQ (0.157 µg/g dw). The mean Vpb4Da2 protein level in MON 95275 was 1.2 µg/g dw in grain.

For details please refer to Appendix 8 [redacted] 2021 (TRR000072)).

Table 22. Summary of Vpb4Da2 Protein Levels in Maize Tissues Collected from MON 95275 Produced from Five U.S. Field Trial Sites in 2019

Tissue Type[1]	Development Stage[2]	Mean (SE) Range (µg/g fw)[3]	Mean (SE) Range (µg/g dw)[4]	LOQ/LOD (µg/g dw)[5]
OSL	V2-V4	5.9 (0.27) 2.8 – 7.6	39 (1.8) 19 – 51	0.313/0.110
OSR	V2-V4	1.5 (0.15) 0.38 – 2.9	14 (1.3) 3.4 – 26	0.313/0.128
Forage	R5	1.0 (0.040) 0.75 – 1.4	3.3 (0.13) 2.5 – 4.8	0.313/0.124
Grain	R6	1.0 (0.076) 0.37– 1.6	1.2 (0.086) 0.42 – 1.9	0.157/0.067
Pollen	VT-R1	<LOQ (NA[6]) NA – NA	<LOQ (NA) NA – NA	0.157/0.082

[1] OSL = over season leaf, OSR = over season root
[2] The crop development stage at which each tissue was collected.
[3] Protein levels are expressed as the arithmetic mean and standard error (SE) as microgram (µg) of protein per gram (g) of tissue converted from a dry weight (dw) to a fresh weight basis (fw). The means, SE, and ranges (minimum and maximum values) were calculated for each tissue across all five sites (n=20)
[4] Protein levels are expressed as the arithmetic mean and standard error (SE) as microgram (µg) of protein per gram (g) of tissue on a dry weight basis (dw).
[5] LOQ=limit of quantitation. LOD=limit of detection.
[6] NA=Not Applicable.

B.1(b) Information about prior history of human consumption of the new substances, if any, or their similarity to substances previously consume in food.

Refer to Section A.2(a)(i).

B.1(c) Information on whether any new protein has undergone any unexpected post-translational modification in the new host

Refer to Section B.1(a)(i)(vi) and Section B.1(a)(ii)(vi).

B.1(d) Where any ORFs have been identified, bioinformatics analysis to indicate the potential for allergenicty and toxicity of the ORFs

Refer to Section A.3(c)(v).

B.2. New Proteins

B.2(a) Information on the potential toxicity of any new proteins, including:

B.2(a)(i) A bioinformatic comparison of the amino acid sequence of each of the new proteins to know protein toxins and anti-nutrients (e.g. protease inhibitors, lectins)

Potential structural similarities shared between the MON 95275 Mpp75Aa1.1 and Vpb4Da2 proteins with sequences in a protein database were evaluated using the FASTA sequence alignment tool. The FASTA program directly compares amino acid sequences (*i.e.*, primary, linear protein structure) and the alignment data may be used to infer shared higher order structural similarities between two sequences (*i.e.*, secondary and tertiary protein structures). Proteins that share a high degree of similarity throughout the entire sequence are often homologous. Homologous proteins often have common secondary structures, common three-dimensional configuration, and, consequently, may share similar functions (Caetano-Anollés *et al.*, 2009; Illergård *et al.*, 2009).

FASTA bioinformatic alignment searches using the Mpp75Aa1.1 and Vpb4Da2 amino acid sequences were performed with a toxin database to identify possible homology with proteins that may be harmful to the health of humans or other animals. When searching the TOX_2021 database, Mpp75Aa1.1 and Vpb4Da2 each returned a single alignment below the significance threshold[9]. Further inspection of each alignment revealed homology to broad families of β-pore forming proteins including epsilon toxins. The results of the TOX_2021 search do not provide any additional information to indicate Mpp75Aa1.1 and Vpb4Da2 could display toxicity towards organisms other than the intended insect pests. To further understand the implications of these results, a structural, domain-based approach for each protein was taken for each protein to illustrate their specificity (Moar *et al.*, 2017b).

B.2(a)(i)(i) Mpp75Aa1.1

Mpp75Aa1.1 is a member of the ETX_MTX2 β-PFP family. Therefore, it is not surprising that Mpp75Aa1.1 displays overall structural similarity with other members in the family such as epsilon toxin. The X-ray crystal structure solved at 1.94 Å resolution reveals that the Mpp75Aa1.1 protein consists of three domains (Kouadio *et al.*, 2021a). The domain I is responsible for receptor-binding/target-specificity while the other two domains (II & III) form the pore-forming loop and oligomerization regions responsible for the beta-pore forming function. Although the level of primary sequence identity between family members can be as low as 25%, the receptor binding domain exhibits significant divergence in both primary amino acid sequence and higher order structure while the pore-forming and oligomerization domains share a relatively higher degree of structural conservation (Moar *et al.*, 2017b; Akiba *et al.*, 2009; Gowda *et al.*, 2016; Bokori-Brown *et al.*, 2013; Cole *et al.*, 2004; Jerga *et al.*, 2016; Xu *et al.*, 2015). The

[9] Mpp75Aa1.1 as the query sequence was aligned to Q02307, which is described as epsilon-toxin type B (ETX) from *Clostridium perfringens*, with 25.9% identity over 297 amino acids and an *E*-score of 1.1e-22. Vpb4Da2 as the query sequence was aligned to P13423, which is described as Protective antigen (PA) from *Bacillus anthracis*, with 32.7% identity over 626 amino acids and an *E*-score of 7.2e-58.

increased divergence in amino acid sequence and structure of the receptor binding domain relative to the rest of the protein underscores its importance in providing specificity to β-PFPs, which has been illustrated by direct comparison of crystal structures (Kouadio *et al.*, 2021a). The head-to-head comparison between the crystal structures of Mpp75Aa1.1 and epsilon toxin reveals significant structural and sequence differences in the receptor binding domain and the C-terminal end of the proteins (Kouadio *et al.*, 2021a). Notably, the receptor binding domains from Mpp75Aa1.1 and epsilon toxin cannot be aligned. Lack of structural homology to the epsilon toxin receptor binding domain highlights functional specificity differences between the Mpp75Aa1.1 and epsilon toxin proteins. The functional specificity of the receptor binding domain was further revealed by amino acid substitutions. Alanine substitution of the surface-exposed amino acids W206, Y212, and G217 within the Mpp75Aa1.1 domain I demonstrates that these three amino acids are essential for its insecticidal activity. The distinctive spatial arrangement of these amino acids in domain I suggests that they are part of a receptor binding epitope unique to Mpp75Aa1.1 and not present in other ETX_MTX2 proteins. Similarly, replacement of two surface exposed tyrosine residues (Y30A and Y196A) in the head region of epsilon toxin significantly reduced cell binding and cytotoxic activities in MDCK 2 cells and abolished toxicity in mice (Bokori-Brown *et al.*, 2014). These tyrosine residues are not present in domain I of Mpp75Aa1.1, thus reflecting their divergence in target organism specificity.

Crystal structure analysis also reveals that Mpp75Aa1.1 has a more extended C-terminal peptide (Kouadio *et al.*, 2021a). Results indicate that removal of the Mpp75Aa1.1 C-terminal peptide by specific proteases, which is required for activation, combined with the neutral to slightly acidic pH-dependent oligomerization also contributes to WCR specificity of Mpp75Aa1.1 (Kouadio *et al.*, 2021a). These analyses demonstrate that the Mpp75Aa1.1 insecticidal activity is regulated by multiple steps, further supporting the conclusion that its target organism specificity is highly selective and its activity is unlikely to happen in humans or other animals. The structural diversity in receptor binding domain as well as their specific activation processes determines the functional specificity of each ETX_MTX2 β-PFP family member. Based upon these bioinformatic and domain structure analyses it is unlikely that Mpp75Aa1.1 is harmful to the health of humans or other animals.

For details, please refer to Appendix 9 ([redacted] 2021 (TRR0001416)).

B.2(a)(i)(ii) Vpb4Da2

The Vpb4Da2 X-ray crystal structure illustrates an architecture of six structural domains and overall structural homology to the bacterial_exotoxin_B family of β-PFP (Kouadio *et al.*, 2021b). The amino-terminal domains 1-3 of Vpb4Da2 share structural homology with the PA protein from *Bacillus anthracis* and encompass a β-pore forming loop constituent of the clostridial binary-toxB module. The carboxyl-terminal half of Vpb4Da2 consists of domains 4 to 6 and is responsible for receptor binding, which confers WCR insecticidal specificity (Kouadio *et al.*, 2021b). The PA protein is one of the most well characterized bacterial_exotoxin_B protein family members. The PA protein itself is non-toxic and has been safely and effectively used as a vaccine in humans and certain animals to provide protection against *B. anthracis* infection (Wesche *et al.*, 1998; Campbell *et al.*, 2007). More broadly, the safe and effective use of specific molecular components of otherwise virulent pathogens is the fundamental basis for the development of

vaccines against a variety of illnesses worldwide (Clem, 2011). Significant sequence homology between Vpb4Da2 domains 1-3 and the PA protein therefore produces no concern with regard to the safety of the Vpb4Da2 protein for exposure by humans or other animals.

While domains 1-3 of Vpb4Da2 display a high degree of amino acid sequence homology with members from the bacterial_exotoxin B family, the domains that confer specificity exhibit a low degree of sequence conservation within the same protein family (Kouadio *et al.*, 2021b). This is not surprising given that the motifs responsible for β-pore forming are present in Vpb4Da2 domains 1-3, and the bacterial_exotoxin_B family shares a similar mechanism of pore formation but with different host receptor specificities (Rigden *et al.*, 2004; Knapp *et al.*, 2016). In fact, the closely related Vpb4Da2 homolog, Vpb4C.6693 which shares ~77% amino acid sequence identity with Vpb4Da2 is natively non-toxic to WCR. However, the Vpb4C.6693 protein can be converted into a WCR-toxic form simply by swapping its domains 4-6 with those from Vpb4Da2 (Kouadio *et al.*, 2021b). The low degree of sequence conservation in Vpb4Da2 domains 4-6 as well as the ability to convert a non-insecticidal homolog to a WCR toxic protein through domain swapping reflects the key role of these domains in host specificity/recognition.

Amino acid sequence analysis further reveals that Vpb4Da2 possesses an alanine residue in position 425 of Domain 2, whereas a phenylalanine residue is conserved in this same position in other bacterial_exotoxin_B family members (Kouadio *et al.*, 2021b). This residue (F427 in *B. anthracis*) is a critical functional component of the φ-clamp of the PA protein heptameric pore, which catalyzes the translocation of the LF and EF components across the membrane that subsequently elicit toxicity (Krantz *et al.*, 2005). The substitution of F427 with Ala drastically reduces the ability of the PA protein to catalyze translocation of LF *in vitro* and in cell-based assays (Krantz *et al.*, 2005). Since this residue is critical for the protein translocation function of the PA protein and related bacterial_exotoxin_B family members, the absence of this residue in Vpb4Da2 indicates that it is highly unlikely to catalyze the translocation of other proteins into host cells, thus providing evidence that Vpb4Da2 exerts its toxicity against WCR without the help of other proteins (Kouadio *et al.*, 2021b; Melnyk and Collier, 2006). The above data clearly indicate that identifying overall homology to a known toxin warrants further investigation but does not by itself demonstrate toxicity. This also further highlights the importance of incorporating a domain-based evaluation into protein safety assessments when using a weight of evidence approach. These domain-based protein characterizations reveal that each member of β_PFP proteins has distinct specificity and activation processes despite displaying overall structural similarity to other toxins (Moar *et al.*, 2017a; Kouadio *et al.*, 2021b). Based upon these bioinformatic and domain structure analyses it is unlikely that Vpb4Da2 is harmful to the health of humans or other mammals.

For details, please refer to Appendix 9 [redacted], 2021 (TRR0001416)).

B.2(a)(ii) Information on the stability of the proteins to proteolysis in appropriate gastrointestinal model systems

B.2(a)(ii)(i) Digestive Fate of the Mpp75Aa1.1 Protein

B.2.(a)(ii)(i)(i) Degradation of the Mpp75A a1.1 by Pepsin

Degradation of the Mpp75Aa1.1 protein by pepsin was evaluated over time by analyzing digestion mixtures incubated for targeted time intervals following a standardized protocol validated in an international, multi-laboratory ring study (Thomas *et al.*, 2004) collected at targeted incubation time points. The susceptibility of Mpp75Aa1.1 protein to pepsin degradation was assessed by visual analysis of a Brilliant Blue G Colloidal stained SDS-PAGE gel and by visual analysis of a western blot probed with an anti-Mpp75Aa1.1 polyclonal antibody. Both visualization methods were run concurrently with separate SDS-PAGE and western blot analyses to estimate the limit of detection (LOD) of the Mpp75Aa1.1 protein.

For SDS-PAGE analysis of the digestibility of the Mpp75Aa1.1 protein in pepsin, the gel was loaded with 1 µg of total test protein (based on pre-digestion protein concentrations) for each of the digestion samples (Figure 29, Panel A). The SDS-PAGE gel for the digestibility assessment was run concurrently with a separate SDS-PAGE gel to estimate the LOD of the Mpp75Aa1.1 protein (Figure 29, Panel B). The LOD of intact Mpp75Aa1.1 protein was approximately 1.6 ng (Figure 29, Panel B, lane 9). Visual examination of SDS-PAGE data showed that the intact Mpp75Aa1.1 protein was digested within 0.5 min of incubation in pepsin (Figure 29, Panel A, lane 5). Therefore, based on the LOD, more than 99.8% (100% - 0.2% = 99.8%) of the intact Mpp75Aa1.1 protein was digested within 0.5 min of incubation in pepsin. A single peptide fragment between 3.5 to 6 kDa was observed during the first 2 min of the pepsin digestion.

No change in the Mpp75Aa1.1 protein band intensity was observed in the absence of pepsin in the 0 min No Pepsin Control and 60 min No Pepsin Control **(**Figure 29, lanes 3 and 12). This indicates that the degradation of the Mpp75Aa1.1 protein was due to the proteolytic activity of pepsin and not due to instability of the protein while incubated in 10 mM HCl, 2 mg/ml NaCl, pH ~1.2 for 60 min.

The 0 min No Test Protein Control and 60 min No Test Protein Control (Figure 29, lanes 2 and 13) demonstrated that the pepsin is stable throughout the experimental phase.

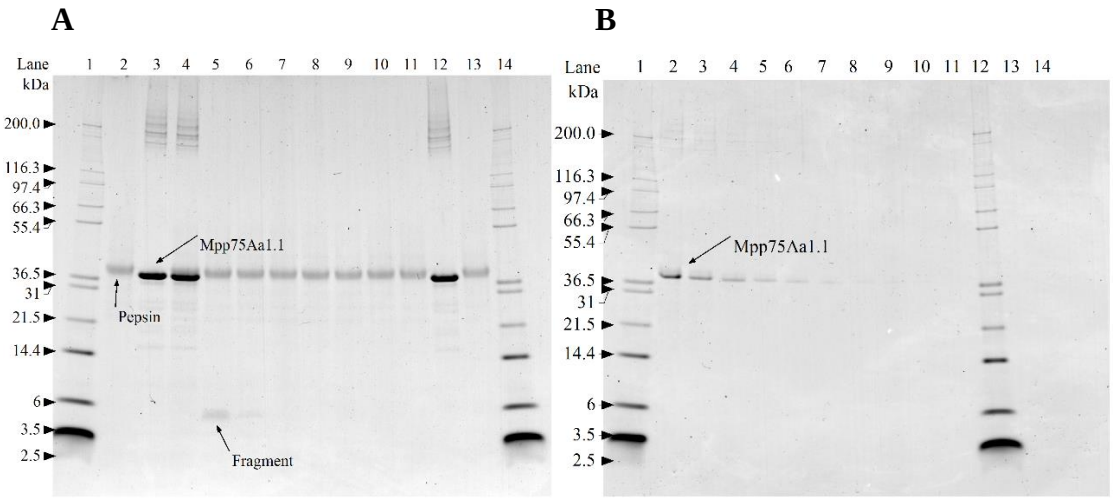

Figure 29. SDS-PAGE Analysis of the Degradation of Mpp75Aa1.1 Protein by Pepsin

Colloidal Brilliant Blue G stained SDS-PAGE gels were used to assess the degradation of Mpp75Aa1.1 protein by pepsin. Molecular weights (kDa) are shown on the left of each gel and correspond to the markers loaded. In each gel, the Mpp75Aa1.1 protein migrated to approximately 34 kDa and pepsin to approximately 38 kDa. Empty lanes were cropped from the images.

A: Mpp75Aa1.1 protein degradation in the presence of pepsin. Based on pre-reaction protein concentrations, 1 µg of test protein was loaded in each lane containing Mpp75Aa1.1 protein.

B: LOD determination. Indicated amounts of the test protein from the Pepsin Treated T0 sample were loaded to estimate the LOD of the Mpp75Aa1.1 protein.

A

Lane	Sample	Incubation Time (min)
1	Mark12 MWM	-
2	0 min No Test Protein Control	0
3	0 min No Pepsin Control	0
4	Pepsin Treated T0	0
5	Pepsin Treated T1	0.5
6	Pepsin Treated T2	2
7	Pepsin Treated T3	5
8	Pepsin Treated T4	10
9	Pepsin Treated T5	20
10	Pepsin Treated T6	30
11	Pepsin Treated T7	60
12	60 min No Pepsin Control	60
13	60 min No Test Protein Control	60
14	Mark12 MWM	-
15	Empty	-

B

Lane	Sample	Amount (ng)
1	Mark12 MWM	-
2	Pepsin Treated T0	200
3	Pepsin Treated T0	100
4	Pepsin Treated T0	50
5	Pepsin Treated T0	25
6	Pepsin Treated T0	12.5
7	Pepsin Treated T0	6.3
8	Pepsin Treated T0	3.1
9	Pepsin Treated T0	1.6
10	Pepsin Treated T0	0.8
11	Pepsin Treated T0	0.4
12	Mark12 MWM	0.2
13	Empty	0.1
14	Empty	-
15	Empty	-

The western blot used to assess Mpp75Aa1.1 protein degradation (Figure 30 Panel A) was run concurrently with the western blot used to estimate the LOD (Figure 30, Panel B). For western analysis, the Mpp75Aa1.1 protein was loaded with approximately 10 ng per lane of total protein (based on pre-reaction total protein concentrations) for each reaction time point examined. The LOD of the Mpp75Aa1.1 protein was approximately 0.031 ng (Figure 30, Panel B, lane 9). Western blot analysis demonstrated that the intact Mpp75Aa1.1 protein was degraded below the LOD within 0.5 min of incubation in the presence of pepsin (Figure 30, Panel A, lane 5). Based on the western blot LOD for the Mpp75Aa1.1 protein, more than 99.7% (100% - 0.3% = 99.7%) of the intact Mpp75Aa1.1 protein was degraded within 0.5 min. No peptide fragments were detected at the 0.5 min and beyond time points in the western blot analysis.

No change in the Mpp75Aa1.1 protein band intensity was observed in the absence of pepsin in the 0 min No Pepsin Control and 60 min No Pepsin Control (Figure 30, lanes 3 and 12). This indicates that the degradation of the Mpp75Aa1.1 protein was due to the proteolytic activity of pepsin and not due to instability of the protein while incubated in 2 mg/ml NaCl, 10 mM HCl, pH ~1.2 for 60 min.

No immunoreactive bands were observed in 0 min No Protein Control and 60 min No Protein Control (Figure 30, lanes 2 and 13). This result indicates that there was no non-specific interaction between the pepsin solution and the Mpp75Aa1.1-specific antibody under these experimental conditions.

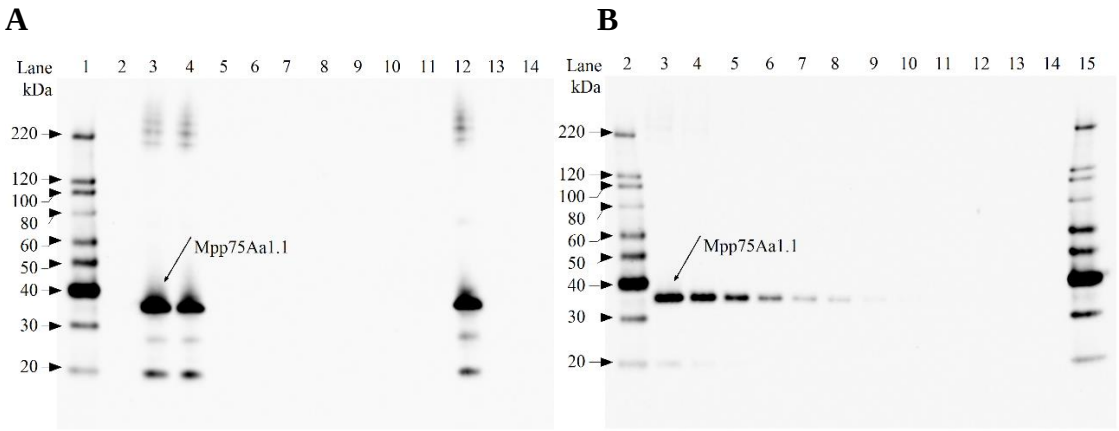

Figure 30. Western Blot Analysis of the Degradation of Mpp75Aa1.1 Protein by Pepsin

Western blots probed with an anti-Mpp75Aa1.1 antibody was used to assess the degradation of Mpp75Aa1.1 by pepsin. Molecular weights (kDa) are shown on the left of each gel and correspond to the MagicMark™ molecular weight marker. Some empty lanes and molecular weight markers that were not visible on the membrane were cropped from the images. A 10 sec exposure is shown.

A: Mpp75Aa1.1protein degradation by pepsin. Based on pre-reaction protein concentrations, 10 ng of test protein was loaded in each lane containing Mpp75Aa1.1protein.
B: LOD determination. Indicated amounts of the test protein from the Pepsin Treated T0 sample were loaded to estimate the LOD of the Mpp75Aa1.1 protein.

A

Lane	Sample	Incubation Time (min)
1	MagicMark MWM	-
2	0 min No Test Protein Control	0
3	0 min No Pepsin Control	0
4	Pepsin Treated T0	0
5	Pepsin Treated T1	0.5
6	Pepsin Treated T2	2
7	Pepsin Treated T3	5
8	Pepsin Treated T4	10
9	Pepsin Treated T5	20
10	Pepsin Treated T6	30
11	Pepsin Treated T7	60
12	60 min No Pepsin Control	60
13	60 min No Test Protein Control	60
14	Precision Plus MWM	-
15	Empty	-

B

Lane	Sample	Amount (ng)
1	Precision Plus MWM	-
2	MagicMark MWM	-
3	Pepsin Treated T0	2
4	Pepsin Treated T0	1
5	Pepsin Treated T0	0.5
6	Pepsin Treated T0	0.25
7	Pepsin Treated T0	0.13
8	Pepsin Treated T0	0.063
9	Pepsin Treated T0	0.031
10	Pepsin Treated T0	0.016
11	Pepsin Treated T0	0.008
12	Pepsin Treated T0	0.004
13	Pepsin Treated T0	0.002
14	Pepsin Treated T0	0.001
15	MagicMark MWM	-

B.2.(a)(ii)(i)(ii) Degradation of the MON 95275 Mpp75Aa1.1 Protein by Pancreatin

The degradation of the Mpp75Aa1.1 protein by pancreatin was assessed by western blot analysis (Figure 31). The western blot used to assess the Mpp75Aa1.1 protein degradation (Figure 31, Panel A) was run concurrently with the western blot used to estimate the LOD (Figure 31, Panel B) of the Mpp75Aa1.1 protein. The LOD of the Mpp75Aa1.1 protein was observed at approximate 0.031 ng protein loading (Figure 31, Panel B, lane 9). The LOD was used to calculate the maximum relative amount of Mpp75Aa1.1 protein that could remain visually undetected after digestion, which corresponded to approximately 0.3% of the total protein loaded.

The Mpp75Aa1.1 protein was loaded with approximately 10 ng per lane of total protein (based on pre-reaction total protein concentrations) for each reaction time point examined. Western blot analysis demonstrated that the intact Mpp75Aa1.1 protein was degraded below the LOD within 15 min of incubation in the presence of pancreatin (Figure 31, Panel A, lane 6). Based on the western blot LOD for the Mpp75Aa1.1 protein, more than 99.7% (100% - 0.3% = 99.7%) of the intact Mpp75Aa1.1 protein was degraded within 15 min. Several bands smaller than 30 kDa corresponding to fragments of Mpp75Aa1.1 were present during the duration of the pancreatin digestion (Figure 31, Panel A, lanes 5-12). The SuperSignal Dura western blot detection reagent improved the detection limit to pg level with approximately 1/300 of the starting amount of Mpp75Aa1.1 still visible. Furthermore, such fragments would not be expected if the protein exposed to pepsin first prior to pancreatin digestion.

No significant change in the intact Mpp75Aa1.1 (~34 kDa) band intensity was observed in the absence of pancreatin in the 0 min No Pancreatin Control and 24 hour No Pancreatin Control (Figure 31, Panel A, lanes 3 and 13). This indicates that the degradation of all immunoreactive forms of the Mpp75Aa1.1 protein was due to the proteolytic activity of pancreatin and not due to instability of the protein when incubated in 50 mM KH_2PO_4, pH 7.5 over the course of the experiment.

No immunoreactive bands were observed in the 0 min No Test Protein Control and 24 hour No Test Protein Control (Figure 31, Panel A, lanes 2 and 14), demonstrating the absence of non-specific antibody interactions with the pancreatin solution.

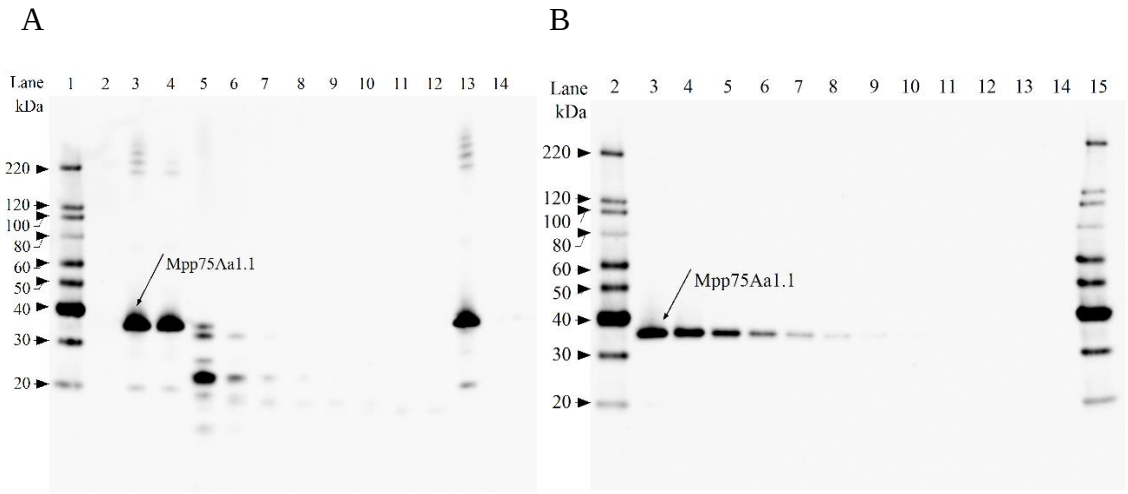

Figure 31. Western Blot Analysis of the Degradation of the Mpp75Aa1.1 Protein by Pancreatin

Western blots probed with an anti-Mpp75Aa1.1antibody was used to assess the degradation of Mpp75Aa1.1by pancreatin. Molecular weights (kDa) are shown on the left of each gel and correspond to the MagicMark™ molecular weight marker. Some empty lanes and molecular weight markers that were not visible on the membrane were cropped from the images. A 510 sec exposure is shown.

A: Mpp75Aa1.1protein degradation by pancreatin. Based on pre-reaction protein concentrations, 10 ng of test protein was loaded in each lane containing Mpp75Aa1.1protein.

B: LOD determination. Indicated amounts of the test protein from the Pancreatin Treated T0 sample were loaded to estimate the LOD of the Mpp75Aa1.1 protein.

A

Lane	Sample	Incubation Time
1	MagicMark MWM	-
2	0 min No Test Protein Control	0
3	0 min No Pancreatin Control	0
4	Pancreatin Treated T0	0
5	Pancreatin Treated T1	5 min
6	Pancreatin Treated T2	15 min
7	Pancreatin Treated T3	30 min
8	Pancreatin Treated T4	1 h
9	Pancreatin Treated T5	2 h
10	Pancreatin Treated T6	4 h
11	Pancreatin Treated T7	8 h
12	Pancreatin Treated T8	24 h
13	24 h No Pancreatin Control	24 h
14	24 h No Test Protein Control	24 h
15	Precision Plus MWM	-

B

Lane	Sample	Amount (ng)
1	Precision Plus MWM	-
2	MagicMark MWM	-
3	Pancreatin Treated T0	2
4	Pancreatin Treated T0	1
5	Pancreatin Treated T0	0.5
6	Pancreatin Treated T0	0.25
7	Pancreatin Treated T0	0.13
8	Pancreatin Treated T0	0.063
9	Pancreatin Treated T0	0.031
10	Pancreatin Treated T0	0.016
11	Pancreatin Treated T0	0.008
12	Pancreatin Treated T0	0.004
13	Pancreatin Treated T0	0.002
14	Pancreatin Treated T0	0.001
15	MagicMark MWM	-

B.2.(a)(ii)(i)(iii) Digestive Fate of the Mpp75Aa1.1 Protein Conclusions

The ability of Mpp75Aa1.1 protein to be degraded by pepsin and by pancreatin was evaluated in this study. The results showed that at least 99.8% of the intact Mpp75Aa1.1 protein was degraded by pepsin within 0.5 min when analyzed by SDS-PAGE and 99.7% of the intact Mpp75Aa1.1 was degraded by pepsin within 0.5 min when analyzed by western blot using a Mpp75Aa1.1-specific antibody. SDS-PAGE analysis showed that a single peptide fragment between 3.5 and 6 kDa was observed during the first 2 min of the pepsin digestion and completely degraded after 5 min. Greater than 99.7% of the intact Mpp75Aa1.1 protein was degraded within 15 min of incubation with pancreatin when analysed by western blot using a Mpp75Aa1.1-specific antibody. These results show that the full-length Mpp75Aa1.1 is rapidly degraded by pepsin and pancreatin. Rapid degradation of the intact Mpp75Aa1.1 protein by pepsin or pancreatin indicates that the Mpp75Aa1.1 protein is highly unlikely to pose any safety concern to human or animal health.

For details, please refer to Appendix 10 ([redacted], 2022 (TRR0000731)).

B.2(a)(ii)(ii) Digestive Fate of Vpb4Da2 Protein

B.2.(a)(ii)(ii)(i) Degradation of Vpb4Da2 Protein in the Presence of Pepsin

Degradation of the Vpb4Da2 protein by pepsin was evaluated over time by analyzing digestion mixtures incubated for targeted time intervals following a standardized protocol validated in an international, multi-laboratory ring study (Thomas *et al.*, 2004) collected at targeted incubation time points. The susceptibility of the Vpb4Da2 protein to pepsin degradation was assessed by visual analysis of a Brilliant Blue G Colloidal stained SDS-PAGE gel and by visual analysis of a western blot probed with an anti-Vpb4Da2 polyclonal antibody. Both visualization methods were run concurrently with separate SDS-PAGE and western blot analyses to estimate the limit of detection (LOD) of the Vpb4Da2 protein.

For SDS-PAGE analysis of the digestibility of the Vpb4Da2 protein in pepsin, the gel was loaded with 1 µg of total test protein (based on pre-digestion protein concentrations) for each of the digestion samples (Figure 32, Panel A). The SDS-PAGE gel for the digestibility assessment was run concurrently with a separate SDS-PAGE gel to estimate the LOD of the Vpb4Da2 protein (Figure 32, Panel B). The LOD of intact Vpb4Da2 protein was approximately 1.6 ng (Figure 32, Panel B, lane 9). Visual examination of SDS-PAGE data showed that the intact Vpb4Da2 protein was digested within 0.5 min of incubation in pepsin (Figure 32, Panel A, lane 5). Therefore, based on the LOD, more than 99.8% (100% - 0.2% = 99.8%) of the intact Vpb4Da2 protein was digested within 0.5 min of incubation in pepsin. Peptide fragments between 2.5 to 6 kDa were observed during the first 5 min of the pepsin digestion.

No change in the Vpb4Da2 protein band intensity was observed in the absence of pepsin in the 0 min No Pepsin Control and 60 min No Pepsin Control (Figure 32, Panel A, lanes 3 and 12). This indicates that the degradation of the Vpb4Da2 protein was due to the proteolytic activity of pepsin and not due to instability of the protein while incubated in 10 mM HCl, 2 mg/ml NaCl, pH ~1.2 for 60 min.

The 0 min No Test Protein Control and 60 min No Test Protein Control (Figure 32, Panel A, lanes 2 and 13) demonstrated that the pepsin is stable throughout the experimental phase.

A **B**

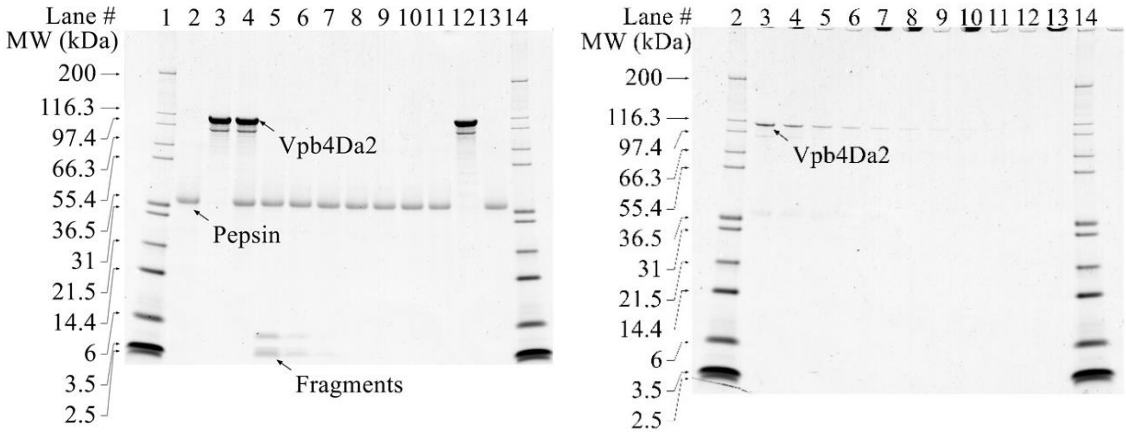

Figure 32. SDS-PAGE Analysis of the Degradation of Vpb4Da2 Protein by Pepsin

Colloidal Brilliant Blue G stained SDS-PAGE gels were used to assess the degradation of Vpb4Da2 protein by pepsin. Molecular weights (kDa) are shown on the left of each gel and correspond to the markers loaded. In each gel, the Vpb4Da2 protein migrated to approximately 103.8 kDa and pepsin to approximately 38 kDa. Empty lanes were cropped from the images.
A: Vpb4Da2 protein degradation in the presence of pepsin. Based on pre-reaction protein concentrations, 1 µg of test protein was loaded in each lane containing Vpb4Da2 protein.
B: LOD determination. Indicated amounts of the test protein from the Pepsin Treated T0 sample were loaded to estimate the LOD of the Vpb4Da2 protein.

A

Lane	Sample	Incubation Time (min)
1	Mark12 MWM	-
2	0 min No Test Protein Control	0
3	0 min No Pepsin Control	0
4	Pepsin Treated T0	0
5	Pepsin Treated T1	0.5
6	Pepsin Treated T2	2
7	Pepsin Treated T3	5
8	Pepsin Treated T4	10
9	Pepsin Treated T5	20
10	Pepsin Treated T6	30
11	Pepsin Treated T7	60
12	60 min No Pepsin Control	60
13	60 min No Test Protein Control	60
14	Mark12 MWM	-
15	Empty	-

B

Lane	Sample	Amount (ng)
1	Empty	-
2	Mark12 MWM	-
3	Pepsin Treated T0	100
4	Pepsin Treated T0	50
5	Pepsin Treated T0	25
6	Pepsin Treated T0	12.5
7	Pepsin Treated T0	6.3
8	Pepsin Treated T0	3.1
9	Pepsin Treated T0	1.6
10	Pepsin Treated T0	0.8
11	Pepsin Treated T0	0.4
12	Pepsin Treated T0	0.2
13	Pepsin Treated T0	0.1
14	Mark12 MWM	-
15	Empty	-

For western blot analysis of Vpb4Da2 pepsin susceptibility, the Vpb4Da2 protein was loaded with approximately 5 ng per lane of total protein (based on pre-reaction total protein concentrations) for each reaction time point examined. The western blot used to assess Vpb4Da2 protein degradation (Figure 33, Panel A) was run concurrently with the western blot used to estimate the LOD (Figure 33, Panel B). The LOD of the Vpb4Da2 protein was approximately 0.063 ng (Figure 33, Panel B, Lane 9). Western blot analysis demonstrated that the intact Vpb4Da2 protein was degraded below the LOD within 0.5 min of incubation in the presence of pepsin (Figure 33, Panel A, lane 6). Based on the western blot LOD for the Vpb4Da2 protein, more than 98.7% (100% - 1.3% = 98.7%) of the intact Vpb4Da2 protein was degraded within 0.5 min. No peptide fragments were detected at the 0.5 min and beyond time points in the western blot analysis.

No change in the Vpb4Da2 protein band intensity was observed in the absence of pepsin in the 0 min No Pepsin Control and 60 min No Pepsin Control (Figure 33, Panel A, lanes 4 and 13). This indicates that the degradation of the Vpb4Da2 protein was due to the proteolytic activity of pepsin and not due to instability of the protein while incubated in 2 mg/ml NaCl, 10 mM HCl, pH ~1.2 for 60 min.

No immunoreactive bands were observed in 0 min No Protein Control and 60 min No Protein Control (Figure 33, Panel A, lanes 3 and 14). This result indicates that there was no non-specific interaction between the pepsin solution and the Vpb4Da2-specific antibody under these experimental conditions.

A **B**

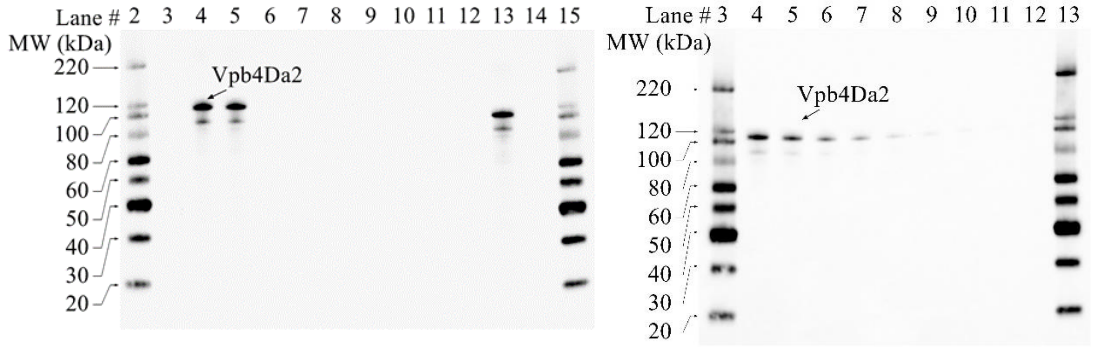

Figure 33. Western Blot Analysis of the Degradation of the Vpb4Da2 Protein by Pepsin

Western blots probed with an anti-Vpb4Da2 antibody were used to assess the degradation of Vpb4Da2 by pepsin. Molecular weights (kDa) are shown on the left of each gel and correspond to the MagicMark™ molecular weight marker. Empty lanes and molecular weight markers that were not visible on the film were cropped from the images. A 10 sec exposure is shown.
A: Vpb4Da2 protein degradation by pepsin. Based on pre-reaction protein concentrations, 5 ng of test protein was loaded in each lane containing Vpb4Da2 protein.
B: LOD determination. Indicated amounts of the test protein from the Pepsin Treated T0 sample were loaded to estimate the LOD of the Vpb4Da2 protein.

A

Lane	Sample	Incubation Time (min)
1	Precision Plus MWM	-
2	MagicMark MWM	-
3	0 min No Test Protein Control	0
4	0 min No Pepsin Control	0
5	Pepsin Treated T0	0
6	Pepsin Treated T1	0.5
7	Pepsin Treated T2	2
8	Pepsin Treated T3	5
9	Pepsin Treated T4	10
10	Pepsin Treated T5	20
11	Pepsin Treated T6	30
12	Pepsin Treated T7	60
13	60 min No Pepsin Control	60
14	60 min No Test Protein Control	60
15	MagicMark MWM	-

B

Lane	Sample	Amount (ng)
1	Empty	-
2	Precision Plus MWM	-
3	MagicMark MWM	-
4	Pepsin Treated T0	2
5	Pepsin Treated T0	1
6	Pepsin Treated T0	0.5
7	Pepsin Treated T0	0.25
8	Pepsin Treated T0	0.13
9	Pepsin Treated T0	0.063
10	Pepsin Treated T0	0.031
11	Pepsin Treated T0	0.016
12	Pepsin Treated T0	0.008
13	MagicMark MWM	-
14	Precision Plus MWM	-
15	Empty	-

B.2.(a)(ii)(ii)(ii) Degradation of Vpb4Da2 Protein in the Presence of Pancreatin

The degradation of the Vpb4Da2 protein by pancreatin was assessed by western blot analysis (Figure 34). The western blot used to assess the Vpb4Da2 protein degradation (Figure 34, Panel A) was run concurrently with the western blot used to estimate the LOD (Figure 34, Panel B) of the Vpb4Da2 protein. The LOD of the Vpb4Da2 protein was observed at approximate 0.063 ng protein loading (Figure 34, Panel B, lane 9). The LOD was used to calculate the maximum relative amount of Vpb4Da2 protein that could remain visually undetected after digestion, which corresponded to approximately 1.3% of the total protein loaded.

The Vpb4Da2 protein was loaded with approximately 5 ng per lane of total protein (based on pre-reaction total protein concentrations) for each reaction time point examined. Western blot analysis demonstrated that the intact Vpb4Da2 protein was degraded below the LOD within 5 min of incubation in the presence of pancreatin (Figure 34, Panel A, lane 6). Based on the western blot LOD for the Vpb4Da2 protein, more than 98.7% (100% - 1.3% = 98.7%) of the intact Vpb4Da2 protein was degraded within 5 min. Several bands smaller than 60 kDa corresponding to fragments of Vpb4Da2 were present during the first hour of the pancreatin digestion (Figure 34, Panel A, lanes 6-9). Those fragments were no longer observed at 2-hour of incubation of pancreatin. Such fragments would not be expected if the protein exposed to pepsin first prior to pancreatin digestion.

No significant change in the intact Vpb4Da2 (~103.8 kDa) band intensity was observed in the absence of pancreatin in the 0 min No Pancreatin Control and 24 hour No Pancreatin Control (Figure 34, Panel A, lanes 4 and 14). This indicates that the degradation of all immunoreactive forms of the Vpb4Da2 protein was due to the proteolytic activity of pancreatin and not due to instability of the protein when incubated in 50 mM KH_2PO_4, pH 7.5 over the course of the experiment.

No immunoreactive bands were observed in the 0 min No Test Protein Control and 24 hour No Test Protein Control (Figure 34, Panel A, lanes 3 and 15), demonstrating the absence of non-specific antibody interactions with the pancreatin solution.

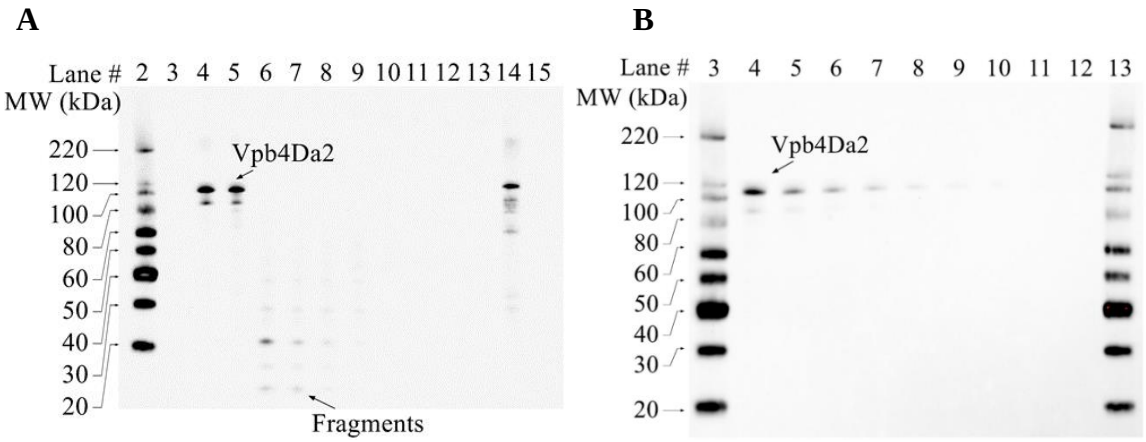

Figure 34. Western Blot Analysis of the Degradation of the Vpb4Da2 Protein by Pancreatin
Western blots probed with an anti-Vpb4Da2 antibody were used to assess the degradation of Vpb4Da2 by pancreatin. Molecular weights (kDa) are shown on the left of each gel and correspond to the MagicMark™ molecular weight marker. Empty lanes and molecular weight markers that were not visible on the film were cropped from the images. A 10 sec exposure is shown.
A: Vpb4Da2 protein degradation by pancreatin. Based on pre-reaction protein concentrations, 5 ng of test protein was loaded in each lane containing Vpb4Da2 protein.
B: LOD determination. Indicated amounts of the test protein from the Pancreatin Treated T0 sample were loaded to estimate the LOD of the Vpb4Da2 protein.

Lane	Sample	Incubation Time
1	Precision Plus MWM	-
2	MagicMark MWM	-
3	0 min No Test Protein Control	0
4	0 min No Pancreatin Control	0
5	Pancreatin Treated T0	0
6	Pancreatin Treated T1	5 min
7	Pancreatin Treated T2	15 min
8	Pancreatin Treated T3	30 min
9	Pancreatin Treated T4	1 h
10	Pancreatin Treated T5	2 h
11	Pancreatin Treated T6	4 h
12	Pancreatin Treated T7	8 h
13	Pancreatin Treated T8	24 h
14	24 h No Pancreatin Control	24 h
15	24 h No Test Protein Control	24 h

Lane	Sample	Amount (ng)
1	Empty	-
2	Precision Plus MWM	-
3	MagicMark MWM	-
4	Pancreatin Treated T0	2
5	Pancreatin Treated T0	1
6	Pancreatin Treated T0	0.5
7	Pancreatin Treated T0	0.25
8	Pancreatin Treated T0	0.13
9	Pancreatin Treated T0	0.063
10	Pancreatin Treated T0	0.031
11	Pancreatin Treated T0	0.016
12	Pancreatin Treated T0	0.008
13	MagicMark MWM	-
14	Precision Plus MWM	-
15	Empty	-

B.2.(a)(ii)(ii)(iii) Digestive Fate of the VpbDa2 Protein Conclusion

The ability of Vpb4Da2 protein to be degraded by pepsin and by pancreatin was evaluated in this study. The results showed that at least 99.8% of the intact Vpb4Da2 protein was degraded by pepsin within 0.5 min when analyzed by SDS-PAGE and 98.7% of the intact Vpb4Da2 was degraded by pepsin within 0.5 min when analyzed by western blot using a Vpb4Da2-specific antibody. SDS-PAGE analysis also showed that peptide fragments between 2.5 to 6 kDa were observed during the first 5 min of the pepsin digestion and completed degraded after 5 min. Greater than 98.7% of the intact Vpb4Da2 protein was degraded within 5 min of incubation with pancreatin when analyzed by western blot using a Vpb4Da2-specific antibody. These results show that the full-length Vpb4Da2 is rapidly degraded by pepsin and pancreatin. Rapid degradation of the intact Vpb4Da2 protein by pepsin or pancreatin indicates that the Vpb4Da2 protein is highly unlikely to pose any safety concern to human or animal health.

For details, please refer to Appendix 11 ([redacted], 2020 (TRR0000596)).

B.2(a)(iii) An animal toxicity study if the bioinformatic comparison and biochemical studies indicate either a relationship with known protein toxins/anti-nutrients or resistance to proteolysis

Not relevant for this product.

B.2(b) Information on the potential allergenicity of any new proteins, including:

B.2(b)(i) Source of the new proteins

The *mpp75Aa1.1* gene encodes the Mpp75Aa1.1 protein, which is derived from the full-length precursor form of the insecticidal protein Mpp75Aa1 from *Brevibacillus laterosporus*. The taxonomy of *Brevibacillus laterosporus* is:

Kingdom: Bacteria
Phylum: Firmicutes
Class: Bacilli
Order: Bacillales
Family: Paenibacillaceae
Genus: *Brevibacillus*

B. laterosporus, formerly classified as *Bacillus laterosporus*, is an endospore-forming insecticidal bacilli and not known for pathogenicity or allergenicity in humans or other vertebrates with the only known report of *B. laterosporus* infection occurring in an immunocomprimised pediatric patient (Shida *et al.*, 1996; Curtis *et al.*, 2020; Laubach, 1916). However, *B. laterosporus* shares a similar habitat to *Bt*, and can be isolated from a wide range of environments including soil, rocks, dust, and both fresh and sea waters (Ruiu, 2013; Panda *et al.*, 2014; Nivetha and Jayachandran, 2017). Furthermore, *B. laterosporus* is also found to be present in many food sources such as cheese (Román-Blanco *et al.*, 1999), curd (Panda *et al.*, 2014), beans (Sarkar *et al.*, 2002), and honey (Iurlina and Fritz, 2005), as well as being listed as a probiotic for humans (Hong *et al.*,

2005) and feed additive for birds (Ruiu, 2013; Ruiu *et al.*, 2014). *B. laterosporus* isolate has a characterized broad-spectrum insecticidal activity and was registered for pest control in horticulture and agriculture in New Zealand (NZ EPA, 2022). Taken together, the widespread presence of *B. laterosporus* in the environment provides a documented history of safe exposure and consumption for human and other vertebrates.

The donor organism for the *vpb4Da2* gene is *Bacillus thuringiensis* (*Bt*). The taxonomy of *Bacillus thuringiensis* is:

Kingdom: Bacteria
Phylum: Firmicutes
Class: Bacilli
Order: Bacillales
Family: Bacillaceae
Genus: *Bacillus*

Bt has a long history of commercial use in the U.S. to produce microbially-derived products with insecticidal activity. Applications of Bt have a documented history of safe use in agriculture, including in organic farming **(**U.S. EPA, 1988**;** WHO, 1999**;** Cannon, 1993**)**. Since the first Bt isolate was registered as a pesticide in 1961, over 180 microbial Bt products have been registered in the United States (U.S.), with more than 120 microbial products registered in the European Union (EU) **(**Hammond, 2004**)**. Microbial pesticides containing Bt insecticidal proteins have been subjected to extensive toxicity testing showing no adverse effects to human health (U.S. EPA, 2005; U.S. EPA, 2001b; Baum *et al.*, 1999; Betz *et al.*, 2000; Mendelsohn *et al.*, 2003; McClintock *et al.*, 1995). Additionally, there are no confirmed cases of allergic reactions to the insecticidal proteins in microbial-derived Bt products during more than 50 years of use (Koch *et al.*, 2015).

Similar to the corn rootworm-protected maize event MON 87411 (A1097), the sequence present in the *DvSnf7.1* suppression cassette in MON 95275 was designed to match the gene present in western corn rootworm (WCR: *Diabrotica virgifera virgifera*) encoding the SNF7 subunit of the ESCRT-III complex (Babst *et al.*, 2002). The taxonomy of *Diabrotica virgifera virgifera* is:

Kingdom: Animalia
Phylum: Arthropoda
Class:Insecta
Order:Coleoptera
Family: Chrysomelidae
Genus: *Diabrotica*

The sequence in MON 95275 utilized to induce the RNAi mechanism in CRW is the same sequence present in MON 87411. Based on the ubiquitous nature of RNAi suppression utilizing endogenous dsRNAs in a wide variety of plant species consumed by humans and animals, demonstration of the specificity of *Snf7* suppression in CRW (Bachman *et al.*, 2013; Bachman *et al.*, 2016), the long history of safe consumption of RNA from a range of sources (Rodrigues and Petrick, 2020), and the apparent lack of toxicity or allergenicity of dietary RNA (Petrick *et al.*, 2016), the *DvSnf7.1* RNAi suppression sequence used in MON 95275 poses no observed risks to humans or other vertebrates.

B.2(b)(ii) A bioinformatics comparison of the amino acid sequence to known allergens

B.2(b)(ii)(i) Structural similarity of the Mpp75Aa1.1 Protein to known allergens

The Codex guidelines for the evaluation of the allergenicity potential of introduced proteins (Codex Alimentarius, 2009) are based on the comparison of amino acid sequences between introduced proteins and allergens, where allergenic cross-reactivity may exist if the introduced protein is found to have at least 35% amino acid identity with an allergen over any segment of at least 80 amino acids. The Codex guideline also suggests that a sliding window search with a scientifically justified peptide size be used to identify immunologically relevant peptides in otherwise unrelated proteins. Therefore, the extent of sequence similarities between the Mpp75Aa1.1 protein sequence and known allergens, gliadins, and glutenins was assessed using the FASTA sequence alignment tool along with an eight-amino acid sliding window search (Thomas *et al.*, 2005; Codex Alimentarius, 2009). The data generated from these analyses confirm that the Mpp75Aa1.1 protein does not share amino acid sequence similarities with known allergens, gliadins, or glutenins.

The FASTA program directly compares amino acid sequences (i.e., primary, linear protein structure). This alignment data may be used to infer shared higher order structural similarities between two sequences (i.e., secondary and tertiary protein structures). Proteins that share a high degree of similarity throughout the entire sequence are often homologous. By definition, homologous proteins have common secondary structures, and three-dimensional configuration, and, consequently, may share similar functions. Periodically, the databases used to evaluate proteins are updated. Since the most recent reports were completed, the allergen (AD_2021) database has been revised and updated. In order to determine if the Mpp75Aa1.1 protein shares significant sequence similarity to new sequences contained in the updated allergen database, protein sequences were used as a query for a FASTA and Sliding Window search of the AD_2021 database. The allergen, gliadin, and glutenin protein sequence database (AD_2021) was obtained as the "COMprehensive Protein Allergen REsource" (COMPARE) database from the Health and Environmental Sciences Institute (HESI) and was used for the evaluation of sequence similarities shared between the Mpp75Aa1.1 protein and all proteins in the database. The AD_2021 database contains 2,348 sequences. When used to align the sequence of the introduced protein to each protein in the database, the FASTA algorithm produces an *E*-score (expectation score) for each alignment. The *E*-score is a statistical measure of the likelihood that the observed similarity score could have occurred by chance in a search. A larger *E*-score indicates a low degree of similarity between the query sequence and the sequence from the database. Typically, alignments between two sequences which have an *E*-score of less than or equal to 1×10-5 are considered to have meaningful homology. Results indicate that the Mpp75Aa1.1 protein sequence does not share meaningful similarity with sequences in the allergen database. No alignment met or exceeded the threshold of 35% identity over 80 amino acids recommended by Codex Alimentarius (2009) or had an *E*-score of less than or equal to 1×10-5.

A second bioinformatic tool, an eight-amino acid sliding window search, was used to specifically identify short linear polypeptide matches to known allergens. It is possible that proteins structurally unrelated to allergens, gliadins, and glutenins may contain smaller immunologically meaningful epitopes. An amino acid sequence may have allergenic potential if it has an exact sequence identity of at least eight linearly contiguous amino acids with a potential allergen epitope

(Hileman *et al.*, 2002; Metcalfe *et al.*, 1996). Using a sliding window of less than eight amino acids can produce matches containing considerable uncertainty depending on the length of the query sequence (Silvanovich *et al.*, 2006), and is not useful to the allergy assessment process (Thomas *et al.*, 2005). No eight contiguous amino acid identities were detected when the Mpp75Aa1.1 protein sequence was compared to the proteins in the AD_2021 sequence database.

The bioinformatic results demonstrated there were no biologically relevant sequence similarities to allergens when the Mpp75Aa1.1 protein sequence was used as a query for a FASTA search of the AD_2021 database. Furthermore, no short (eight amino acid) polypeptide matches were shared between the Mpp75Aa1.1 protein sequence and proteins in the allergen database. These data show that Mpp75Aa1.1 protein sequence lacks both structurally and immunologically relevant similarities to known allergens, gliadins, and glutenins.

For details, please refer to Appendix 9[redacted], 2021 (TRR0001416)).

B.2(b)(ii)(ii) Structural Similarity of Vpb4Da2 Protein to Known Allergens

As previously stated, the extent of sequence similarities between the Vpb4Da2 protein sequence and known allergens, gliadins, and glutenins was assessed using the FASTA sequence alignment tool along with an eight-amino acid sliding window search (Thomas *et al.*, 2005; Codex Alimentarius, 2009). The data generated from these analyses confirm that the Vpb4Da2 protein does not share amino acid sequence similarities with known allergens, gliadins, or glutenins.

The bioinformatic results demonstrated there were no biologically relevant sequence similarities to allergens when the Vpb4Da2 protein sequence was used as a query for a FASTA search of the AD_2021 database. Furthermore, no short (eight amino acid) polypeptide matches were shared between the Vpb4Da2 protein sequence and proteins in the allergen database. These data show that Vpb4Da2 protein sequence lacks both structurally and immunologically relevant similarities to known allergens, gliadins, and glutenins.

For details, please refer to Appendix 9[redacted] 2021 (TRR0001416)).

B.2(b)(iii) The new protein's structural properties, including, but not limited to, its susceptibility to enzymatic degregation (e.g. proteolysis), heat and/or acid stability

B.2(b)(iii)(i) Heat susceptibility of the MON 95275 Mpp75Aa1.1 Protein

The effect of heat treatment on the activity of the *E. coli*-produced Mpp75Aa1.1 protein was evaluated. Heat treated samples and an unheated control sample of Mpp75Aa1.1 protein were analyzed: 1) using an insect bioassay to assess the impact of temperature on the functional activity of the Mpp75Aa1.1 protein; and 2) using SDS-PAGE to assess the impact of temperature on protein integrity.

Aliquots of Mpp75Aa1.1 protein were heated to 25, 37, 55, 75 and 95 ºC for either 15 or 30 minutes, while a separate aliquot of Mpp75Aa1.1 protein was maintained on ice for the duration of the heat treatments to serve as a temperature control. The effect of heat treatment on the

activity of Mpp75Aa1.1 was evaluated using an insect bioassay. The effect of heat treatment on the integrity of the Mpp75Aa1.1 protein was evaluated using SDS-PAGE analysis of the heated and temperature control Mpp75Aa1.1 protein samples.

Results of the functional activity assay for Mpp75Aa1.1 protein incubated for 15 and 30 minutes are listed in Table 23 and Table 24, respectively. The control sample had an EC_{50} of 7.3 µg Mpp75Aa1.1 protein/ml diet, thus demonstrating that protein activity was maintained during incubation on ice. Protein activity was retained when incubated for 15 and 30 minutes at a temperature of 25 and 37°C. Protein activity was likewise retained when incubated at a temperature of 55°C for 15 minutes however, when incubated for 30 minutes at a temperature of 55°C, the protein activity was significantly lost such that an EC_{50} value could not be established. No dose-response relationship was observed from the 55°C heat-treated sample for 30 min or 75 and 95°C heat-treated samples for the 15 minute or 30 minute heat treatments, respectively. As a result, no EC_{50} values were estimated, indicating that Mpp75Aa1.1 protein had no functional activity in WCR bioassay after the incubation at 55°C for 30 minutes or ≥75°C temperatures for 15 or 30 minutes.

The results of the SDS-PAGE analysis of the heat-treated samples incubated for 15 and 30 minutes are illustrated in Figure 35 and Figure 36, respectively. The control sample loaded on each gel (Figure 35 and Figure 36, lane 2) showed equivalent band intensity to the 100% reference standard (Figure 35 and Figure 36, lane 8), demonstrating that the Mpp75Aa1.1 protein was stable on wet ice during the incubation period. No apparent decrease in band intensity of the ~34.0 kDa Mpp75Aa1.1 protein was observed in the test samples when heated at temperatures of 25, 37, 55 and 75°C for 15 or 30 minutes. High molecular weight protein aggregates wereevident at 37, 55 and 75°C with decreasing aggregation apparent at higher temperatures. Degradation products were evident at 75 and 95°C for both 15 and 30 minutes with increasing degradation at higher temperatures. A decrease in the intensity of the main Mpp75Aa1.1 band was evident at 95°C with the most prominent loss of band intensity observed at 30 minutes.

These data demonstrate that the Mpp75Aa1.1 protein behaves with a predictable tendency toward protein denaturation and loss of functional activity at elevated temperatures. Heat treatment is widely used in the preparation of foods containing components derived from maize grain. Therefore, it is reasonable to conclude that Mpp75Aa1.1 protein would not be consumed as an active protein in food products derived from MON 95275 due to standard processing practices that include heat treatment at 55 ºC for 30 minutes or ≥75 ºC for the majority of foods derived from processed maize (Hammond and Jez, 2011).

For details, please refer to Appendix 12 [redacted], 2021 (TRR0000870)).

Table 23. EC50 Values and 95% Confidence Limits (CI) for the Heat Treated Mpp75Aa1.1 Protein After 15 Minutes

Temperature	EC_{50} (µg Mpp75Aa1.1/ml diet)	95% CI (µg Mpp75Aa1.1/ml diet)
0 ºC (control)	7.3	4.2 - 13
25 ºC	15	6.8 - 34
37 ºC	12	8.1 - 18
55 ºC	15	8.4 - 28
75 ºC[1]	N/A[2]	N/A
95 ºC[1]	N/A	N/A

[1]No EC_{50} value and 95% CI were estimated since no dose-response relationship was observed.
[2]N/A: not available

Table 24. EC50 Values and 95% Confidence Limits (CI) for the Heat Treated Mpp75Aa1.1 Protein After 30 Minutes

Temperature	EC50 (µg Mpp75Aa1.1/ml diet)	95% CI (µg Mpp75Aa1.1/ml diet)
0 ºC (control)	7.3	4.2 - 13
25 ºC	12	6.2 - 23
37 ºC	7.1	4.8 - 11
55 ºC[3]	N/A[2]	N/A
75 ºC[1]	N/A	N/A
95 ºC[1]	N/A	N/A

[1]No EC_{50} value and 95% CI were estimated since no dose-response relationship was observed.
[2]N/A: not available
[3]The EC_{50} value could not be estimated since <50% growth inhibition was observed at the highest test concentration

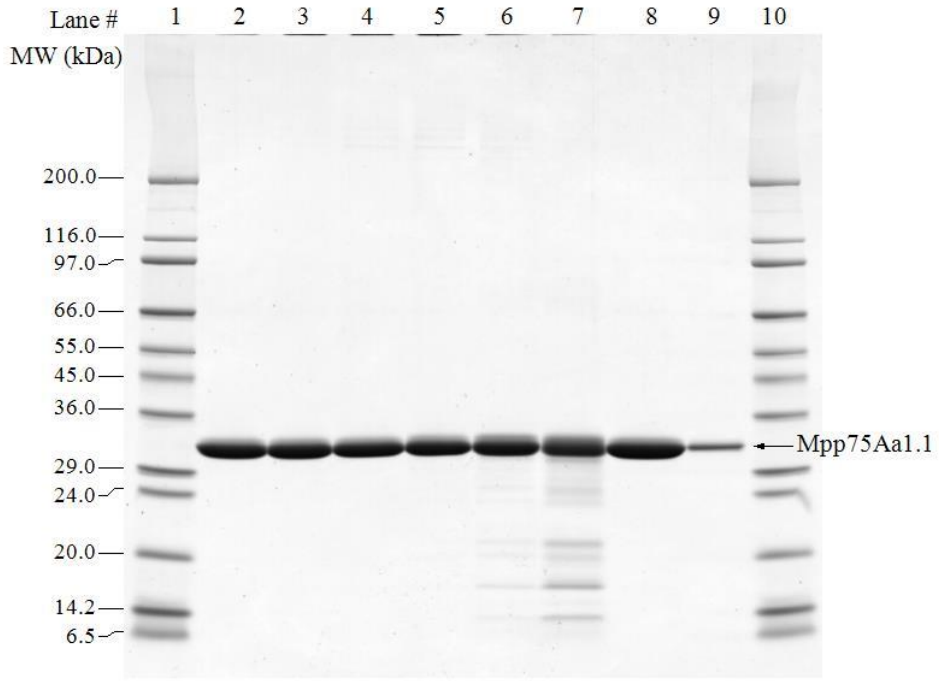

Figure 35. SDS-PAGE of Mpp75Aa1.1 Protein Demonstrating the Effect After 15 Minutes at Elevated Temperatures on Protein Structural Stability

Heat-treated samples of Mpp75Aa1.1 (3.0 µg total protein) separated on a Tris-glycine 4-20 % polyacrylamide gel under denaturing and reducing conditions. The gel was stained with Brilliant Blue G Colloidal. Approximate molecular weights (kDa) are shown on the left and correspond to molecular weight standards in lanes 1 and 10.

Lane	Description	Total Amount
1	SigmaMarker Wide Standards	5.0 µl
2	Mpp75Aa1.1 Protein Control	3.0 µg
3	Mpp75Aa1.1 Protein 25ºC	3.0 µg
4	Mpp75Aa1.1 Protein 37ºC	3.0 µg
5	Mpp75Aa1.1 Protein 55ºC	3.0 µg
6	Mpp75Aa1.1 Protein 75ºC	3.0 µg
7	Mpp75Aa1.1 Protein 95ºC	3.0 µg
8	Mpp75Aa1.1 Protein Reference 100% Equivalence	3.0 µg
9	Mpp75Aa1.1 Protein Reference 10% Equivalence	0.3 µg
10	SigmaMarker Wide Standards	5.0 µl

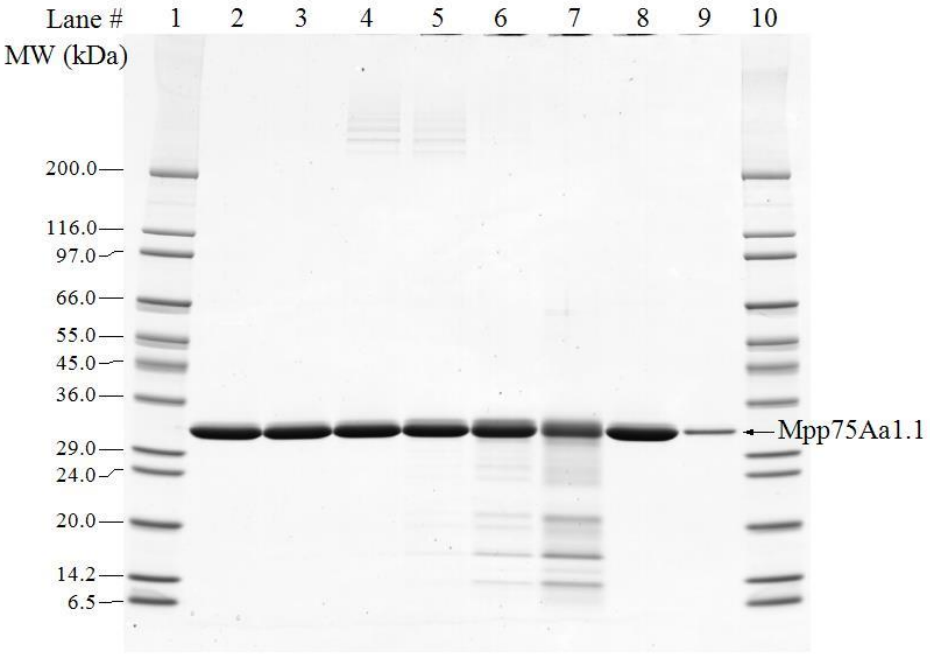

Figure 36. SDS-PAGE of Mpp75Aa1.1 Protein Demonstrating the Effect After 30 Minutes at Elevated Temperatures on Protein Structural Stability

Heat-treated samples of Mpp75Aa1.1 (3.0 µg total protein) separated on a Tris-glycine 4-20 % polyacrylamide gel under denaturing and reducing conditions. The gel was stained with Brilliant Blue G Colloidal. Approximate molecular weights (kDa) are shown on the left and correspond to molecular weight standards in lanes 1 and 10.

Lane	Description	Total Amount
1	SigmaMarker Wide Standards	5.0 µl
2	Mpp75Aa1.1 Protein Control	3.0 µg
3	Mpp75Aa1.1 Protein 25ºC	3.0 µg
4	Mpp75Aa1.1 Protein 37ºC	3.0 µg
5	Mpp75Aa1.1 Protein 55ºC	3.0 µg
6	Mpp75Aa1.1 Protein 75ºC	3.0 µg
7	Mpp75Aa1.1 Protein 95ºC	3.0 µg
8	Mpp75Aa1.1 Protein Reference 100% Equivalence	3.0 µg
9	Mpp75Aa1.1 Protein Reference 10% Equivalence	0.3 µg
10	SigmaMarker Wide Standards	5.0 µl

B.2(b)(iii)(ii) Heat susceptibility of the MON 95275 Vpb4Da2 Protein

The effect of heat treatment on the activity of the *E. coli*-produced Vpb4Da2 protein was evaluated using purified protein. Heat treated samples and an unheated control sample of Vpb4Da2 protein were analyzed: 1) using an insect bioassay to assess the impact of temperature on the functional activity of the Vpb4Da2 protein; and 2) using SDS-PAGE to assess the impact of temperature on protein integrity.

Aliquots of Vpb4Da2 protein were heated to 25, 37, 55, 75 and 95 ºC for either 15 or 30 minutes, while a separate aliquot of Vpb4Da2 protein was maintained on ice for the duration of the heat treatments to serve as a temperature control. The effect of heat treatment on the activity of Vpb4Da2 was evaluated using a insect bioassay. The effect of heat treatment on the integrity of the Vpb4Da2 protein was evaluated using SDS-PAGE analysis of the heated and temperature control Vpb4Da2 protein samples.

Results of the functional activity assay for Vpb4Da2 protein incubated for 15 and 30 minutes are listed in Table 25 and Table 26, respectively. The control sample had an EC_{50} of 10 µg Vpb4Da2 protein/ml diet, thus demonstrating that protein activity was maintained during incubation on ice. Protein activity was retained when incubated for 15 and 30 minutes at a temperature of 25 and 37ºC. No dose-response relationship was observed from the 55, 75 and 95°C heat-treated samples for the 15 minute or 30 minute treatments, respectively. As a result, no EC_{50} values were estimated, indicating that Vpb4Da2 protein had no functional activity in WCR bioassay after the incubation at ≥55°C temperatures for 15 or 30 minutes.

The results of the SDS-PAGE analysis of the heat-treated samples incubated for 15 and 30 minutes are illustrated in Figure 37 and Figure 38, respectively. The control sample loaded on each gel (Figure 37 and Figure 38, lane 2) showed equivalent band intensity to the 100% reference standard (Figure 37 and Figure 38, lane 8), demonstrating that the Vpb4Da2 protein was stable on wet ice during the incubation period. No apparent decrease in band intensity of the ~103.8 kDa Vpb4Da2 protein was observed in the test samples when heated at temperatures of 25, 37 and 55°C for 15 or 30 minutes. Degradation and aggregation products were evident at 55°C for both 15 and 30 minutes. A decrease in the intensity of the main Vpb4Da2 band was evident at 75°C with the most prominent loss of band intensity observed at 30 minutes. In addition, degradation and aggregation products were also evident at 75°C for both the 15 and 30 heat treatments. Incubation for 15 and 30 minutes at 95°C resulted in a significant loss of the Vpb4Da2 band intensity with less than 10% remaining after the 30 minute heat treatment compared to the 10% reference standard. Additionally, both the 15 and 30 minute heat treatments at 95°C exhibited increased smaller molecular weight degradation with less higher molecular weight aggregation as compared to the 55 and 75°C heat-treated samples.

These data demonstrate that the Vpb4Da2 protein remains largely intact but behaves with a predictable tendency toward protein denaturation and loss of functional activity at elevated temperatures. Heat treatment is widely used in the preparation of foods containing components derived from maize grain. Therefore, it is reasonable to conclude that Vpb4Da2 protein would not be consumed as an active protein in food products derived from MON 95275 due to standard processing practices that include heat treatment at or above 55ºC for the majority of foods derived from processed maize (Hammond and Jez, 2011).

For details, please refer to Appendix 13 [redacted], 2021 (TRR0000871)).

Table 25. EC_{50} Values and 95% Confidence Limits (CI) for the Heat Treated Vpb4Da2 Protein After 15 Minutes

Temperature	EC_{50} (µg Vpb4Da2/ml diet)	95% CI (µg Vpb4Da2/ml diet)
0 ºC (control)	10	7.4 - 14
25 ºC	14	11 - 18
37 ºC	14	8.0 - 26
55 ºC[1]	N/A	N/A
75 ºC[1]	N/A	N/A
95 ºC[1]	N/A	N/A

[1] No EC50 value and 95% CI were estimated since no dose-response relationship was observed.

Table 26. EC_{50} Values and 95% Confidence Limits (CI) for the Heat Treated Vpb4Da2 Protein After 30 Minutes

Temperature	EC50 (µg Vpb4Da2/ml diet)	95% CI (µg Vpb4Da2/ml diet)
0 ºC (control)	10	7.4 - 14
25 ºC	10	6.1 - 16
37 ºC	12	6.4 - 24
55 ºC[1]	N/A[2]	N/A
75 ºC[1]	N/A	N/A
95 ºC[1]	N/A	N/A

[1] No EC50 value and 95% CI were estimated since no dose-response relationship was observed

[2] N/A, not available

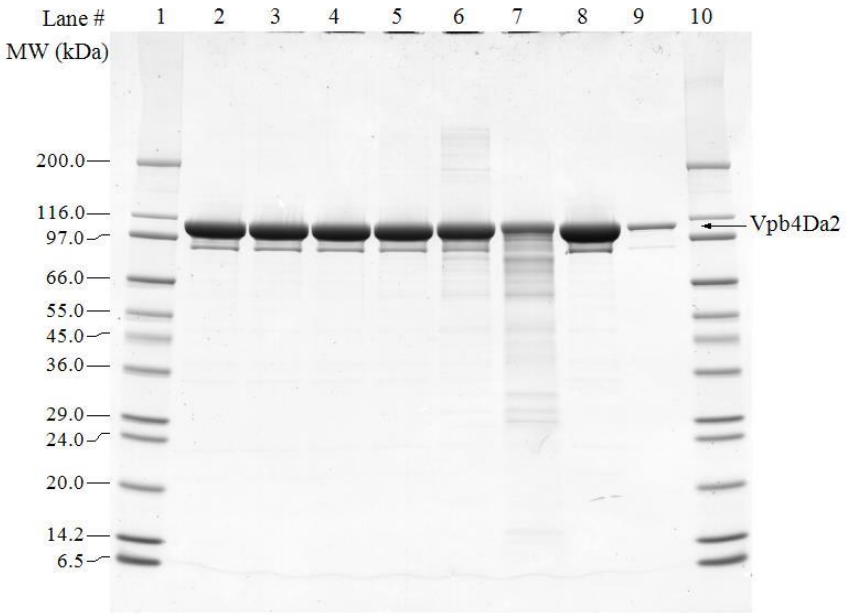

Figure 37. SDS-PAGE of Vpb4Da2 Protein Demonstrating the Effect After 15 Minutes at Elevated Temperatures on Protein Structural Stability

Heat-treated samples of Vpb4Da2 (3.0 µg total protein) separated on a Tris-glycine 4-20 % polyacrylamide gel under denaturing and reducing conditions. The gel was stained with Brilliant Blue G Colloidal. Approximate molecular weights (kDa) are shown on the left and correspond to molecular weight standards in lanes 1 and 10.

Lane	Description	Total Amount
1	SigmaMarker Wide Standards	5.0 µl
2	Vpb4Da2 Protein Control	3.0 µg
3	Vpb4Da2 Protein 25ºC	3.0 µg
4	Vpb4Da2 Protein 37ºC	3.0 µg
5	Vpb4Da2 Protein 55ºC	3.0 µg
6	Vpb4Da2 Protein 75ºC	3.0 µg
7	Vpb4Da2 Protein 95ºC	3.0 µg
8	Vpb4Da2 Protein Reference 100% Equivalence	3.0 µg
9	Vpb4Da2 Protein Reference 10% Equivalence	0.3 µg
10	SigmaMarker Wide Standards	5.0 µl

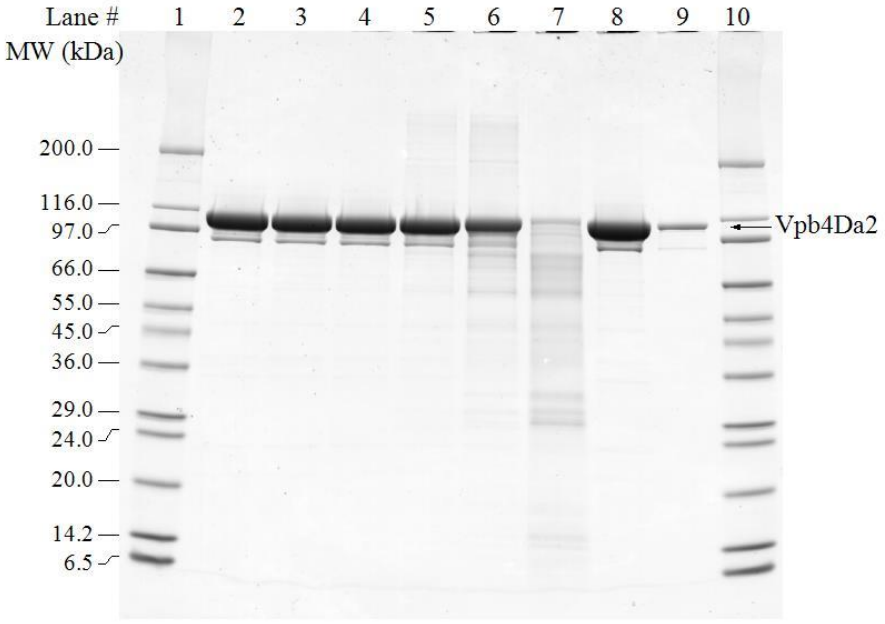

Figure 38. SDS-PAGE of Vpb4Da2 Protein Demonstrating the Effect After 30 Minutes at Elevated Temperatures on Protein Structural Stability

Heat-treated samples of Vpb4Da2 (3.0 µg total protein) separated on a Tris-glycine 4-20 % polyacrylamide gel under denaturing and reducing conditions. The gel was stained with Brilliant Blue G Colloidal. Approximate molecular weights (kDa) are shown on the left and correspond to molecular weight standards in lanes 1 and 10.

Lane	Description	Total Amount
1	SigmaMarker Wide Standards	5.0 µl
2	Vpb4Da2 Protein Control	3.0 µg
3	Vpb4Da2 Protein 25ºC	3.0 µg
4	Vpb4Da2 Protein 37ºC	3.0 µg
5	Vpb4Da2 Protein 55ºC	3.0 µg
6	Vpb4Da2 Protein 75ºC	3.0 µg
7	Vpb4Da2 Protein 95ºC	3.0 µg
8	Vpb4Da2 Protein Reference 100% Equivalence	3.0 µg
9	Vpb4Da2 Protein Reference 10% Equivalence	0.3 µg
10	SigmaMarker Wide Standards	5.0 µl

B.2(b)(iii)(ii) Degradation and Heat Susceptibility of the MON 95275 Mpp75Aa1.1 and Vpb4Da2 Proteins– Conclusions

The stability of a protein to heat or its degradation in the presence of pepsin and pancreatin is a factor in the assessment of its potential toxicity. The degradation of Mpp75Aa1.1 and Vpb4Da2 proteins were evaluated by incubation with solutions containing pepsin and pancreatin, and the results show that Mpp75Aa1.1 and Vpb4Da2 proteins were readily degraded (Sections B.2(a)(ii)(i) and B.2(a)(ii)(ii) respectively). Exposure to heat during food processing or cooking, and to digestive fluids is likely to have a profound effect on the structure and function of proteins.

The effect of heat treatment on the activity of Mpp75Aa1.1 and Vpb4Da2 proteins was evaluated using insect bioassays to assess the impact of temperature on functional activity, and using SDS-PAGE to assess the impact of temperature on protein integrity. The results show that Mpp75Aa1.1 protein was completely deactivated by heating at 55ºC for 30 min or ≥75ºC for 15 min or more (Section B.2(b)(iii)(i)) and Vpb4Da2 protein was completely deactivated by heating at 55ºC or above for 15 min or more (Section B.2(b)(iii)(ii)). Therefore, it is anticipated that exposure to functionally active Mpp75Aa1.1 and Vpb4Da2 proteins from the consumption of MON 95275 or foods derived from MON 95275 is unlikely.

B.2(b)(iv) Specific serum screening where a new protein is derived from a source known to be allergenic or has sequence homology with a know allergen

Not relevant for this product.

B.2(b)(v) Information on whether the new protein(s) have a role in the elicitation of gluten-sensitive enteropathy, in cases where the introduced genetic material is obtained from wheat, rye, barley, oats, or related cereal grains

Not relevant for this product.

B.3 Other (non-protein) New Substances

As described in Section A.3.(f), MON 95275 contains a DvSnf7.1 suppression cassette that expresses an inverted repeat sequence designed to match the sequence in WCR and thereby utilizes the RNAi pathway to control CRW (*Diabrotica* spp.). The expression of the suppression cassette results in the formation of a dsRNA transcript containing a 240 bp fragment of the WCR Snf7 gene (DvSnf7). Upon consumption of MON 95275 by WCR, DvSnf7 dsRNA is recognized by the pest's RNAi machinery, resulting in the down-regulation of the targeted DvSnf7 gene leading to WCR mortality (Bolognesi *et al.*, 2012). The DNA sequence of the 240bp dsRNA (DvSnf7 dsRNA) responsible for an RNAi-based mode of action (MOA) in MON 95275 is identical to that in MON 87411 approved by FSANZ in 2015, A1097) also used to induce the RNAi mechanism in the CRW pests. The only difference between the full length DvSnf7.1 RNA expressed in MON 95275 and the full length DvSnf7 RNA expressed in MON 87411 is 5′ UTR, which was optimized to increase in planta expression.

B.3(a) History of Safe Use of RNA-mediated Gene Suppression in Plants

RNAi-mediated gene suppression is a naturally occurring, ubiquitous process in eukaryotes, including plants and animals consumed as food and feed. Endogenous RNA-mediated gene modulation is responsible for certain characteristics of conventional crops (Tuteja *et al.*, 2004; Kusaba *et al.*, 2003; Della Vedova *et al.*, 2005) and has also been utilized in some biotechnology-derived crops approved for cultivation and use as food and feed (Ivashuta *et al.*, 2009; Petrick *et al.*, 2013; Parrott *et al.*, 2010). The RNAi mechanism has also been leveraged in the development of biotechnology-derived crops with quality traits and with virus resistance (Frizzi and Huang, 2010; Parrott *et al.*, 2010; Kamthan *et al.*, 2015) and has been recently developed as a highly selective tool for insect control (Bachman *et al.*, 2013; Baum *et al.*, 2007a; Mao *et al.*, 2007). Therefore, there is a history of safe consumption of the RNA molecules mediating gene suppression in plants, including those with homology to genes in humans and other animals (Ivashuta *et al.*, 2009; Jensen *et al.*, 2013). Additionally, there is no evidence to suggest that dietary consumption of nucleic acids is associated with toxicity (U.S. FDA, 1992; Petrick *et al.*, 2013) and U.S. EPA has an established tolerance exemption for nucleic acids that are part of PIP products (U.S. EPA, 2001a). U.S. FDA recognizes that all food allergens are proteins (U.S. FDA, 1992; U.S. FDA, 2001) and there is also no evidence of allergenicity of dietary RNA in the peer-reviewed scientific literature. This lack of toxicity or allergenicity for ingested RNA also extends to RNA molecules associated with dsRNA-mediated gene regulation. Therefore an extensive history of safe consumption for dietary RNAs, including dsRNAs, has been established, as reviewed (Dickinson *et al.*, 2013). The reason for this history of safe consumption of dietary RNAs is that extensive sequence-independent physiological and biochemical barriers are known to exist in humans and other animals that limit the potential for uptake or activity of ingested nucleic acids (Juliano *et al.*, 2009; Petrick *et al.*, 2013; O'Neill *et al.*, 2011).

A publication by Zhang et al. (2012a) reported that ingestion of large doses of a particular small (micro) RNA (miRNA) from rice led to some absorption of the miRNA, detection of the miRNA in serum and liver, and an apparent impact on a target protein and plasma LDL in mice Zhang *et al.* (2012a). The authors suggest that a "cross-kingdom" effect – a plant gene product (miR168a) regulating animal gene expression – may be a common phenomenon; and that miRNAs in food may regulate specific genes in animals based upon sequence identity between plant miRNAs and mammalian genes. A second publication (Heinemann *et al.*, 2013), a review article relying almost exclusively on the Zhang et al. (2012a) study, suggests that the current safety/risk assessment approach is insufficient for RNA-based biotechnology-derived products. As previously stated, there are no safety concerns related to the consumption of RNA and RNAi in plants and therefore the current safety assessment approach for biotechnology-derived crops is appropriate for assessing the safety of products expressing RNA-mediated traits. This approach was applied successfully to evaluate the safety of MON 87411 maize, a corn rootworm control trait utilizing RNAi and is also appropriate for evaluation of MON 95275. The following evidence supports this conclusion:

Humans regularly consume plants that contain small RNAs. It has been demonstrated that many existing plant RNAs share sequences with human genes (Ivashuta *et al.*, 2009). In addition to small RNAs, there are also long dsRNAs in plants encoding small RNAs that share sequence identity to human transcripts (Jensen *et al.*, 2013). Further, humans regularly consume animal-

derived foods that are likely to contain more animal miRNAs that have 100% identity to human genes than those miRNAs contained within plants. Despite this routine ingestion of plant and animal small RNAs, no impacts on human health have been reported

A follow-up study to Zhang et al. (2012a) involving Monsanto scientists (Zhang *et al.*, 2012b) revealed confounding factors which likely explain, in part, the unexpected findings in the 2012 study (Zhang *et al.*, 2012a). In this follow-up study, plant miRNAs (including miR168a) were shown to be over-represented relative to their dietary abundance in some public animal small RNA datasets. This indicates that their apparent presence in mouse tissues likely resulted, at least in part, from cross-contamination during the sequencing procedure, thus calling into question the potential for significant uptake of ingested plant miRNAs (Zhang *et al.*, 2012b).

Differences in diet composition, rather than cross-kingdom gene regulation by plant miRNAs, were likely responsible for alterations in plasma LDL cholesterol when Zhang et al. (2012a), fed an all-rice diet to mice (Petrick *et al.*, 2013). These results are consistent with the known challenges to oral delivery of nucleic acids (O'Neill *et al.*, 2011).

Monsanto and miRagen Therapeutics scientists collaborated on a rice feeding study in mice to evaluate claims of dietary miRNA uptake and physiological impact (Dickinson *et al.*, 2013). In this study, miR168a uptake was not reproduced, LDLRAP1 protein levels were unaffected, and LDL was only modulated with a high rice diet and not with a nutritionally balanced rice diet. These results support the conclusion that previously reported observations (Zhang *et al.*, 2012a) were due to variability in gene expression and protein expression data and nutritional differences in animal diets, rather than dietary exposure to miR168a.

Endogenous miRNAs are present in substantial levels in the diets of humans, mice, and honey bees. Snow *et al.* (2013) provide empirical data to demonstrate that despite consumption of these miRNAs, horizontal delivery via oral ingestion from a typical diet is neither frequent nor prevalent in these consuming organisms.

A feeding study in nonhuman primates with a miRNA-rich food source found that, “there is little evidence for presence of these plant miRNA in nonhuman primate blood prior to or following dietary intake of a plant miRNA-rich substance (Witwer *et al.*, 2013).”

Observations of limited RNA uptake due to biological barriers have been made with ingested/orally administered RNA molecules (Rodrigues and Petrick, 2020). USDA and NIH scientists found that miRNA was extensively degraded under *in vitro* digestion conditions and conducted a feeding study in mice with corn, finding that corn miRNAs were not detected in whole blood or tissues after dietary consumption over two weeks (Huang *et al.*, 2018).

A controlled 28-day feeding study in rats did not result in apparent transfer of plant miRNAs to the bloodstream as evaluated in serum (Kang *et al.*, 2017). In addition, these authors conducted a comprehensive survey of more than 800 human data sets within this same publication. They found that dietary miRNAs are detected a very low levels (<5 copies per cell compared to thousands needed for gene suppression) and appear to result from technical artifacts rather than dietary uptake thus supporting the conclusion that contamination (not dietary uptake) is the most

plausible explanation for detection of exogenous miRNAs in mammalian blood samples (Rodrigues and Petrick, 2020).

Numerous barriers (e.g., salivary enzymes, stomach acids/digestive enzymes, nucleases in serum, etc.) to the systemic and cellular uptake of exogenous nucleic acids exist (Petrick *et al.*, 2013; Haupenthal *et al.*, 2006; O'Neill *et al.*, 2011; Akhtar, 2009; Jain, 2008).

Other authors, organizations, and regulatory bodies have looked specifically at biotechnology-derived RNA-based products and support current risk assessment approaches (ILSI-CERA, 2011; Parrott *et al.*, 2010; FSANZ, 2013).

The FSANZ, The U.S. FDA, USDA, and U.S. EPA have approved MON 87411, a RNAi-based trait for corn rootworm control in maize. The U.S. EPA approval carefully considered the food and feed safety of the dsRNA molecule expressed in MON 87411 maize, and conducted an extensive consideration of the safety of the technology and the specific trait by independent experts through use of Scientific Advisory Panels.

Finally, these numerous points regarding the ubiquitous nature of RNA in foods, the known barriers to systemic and cellular uptake of exogenous nucleic acids, the known sequence similarity between some plant and human RNAs, and empirical data demonstrating the lack of adverse impacts on non-target organisms lead us to conclude that expression of DvSnf7 RNA in MON 95275 poses no unique or novel risks.

B.3(b) Characterization and Equivalence of DvSnf7.1 RNA from MON 95275

Despite the long history of exposure to and consumption of nucleic acids, a characterization and safety assessment of the DvSnf7.1 RNA produced in MON 95275 was conducted. The *DvSnf7.1* suppression cassette produces the DvSnf7.1 RNA transcript, which contains an inverted repeat with sequence designed to match the essential gene *Snf7* from *D. virgifera virgifera* and form the 240 bp DvSnf7 dsRNA in MON 95275. The DNA sequence of the inverted repeat in MON 95275 is identical to that in MON 87411. Furthermore, the 240 bp DvSnf7 dsRNA sequence expressed in MON 95275, responsible for an RNAi-based mode of action (MOA), is exactly the same as that expressed in MON 87411, which was previously deregulated/approved. The only difference between DvSnf7.1 RNA expressed in MON 95275 and DvSnf7 RNA expressed in MON 87411 is the leader sequence (See Appendix 1).

A two tiered approach was taken to validate the use of the previously assessed MON 87411 DvSnf7 RNA safety data to support the safety of MON 95275 DvSnf7.1 RNA (Figure 39). First, the equivalence of the plant-produced DvSnf7.1 and *in vitro*-produced DvSnf7.1 RNAs in MON 95275 was demonstrated. To then leverage the previously assessed safety data generated using the *in vitro*-produced DvSnf7 RNA from MON 87411, equivalence between the MON 95275 *in vitro*-produced DvSnf7.1 RNA and MON 87411 *in vitro*-produced RNA (DvSnf7_968) was demonstrated. Confirmation that the *in planta*-produced and *in vitro*-produced DvSnf7.1 RNA in MON 95275 is equivalent allows for the direct comparison of the *in vitro*-produced MON 95275 DvSn7.1 RNA to the *in vitro*-produced MON 87411 RNA (DvSnf7_968). Further confirmation of the equivalence in functional activity between the DvSnf7.1 and DvSnf7 *in vitro*-produced RNAs demonstrates the use of the same RNAi MOA and therefore provides strong support for the use of the MON 87411 DvSnf7 RNA safety data to support the safety of MON 95275 DvSn7.1 RNA.

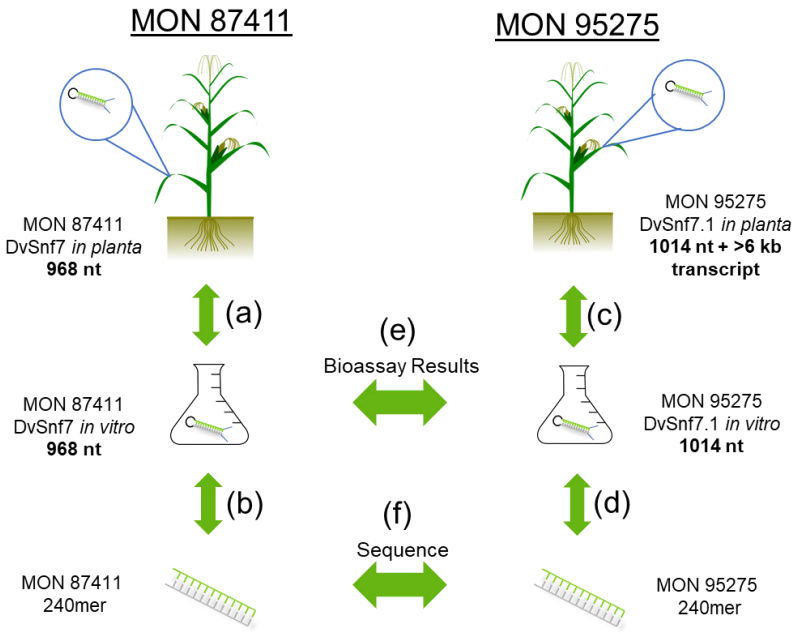

Figure 39. Data to Support Use of MON 87411 DvSnf7 RNA Safety Data to Support the Safety of MON 95275 DvSnf7.1 RNA

(**a**) The functional and molecular equivalence between the MON 87411 mRNA (including *in planta* DvSnf7 RNA) and the MON 87411 *in vitro*-produced DvSnf7 RNA was demonstrated using an insect bioassay and molecular analyses, previously assessed. All submitted safety studies for DvSnf7 RNA were done using the MON 87411 *in vitro*-produced DvSnf7 RNA. (**b**) RNase I_f protection assay and northern blot analysis confirmed the the presence and the size of the 240 nucleotide sized dsRNA active region of DvSnf7 RNA both MON 87411 produced and *in vitro* produced DvSnf7 RNA. Insect bioassay on 240 bp dsRNA sequence adds to weight of evidence supporting the 240 bp sequence of DvSnf7 is the active region, previously assessed. (**c**) The functional and molecular equivalence between MON 95275 mRNA (including *in planta* DvSnf7.1 RNA and the DvSn7.1 read-through transcripts) and the MON 95275 *in vitro*-produced DvSnf7.1 RNA was demonstrated using an insect bioassay and molecular analyses. (**d**) RNase I_f protection assay and northern blot analysis confirmed the the presence and the size of the 240 nucleotide sized dsRNA active region of DvSnf7.1 RNA from both MON 95275 produced and *in vitro* produced DvSnf7.1 RNA (**e**) The functional and molecular equivalence between the MON 87411 *in vitro*-produced DvSnf7 and MON 95275 *in vitro*-produced DvSnf7.1 RNA was demonstrated using an insect bioassay and molecular analysis. (**f**) The DNA sequence of the inverted repeat in MON 95275 is identical to that in MON 87411. Furthermore, the 240 bp DvSnf7 dsRNA sequence expressed in MON 95275, responsible for an RNAi-based mode of action (MOA), is exactly the same as that expressed in MON 87411. This multi tiered approach validates the use of the previously assessed MON 87411 DvSnf7 RNA safety data to support the safety of MON 95275 DvSnf7.1 RNA.

B.3(b)(i) Characterization and Equivalence of the Molecular and Functional Properties of DvSnf7.1 RNA from MON 95275

The characterization and molecular equivalence between MON 95275 DvSnf7.1 RNA and *in vitro*-produced DvSnf7.1 RNA was established by two molecular analyses and a functional assay. The molecular assays include 1) DNA sequencing of the reverse transcribed RNA determined that the sequence of the MON 95275 full length DvSnf7.1 and *in vitro* DvSnf7.1 RNAs was identical, including the sequence within the 240 bp inverted repeat regions; and 2) RNase I_f digestion

followed by northern blot analysis detected the 240 bp dsRNA in MON 95275 DvSnf7.1 RNA and demonstrated its equivalence to the *in vitro* produced DvSnf7.1 RNA. The functional assay also demonstrated equivalent activity for the MON 95275 DvSnf7.1 RNA and *in vitro*-produced DvSnf7.1 RNA.

Taken together, these molecular and functional assay data provide a detailed characterization of MON 95275 DvSnf7.1 RNA and establish its equivalence to the *in vitro*-produced DvSnf7.1 RNA. The equivalence justifies the use of the *in vitro*-produced DvSnf7.1 RNA as a test subtance in the equivalence assessments of MON 87411 *in vitro*-produced RNA (DvSnf7_968) and MON 95275 *in vitro*-produced DvSnf7.1 RNA to support the use of MON 87411 DvSnf7 RNA safety data to support the safety of MON 95275 DvSn7.1 RNA.

For details, please refer to Appendix 14 ([redacted], 2022 (TRR0000514)).

B.3(b)(i)(i) Results of cDNA Sequence Analyses

In order to characterize the MON 95275 DvSnf7.1 RNA, and to demonstrate molecular equivalence between it and *in vitro*-produced DvSnf7.1 RNA, the sequence of MON 95275 DvSnf7.1 cDNA (complementary DNA) was determined. MON 95275 DvSnf7.1 RNA was reverse transcribed to cDNA and amplified by PCR. The consensus sequence of MON 95275 DvSnf7.1 cDNA was aligned to the sequence of cDNA from in vitro-produced DvSnf7.1 RNA, which was previously characterized. This analysis demonstrated that the sequenced regions between MON 95275 DvSnf7.1 cDNA and in vitro-produced DvSnf7.1 cDNA are identical. More importantly, it was shown that there is a 100% sequence identity in the inverted repeat regions between the MON 95275 DvSnf7.1 cDNA consensus sequence and the in vitro-produced DvSnf7.1 cDNA reference sequence. This analysis serves as identity confirmation of the MON 95275 DvSnf7.1 RNA as well as demonstrating the molecular equivalence between MON 95275 DvSnf7.1 RNA and in vitro-produced DvSnf7.1 RNA (Appendix 14).

B.3(b)(i)(ii) Results of RNase I_f Protection Assay and Northern Blot Analysis

MON 95275 mRNA and the *in vitro*-produced DvSnf7.1 RNA were digested by RNase I_f which preferentially digests single-stranded RNA leaving double-stranded RNA regions intact. Each RNase I_f digested sample was loaded in triplicate and subjected to northern blot analysis. The northern blot was hybridized with a DNA probe specific to the 240 nt dsRNA region of the DvSnf7.1 RNA in order to characterize MON 95275 DvSnf7.1 RNA by identifying the presence of the functionally active inverted repeat region of DvSnf7. Additionally, a comparison of the dsRNA regions of the MON 95275 DvSnf7.1 RNA and *in vitro*-produced DvSnf7.1 RNA was conducted using this northern blot analysis to determine equivalence. The results are shown in Figure 40. MON 95275 DvSnf7.1 RNA contains the expected 240 nt dsRNA region of DvSnf7 (Lanes 4-6). This is the expected size of the double stranded functionally active region of the DvSnf7 (Bolognesi *et al.*, 2012). Furthermore, the RNase I_f digested *in vitro*-produced DvSnf7.1 RNA exhibits a single dsRNA species, at approximately 240 nt (Lanes 1-3), similar to MON 95275 DvSnf7.1 RNA (Lanes 4-6), indicating that MON 95275 DvSnf7.1 RNA and the *in*

vitro-produced DvSnf7.1 RNA are equivalent with respects to the size of their dsRNA functionally active regions.

For details, please refer to Appendix 14 ([redacted], 2022 (TRR0000514)).

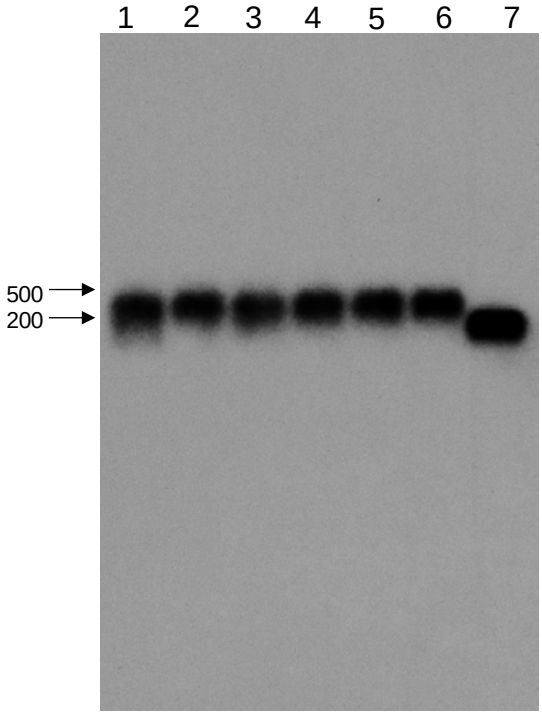

Figure 40. Northern Blot Analysis to Confirm the Equivalence between the dsRNA *in in vitro*-produced DvSnf7.1 RNA and MON 95275 DvSnf7.1 RNA

The blot was hybridized with a ^{32}P-labled, DvSnf7 probe specific to the 240 bp dsRNA. Lanes 1-3 contain ~0.42 ng of *in vitro* DvSnf7.1 RNA that was RNase I_f digested and lanes 4-6 contain an equivalence of ~0.42 ng MON 95275 DvSnf7.1 RNA presented in the MON 95275 poly (A) RNA also subjected to RNase I_f digestion. Lane 7 contains ~0.22 ng of the DvSnf7 probe template. Lane designations are as follows:

Lane	**Sample**
1	*In vitro*-produced DvSnf7.1 RNA (RNase I_f digested)
2	*In vitro*-produced DvSnf7.1 RNA (RNase I_f digested)
3	*In vitro*-produced DvSnf7.1 RNA (RNase I_f digested)
4	MON 95275 poly (A) RNA (RNase I_f digested)
5	MON 95275 poly (A) RNA (RNase I_f digested)
6	MON 95275 poly (A) RNA (RNase I_f digested)
7	DvSnf7 DNA template

Arrows denote the size of the RNA, in bases, obtained from the High Range Ribo Ruler ladder.

B.3(b)(i)(iii) Results of Functional Activity Analysis

Southern corn rootworm (SCR, *Diabrotica undecimpunctata*) larvae were used to measure the functional activity, measured as an LC_{50}, of the test and reference substances. Three bioassay replicates were conducted on different days, each using a separate batch of insects. MON 95275 DvSnf7.1 RNA contained in MON 95275 mRNA and *in vitro* DvSnf7.1 RNA were assessed in parallel during each bioassay replicate which consisted of a geometric series of dilutions expected to elicit a response from the SCR larvae that allowed for the estimation of an LC_{50} value.

The mean LC_{50} values estimated for the MON 95275 mRNA and *in vitro*-produced DvSnf7.1 RNA were 2.1 (± SE 0.27) and 4.2 (± SE 1.55) ng DvSnf7.1 RNA/mL diet, respectively (Table 27). The results confirm that the functional activity of the MON 95275 mRNA is not significantly different from the activity of the *in vitro*-produced DvSnf7.1 RNA ($p = 0.260$, $\alpha = 0.05$) (Table 28).

Table 27. LC50 Values and 95% Confidence Intervals (CIs) for the *in vitro*-Produced DvSnf7.1 RNA and MON 95275 mRNA in a 12-day SCR Diet-Incorporation Bioassay

Test or Reference Substance	Bioassay Replicate	LC_{50} Values (ng DvSnf7.1 RNA/mL diet)	95% CI (ng DvSnf7.1 RNA/mL diet)
In vitro DvSnf7.1	1	4.2	2.8 – 6.0
In vitro DvSnf7.1	2	6.8	2.3 – 114.6
In vitro DvSnf7.1	3	1.5	0.4 – 3.9
Mean LC_{50} value of *in vitro*-produced DvSnf7.1: 4.2 (± SE 1.55) ng DvSnf7.1 RNA/mL diet			
MON 95275 mRNA	1	2.6	1.4 – 4.7
MON 95275 mRNA	2	1.7	1.1 – 2.5
MON 95275 mRNA	3	2.0	1.2 – 3.1
Mean LC_{50} value of MON 95275 DvSnf7.1: 2.1 (± SE 0.27) ng DvSnf7.1 RNA/mL diet			

Table 28. Comparison between *in vitro* DvSnf7.1 RNA and MON 95275 mRNA

Source	Source	Difference	Standard Error	DF	P-value
in vitro-produced DvSnf7.1 RNA	MON 95275 mRNA	2.1	1.57	4	0.260

B.3(b)(ii) Comparison and Equivalence of DvSnf7.1 RNA in MON 95275 and DvSnf7 RNA in MON 87411

The *DvSnf7.1* suppression cassette produces the DvSnf7.1 RNA transcript, which contains an inverted repeat with sequence designed to match the essential gene *Snf7* from *D. virgifera virgifera* and form the 240 bp DvSnf7 dsRNA in MON 95275. The DNA sequence of the inverted repeat in MON 95275 is identical to that in MON 87411. Furthermore, the 240 bp DvSnf7 dsRNA sequence expressed in MON 95275, responsible for an RNAi-based mode of action (MOA), is exactly the same as that expressed in MON 87411, which was previously deregulated/approved. The only difference between DvSnf7.1 RNA expressed in MON 95275 and DvSnf7 RNA expressed in MON 87411 is the leader sequence.

The comparison and equivalence between DvSnf7.1 RNA in MON 95275 and DvSnf7 RNA in MON 87411 was established by molecular and a functional assay. The molecular assessment used RNase I_f digestion followed by northern blot analysis to demonstrate that the expected 240 bp dsRNA was contained in both the full length DvSnf7.1 and full length DvSnf7_968 RNA. Lastly, functional equivalence between the two *in vitro*-produced full length DvSnf7.1 RNA and DvSnf7 RNA was demonstrated by diet-incorporation bioassay, and each elicited comparable concentration-dependent mortality responses in a sensitive insect.

The molecular and functional assay data demonstrate that the DvSnf7.1 RNA in MON 95275 and the DvSnf7_968 RNA in MON 87411 share the same ~240 bp dsRNA responsible for the RNAi MOA and are functionally equivalent. Taken together, this information provides justification for the use of previously assessed DvSnf7 RNA safety data from MON 87411 to support the safety of Dvsnf7.1 RNA in MON 95275.

For details, please refer to Appendix 15 ([redacted], 2022 (TRR0001178)).

B.3(b)(ii)(i) RNase I_f Protection Assay and Northern Blot Analysis

The in vitro DvSnf7.1 and in-planta mRNA present in MON 95275, and in vitro DvSnf7_968 and in-planta mRNA present in MON 87411 were digested by RNase If which preferentially digests single stranded RNA leaving dsRNA regions intact. Each RNase If digested sample was loaded in triplicate and subjected to Northern blot analyses. By hybridizing with the DvSnf7 probe that is specific to 240 nt DvSnf7 inverted repeat sequence, any RNA molecules that contain the DvSnf7 sequence will produce a hybridization signal.

The expected ~240 nt dsRNA was detected in RNase If-digested in vitro DvSnf7.1 (Figure 41, lanes 1-3), RNase If-digested in-planta mRNA from MON 95275 (Figure 41, lanes 4-6), RNase If digested in vitro DvSnf7_968 (Figure 41, lanes 7-9), and RNase I-f-digested in-planta mRNA from MON 87411 (Figure 41, lanes 10-12).

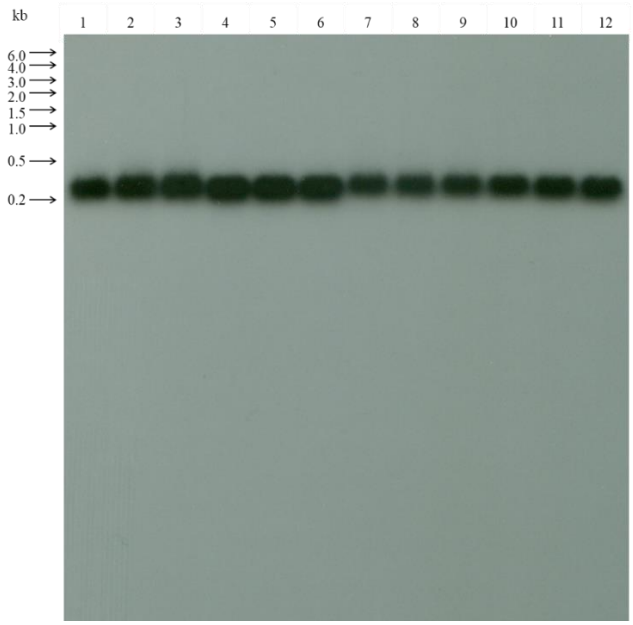

Figure 41. Northern Blot Analysis of RNase If-digested DvSnf7.1, MON 95275 mRNA, DvSnf7_968, and MON 87411 mRNA

RNase I_f-digested DvSnf7.1, MON 95275 mRNA, DvSnf7_968, and MON 87411 mRNA were resolved on a 2% agarose/~6.7% formaldehyde gel and hybridized with the DvSnf7 probe. Lane designations are as follows:

Lane	
1	~0.42 ng RNase I_f-digested DvSnf7.1 RNA
2	~0.42 ng RNase I_f-digested DvSnf7.1 RNA
3	~0.42 ng RNase I_f-digested DvSnf7.1 RNA
4	~2.5 µg RNase I_f-digested MON 95275 mRNA
5	~2.5 µg RNase I_f-digested MON 95275 mRNA
6	~2.5 µg RNase I_f-digested MON 95275 mRNA
7	~0.42 ng RNase I_f-digested DvSnf7_968 RNA
8	~0.42 ng RNase I_f-digested DvSnf7_968 RNA
9	~0.42 ng RNase I_f-digested DvSnf7_968 RNA
10	~0.75 µg RNase I_f-digested MON 87411mRNA
11	~0.75 µg RNase I_f-digested MON 87411 mRNA
12	~0.75 µg RNase I_f-digested MON 87411 mRNA

Arrows denote the size of the RNA, in kilobases, obtained from the RiboRuler High Range RNA Ladder (Thermo Scientific) on the ethidium bromide stained gel.

B.3(b)(ii)(ii) Functional Activity Analysis

In a 12-day diet-incorporation bioassay, the southern corn rootworm (SCR, *Diabrotica undecimpunctata*) demonstrated nearly identical concentration-dependent mortality response to the *in vitro*-produced full length MON 95275 DvSnf7.1 RNA and MON 87411 DvSnf7_968 RNA. Mean LC_{50} values for DvSnf7.1 and DvSnf7_968 were 4.5 ± 2.13 ng/mL diet and 5.2 ± 0.26 ng/mL diet, respectively (Table 29). A t-test indicated no significant difference between these values (p = 0.758) (Table 30).

Table 29. Individual and Mean LC50 Values and 95% Confidence Intervals (CIs) for DvSnf7.1 and DvSnf7_968 in a 12-Day Diet Incorporation Bioassay

Treatment	Bioassay Replicate	LC_{50} (ng DvSnf7/mL diet)	95% CI (ng DvSnf7 /mL diet)
DvSnf7.1 RNA	1	8.8	5.6 - 14
	2	2.3	1.4 – 3.9
	3	2.5	1.6 – 3.9
Mean LC_{50} ± SE: 4.5 ± 2.13 ng DvSnf7.1/mL diet			
DvSnf7_968 RNA	1	5.7	3.6 – 9.2
	2	5.1	3.2 – 8.3
	3	4.8	3.9 – 5.9
Mean LC_{50} ± SE: 5.2 ± 0.26 ng DvSnf7 968/mL diet			

Table 30. t-Test Comparison between DvSnf7.1 and DvSnf7_968

Source	Source	Difference	Standard Error	p-Value
DvSnf7.1 RNA	DvSnf7_968 RNA	-0.67	1.889	0.758

*Significant at α=0.05

B.3(c) Characterization of DvSnf7.1 Read-through Transcripts in MON 95275

Analysis of DvSnf7.1 expression by high molecular weight (HMW) northern blot showed the expected full length transcript of ~1.4 kb and smaller transcripts, which most likely represent a population of processed intermediates derived from DvSnf7.1, across all generations. In addition, the HMW northern blot for DvSnf7.1 RNA also showed an additional, but less intense > 6kb band. Additional analysis of this > 6kb band by sequencing demonstrated three read-through transcripts from the DvSnf7.1 suppression cassette containing sequence from the plant genomic region flanking the 3' end of the insert. Digestion of the MON 95275 RNA with RNase If, an enzyme that digests single stranded RNA, followed by northern blotting with a DvSnf7 probe produces only the expected 240 bp DvSnf7 dsRNA (see Section B.3(b)(i)(ii)) indicating that the full length DvSnf7.1 transcript and >6 kb read-through transcripts are processed to generate only the expected 240 bp dsRNA responsible for the RNAi MOA and no other dsRNAs, the same as MON 87411. Limited RNA transcriptional read-through is a normal phenomenon of gene expression (Xing *et al.*, 2010).

As with the full length DvSnf7.1 transcript, these additional low-abundance transcripts are not expected to be translated to generate any peptide(s) or protein(s), because it is known that the stem-loop structure of dsRNA inhibits ribosome scanning and protein translation (Kozak, 1989). Even though no peptides or proteins are expected to be produced from the read-through transcripts, start codon analysis and bioinformatics using all potential putative peptides sequences against a curated protein allergen database (AD_2021), a comprehensive protein toxin database (TOX_2021) and an "all proteins" database (PRT_2021) confirmed none of the theoretical peptides yielded meaningful alignments that reflected potential allergenicity or toxicity. Therefore, the read-through transcripts produced by the DvSnf7.1 suppression cassette are not expected to be translated to any peptides(s) or protein(s) that may cause any safety concern.

For details of the materials and methods for the read-through DvSn7.1 RNA transcripts, please refer to Appendix 16 [redacted] 2021 (TRR0001021)). A summary of the data obtained to support a conclusion of RNA equivalence and no safety concern of the read-through transcripts is provided below.

B.3(c)(i) Northern Blot Analysis of DvSnf7.1 RNA in MON 95275 Tissues

Total RNA extracted from the leaf, root, pollen and grain tissues of MON 95275, and leaf tissue from the control substance were subjected to Northern blot analyses. By hybridizing with the DvSnf7 probe generated from the DvSnf7.1 suppression cassette, any RNA molecules that contain the DvSnf7 sequence will produce a hybridization signal.

Approximately 10 µg of total RNA were resolved on a 1.5% agarose/ ~7% formaldehyde gel. After the transfer of the RNA onto a nylon membrane, the blot was hybridized with the DvSnf7 probe (Figure 42, Panel A). Total RNA from the conventional controls showed no detectable hybridization bands, as expected (Figure 42, Panel A, Lane 1). The total RNA isolated from root and leaf of MON 95275 produced the expected hybridization bands of ~1.4 kb unprocessed transcripts and smaller transcripts which most likely represent a population of processed intermediates derived from DvSnf7.1 (Figure 42, Panel A, Lane 2 and Lane 5). In addition,

unexpected larger bands were also detected in leaf (Figure 42, Panel A, Lane 5). Neither expected nor unexpected bands were detected in both grain and pollen tissues indicating the DvSnf7.1 expression is below the level of detection by northern blot (Figure 42, Panel A, Lane 3 and Lane 4). Ethidium bromide staining of the agarose/formaldehyde gel indicated that the total RNA from conventional and test substance tissues were of similar intensity, suggesting equal loading of the test and control RNA samples (Figure 42, Panel B).

For details, please refer to Appendix 16 ([redacted] 2021 (TRR0001021)).

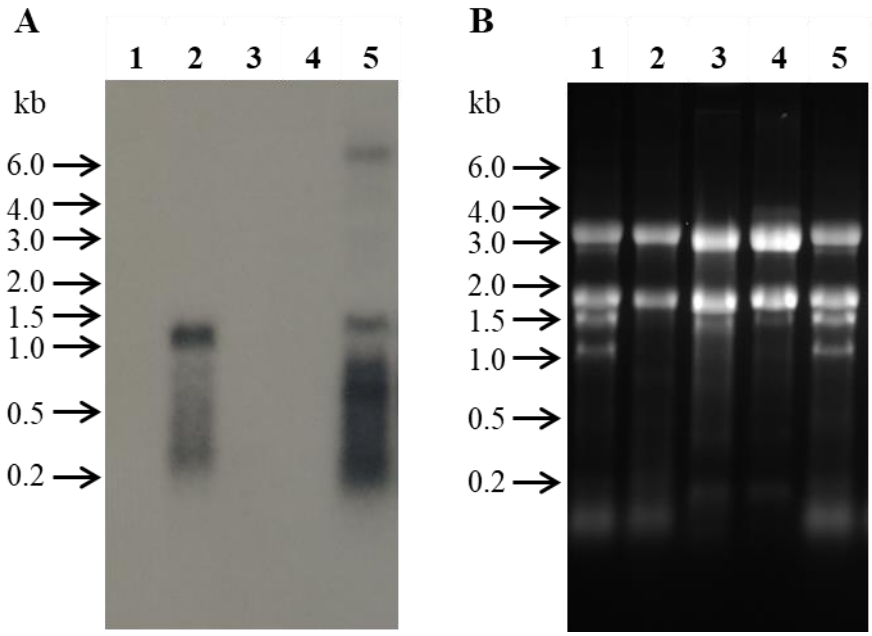

Figure 42. Northern Blot Analysis of DvSnf7.1 RNA in MON 95275 Tissues

Approximately 10 µg of total RNA from control and test substances were resolved on a 1.5% agarose/~7% formaldehyde gel. Panel A is the Northern blot hybridized with the DvSnf7 probe. Panel B is the fluorescent image of the ethidium bromide stained formaldehyde/agarose gel prior to transfer onto a nylon membrane. Lane designations are as follows:

Lane	
1	Conventional Control Leaf
2	MON 95275 Root
3	MON 95275 Grain
4	MON 95275 Pollen
5	MON 95275 Leaf

Arrows denote the size of the RNA, in kilobases, obtained from the RiboRuler High Range RNA Ladder (Thermo Scientific) on the ethidium bromide stained gel.

B.3(c)(ii) Sequence of the Extra Transcripts

In order to determine the sequence of the unexpected transcripts, cDNA from MON 95725 leaf tissue was synthesized and sequenced using PacBio. Raw PacBio reads from MON 95275 leaf cDNA were used to generate circular consensus sequence (CCS) reads, which were then clustered to generate high quality isoforms (Predicted accuracy > 99%). Redundant isoforms were merged and grouped. Northern blot analyses§ (data not shown) with a probe specific to S-Isr-1, which is upstream of Dvsnf7.1 suppression cassette (Figure 1 in Appendix 6), or with a probe specific to 390 bp genomic sequence, which is downstream of the DvSnf7.1 suppression cassette (Figure 43), demonstrated that extra transcripts are likely read-through transcripts from the DvSnf7.1 suppression cassette into the neighboring genomic DNA. To confirm this hypothesis, these nonredundant isoforms were BLASTed with 390 bp genomic sequence downstream of the DvSnf7.1 suppression cassette or ~1000 bp sequence 5′ of gene GRMZM2G017404-, which is further downstream of DvSnf7.1 suppression cassette (see Figure 43, panel B).

The DvSnf7.1 transcript isoforms identified by BLAST matched the sequence from downstream of DvSnf7.1 suppression cassette, indicating that they are read-through transcripts. The DvSnf7.1 read-through transcription initiates predominantly at base 3 in the L-35Sa leader sequence. The rest of the isoforms initiate either at the last base of P-35S[a] Promoter or at base 2 of the L-35S[a] leader sequence. All read-through transcript isoforms contain T-E9 terminator, T-DNA right border and flanking genomic sequence. In addition, read-through transcripts also contain the sequence from the adjacent endogenous gene GRMZM2G017404, and terminate at the end of the last exon of GRMZM2G017404 (Figure 43, panel A). Since both 3′ RACE (see below) and PacBio rely on the poly A tail of mRNA to amplify and sequence products, the identification of products indicates that read-through transcripts are polyadenylated. There is a gap in the sequence corresponding to the inverted repeat region. The isoforms likely contain this double stranded region, though we were not able to sequence through it. This is not unexpected, given the strong secondary structure formed with the inverted repeat. It has been demonstrated that polymerases involved in reverse transcription (Zhang *et al.*, 2001) and PCR (Viswanathan *et al.*, 1999), both necessary steps in the PacBio RNA sequencing procedure, can jump over double stranded nucleic acid regions of the template. Consistent with this hypothesis, the attempt to amplify through the inverted repeat region by 3′ RACE from the read-through transcript also failed, due to the secondary structure from inverted repeat. Instead, two overlapping fragments spanning one DvSnf7[p] repeat, T-E9 terminator, the flanking genomic region, and the downstream endogenous gene GRMZM2G017404 were amplified and sequenced (Figure 43, panel B). Sequencing of these RT-PCR products demonstrates that read-through transcripts contain one of the expected DvSnf7[p] repeat sequences. Although there is no direct evidence for the presence of the other DvSnf7[p] repeat, it is likely that it is also present in the read-through transcripts, therefore, this DvSnf7[p] repeat sequence was included in the bioinformatics analysis (described below) to evaluate the potential outcome of the read-through transcript.

§ Northern blot analyses are in the data package of REG-2020-0035.
a Superscript in P-35S and L-35S indicates that these two elements are merged and labeled as P-35S in plasmid map of PV-ZMIR525664 in Figure 1 in Appendix 16
p Superscript in DvSnf7 indicates the partial sequence.

There are three major read-through transcript variants: one has two unspliced introns (intron 1 and intron 7) for GRMZM2G017404, one has one unspliced intron (intron 1) for GRMZM2G017404, and one has no intron retention for GRMZM2G017404, transcripts 1, 2 and 3, respectively in Figure 43, panel A. The sequence alignment of read-through transcript variants with the first DvSnf7^{P} repeat sequence added are shown in Figure 44.

For details, please refer to Appendix 16 [redacted]., 2021 (TRR0001021)).

B.3(c)(iii) Bioinformatic Analysis of Read-Through Transcripts

B.3(c)(iii)(i) Assessment of Start Codon

Although the likelihood of translation of ORFs from any of the three transcripts is low due to the positioning of any start codons downstream of the DvSnf7 inverted repeat which would restrict, if not eliminate, the potential for translation initiation (see discussion below), start codon analysis was performed on three read-through transcripts identified in MON 95275 by long read (PacBio) sequencing. The relationship among the three transcripts is shown in Figure 43, panel A).

Each transcript was evaluated for the presence of ATG codons, the likelihood of translation initiation from that codon and the resultant ORFs (open reading frames) of 8 amino acids or greater as depicted in Appendix 16, Figures 1-3. General features in Appendix 16, Figures 1-3 include, a low number of start codons with favorable context as shown in green and to a lesser extent yellow ORF color, a low density of ORFs in the interval of ~1500 nucleotides through ~3000 nucleotides and a long ORF that includes a favorable start codon in transcript 3 that reflects a presumptive gene, GRMZM2G017404, in the genomic DNA. The assignments of start context were based upon the work of Gupta et al., 2016 where they evaluated a dataset of 107,659 monocot start codons found in published coding sequences and mRNAs.

As is depicted in Appendix 16, the context of the majority of the start codons in the three read-through transcripts is poor. Of those that are of the highest start context quality, all appear to be associated with the presumptive endogenous gene located downstream of nucleotide coordinate ~2600 and would likely be present in endogenous transcripts. Likewise, nucleotide coordinates 1 to ~1000 would be expected to be found in transcripts as they are part of the DvSnf7.1 RNA molecule produced by the transgene. Therefore, the region of most interest lies between nucleotide coordinates ~1000-2600 as this is a transcription product that is unique to and common among the three read-through transcripts.

In addition to having potential start codons whose contexts are of low quality that limit the likelihood that they could effectively initiate translation, the positioning of these start codons downstream of the DvSnf7 would further restrict, if not eliminate, the potential for translation initiation. In eukaryotes, translation is initiated through recruitment of ribosome components binding to the 5′ cap structure and assembling into a 43S complex that scans the mRNA until a contextually correct start codon is identified. Once such a codon is identified the 60S ribosomal subunit is added yielding a translation competent ribosome. While the 43S complex can melt dsRNA, there is an upper limit to inverted repeat length of 20 bp at which point the complex stalls

and scanning ceases (Kozak, 1989). Under such a scenario the DvSnf7 inverted repeat will prevent translation of the read-through transcripts.

Since inverted repeat RNA is degraded by endogenous RNase activity, the remaining ssRNA would extend from a nucleotide coordinate of ~1000 through the respective distal end of the three read-through transcripts. Assuming it too was not degraded by endogenous RNase, it could potentially serve a mRNA-like function. However, since this RNA would not have a 5′ cap structure, it would not facilitate ribosome component binding, scanning and 80S ribosome assembly. Moreover, de-capped RNA is subject to nucleolytic degradation (Łabno et.al., 2016 and references therein).

A number of mechanisms are known to facilitate translation of uncapped RNA or an mRNA that has dsRNA blocking 43S complex scanning are known to exist. Such non-canonical translation initiation involves CITEs (Cap Independent Translation Elements, TISUs (Translation Initiator of Short 5′ UTR), ribosomal shunting or IRES (Internal Ribosome Entry Site) sequences (Kwan and Thompson, 2019). Both CITEs and TISUs are highly specialized mechanisms and are unlikely to be of consequence for the read-through transcripts. CITEs mediated translation occurs on mRNAs derived from plant viruses that lack 5′ cap structures and poly-A tails. CITEs are found in the 3′ UTR where they recruit the 40S ribosomal subunit which is then brought into proximity of the 5′ UTR through RNA-RNA interactions that lead to ribosome assembly on the 5′ UTR and mRNA scanning. TISU is a 5′ cap dependent mechanism that is employed by housekeeping gene transcripts having 5′ UTRs of fewer than 30 nucleotides. Ribosomal shunting and IRES mediated non-canonical translation initiation are employed in response to environmental stresses such as hypoxia, apoptosis, or starvation. Furthermore, hosts responding to viral infection and viruses themselves employ mechanisms of non-canonical translation initiation. Ribosomal shunting involves limited cap-dependent scanning until the ribosomal complex reaches a donor site upstream of a structurally complex segment in the 5′ untranslated region. At this point it "shunts" over the complex region and lands at a start codon acceptor site where translation is initiated. IRES sequences were first identified in viral genomes and more recently have been identified in a number of cellular genes involved in stress response. They vary in size from 9 to ~1000 nucleotides and as of this time do not have any identifiable consensus sequence feature. Moreover, IRES elements have a broad range of initiation factor requirements. Non-canonical translation initiation through shunting or IRES elements occurs in response to extreme environmental stress or as a means of viral propagation. Therefore, it is unlikely that non-canonical translation initiation occurs with any transcript be it endogenous or read-though under most environmental conditions. If environmental conditions were such that non-canonical translation initiation of endogenous transcripts was to occur, there is still no identifiable characteristic in the read-through transcripts to indicate they would support non-canonical translation initiation. In conclusion it is highly unlikely that the read-through transcripts would yield translation products.

B.3.(c)(iii)(ii) Assessment of Potential Allergenicity, Toxicity, Adverse Biological Activity

However, if one of the three read-through transcripts was able to initiate non-canonical translation, all putative peptide sequences were evaluated using the FASTA36 algorithm and the AD_2021, TOX_2021 and PRT_2021 databases. Since the three transcripts shared common putative

translation products and also had unique transcript specific putative translation products, the analyses are reported as groups in Tables 1-12 in Appendix 16. Tables 1-3 reflect the common putative peptides and Tables 4-6, 7-9 and 10-12 reflect unique putative peptides from transcripts 1, 2 and 3, respectively. Searches of the AD_2021 database did not yield alignments displaying exact eight amino acids match, alignments displaying 35% identity with 80 amino acids or an E-value ≤ 1e-5. Likewise, no alignments displaying an E-value ≤ 1e-5 were recovered in searches of the TOX_2021 database. Searches of the PRT_2021 database positively identified the DvSnf7 sequence among the common putative peptides (described as "Sequence 21980 from patent US 9238822" in Table 3 in Appendix 16). Similarly, the presumptive downstream product of GRMZM2G017404, "BTB/POZ domain-containing protein" was identified in the three read-through transcripts and reported in Tables 6, 9 and 12 both as protein segments due to the retention of introns and as a complete protein. Finally, isolated alignments were identified with unnamed protein products from a grass species *Digitaria_exelis* that are full contained within BTB/POZ domain-containing protein coding sequence albeit on a different reading frame.

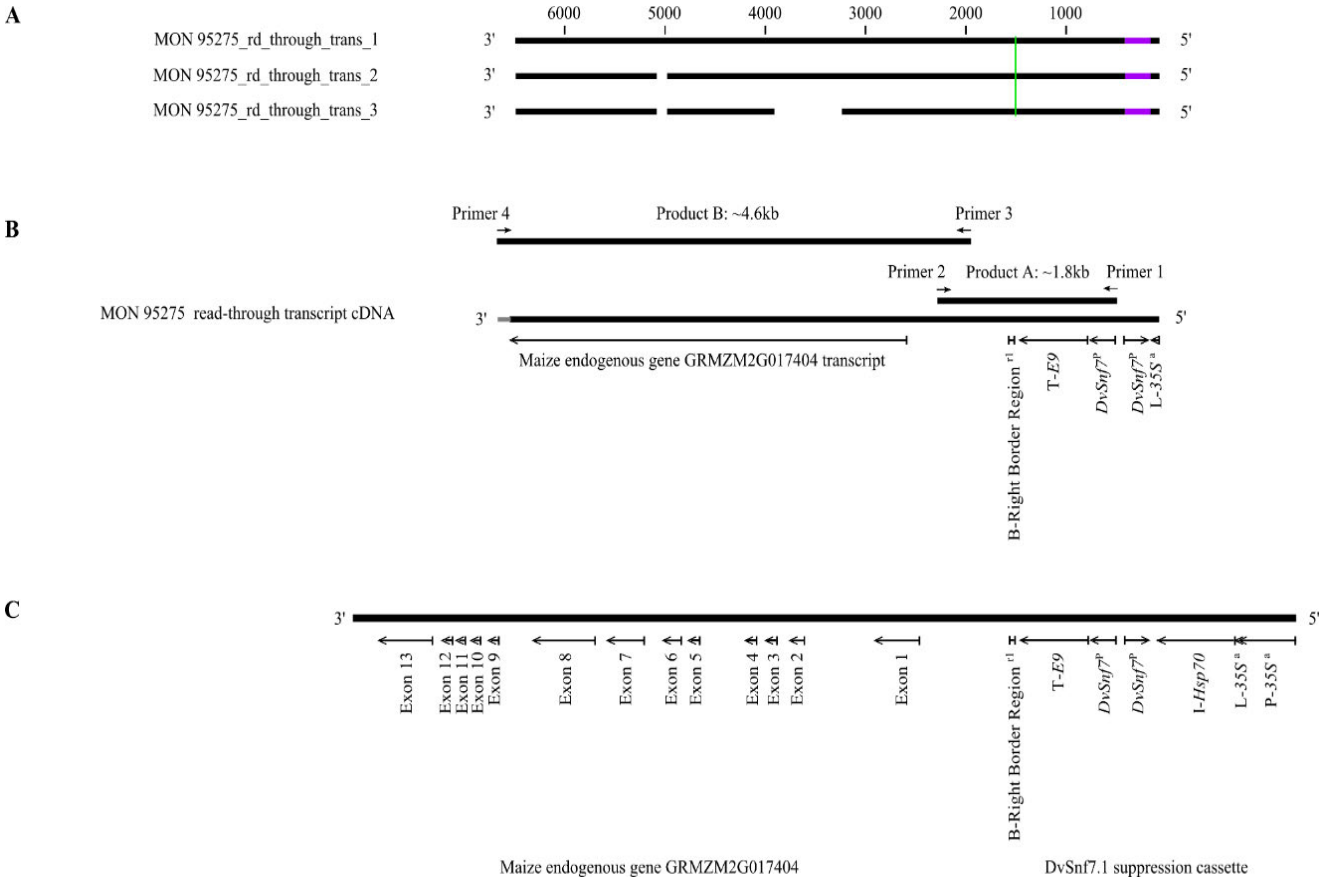

Figure 43. Transcript Mapping, PCR Amplification, and DNA Sequence Map of DvSnf7.1 Read-through from MON 95275

A) MON 95275 DvSnf7.1 read-through transcript mapping. The three transcripts were mapped relative to the longest transcript (MON_95275_rd_through_trans_1), which contains intron 1 and intron 7 from GRMZM2G017404. Transcript 2 (MON_95275_rd_through_trans_2) contains intron 1 from GRMZM2G017404 and transcript 3 (MON_95275_rd_through_trans_3) contains no introns from GRMZM2G017404. The green vertical line shows the location of the inserted DNA-Genomic DNA junction and the scale reflects 1000 nucleotide intervals in the sequences. The purple segment represents the first DvSnf7 inverted repeat sequence that was not confirmed by PacBio or RT-PCR. The gaps in transcripts 2 and 3 indicate the removal of introns. B) The illustration of the DvSnf7.1 read-through transcript cDNA. PCR was performed on MON 95275 DvSnf7.1 read-through transcript cDNA using two pairs of primers to generate overlapping PCR fragments for NovaSeq. The expected product size for each amplicon and the primers used are provided in the illustration. The gray segment at 3′ end of DvSnf7.1 read-through transcript cDNA represents sequence of GeneRacer Oligo dT primer. The gene specific PCR primers used for the amplification of Product A are: Primer 1 (5′-CGCTTTATCACGATACCTTCTACCAC) and Primer 2 (5′-AAACAATAAGTCAGTACGACCC). The PCR primers used for the amplification of Product B is gene specific Primer 3 (5′-ATTTAGATCATCCTTCACCCTC) and GeneRacer 3′ specific Primer 4. C) The depiction of the DvSnf7.1 suppression cassette and adjacent gene GRMZM2G017404. The introns for GRMZM2G017404 are between the exons, numbered from right to left with the intron 1 being between exons 1 and 2.

p Superscript in DvSnf7 indicates the partial sequence.
r1 Superscript in Right Border Region indicates that the sequence in MON 95275 was truncated compared to the sequence in the plasmid vector PV-ZMIR525664.
a Superscript in P-35S and L-35S indicates that these two elements are merged and labeled as P-35S in plasmid map of PV-ZMIR525664 in Figure 1 in Appendix 16.
GRMZM2G017404 is an uncharacterized maize endogenous gene (https://maizegdb.org/gene_center/gene/GRMZM2G017404).

```
Variant 3       ACGCTGAAATCACCAGTCTCTCTCTACAAATCTATCTCTCTCTATTTTCCGTACGACCGT
Variant 2       ACGCTGAAATCACCAGTCTCTCTCTACAAATCTATCTCTCTCTATTTTCCGTACGACCGT
Variant 1       ACGCTGAAATCACCAGTCTCTCTCTACAAATCTATCTCTCTCTATTTTCCGTACGACCGT

Variant 3       CTTCGATACCAAGCGGGAGCTCGACGTCCCTCAGCAGTCGCTGTGCGATACCATCCATGA
Variant 2       CTTCGATACCAAGCGGGAGCTCGACGTCCCTCAGCAGTCGCTGTGCGATACCATCCATGA
Variant 1       CTTCGATACCAAGCGGGAGCTCGACGTCCCTCAGCAGTCGCTGTGCGATACCATCCATGA

Variant 3       TATCGTGAACATCATCTACATTCAAATTCTTATGAGCTTTCTTAAGGGCATCTGCAGCAT
Variant 2       TATCGTGAACATCATCTACATTCAAATTCTTATGAGCTTTCTTAAGGGCATCTGCAGCAT
Variant 1       TATCGTGAACATCATCTACATTCAAATTCTTATGAGCTTTCTTAAGGGCATCTGCAGCAT

Variant 3       TTTTCATAGAATCTAATACAGCAGTATTTGTGCTAGCTCCTTCGAGGGCTTCCCTCTGCA
Variant 2       TTTTCATAGAATCTAATACAGCAGTATTTGTGCTAGCTCCTTCGAGGGCTTCCCTCTGCA
Variant 1       TTTTCATAGAATCTAATACAGCAGTATTTGTGCTAGCTCCTTCGAGGGCTTCCCTCTGCA

Variant 3       TTTCAATAGTTGTAAGGGTTCCATCTATTTGTAGTTGGGTCTTTTCCAATCGTTTCTTCT
Variant 2       TTTCAATAGTTGTAAGGGTTCCATCTATTTGTAGTTGGGTCTTTTCCAATCGTTTCTTCT
Variant 1       TTTCAATAGTTGTAAGGGTTCCATCTATTTGTAGTTGGGTCTTTTCCAATCGTTTCTTCT

Variant 3       TTTTGAGGGCTTGGAGTGCAACTCTTTTATTTTTCGACGCATTTTTCTTTGCAAGTACTG
Variant 2       TTTTGAGGGCTTGGAGTGCAACTCTTTTATTTTTCGACGCATTTTTCTTTGCAAGTACTG
Variant 1       TTTTGAGGGCTTGGAGTGCAACTCTTTTATTTTTCGACGCATTTTTCTTTGCAAGTACTG

Variant 3       CGATCGCGTTAACGCTTTATCACGATACCTTCTACCACATATCACTAACAACATCAACAC
Variant 2       CGATCGCGTTAACGCTTTATCACGATACCTTCTACCACATATCACTAACAACATCAACAC
Variant 1       CGATCGCGTTAACGCTTTATCACGATACCTTCTACCACATATCACTAACAACATCAACAC

Variant 3       TCATCACTCTCGACGACATCCACTCGATCACTACTCTCACACGACCGATTAACTCCTCAT
Variant 2       TCATCACTCTCGACGACATCCACTCGATCACTACTCTCACACGACCGATTAACTCCTCAT
Variant 1       TCATCACTCTCGACGACATCCACTCGATCACTACTCTCACACGACCGATTAACTCCTCAT

Variant 3       CCACGCGGCCGCCTGCAGGAGCGCAAAGAAAAATGCGTCGAAAAATAAAAGAGTTGCACT
Variant 2       CCACGCGGCCGCCTGCAGGAGCGCAAAGAAAAATGCGTCGAAAAATAAAAGAGTTGCACT
Variant 1       CCACGCGGCCGCCTGCAGGAGCGCAAAGAAAAATGCGTCGAAAAATAAAAGAGTTGCACT

Variant 3       CCAAGCCCTCAAAAAGAAGAAACGATTGGAAAAGACCCAACTACAAATAGATGGAACCCT
Variant 2       CCAAGCCCTCAAAAAGAAGAAACGATTGGAAAAGACCCAACTACAAATAGATGGAACCCT
Variant 1       CCAAGCCCTCAAAAAGAAGAAACGATTGGAAAAGACCCAACTACAAATAGATGGAACCCT

Variant 3       TACAACTATTGAAATGCAGAGGGAAGCCCTCGAAGGAGCTAGCACAAATACTGCTGTATT
Variant 2       TACAACTATTGAAATGCAGAGGGAAGCCCTCGAAGGAGCTAGCACAAATACTGCTGTATT
Variant 1       TACAACTATTGAAATGCAGAGGGAAGCCCTCGAAGGAGCTAGCACAAATACTGCTGTATT

Variant 3       AGATTCTATGAAAAATGCTGCAGATGCCCTTAAGAAAGCTCATAAGAATTTGAATGTAGA
Variant 2       AGATTCTATGAAAAATGCTGCAGATGCCCTTAAGAAAGCTCATAAGAATTTGAATGTAGA
Variant 1       AGATTCTATGAAAAATGCTGCAGATGCCCTTAAGAAAGCTCATAAGAATTTGAATGTAGA

Variant 3       TGATGTTCACGATATCATGGATTAGATCGCCAGCGGTACTCGCTGAGGCCTAGCTTTCGT
Variant 2       TGATGTTCACGATATCATGGATTAGATCGCCAGCGGTACTCGCTGAGGCCTAGCTTTCGT
Variant 1       TGATGTTCACGATATCATGGATTAGATCGCCAGCGGTACTCGCTGAGGCCTAGCTTTCGT
```

```
Variant 3        TCGTATCATCGGTTTCGACAACGTTCGTCAAGTTCAATGCATCAGTTTCATTGCGCACAC
Variant 2        TCGTATCATCGGTTTCGACAACGTTCGTCAAGTTCAATGCATCAGTTTCATTGCGCACAC
Variant 1        TCGTATCATCGGTTTCGACAACGTTCGTCAAGTTCAATGCATCAGTTTCATTGCGCACAC

Variant 3        ACCAGAATCCTACTGAGTTTGAGTATTATGGCATTGGGAAAACTGTTTTTCTTGTACCAT
Variant 2        ACCAGAATCCTACTGAGTTTGAGTATTATGGCATTGGGAAAACTGTTTTTCTTGTACCAT
Variant 1        ACCAGAATCCTACTGAGTTTGAGTATTATGGCATTGGGAAAACTGTTTTTCTTGTACCAT

Variant 3        TTGTTGTGCTTGTAATTTACTGTGTTTTTTATTCGGTTTTCGCTATCGAACTGTGAAATG
Variant 2        TTGTTGTGCTTGTAATTTACTGTGTTTTTTATTCGGTTTTCGCTATCGAACTGTGAAATG
Variant 1        TTGTTGTGCTTGTAATTTACTGTGTTTTTTATTCGGTTTTCGCTATCGAACTGTGAAATG

Variant 3        GAAATGGATGGAGAAGAGTTAATGAATGATATGGTCCTTTTGTTCATTCTCAAATTAATA
Variant 2        GAAATGGATGGAGAAGAGTTAATGAATGATATGGTCCTTTTGTTCATTCTCAAATTAATA
Variant 1        GAAATGGATGGAGAAGAGTTAATGAATGATATGGTCCTTTTGTTCATTCTCAAATTAATA

Variant 3        TTATTTGTTTTTTCTCTTATTTGTTGTGTGTTGAATTTGAAATTATAAGAGATATGCAAA
Variant 2        TTATTTGTTTTTTCTCTTATTTGTTGTGTGTTGAATTTGAAATTATAAGAGATATGCAAA
Variant 1        TTATTTGTTTTTTCTCTTATTTGTTGTGTGTTGAATTTGAAATTATAAGAGATATGCAAA

Variant 3        CATTTTGTTTTGAGTAAAAATGTGTCAAATCGTGGCCTCTAATGACCGAAGTTAATATGA
Variant 2        CATTTTGTTTTGAGTAAAAATGTGTCAAATCGTGGCCTCTAATGACCGAAGTTAATATGA
Variant 1        CATTTTGTTTTGAGTAAAAATGTGTCAAATCGTGGCCTCTAATGACCGAAGTTAATATGA

Variant 3        GGAGTAAAACACTTGTAGTTGTACCATTATGCTTATTCACTAGGCAACAAATATATTTTC
Variant 2        GGAGTAAAACACTTGTAGTTGTACCATTATGCTTATTCACTAGGCAACAAATATATTTTC
Variant 1        GGAGTAAAACACTTGTAGTTGTACCATTATGCTTATTCACTAGGCAACAAATATATTTTC

Variant 3        AGACCTAGAAAAGCTGCAAATGTTACTGAATACAAGTATGTCCTCTTGTGTTTTAGACAT
Variant 2        AGACCTAGAAAAGCTGCAAATGTTACTGAATACAAGTATGTCCTCTTGTGTTTTAGACAT
Variant 1        AGACCTAGAAAAGCTGCAAATGTTACTGAATACAAGTATGTCCTCTTGTGTTTTAGACAT

Variant 3        TTATGAACTTTCCTTTATGTAATTTTCCAGAATCCTTGTCAGATTCTAATCATTGCTTTA
Variant 2        TTATGAACTTTCCTTTATGTAATTTTCCAGAATCCTTGTCAGATTCTAATCATTGCTTTA
Variant 1        TTATGAACTTTCCTTTATGTAATTTTCCAGAATCCTTGTCAGATTCTAATCATTGCTTTA

Variant 3        TAATTATAGTTATACTCATGGATTTGTAGTTGAGTATGAAAATATTTTTTAATGCATTTT
Variant 2        TAATTATAGTTATACTCATGGATTTGTAGTTGAGTATGAAAATATTTTTTAATGCATTTT
Variant 1        TAATTATAGTTATACTCATGGATTTGTAGTTGAGTATGAAAATATTTTTTAATGCATTTT

Variant 3        ATGACTTGCCAATTGATTGACAACGGCGCGCCAAGAAGAACGATTGGCAAACAGCTATTA
Variant 2        ATGACTTGCCAATTGATTGACAACGGCGCGCCAAGAAGAACGATTGGCAAACAGCTATTA
Variant 1        ATGACTTGCCAATTGATTGACAACGGCGCGCCAAGAAGAACGATTGGCAAACAGCTATTA

Variant 3        TGGGTATTATGGGTAGGCCTGCCCGGGCTCAGCCTAAGTCGCTACCTTAGGACCGTTATA
Variant 2        TGGGTATTATGGGTAGGCCTGCCCGGGCTCAGCCTAAGTCGCTACCTTAGGACCGTTATA
Variant 1        TGGGTATTATGGGTAGGCCTGCCCGGGCTCAGCCTAAGTCGCTACCTTAGGACCGTTATA

Variant 3        GTTACCGGGAAACTATCAGTGTTTGATCGGGCCGGCTGCTACAGACCTGAAACTTCATGC
```

```
Variant 2        GTTACCGGGAAACTATCAGTGTTTGATCGGGCCGGCTGCTACAGACCTGAAACTTCATGC
Variant 1        GTTACCGGGAAACTATCAGTGTTTGATCGGGCCGGCTGCTACAGACCTGAAACTTCATGC

Variant 3        GCCAAAAAAGGGACGGTATCCGTTGATTTGTTGAGTTTTGACCCGTCTTCATAAAAAATT
Variant 2        GCCAAAAAAGGGACGGTATCCGTTGATTTGTTGAGTTTTGACCCGTCTTCATAAAAAATT
Variant 1        GCCAAAAAAGGGACGGTATCCGTTGATTTGTTGAGTTTTGACCCGTCTTCATAAAAAATT

Variant 3        GGAGTCTATCTATCTTCTTTACAAACGCCAAGACTAGTTTAAAAACACTATTGTTCCAAG
Variant 2        GGAGTCTATCTATCTTCTTTACAAACGCCAAGACTAGTTTAAAAACACTATTGTTCCAAG
Variant 1        GGAGTCTATCTATCTTCTTTACAAACGCCAAGACTAGTTTAAAAACACTATTGTTCCAAG

Variant 3        AGATTTCTATTTCCCAAAGAAAAATAAACTATTTTTTTGAAAAAATAAAAATCTCTTGGC
Variant 2        AGATTTCTATTTCCCAAAGAAAAATAAACTATTTTTTTGAAAAAATAAAAATCTCTTGGC
Variant 1        AGATTTCTATTTCCCAAAGAAAAATAAACTATTTTTTTGAAAAAATAAAAATCTCTTGGC

Variant 3        AAGACTCTAAATTTAGCTAGGATTTATATCTAAACTGTTGGGGTTGCTCTTACTCACTCA
Variant 2        AAGACTCTAAATTTAGCTAGGATTTATATCTAAACTGTTGGGGTTGCTCTTACTCACTCA
Variant 1        AAGACTCTAAATTTAGCTAGGATTTATATCTAAACTGTTGGGGTTGCTCTTACTCACTCA

Variant 3        AATCCAGCGAACAATATTATTTAGATCATCCTTCACCCTCCCCACAACATCGTCGCCCCA
Variant 2        AATCCAGCGAACAATATTATTTAGATCATCCTTCACCCTCCCCACAACATCGTCGCCCCA
Variant 1        AATCCAGCGAACAATATTATTTAGATCATCCTTCACCCTCCCCACAACATCGTCGCCCCA

Variant 3        ACCTTCCTCCTCCCACTCACTTGGGTCGTTGCTATCGACCCCCTTCTCTCTTGCTCACAA
Variant 2        ACCTTCCTCCTCCCACTCACTTGGGTCGTTGCTATCGACCCCCTTCTCTCTTGCTCACAA
Variant 1        ACCTTCCTCCTCCCACTCACTTGGGTCGTTGCTATCGACCCCCTTCTCTCTTGCTCACAA

Variant 3        TATCATAACATTAACACAGTCTACTCCTTCCGTTCCAGAAAGAATATCGGTTTAACTTTT
Variant 2        TATCATAACATTAACACAGTCTACTCCTTCCGTTCCAGAAAGAATATCGGTTTAACTTTT
Variant 1        TATCATAACATTAACACAGTCTACTCCTTCCGTTCCAGAAAGAATATCGGTTTAACTTTT

Variant 3        TGTCAAATTTGACTGGCTCATCTTATTAAAAAATTATAACTATTATTTATTTTCATTCCG
Variant 2        TGTCAAATTTGACTGGCTCATCTTATTAAAAAATTATAACTATTATTTATTTTCATTCCG
Variant 1        TGTCAAATTTGACTGGCTCATCTTATTAAAAAATTATAACTATTATTTATTTTCATTCCG

Variant 3        ATTTAGTTTATCATACAATTTACTTTAACCAGCAACTGTTTTTAATGTTTTTTCAAATAT
Variant 2        ATTTAGTTTATCATACAATTTACTTTAACCAGCAACTGTTTTTAATGTTTTTTCAAATAT
Variant 1        ATTTAGTTTATCATACAATTTACTTTAACCAGCAACTGTTTTTAATGTTTTTTCAAATAT

Variant 3        TTTGGTAATATAAGCCGGTTAAATTTGGCGTCAAAATGGTCAAACAACTTTTTTTTATGG
Variant 2        TTTGGTAATATAAGCCGGTTAAATTTGGCGTCAAAATGGTCAAACAACTTTTTTTTATGG
Variant 1        TTTGGTAATATAAGCCGGTTAAATTTGGCGTCAAAATGGTCAAACAACTTTTTTTTATGG

Variant 3        ATAGGAGTAGTAACTAGGCCTTGTTTGGGTCGTACTGACTTATTGTTTAGCAGTGGCTAA
Variant 2        ATAGGAGTAGTAACTAGGCCTTGTTTGGGTCGTACTGACTTATTGTTTAGCAGTGGCTAA
Variant 1        ATAGGAGTAGTAACTAGGCCTTGTTTGGGTCGTACTGACTTATTGTTTAGCAGTGGCTAA

Variant 3        TAATTAATCAGAAAATAAATAATTAACTAGCAAATATTAGTCAGGGTATATTTGAAGACT
Variant 2        TAATTAATCAGAAAATAAATAATTAACTAGCAAATATTAGTCAGGGTATATTTGAAGACT
Variant 1        TAATTAATCAGAAAATAAATAATTAACTAGCAAATATTAGTCAGGGTATATTTGAAGACT
```

```
Variant 3        TGACTATTTATATGATTTATTAATATCTATTAGTAAGGTCAAATAGCTAATGGACAAATA
Variant 2        TGACTATTTATATGATTTATTAATATCTATTAGTAAGGTCAAATAGCTAATGGACAAATA
Variant 1        TGACTATTTATATGATTTATTAATATCTATTAGTAAGGTCAAATAGCTAATGGACAAATA

Variant 3        ATTTATCAGTTCTTCGGCTAACAATTAGCTACTTTTTTAGCTGACCTATTTAAATGTTAA
Variant 2        ATTTATCAGTTCTTCGGCTAACAATTAGCTACTTTTTTAGCTGACCTATTTAAATGTTAA
Variant 1        ATTTATCAGTTCTTCGGCTAACAATTAGCTACTTTTTTAGCTGACCTATTTAAATGTTAA

Variant 3        GGTACTAAAATTAGCTGGTAAACTGTTTGACACAATGATAAAAAAAAAGCCCTTAGGTTTA
Variant 2        GGTACTAAAATTAGCTGGTAAACTGTTTGACACAATGATAAAAAAAAAGCCCTTAGGTTTA
Variant 1        GGTACTAAAATTAGCTGGTAAACTGTTTGACACAATGATAAAAAAAAAGCCCTTAGGTTTA

Variant 3        GTTTGGGAACCACGTTATTCCAAGGGATTTTCATTTTCACAAGGGAAATTAGTTTATTTT
Variant 2        GTTTGGGAACCACGTTATTCCAAGGGATTTTCATTTTCACAAGGGAAATTAGTTTATTTT
Variant 1        GTTTGGGAACCACGTTATTCCAAGGGATTTTCATTTTCACAAGGGAAATTAGTTTATTTT

Variant 3        CCCTTGGGAAAATAAGAATCTCTTGGGAAAATTGAGCTTCCAAACTAGCCCTTAAAACAT
Variant 2        CCCTTGGGAAAATAAGAATCTCTTGGGAAAATTGAGCTTCCAAACTAGCCCTTAAAACAT
Variant 1        CCCTTGGGAAAATAAGAATCTCTTGGGAAAATTGAGCTTCCAAACTAGCCCTTAAAACAT

Variant 3        GTTCTTCCGCCAAATGTTCCTCCGTCAAATCAAATCAGGTCTGGAGGAGATGTCGCTTGC
Variant 2        GTTCTTCCGCCAAATGTTCCTCCGTCAAATCAAATCAGGTCTGGAGGAGATGTCGCTTGC
Variant 1        GTTCTTCCGCCAAATGTTCCTCCGTCAAATCAAATCAGGTCTGGAGGAGATGTCGCTTGC

Variant 3        TGGGCATTGGCTAACCGTACTAACCGTAGATCGCAGTACATTTCCTGAATCCGAGCGATC
Variant 2        TGGGCATTGGCTAACCGTACTAACCGTAGATCGCAGTACATTTCCTGAATCCGAGCGATC
Variant 1        TGGGCATTGGCTAACCGTACTAACCGTAGATCGCAGTACATTTCCTGAATCCGAGCGATC

Variant 3        GCTGCTTTTCTCGTTTCTACTTTCTTCTACCTCCCGATTCGCTGGCCTCTCCCGACCCTG
Variant 2        GCTGCTTTTCTCGTTTCTACTTTCTTCTACCTCCCGATTCGCTGGCCTCTCCCGACCCTG
Variant 1        GCTGCTTTTCTCGTTTCTACTTTCTTCTACCTCCCGATTCGCTGGCCTCTCCCGACCCTG

Variant 3        CCCCGCCTCATCACTCCCCATCCCACCGACACACGGCGTGTCAGGTGTCACGCGCCTCCG
Variant 2        CCCCGCCTCATCACTCCCCATCCCACCGACACACGGCGTGTCAGGTGTCACGCGCCTCCG
Variant 1        CCCCGCCTCATCACTCCCCATCCCACCGACACACGGCGTGTCAGGTGTCACGCGCCTCCG

Variant 3        CTAAAACCCTAGCCCCACCCAGGCCTGATGGCTGCTCCGCGGCAGCCGCACCCACCGGCA
Variant 2        CTAAAACCCTAGCCCCACCCAGGCCTGATGGCTGCTCCGCGGCAGCCGCACCCACCGGCA
Variant 1        CTAAAACCCTAGCCCCACCCAGGCCTGATGGCTGCTCCGCGGCAGCCGCACCCACCGGCA

Variant 3        GCGGAGGAGGGAGCCGCGCCGGCGGGTCCCCTGCCCGCCGCCGCGCCAGGTCCGCGTCCG
Variant 2        GCGGAGGAGGGAGCCGCGCCGGCGGGTCCCCTGCCCGCCGCCGCGCCAGGTCCGCGTCCG
Variant 1        GCGGAGGAGGGAGCCGCGCCGGCGGGTCCCCTGCCCGCCGCCGCGCCAGGTCCGCGTCCG

Variant 3        TACGACGTGACGGTCGCGGCAACGGAGCTCCGGCCGGTGGACTGCAATCTCGCCGCGCTC
Variant 2        TACGACGTGACGGTCGCGGCAACGGAGCTCCGGCCGGTGGACTGCAATCTCGCCGCGCTC
Variant 1        TACGACGTGACGGTCGCGGCAACGGAGCTCCGGCCGGTGGACTGCAATCTCGCCGCGCTC

Variant 3        TGTGACCACGTTCAGGCGGAGGGCTTCGGCTCCGGGGCCTTCTCCGACCTCGTCGTGGAG
Variant 2        TGTGACCACGTTCAGGCGGAGGGCTTCGGCTCCGGGGCCTTCTCCGACCTCGTCGTGGAG
```

```
Variant 1       TGTGACCACGTTCAGGCGGAGGGCTTCGGCTCCGGGGCCTTCTCCGACCTCGTCGTGGAG

Variant 3       GCCATGGGCGCCACCTACCGCCTCCATCGCCTCATCCTCTCCCGCAGCGCCTACTTCAGG
Variant 2       GCCATGGGCGCCACCTACCGCCTCCATCGCCTCATCCTCTCCCGCAGCGCCTACTTCAGG
Variant 1       GCCATGGGCGCCACCTACCGCCTCCATCGCCTCATCCTCTCCCGCAGCGCCTACTTCAGG

Variant 3       ------------------------------------------------------------
Variant 2       TGAGCAGAGCCTTGGCGCGCTCGCCGCCTTCGCGGATTGAAGTGCCTGTTTGGCTGTTTC
Variant 1       TGAGCAGAGCCTTGGCGCGCTCGCCGCCTTCGCGGATTGAAGTGCCTGTTTGGCTGTTTC

Variant 3       ------------------------------------------------------------
Variant 2       GATCTGGGTCGTCTGCAGCTGCTCAAAGTACTTAATTGAATTTCTGTGTGGACATTTTTG
Variant 1       GATCTGGGTCGTCTGCAGCTGCTCAAAGTACTTAATTGAATTTCTGTGTGGACATTTTTG

Variant 3       ------------------------------------------------------------
Variant 2       TCTTGGTTGGGACGTCTCCACCCCTTTCCTGTAAAATTTCCATGTGCTTTGATTCCTAAC
Variant 1       TCTTGGTTGGGACGTCTCCACCCCTTTCCTGTAAAATTTCCATGTGCTTTGATTCCTAAC

Variant 3       ------------------------------------------------------------
Variant 2       GTTCAATCTAAGAATATGACCTTATCAAGTGATTAGGATTCTGTTTTTCCCCCCAGAAAG
Variant 1       GTTCAATCTAAGAATATGACCTTATCAAGTGATTAGGATTCTGTTTTTCCCCCCAGAAAG

Variant 3       ------------------------------------------------------------
Variant 2       TAACAGCCTGCAAATAGCATGCCGATTGAAATCTTACACTCTTAACCGAACATGTTAGAT
Variant 1       TAACAGCCTGCAAATAGCATGCCGATTGAAATCTTACACTCTTAACCGAACATGTTAGAT

Variant 3       ------------------------------------------------------------
Variant 2       TTTCATTTACTCTGTATATATCATATTGCATCCTTCAATGTTCAGTTTGCCTTATGATTT
Variant 1       TTTCATTTACTCTGTATATATCATATTGCATCCTTCAATGTTCAGTTTGCCTTATGATTT

Variant 3       ------------------------------------------------------------
Variant 2       CCAGATTTCCATTTATGCCAAGAATCGCTATTGAAGCTAAAATTGATTTAATAAAAGTCA
Variant 1       CCAGATTTCCATTTATGCCAAGAATCGCTATTGAAGCTAAAATTGATTTAATAAAAGTCA

Variant 3       ------------------------------------------------------------
Variant 2       GGCACTATTTTTTTCTGTTGAGATTTCAAGTTCAGAACTTTTGGATGGAAGTATAGGCAT
Variant 1       GGCACTATTTTTTTCTGTTGAGATTTCAAGTTCAGAACTTTTGGATGGAAGTATAGGCAT

Variant 3       ------------------------------------------------------------
Variant 2       CAACCAATAGTGTGGCTCATGAAAAATGAAATCATAGTTTTTCTCCCTTCCCTTTAGCGT
Variant 1       CAACCAATAGTGTGGCTCATGAAAAATGAAATCATAGTTTTTCTCCCTTCCCTTTAGCGT

Variant 3       ------------------------------------------------------------
Variant 2       CGTGCACACATATTTCCCTTATTACATTACTTCCCTACTGGCACATCCCCACATAGAATG
Variant 1       CGTGCACACATATTTCCCTTATTACATTACTTCCCTACTGGCACATCCCCACATAGAATG

Variant 3       ------------------------------------------------------------
Variant 2       TTCATGTAAATTAAAACAAGTAAAATGCTTAACAACTTCTGTATGGTAATTTCTTGAAGG
Variant 1       TTCATGTAAATTAAAACAAGTAAAATGCTTAACAACTTCTGTATGGTAATTTCTTGAAGG
```

```
Variant 3        AATATGCTACATGGTCCTTGGAGAGAGTCGGGAGCACCCACAGTGGTTTTGCACATAGAT
Variant 2        AATATGCTACATGGTCCTTGGAGAGAGTCGGGAGCACCCACAGTGGTTTTGCACATAGAT
Variant 1        AATATGCTACATGGTCCTTGGAGAGAGTCGGGAGCACCCACAGTGGTTTTGCACATAGAT

Variant 3        GATGCCAATGTCGATTCAGATGCAATTGCAATTGCGCTCGCATATCTTTATGGGCAACCC
Variant 2        GATGCCAATGTCGATTCAGATGCAATTGCAATTGCGCTCGCATATCTTTATGGGCAACCC
Variant 1        GATGCCAATGTCGATTCAGATGCAATTGCAATTGCGCTCGCATATCTTTATGGGCAACCC

Variant 3        CCCAAGCTTACTGATAGCAATGCATTCCGAGTGCTTGCAGCTGCATCATTTCTGGATCTT
Variant 2        CCCAAGCTTACTGATAGCAATGCATTCCGAGTGCTTGCAGCTGCATCATTTCTGGATCTT
Variant 1        CCCAAGCTTACTGATAGCAATGCATTCCGAGTGCTTGCAGCTGCATCATTTCTGGATCTT

Variant 3        CAGGACTTATGTACAATATGTACAGATTTTATCATTTCCGAGCTCTGGACATCAAACTTT
Variant 2        CAGGACTTATGTACAATATGTACAGATTTTATCATTTCCGAGCTCTGGACATCAAACTTT
Variant 1        CAGGACTTATGTACAATATGTACAGATTTTATCATTTCCGAGCTCTGGACATCAAACTTT

Variant 3        TTACAATACCAGTTGTTTGCTGAGAGTCAAGATTATGGGAGCCATGGAGAACGTGTTAGG
Variant 2        TTACAATACCAGTTGTTTGCTGAGAGTCAAGATTATGGGAGCCATGGAGAACGTGTTAGG
Variant 1        TTACAATACCAGTTGTTTGCTGAGAGTCAAGATTATGGGAGCCATGGAGAACGTGTTAGG

Variant 3        AACGCTTGCTGGGGTTATCTTTGTCAAAGTGCCACAATGGAATTACGAGAGGTGCTACCA
Variant 2        AACGCTTGCTGGGGTTATCTTTGTCAAAGTGCCACAATGGAATTACGAGAGGTGCTACCA
Variant 1        AACGCTTGCTGGGGTTATCTTTGTCAAAGTGCCACAATGGAATTACGAGAGGTGCTACCA

Variant 3        AAGCTTTCTTCACAAACTTTGCATGCTCTTCTTACATCTGACGAATTATGGGTACCTAAC
Variant 2        AAGCTTTCTTCACAAACTTTGCATGCTCTTCTTACATCTGACGAATTATGGGTACCTAAC
Variant 1        AAGCTTTCTTCACAAACTTTGCATGCTCTTCTTACATCTGACGAATTATGGGTACCTAAC

Variant 3        GAGGAGAAAAGGTTTGAACTAGCATTACTTACTCTACTTGCAAAGGTTGCTATGTGTGAG
Variant 2        GAGGAGAAAAGGTTTGAACTAGCATTACTTACTCTACTTGCAAAGGTTGCTATGTGTGAG
Variant 1        GAGGAGAAAAGGTTTGAACTAGCATTACTTACTCTACTTGCAAAGGTTGCTATGTGTGAG

Variant 3        ATACAAGTTAGTGGTAATGAAACAAATTTACCAAGTGCTGATCGATCCATGAGGAAGGGG
Variant 2        ATACAAGTTAGTGGTAATGAAACAAATTTACCAAGTGCTGATCGATCCATGAGGAAGGGG
Variant 1        ATACAAGTTAGTGGTAATGAAACAAATTTACCAAGTGCTGATCGATCCATGAGGAAGGGG

Variant 3        AAGACTCCAATGAATGAATCTGGGGAGGAACTGCTAATGGACTCTGAATTGCAGAACTTG
Variant 2        AAGACTCCAATGAATGAATCTGGGGAGGAACTGCTAATGGACTCTGAATTGCAGAACTTG
Variant 1        AAGACTCCAATGAATGAATCTGGGGAGGAACTGCTAATGGACTCTGAATTGCAGAACTTG

Variant 3        AAGTTGCATGATAACTTGGGGAATGAAATTTCCCATAACATTATTGCTATTTCAGATATG
Variant 2        AAGTTGCATGATAACTTGGGGAATGAAATTTCCCATAACATTATTGCTATTTCAGATATG
Variant 1        AAGTTGCATGATAACTTGGGGAATGAAATTTCCCATAACATTATTGCTATTTCAGATATG

Variant 3        AATGGTGAAGCTCCCAAGAGAATGGAGATTGATTGTTCTACCGGAGGACCATCAGGAGAA
Variant 2        AATGGTGAAGCTCCCAAGAGAATGGAGATTGATTGTTCTACCGGAGGACCATCAGGAGAA
Variant 1        AATGGTGAAGCTCCCAAGAGAATGGAGATTGATTGTTCTACCGGAGGACCATCAGGAGAA

Variant 3        AGCACTTCATATCAATTTAATGAAAATAACTGGATTTCTAGTGAGCAAACTGCAAATAAT
Variant 2        AGCACTTCATATCAATTTAATGAAAATAACTGGATTTCTAGTGAGCAAACTGCAAATAAT
Variant 1        AGCACTTCATATCAATTTAATGAAAATAACTGGATTTCTAGTGAGCAAACTGCAAATAAT
```

```
Variant 3       TATTTCTCAAGAACTTCCAGTAGTGTTGTTGTTCCTACTGAGTGGGGAAGGCCCAATGCA
Variant 2       TATTTCTCAAGAACTTCCAGTAGTGTTGTTGTTCCTACTGAGTGGGGAAGGCCCAATGCA
Variant 1       TATTTCTCAAGAACTTCCAGTAGTGTTGTTGTTCCTACTGAGTGGGGAAGGCCCAATGCA

Variant 3       CCACTTTGGGGTGGCAGGGTCGTTGGACGGCGGCAAATTAGATACATTAGAGGAAGCTCT
Variant 2       CCACTTTGGGGTGGCAGGGTCGTTGGACGGCGGCAAATTAGATACATTAGAGGAAGCTCT
Variant 1       CCACTTTGGGGTGGCAGGGTCGTTGGACGGCGGCAAATTAGATACATTAGAGGAAGCTCT

Variant 3       TGTCTATCTACTGATGAATATAATGCTTTTATGAATATATTTGAGAGAGGTTCTCTTCTC
Variant 2       TGTCTATCTACTGATGAATATAATGCTTTTATGAATATATTTGAGAGAGGTTCTCTTCTC
Variant 1       TGTCTATCTACTGATGAATATAATGCTTTTATGAATATATTTGAGAGAGGTTCTCTTCTC

Variant 3       TACTGCAATATGTCCTTTGATGCACTGCTAAGTGTTCGAAAGCAACTCGAAGAATTTGGA
Variant 2       TACTGCAATATGTCCTTTGATGCACTGCTAAGTGTTCGAAAGCAACTCGAAGAATTTGGA
Variant 1       TACTGCAATATGTCCTTTGATGCACTGCTAAGTGTTCGAAAGCAACTCGAAGAATTTGGA

Variant 3       TTCCCTTGTAAAGCTGTCAATGATAGTCTATGGCTACAG----------------------
Variant 2       TTCCCTTGTAAAGCTGTCAATGATAGTCTATGGCTACAG----------------------
Variant 1       TTCCCTTGTAAAGCTGTCAATGATAGTCTATGGCTACAGGTATTTAATCTACTCCCTGCC

Variant 3       ------------------------------------------------------------ATG
Variant 2       ------------------------------------------------------------ATG
Variant 1       TTGTGGTACTCTGTTCCTTTCAAGACTTTATAAAACCTTGATGCTTTGTTATTGTAGATG

Variant 3       CTTCTGTGTCACAGGGTGCAAGCGATTGTTGCTGATACTTGCAGGAATTGTTGCCTTATG
Variant 2       CTTCTGTGTCACAGGGTGCAAGCGATTGTTGCTGATACTTGCAGGAATTGTTGCCTTATG
Variant 1       CTTCTGTGTCACAGGGTGCAAGCGATTGTTGCTGATACTTGCAGGAATTGTTGCCTTATG

Variant 3       AATAGTTCTTGTGCTTGCAAGCAAGCATATGTGAGCTCGCATACACATTACAGGCAGGAG
Variant 2       AATAGTTCTTGTGCTTGCAAGCAAGCATATGTGAGCTCGCATACACATTACAGGCAGGAG
Variant 1       AATAGTTCTTGTGCTTGCAAGCAAGCATATGTGAGCTCGCATACACATTACAGGCAGGAG

Variant 3       CATGACAGGAGCAGTGCCTCCGACAACATAGGTAATGTCTACCTTGCGGATGGCCAGGGT
Variant 2       CATGACAGGAGCAGTGCCTCCGACAACATAGGTAATGTCTACCTTGCGGATGGCCAGGGT
Variant 1       CATGACAGGAGCAGTGCCTCCGACAACATAGGTAATGTCTACCTTGCGGATGGCCAGGGT

Variant 3       GATGGGAATGGTGTACTTGGGCCTGTCCGTGTTAATGTAAGAGGAGCAGTCGATGGACTT
Variant 2       GATGGGAATGGTGTACTTGGGCCTGTCCGTGTTAATGTAAGAGGAGCAGTCGATGGACTT
Variant 1       GATGGGAATGGTGTACTTGGGCCTGTCCGTGTTAATGTAAGAGGAGCAGTCGATGGACTT

Variant 3       GCTGGTATTGGGAGAGGGAACTCAAATGTGCCTGGTGCAGCTTGGGCTCCTACACGATAT
Variant 2       GCTGGTATTGGGAGAGGGAACTCAAATGTGCCTGGTGCAGCTTGGGCTCCTACACGATAT
Variant 1       GCTGGTATTGGGAGAGGGAACTCAAATGTGCCTGGTGCAGCTTGGGCTCCTACACGATAT

Variant 3       GTCTTCTCCCGTGTCCCTTATGGGCTTGGTTCAAGAAATGGCCAGCAATTTGCCATTGAT
Variant 2       GTCTTCTCCCGTGTCCCTTATGGGCTTGGTTCAAGAAATGGCCAGCAATTTGCCATTGAT
Variant 1       GTCTTCTCCCGTGTCCCTTATGGGCTTGGTTCAAGAAATGGCCAGCAATTTGCCATTGAT

Variant 3       GAATCAGAACCTAGAATTGACCGCAATGGAGATATTTCAGCAGATGGTCTGACTGCATTG
```

```
Variant 2        GAATCAGAACCTAGAATTGACCGCAATGGAGATATTTCAGCAGATGGTCTGACTGCATTG
Variant 1        GAATCAGAACCTAGAATTGACCGCAATGGAGATATTTCAGCAGATGGTCTGACTGCATTG

Variant 3        GTTAACCTTAGCCAAGAAAACAATGCTGCTCATCTGCAGGATCAAAGTCTATTTGAGACA
Variant 2        GTTAACCTTAGCCAAGAAAACAATGCTGCTCATCTGCAGGATCAAAGTCTATTTGAGACA
Variant 1        GTTAACCTTAGCCAAGAAAACAATGCTGCTCATCTGCAGGATCAAAGTCTATTTGAGACA

Variant 3        GGGATGCAGACAAGATATCGCAGTGTTCCATCTGTTTCCACTCCAGGTGGTTCTTCTGTC
Variant 2        GGGATGCAGACAAGATATCGCAGTGTTCCATCTGTTTCCACTCCAGGTGGTTCTTCTGTC
Variant 1        GGGATGCAGACAAGATATCGCAGTGTTCCATCTGTTTCCACTCCAGGTGGTTCTTCTGTC

Variant 3        CAGATGCAGGAGTCAAAGGAGCATGAACTTGGATCAGATTGGGAAACCACAAAGGATGCA
Variant 2        CAGATGCAGGAGTCAAAGGAGCATGAACTTGGATCAGATTGGGAAACCACAAAGGATGCA
Variant 1        CAGATGCAGGAGTCAAAGGAGCATGAACTTGGATCAGATTGGGAAACCACAAAGGATGCA

Variant 3        ACTATATCATTAGACATGAAAACACCTCTTAGCCATTTTCCACCTTTCCGCTTTGGGGTT
Variant 2        ACTATATCATTAGACATGAAAACACCTCTTAGCCATTTTCCACCTTTCCGCTTTGGGGTT
Variant 1        ACTATATCATTAGACATGAAAACACCTCTTAGCCATTTTCCACCTTTCCGCTTTGGGGTT

Variant 3        GAGTTCGAGGATGTGCACAGGCTTGCTGATGGTCAGGTGAAACATTCGACTGAAGTGTTT
Variant 2        GAGTTCGAGGATGTGCACAGGCTTGCTGATGGTCAGGTGAAACATTCGACTGAAGTGTTT
Variant 1        GAGTTCGAGGATGTGCACAGGCTTGCTGATGGTCAGGTGAAACATTCGACTGAAGTGTTT

Variant 3        TATGCAGGCTCTCTATGGAAGGTGAGTGTCCAGCCATTCAATGATGAGGATCCTCATGGG
Variant 2        TATGCAGGCTCTCTATGGAAGGTGAGTGTCCAGCCATTCAATGATGAGGATCCTCATGGG
Variant 1        TATGCAGGCTCTCTATGGAAGGTGAGTGTCCAGCCATTCAATGATGAGGATCCTCATGGG

Variant 3        CGACGCACCCTTGGACTATTTCTCCACCGACGCAAGGCTGAGTTGTTAGATCCCTTGAGG
Variant 2        CGACGCACCCTTGGACTATTTCTCCACCGACGCAAGGCTGAGTTGTTAGATCCCTTGAGG
Variant 1        CGACGCACCCTTGGACTATTTCTCCACCGACGCAAGGCTGAGTTGTTAGATCCCTTGAGG

Variant 3        AAGGCTCACTTGTACGTTGACCCCCGGGAAAAGGTCACTGCTCGGTATCAGCTCATCTGT
Variant 2        AAGGCTCACTTGTACGTTGACCCCCGGGAAAAGGTCACTGCTCGGTATCAGCTCATCTGT
Variant 1        AAGGCTCACTTGTACGTTGACCCCCGGGAAAAGGTCACTGCTCGGTATCAGCTCATCTGT

Variant 3        CCATCAAAGAGAGAGGTCATGATATTTGGAAGCCTGAAGCAGGCTGGGACGCTGCTACCA
Variant 2        CCATCAAAGAGAGAGGTCATGATATTTGGAAGCCTGAAGCAGGCTGGGACGCTGCTACCA
Variant 1        CCATCAAAGAGAGAGGTCATGATATTTGGAAGCCTGAAGCAGGCTGGGACGCTGCTACCA

Variant 3        AAAGCGCCGAAGGGCTGGGGCTGGCGCACTGCTATACTATTTGATGAGCTTGCTGATCTT
Variant 2        AAAGCGCCGAAGGGCTGGGGCTGGCGCACTGCTATACTATTTGATGAGCTTGCTGATCTT
Variant 1        AAAGCGCCGAAGGGCTGGGGCTGGCGCACTGCTATACTATTTGATGAGCTTGCTGATCTT

Variant 3        CTCCAGGGTGGTGCCCTGCGAATTGCTGCAGTGGTCCAGCTTGTCTAGATTAGTTGCAGA
Variant 2        CTCCAGGGTGGTGCCCTGCGAATTGCTGCAGTGGTCCAGCTTGTCTAGATTAGTTGCAGA
Variant 1        CTCCAGGGTGGTGCCCTGCGAATTGCTGCAGTGGTCCAGCTTGTCTAGATTAGTTGCAGA

Variant 3        AAACAACTGCTTGCAAGGATGGTGATAGCACAGCAGTTTGTGTAATTGATATACTCCCTC
Variant 2        AAACAACTGCTTGCAAGGATGGTGATAGCACAGCAGTTTGTGTAATTGATATACTCCCTC
Variant 1        AAACAACTGCTTGCAAGGATGGTGATAGCACAGCAGTTTGTGTAATTGATATACTCCCTC
```

```
Variant 3        CGTCCTAAAATATAGTTTTTTCTGGTCCTTTTTTCCGTCCACATTCGAACAAATGATAAT
Variant 2        CGTCCTAAAATATAGTTTTTTCTGGTCCTTTTTTCCGTCCACATTCGAACAAATGATAAT
Variant 1        CGTCCTAAAATATAGTTTTTTCTGGTCCTTTTTTCCGTCCACATTCGAACAAATGATAAT

Variant 3        GAATAGACATACATACAAACTACATTCATAAATTAAGTTAAGTAGTCAATGCTTGTTTAG
Variant 2        GAATAGACATACATACAAACTACATTCATAAATTAAGTTAAGTAGTCAATGCTTGTTTAG
Variant 1        GAATAGACATACATACAAACTACATTCATAAATTAAGTTAAGTAGTCAATGCTTGTTTAG

Variant 3        TGTAAAACGAATTATATTTTAGGACGGGGTGAGTATGTAAGAACTCAATCTGTCATGTAC
Variant 2        TGTAAAACGAATTATATTTTAGGACGGGGTGAGTATGTAAGAACTCAATCTGTCATGTAC
Variant 1        TGTAAAACGAATTATATTTTAGGACGGGGTGAGTATGTAAGAACTCAATCTGTCATGTAC

Variant 3        TCGTTGTCATGTACTCGTGCTCTGAAATATTGTATAATCTATAGCGGTTTGCTGTTTGGT
Variant 2        TCGTTGTCATGTACTCGTGCTCTGAAATATTGTATAATCTATAGCGGTTTGCTGTTTGGT
Variant 1        TCGTTGTCATGTACTCGTGCTCTGAAATATTGTATAATCTATAGCGGTTTGCTGTTTGGT

Variant 3        ATATAAAAGAGAATATATCAGATGCAAACCAACCACTTGTACAAACCGTGTAAACCAACA
Variant 2        ATATAAAAGAGAATATATCAGATGCAAACCAACCACTTGTACAAACCGTGTAAACCAACA
Variant 1        ATATAAAAGAGAATATATCAGATGCAAACCAACCACTTGTACAAACCGTGTAAACCAACA

Variant 3        TATTGATGGAGG 5634
Variant 2        TATTGATGGAGG 6294
Variant 1        TATTGATGGAGG 6372
```

Figure 44. Alignment of DvSnf7.1 Read-through Transcript Variants cDNA Sequences from MON 95275

The bases match to plasmid PV-ZMIR525664 are single underlined, while the bases match to maize endogenous gene GRMZM2G017404 are double underlined. The sequence in bold was not observed in sequencing data, though is expected to be present in the read-through isoforms. The bolded sequence contains one DvSnf7P repeat. The gaps in DvSnf7.1 read-through variant 2 and variant 3 indicate spliced out introns.

B.3(c)(iii)(iii) Conclusion for the Characterizatoin of DvSnf7.1 Read-through Transcripts in MON 95275

In addition to expected hybridization bands of DvSnf7.1, unexpected larger bands of read-through transcripts were also detected in leaf tissue of MON 95275 by Northern blot analysis. Three variants of the read-through transcripts in leaf RNA of MON 95275 were identified by PacBio Sequencing and confirmed by RT-PCR. The positioning of any new start codons downstream of the DvSnf7 inverted repeat would restrict, if not eliminate, the potential for translation initiation. Even in the highly unlikely event that one of the three read-through transcripts yielded a translation product, bioinformatic analyses demonstrate that the resultant peptides do not provide any indication of hazard as they share no significant similarity with allergens, toxins or proteins that would display untoward biological activity.

For details, please refer to Appendix 16 [redacted]., 2021 (TRR0001021)).

B.4 Novel Herbicide Metabolites in GM Herbicide-Tolerant Plants

Not applicable.

B.5 Compositional Assessment

The introduced Mpp75Aa1.1 and Vpb4Da2 proteins and DvSnf7.1 RNA in MON 95275 confer protection from feeding damage caused by targeted coleopteran insect pests. These expressed products lack catalytic activity and are not intended or expected to affect the plant's metabolism as predicted by the molecular characterization. Given the nature of these introduced traits and the general lack of meaningful unintended compositional characteristics observed for biotechnology-derived products over the past several decades, biologically relevant compositional changes in MON 95275 maize were not expected (Brune *et al.*, 2021).

Food and feed safety assessments of biotechnology-derived crops follow the comparative safety assessment process (Codex Alimentarius, 2009) in which the composition of grain and/or other raw agricultural commodities of the biotechnology-derived crop are compared to the appropriate conventional control that has a history of safe use. For maize, assessments are performed based on the general principles outlined in the OECD consensus document for maize composition (OECD, 2002b).

A review of compositional assessments, that encompassed a total of seven biotechnology-derived crop traits, four maize and three soybean, nine countries, and eleven growing seasons, concluded that incorporation of biotechnology-derived agronomic traits has had little impact on crop composition. Most compositional variation is attributable to growing region, agronomic practices, and genetic background (Harrigan *et al.*, 2010). Numerous scientific publications have further documented the extensive variability in the concentrations of crop nutrients, anti-nutrients, and secondary metabolites that reflect the influence of environmental and genetic factors as well as extensive conventional breeding efforts to improve nutrition, agronomics, and yield (Harrigan *et al.*, 2010; Harrigan *et al.*, 2009; Ridley *et al.*, 2011; Zhou *et al.*, 2011). Compositional equivalence between biotechnology-derived and conventional crops supports an "equal or increased assurance of the safety of foods derived from genetically modified plants" (OECD, 2002a). OECD consensus documents on compositional considerations for new crop varieties emphasize quantitative measurements of essential nutrients and known anti-nutrients or toxicants. These quantitative measurements effectively discern compositional changes that imply potential nutritional or safety (e.g., anti-nutritional) concerns. Levels of the components in grain and/or other raw agricultural commodities of the biotechnology-derived crop product are compared to: 1) corresponding levels in a conventional comparator, a genetically similar conventional line, grown concurrently under similar field conditions, and 2) natural ranges from data published in the scientific literature or in publically available databases (e.g. AFSI[10] Crop Composition Database,

[10] Effective May 1, 2020, the ILSI RF publishing the CCDB became an unaffiliated non-profit scientific organization, no longer part of the ILSI federation, and changed its name to Agriculture and Food Systems Institute (AFSI). There is no change to the current structure or function of the CCDB, only name change: AFSI CCDB. The CCDB working group and their website are still the same. https://www.cropcomposition.org/"

(AFSI, 2019)). This second comparison places any potential differences between the assessed biotechnology-derived crop and its comparator in the context of the well-documented variation within and among maize lines in the concentrations of crop nutrients, anti-nutrients and secondary metabolites.

This section provides a summary of the analyses conducted to evaluate key nutrients, anti-nutrients and secondary metabolites in grain and forage of MON 95275 compared to that of a conventional control maize LH244+HCL617 grown and harvested under similar conditions. The production of materials for compositional analyses used a sufficient variety of field trial sites, robust experimental design (randomized complete block design with four block replicates), and sensitive analytical methods that allow accurate assessments of compositional characteristics over a range of environmental conditions typical for maize production. The information provided in this section addresses relevant factors in Codex Plant Guidelines, Section 4, paragraphs 44 and 45 for compositional analyses (Codex Alimentarius, 2009).

B.5(a) Levels of key nutrients, toxicants and anti-nutrients in the food produced using gene technology compared with the levels in an appropriate comparator

The evaluation of MON 95275 followed considerations relevant to the compositional quality of maize as defined by the OECD consensus document (OECD, 2002b). Harvested grain samples were assessed for moisture and levels of nutrients including protein and 18 amino acids (Table 31), total fat and 22 fatty acids (Table 32), carbohydrates by calculation and fiber (acid detergent fiber (ADF), neutral detergent fiber (NDF) and total dietary fiber (TDF) (Table 33), ash and minerals (calcium, copper, iron, magnesium, manganese, phosphorus, potassium, sodium and zinc (Table 34) and vitamins (vitamin A, vitamin B_1, vitamin B_2,, vitamin B_3, vitamin B_6, vitamin B_9 and vitamin E (Table 35). Grain samples were also assessed for levels of antinutrients (phytic acid and raffinose) and secondary metabolites (ferulic acid, furfural and p-coumaric acid (Table 36). Harvested forage samples were assessed for moisture and levels of nutrients including proximates (protein, total fat and ash; carbohydrates by calculation and fiber (ADF and NDF), and calcium and phosphorus (Table 37) In all, 78 different components were analyzed. Of the 78 measured components, 15 components (caprylic acid, capric acid, lauric acid, myristic acid, myristoleic acid, pentadecanoic acid, pentadecenoic acid, heptadecanoic acid, heptadecenoic acid, gamma linolenic acid, eicosadienoic acid, eicosatrienoic acid, arachidonic acid, sodium and furfural in grain) had more than 50% of the observations below the assay limit of quantitation (LOQ) and were excluded from statistical analysis. Moisture values for grain and forage were measured for conversion of components to dry weight but were not statistically analyzed. Therefore, 61 components were statistically analyzed for all samples.

The statistical comparison of MON 95275 and the conventional control was based on compositional data combined across all field sites. Statistically-significant differences were identified at the 5% level ($\alpha = 0.05$). A statistically-significant difference between MON 95275 and the conventional control does not necessarily imply biological relevance from a food and feed safety perspective. Therefore, any statistically-significant differences observed between MON 95275 and the conventional control were evaluated further to determine whether the detected difference indicated a biologically relevant compositional change or supported a conclusion of compositional equivalence, as follows:

Step 1 – Determination of the Magnitude of Difference between Test (MON 95275) and Conventional Control Means

The difference in means between MON 95275 and the conventional control was determined for use in subsequent steps.

Step 2 – Assessment of the Difference in the Context of Natural Variation within the Conventional Control

The relative impact of MON 95275 was evaluated in the context of variation within the conventional control germplasm grown across multiple sites. This step assessed the mean difference between MON 95275 and the conventional control in the context of the conventional control range value (maximum value minus the minimum value). When a mean difference is less than the variability seen due to natural environmental variation within the conventional control, the difference is typically not a food or feed safety concern (Venkatesh *et al.*, 2014).

Step 3 – Assessment of the Difference in the Context of Natural Variation Due to Multiple Factors

The relative impact of MON 95275 on composition was evaluated in the context of sources of natural variation such as environmental and germplasm influences. This assessment determined whether the component mean value of MON 95275 was within the natural variability defined by the literature values and/or the AFSI Crop Composition Database (AFSI-CCDB, Table 38) values. This naturally occurring variability is important in assessing the biological relevance to food and feed safety of statistically-significant differences in composition between MON 95275 and the conventional control.

These evaluations of natural variation are important as crop composition is known to be greatly influenced by environment and variety (Harrigan *et al.*, 2010). Although used in the comparative assessment process, detection of statistically-significant differences between MON 95275 and the conventional control mean values for an analyzed component does not imply a meaningful contribution by MON 95275 to compositional variability. Only if the impact of MON 95275 on levels of components was large relative to natural variation inherent to conventional maize would further assessments be required to establish whether the change in composition would have an impact from a food and feed safety and nutritional perspective. The steps reviewed in this assessment therefore describe the process for determining whether the differences between MON 95275 and the conventional control are meaningful from a food and feed safety perspective or whether they support a conclusion of compositional equivalence.

Compositional analysis was conducted on grain and forage of MON 95275 and a conventional control grown at five sites in the U.S. during 2019. In all, 78 different analytical components were measured. Of these, 15 components had more than 50% of the observations below the assay limit of quantitation (LOQ) and were excluded from statistical analysis. Moisture values for grain and forage were measured for conversion of components to dry weight but were not statistically analyzed. There were no statistically significant differences ($p<0.05$) for 43 of the 61 components analyzed (Table 31 to Table 37). There were seven components in grain (palmitic acid, stearic acid, oleic acid, linoleic acid, arachidic acid, calcium and vitamin B6) that showed a statistically

significant difference ($p<0.05$) between MON 95275 and the conventional control. No statistical differences ($p<0.05$) were observed for forage analytes.

For palmitic acid, the mean difference was -0.16% total Fatty Acid (Table 32). As shown in Table 32, the magnitude of the difference for palmitic acid between MON 95275 and the conventional control was less than the corresponding conventional control range value. This indicates that MON 95275 does not impact the levels of this component more than the natural variation within the conventional control grown at multiple locations. The mean level of palmitic acid was within the natural variability of this component as published in the scientific literature on maize composition and/or the AFSI-CCDB (Table 38).

For stearic acid, the mean difference was -0.069% Total Fatty Acid (Table 32). As shown in Table 32, the magnitude of the difference for stearic acid between MON 95275 and the conventional control was less than the corresponding conventional control range value. This indicates that MON 95275 does not impact the level of this component more than the natural variation within the conventional control grown at multiple locations. The mean level of stearic acid was within the natural variability of this component as published in the scientific literature on maize composition and/or the AFSI-CCDB (Table 38).

For oleic acid, the mean difference was -0.56% Total Fatty Acid (Table 32). As shown in Table 32(Table 30), the magnitude of the difference for oleic acid between MON 95275 and the conventional control was less than the corresponding conventional control range value. This indicates that MON 95275 does not impact the level of this component more than the natural variation within the conventional control grown at multiple locations. The mean level of oleic acid was within the natural variability of this component as published in the scientific literature on maize composition and/or the AFSI-CCDB (Table 38).

For linoleic acid, the mean difference was 0.81% Total Fatty Acid (Table 32). As shown in Table 32, the magnitude of the difference for linoleic acid between MON 95275 and the conventional control was less than the corresponding conventional control range value. This indicates that MON 95275 does not impact the level of this component more than the natural variation within the conventional control grown at multiple locations. The mean level of linoleic acid was within the natural variability of this component as published in the scientific literature on maize composition and/or the AFSI-CCDB (Table 38).

For arachidic acid, the mean difference was -0.011% Total Fatty Acid (Table 32). As shown in Table 32, the magnitude of the difference for arachidic acid between MON 95275 and the conventional control was less than the corresponding conventional control range value. This indicates that MON 95275 does not impact the level of this component more than the natural variation within the conventional control grown at multiple locations. The mean level of arachidic acid was within the natural variability of this component as published in the scientific literature on maize composition and/or the AFSI-CCDB (Table 38).

For calcium, the mean difference was -0.00019% dw (Table 34). As shown in Table 34, the magnitude of the difference for calcium between MON 95275 and the conventional control was less than the corresponding conventional control range values. This indicates that MON 95275

does not impact the level of this component more than the natural variation within the conventional control grown at multiple locations. The mean level of calcium was within the natural variability of this component as published in the scientific literature on maize composition and/or the AFSI-CCDB (Table 38).

For vitamin B6, the difference was 0.38 mg/kg dw (Table 35). As shown in Table 35, the magnitude of the difference for vitamin B6, between MON 95275 and the conventional control was less than the corresponding conventional control range value. This indicates that MON 95275 does not impact the level of this component more than the natural variation within the conventional control grown at multiple locations. The mean level of vitamin B6, was within the natural variability of this component as published in the scientific literature on maize composition and/or the AFSI-CCDB (Table 38).

These data indicate that the statistically significant differences observed were not biologically meaningful from a food and feed safety perspective. These results support the conclusion that MON 95275 was not a major contributor to variation in component levels in maize grain or forage and confirmed the compositional equivalence of MON 95275 to the conventional control in levels nutrients, anti-nutrients, and secondary metabolites in grain, as well as, nutrients in forage.

For details, please refer to Appendix 17 ([redacted]., 2020 (MSL0030998)).

Table 31. Summary of Maize Grain Protein and Amino Acids for MON 95275 and the Conventional Control

				Difference (Test minus Control)		
Component (% dw)[1]	MON 95275 Mean (S.E.)[2] Range	Control Mean (S.E.) Range	Control Range Value[3]	Mean (S.E.)	p-Value	% Relative[4]
Protein	9.86 (0.15) 8.89 - 10.84	9.75 (0.15) 8.72 - 10.53	1.81	0.11 (0.21)	0.595	1.17
Alanine	0.78 (0.016) 0.67 - 0.87	0.75 (0.016) 0.64 - 0.85	0.21	0.023 (0.023)	0.347	3.07
Arginine	0.47 (0.012) 0.40 - 0.53	0.47 (0.012) 0.41 - 0.52	0.12	-0.00036 (0.014)	0.981	-0.076
Aspartic acid	0.65 (0.011) 0.58 - 0.71	0.63 (0.011) 0.58 - 0.71	0.13	0.012 (0.016)	0.473	1.96
Cystine	0.21 (0.011) 0.15 - 0.28	0.20 (0.011) 0.16 - 0.26	0.10	0.0043 (0.0063)	0.534	2.12
Glutamic acid	1.87 (0.040) 1.59 - 2.11	1.81 (0.040) 1.52 - 2.02	0.50	0.061 (0.057)	0.314	3.38

Table 31. Summary of Maize Grain Protein and Amino Acids for MON 95275 and the Conventional Control (Continued)

Component (% dw)[1]	MON 95275 Mean (S.E.)[2] Range	Control Mean (S.E.) Range	Control Range Value[3]	Difference (Test minus Control) Mean (S.E.)	p-Value	% Relative[4]
Glycine	0.37 (0.0075) 0.32 - 0.40	0.36 (0.0075) 0.32 - 0.40	0.074	0.0050 (0.0094)	0.624	1.38
Histidine	0.27 (0.0055) 0.24 - 0.29	0.26 (0.0055) 0.23 - 0.30	0.061	0.0052 (0.0077)	0.522	1.96
Isoleucine	0.36 (0.0067) 0.31 - 0.41	0.34 (0.0067) 0.30 - 0.38	0.078	0.012 (0.0095)	0.252	3.41
Leucine	1.28 (0.031) 1.06 - 1.49	1.23 (0.031) 1.01 - 1.38	0.37	0.051 (0.041)	0.287	4.10
Lysine	0.28 (0.0042) 0.24 - 0.30	0.27 (0.0042) 0.24 - 0.30	0.055	0.0066 (0.0054)	0.288	2.44
Methionine	0.21 (0.012) 0.15 - 0.26	0.20 (0.012) 0.15 - 0.25	0.097	0.0026 (0.0077)	0.751	1.29

Table 31. Summary of Maize Grain Protein and Amino Acids for MON 95275 and the Conventional Control (Continued)

Component (% dw)[1]	MON 95275 Mean (S.E.)[2] Range	Control Mean (S.E.) Range	Control Range Value[3]	Difference (Test minus Control) Mean (S.E.)	p-Value	% Relative[4]
Phenylalanine	0.51 (0.011) 0.43 - 0.57	0.49 (0.011) 0.42 - 0.54	0.13	0.020 (0.016)	0.286	3.99
Proline	0.92 (0.016) 0.84 - 1.02	0.88 (0.016) 0.78 - 0.97	0.19	0.038 (0.022)	0.129	4.24
Serine	0.49 (0.0098) 0.44 - 0.54	0.48 (0.0098) 0.42 - 0.53	0.11	0.014 (0.014)	0.336	2.97
Threonine	0.35 (0.0060) 0.32 - 0.38	0.35 (0.0060) 0.31 - 0.38	0.072	0.0083 (0.0084)	0.355	2.40
Tryptophan	0.072 (0.0023) 0.062 - 0.084	0.072 (0.0023) 0.060 - 0.086	0.025	0.00011 (0.0013)	0.929	0.16
Tyrosine	0.43 (0.0074) 0.37 - 0.48	0.41 (0.0074) 0.35 - 0.47	0.11	0.015 (0.010)	0.181	3.70

Table 31. Summary of Maize Grain Protein and Amino Acids for MON 95275 and the Conventional Control (Continued)

				Difference (Test minus Control)		
Component (% dw)1	MON 95275 Mean (S.E.)[2] Range	Control Mean (S.E.) Range	Control Range Value[3]	Mean (S.E.)	p-Value	% Relative[4]
Valine	0.47 (0.0077) 0.43 - 0.52	0.45 (0.0077) 0.41 - 0.51	0.099	0.015 (0.011)	0.204	3.33

[1] dw=dry weight
[2] Mean (S.E.) = least-square mean (standard error)
[3] Maximum value minus minimum value for the control maize hybrid
[4] The relative magnitude of the difference in mean values between MON 95275 and the control, expressed as a percent of the control

Table 32. Summary of Maize Grain Total Fat and Fatty Acids for MON 95275 and the Conventional Control

				Difference (Test minus Control)	
Component	MON 95275 Mean (S.E.)[1] Range	Control Mean (S.E.) Range	Control Range Value[2]	Mean (S.E.)	p-Value
Total fat (% dw)[3]	3.73 (0.088) 3.36 - 4.00	3.73 (0.088) 3.20 - 4.07	0.87	0.0035 (0.058)	0.954
Palmitic acid (% Total FA)[4]	12.65 (0.057) 12.39 - 13.02	12.81 (0.056) 12.36 - 13.21	0.85	-0.16 (0.064)	0.016
Palmitoleic acid (% Total FA)	0.12 (0.0023) 0.12 - 0.14	0.13 (0.0022) 0.11 - 0.13	0.022	-0.00037 (0.0012)	0.763
Stearic acid (% Total FA)	1.63 (0.033) 1.51 - 1.74	1.70 (0.033) 1.47 - 1.83	0.36	-0.069 (0.014)	<0.001
Oleic acid (% Total FA)	27.95 (0.21) 26.91 - 28.79	28.52 (0.20) 26.70 - 30.08	3.38	-0.56 (0.19)	0.041
Linoleic acid (% Total FA)	55.65 (0.20) 54.56 - 56.60	54.84 (0.20) 53.71 - 56.21	2.50	0.81 (0.16)	<0.001

Table 32. Summary of Maize Grain Total Fat and Fatty Acids for MON 95275 and the Conventional Control (Continued)

Component	MON 95275 Mean (S.E.)[1] Range	Control Mean (S.E.) Range	Control Range Value[2]	Difference (Test minus Control) Mean (S.E.)	p-Value
Linolenic acid (% Total FA)	1.18 (0.013) 1.11 - 1.29	1.18 (0.013) 1.09 - 1.28	0.18	0.00068 (0.011)	0.951
Arachidic acid (% Total FA)	0.40 (0.010) 0.37 - 0.44	0.41 (0.010) 0.36 - 0.45	0.089	-0.011 (0.0035)	0.004
Eicosenoic acid (% Total FA)	0.25 (0.0060) 0.24 - 0.28	0.25 (0.0060) 0.23 - 0.29	0.057	-0.0023 (0.0019)	0.232
Behenic acid (% Total FA)	0.15 (0.0068) 0.13 - 0.18	0.16 (0.0068) 0.13 - 0.19	0.057	-0.0044 (0.0027)	0.184

[1] Mean (S.E.) = least-square mean (standard error)
[2] Maximum value minus minimum value for the control maize hybrid
[3] dw=dry weight
[4] FA=Fatty Acid
The following components with more than 50% of observations below the assay LOQ were excluded from statistical analysis: caprylic acid, capric acid, lauric acid, myristic acid, myristoleic acid, pentadecanoic acid, pentadecenoic acid, heptadecanoic acid, heptadecenoic acid, gamma linolenic acid, eicosadienoic acid, eicosatrienoic acid and arachidonic acid.

Table 33. Summary of Maize Grain Carbohydrates by Calculation and Fiber for MON 95275 and the Conventional Control

				Difference (Test minus Control)	
Component (% dw)[1]	MON 95275 Mean (S.E.)[2] Range	Control Mean (S.E.) Range	Control Range Value[3]	Mean (S.E.)	p-Value
Carbohydrates by calculation	85.11 (0.14) 83.88 - 86.10	85.24 (0.14) 84.21 - 86.28	2.07	-0.13 (0.20)	0.534
ADF	3.44 (0.13) 2.60 - 4.01	3.44 (0.13) 2.34 - 4.54	2.20	0.00018 (0.14)	0.999
NDF	8.93 (0.25) 6.68 - 10.71	8.91 (0.25) 6.63 - 11.51	4.89	0.018 (0.33)	0.960
TDF	11.25 (0.27) 9.46 - 12.99	11.35 (0.27) 9.82 - 13.33	3.50	-0.099 (0.30)	0.740

[1] dw=dry weight
[2] Mean (S.E.) = least-square mean (standard error)
[3] Maximum value minus minimum value for the control maize hybrid

Table 34. Summary of Maize Grain Ash and Minerals for MON 95275 and the Conventional Control

Component	MON 95275 Mean (S.E.)[1] Range	Control Mean (S.E.) Range	Control Range Value[2]	Difference (Test minus Control) Mean (S.E.)	p-Value
Ash (% dw)[3]	1.29 (0.042) 1.12 - 1.42	1.28 (0.042) 1.06 - 1.51	0.45	0.0089 (0.020)	0.685
Calcium (% dw)	0.0033 (0.00014) 0.0028 - 0.0038	0.0035 (0.00014) 0.0030 - 0.0041	0.0012	-0.00019 (0.00006)	0.005
Copper (mg/kg dw)	1.11 (0.056) 0.92 - 1.45	1.20 (0.056) 0.95 - 2.44	1.49	-0.082 (0.079)	0.310
Iron (mg/kg dw)	15.86 (0.42) 13.94 - 17.94	16.23 (0.42) 13.83 - 20.05	6.21	-0.37 (0.29)	0.212
Magnesium (% dw)	0.11 (0.0018) 0.095 - 0.12	0.11 (0.0018) 0.098 - 0.12	0.024	0.00020 (0.0021)	0.927
Manganese (mg/kg dw)	4.82 (0.23) 3.92 - 5.52	4.79 (0.23) 3.42 - 5.70	2.28	0.029 (0.18)	0.881

Table 34. Summary of Maize Grain Ash and Minerals for MON 95275 and the Conventional Control (Continued)

Component	MON 95275 Mean (S.E.)[1] Range	Control Mean (S.E.) Range	Control Range Value[2]	Difference (Test minus Control) Mean (S.E.)	p-Value
Phosphorus (% dw)	0.29 (0.011) 0.23 - 0.33	0.29 (0.011) 0.21 - 0.33	0.12	0.0053 (0.0070)	0.488
Potassium (% dw)	0.35 (0.011) 0.30 - 0.38	0.36 (0.011) 0.30 - 0.39	0.090	-0.0058 (0.0039)	0.208
Zinc (mg/kg dw)	18.57 (1.15) 14.67 - 23.81	18.44 (1.15) 14.25 - 23.73	9.48	0.13 (0.34)	0.705

[1] Mean (S.E.) = least-square mean (standard error)
[2] Maximum value minus minimum value for the control maize hybrid
[3] dw=dry weight
The following components with more than 50% of observations below the assay LOQ were excluded from statistical analysis: sodium.

Table 35. Summary of Maize Grain Vitamins for MON 95275 and the Conventional Control

Component (mg/kg dw)[1]	MON 95275 Mean (S.E.)[2] Range	Control Mean (S.E.) Range	Control Range Value[3]	Difference (Test minus Control) Mean (S.E.)	p-Value
Vitamin A	0.97 (0.029) 0.81 - 1.25	0.94 (0.029) 0.76 - 1.11	0.36	0.030 (0.023)	0.221
Vitamin B1	3.68 (0.11) 3.01 - 4.04	3.77 (0.11) 3.22 - 4.31	1.09	-0.095 (0.060)	0.124
Vitamin B2	1.49 (0.065) 1.15 - 1.89	1.55 (0.065) 1.24 - 1.86	0.63	-0.055 (0.051)	0.292
Vitamin B3	22.36 (0.57) 17.99 - 27.03	22.24 (0.57) 18.89 - 26.65	7.77	0.11 (0.65)	0.861
Vitamin B6	6.06 (0.077) 5.58 - 6.63	5.68 (0.077) 4.94 - 6.63	1.68	0.38 (0.11)	0.001
Vitamin B9	0.41 (0.026) 0.29 - 0.69	0.42 (0.026) 0.32 - 0.81	0.49	-0.0090 (0.036)	0.815

Table 35. Summary of Maize Grain Vitamins for MON 95275 and the Conventional Control (Continued)

Component (mg/kg dw)1	MON 95275 Mean (S.E.)2 Range	Control Mean (S.E.) Range	Control Range Value3	Difference (Test minus Control) Mean (S.E.)	p-Value
Vitamin E	14.15 (0.70) 11.03 - 25.57	13.45 (0.70) 10.41 - 16.86	6.45	0.70 (0.66)	0.297

[1] dw=dry weight; Common names of vitamins: A=β-Carotene; B1= Thiamine HCl; B2=Riboflavin; B3=Niacin; B6= Pyridoxine HCl; B9=Folic Acid; E=α-Tocopherol

[2] Mean (S.E.) = least-square mean (standard error)

[3] Maximum value minus minimum value for the control maize hybrid

Table 36. Summary of Maize Grain Anti-Nutrients and Secondary Metabolites for MON 95275 and the Conventional Control

Component	MON 95275 Mean (S.E.)[1] Range	Control Mean (S.E.) Range	Control Range Value[2]	Difference (Test minus Control) Mean (S.E.)	p-Value
Phytic acid (% dw)[3]	0.75 (0.056) 0.33 - 0.96	0.71 (0.056) 0.33 - 0.99	0.67	0.041 (0.051)	0.469
Raffinose (% dw)	0.20 (0.014) 0.15 - 0.24	0.19 (0.014) 0.14 - 0.23	0.094	0.0097 (0.0055)	0.153
Ferulic acid (µg/g dw)	2105.37 (31.77) 2004.50 - 2313.77	2114.78 (31.77) 1934.76 - 2317.21	382.45	-9.42 (23.51)	0.691
p-coumaric acid (µg/g dw)	133.22 (9.13) 107.68 - 194.13	133.48 (9.13) 104.61 - 229.12	124.51	-0.26 (4.05)	0.952

[1] Mean (S.E.) = least-square mean (standard error)
[2] Maximum value minus minimum value for the control maize hybrid
[3] dw=dry weight
The following components with more than 50% of observations below the assay LOQ were excluded from statistical analysis: furfural.

Table 37. Summary of Maize Forage Proximates, Carbohydrates by Calculation, Fiber and Minerals for MON 95275 and the Conventional Control

				Difference (Test minus Control)	
Component (% dw)[1]	MON 95275 Mean (S.E.)[2] Range	Control Mean (S.E.) Range	Control Range Value[3]	Mean (S.E.)	p-Value
Protein	6.96 (0.32) 5.69 - 7.81	7.20 (0.32) 5.41 - 9.03	3.62	-0.23 (0.28)	0.457
Total fat	3.12 (0.15) 2.23 - 4.34	2.84 (0.15) 1.33 - 3.53	2.20	0.28 (0.18)	0.183
Carbohydrates by calculation	86.35 (0.37) 83.81 - 87.91	86.50 (0.37) 83.66 - 88.31	4.65	-0.15 (0.33)	0.681
ADF	21.45 (1.07) 17.07 - 27.79	20.76 (1.07) 16.13 - 27.09	10.95	0.69 (0.61)	0.272
NDF	35.09 (1.15) 28.07 - 44.98	33.62 (1.15) 26.62 - 41.16	14.54	1.47 (1.20)	0.287
Ash	3.57 (0.12) 2.84 - 4.86	3.47 (0.12) 2.55 - 4.57	2.01	0.090 (0.093)	0.343

Table 37. Summary of Maize Forage Proximates, Carbohydrates by Calculation, Fiber and Minerals for MON 95275 and the Conventional Control (Continued)

				Difference (Test minus Control)	
Component (% dw)[1]	MON 95275 Mean (S.E.)[2] Range	Control Mean (S.E.) Range	Control Range Value[3]	Mean (S.E.)	p-Value
Calcium	0.22 (0.012) 0.16 - 0.28	0.22 (0.012) 0.15 - 0.30	0.15	-0.0057 (0.0088)	0.525
Phosphorus	0.18 (0.014) 0.13 - 0.25	0.18 (0.014) 0.12 - 0.24	0.13	-0.00040 (0.0065)	0.950

[1] dw=dry weight
[2] Mean (S.E.) = least-square mean (standard error)
[3] Maximum value minus minimum value for the control maize hybrid

B.5(b) Information on the range of natural variation for each constituent measure to allow for assessment of biological significance

Table 38. Literature and AFSI Database Ranges for Components in Maize Grain and Forage

Tissue Components[1]	Literature Range[2]	AFSI Range[3]
Grain Nutrients		
Proximates		
protein (% dw)	8.27-13.33[a]; 9.17-12.19[b]	5.72-17.26
total fat (% dw)	2.95-4.40[a]; 3.18-4.23[b]	1.363-7.830
ash (% dw)	1.17-2.01[a]; 1.27-1.63[b]	0.616-6.282
Amino Acids		
alanine (% dw)	0.60-1.04[a]; 0.68-0.96[b]	0.40-1.48
arginine (% dw)	0.34-0.52[a]; 0.34-0.50[b]	0.12-0.71
aspartic acid (% dw)	0.52-0.78[a]; 0.59-0.76[b]	0.30-1.21
cystine (% dw)	0.19-0.26[a]; 0.20-0.26[b]	0.12-0.51
glutamic acid (% dw)	1.54-2.67[a]; 1.71-2.44[b]	0.83-3.54
glycine (% dw)	0.33-0.43[a]; 0.33-0.42[b]	0.184-0.685
histidine (% dw)	0.25-0.37[a]; 0.27-0.34[b]	0.14-0.46
isoleucine (% dw)	0.30-0.48[a]; 0.32-0.44[b]	0.18-0.69
leucine (% dw)	1.02-1.87[a]; 1.13-1.65[b]	0.60-2.49
lysine (% dw)	0.26-0.33[a]; 0.28-0.31[b]	0.129-0.668
methionine (% dw)	0.17-0.26[a]; 0.16-0.30[b]	0.11-0.47
phenylalanine (% dw)	0.43-0.72[a]; 0.45-0.63[b]	0.24-0.93
proline (% dw)	0.74-1.21[a]; 0.78-1.11[b]	0.46-1.75
serine (% dw)	0.39-0.67[a]; 0.43-0.6[b]	0.15-0.77
threonine (% dw)	0.29-0.45[a]; 0.31-0.39[b]	0.17-0.67
tryptophan (% dw)	0.047-0.085[a]; 0.042-0.07[b]	0.027-0.215
tyrosine (% dw)	0.13-0.43[a]; 0.12-0.41[b]	0.10-0.73
valine (% dw)	0.42-0.62[a]; 0.45-0.58[b]	0.27-0.86
Fatty Acids		
palmitic acid (% Total FA)	8.80-13.33[a]; 9.84-12.33[b]	6.81-26.55
palmitoleic acid (% Total FA)	0.059-0.23[a]	0.067-0.453
stearic acid (% Total FA)	1.36-2.14[a]; 1.3-2.1[b]	1.02-3.83
oleic acid (% Total FA)	19.50-33.71[a]; 19.59-29.13[b]	16.38-42.81
linoleic acid (% Total FA)	49.31-64.70[a]; 56.51-65.65[b]	34.27-67.68
linolenic acid (% Total FA)	0.89-1.56[a]; 1.03-1.38[b]	0.55-2.33
arachidic acid (% Total FA)	0.30-0.49[a]; 0.30-0.41[b]	0.267-0.993
eicosenoic acid (% Total FA)	0.17-0.29[a]; 0.17-0.27[b]	0.098-1.952
behenic acid (% Total FA)	0.069-0.28[a]; 0.059-0.18[b]	0.093-0.417
Carbohydrates By Calculation		
carbohydrates by calculation (% dw)	81.31-87.06[a]; 82.10-85.98[b]	77.4-89.7
Fiber		
ADF (% dw)	1.82-4.48[a]; 1.83-3.39[b]	1.41-11.34
NDF (% dw)	6.51-12.28[a]; 6.08-10.36[b]	4.28-24.30
TDF (% dw)	10.65-16.26[a]; 10.57-14.56[b]	5.78-35.31

Table 38. Literature and AFSI Database Ranges for Components in Maize Grain and Forage (Continued)

Tissue Components[1]	Literature Range[2]	AFSI Range[3]
Minerals		
calcium (% dw)	0.0036-0.0068[a]; 0.0035-0.007[b]	0.001-0.101
copper (mg/kg dw)	0.85-3.54[c]	0.55-21.2
iron (mg/kg dw)	14.17-23.40[a]; 15.90-24.66[b]	9.51-191.00
magnesium (% dw)	0.091-0.14[a]; 0.1-0.14[b]	0.06-0.19
manganese (mg/kg dw)	4.83-8.34[a]; 4.78-9.35[b]	1.69-14.30
phosphorus (% dw)	0.24-0.37[a]; 0.27-0.38[b]	0.13-0.55
potassium (% dw)	0.29-0.39[a]; 0.36-0.43[b]	0.18-0.60
zinc (mg/kg dw)	16.78-28.17[a]; 18.25-30.44[b]	6.5-42.6
Vitamins		
vitamin A (mg/kg dw)	0.14-11.27[d]	0.19-80.20
vitamin B_1 (mg/kg dw)	2.33-4.17[a]; 2.71-4.33[b]	1.26-40.00
vitamin B_2 (mg/kg dw)	0.94-2.42[a]; 1.64-2.81[b]	0.50-7.35
vitamin B_3 (mg/kg dw)	15.07-32.38[a]; 13.64-42.06[b]	7.42-46.94
vitamin B_6 (mg/kg dw)	4.93-7.53[a]; 4.97-8.27[b]	1.18-12.14
vitamin B_9 (mg/kg dw)	0.19-0.35[a]; 0.23-0.42[b]	0.09-3.50
vitamin E (mg/kg dw)	5.96-18.44[a]; 2.84-15.53[b]	0.84-68.67
Grain Other		
Anti-Nutrients		
phytic acid (% dw)	0.69-1.09[a]; 0.60-0.94[b]	0.111-1.940
raffinose (% dw)	0.079-0.22[a]; 0.061-0.15[b]	0.020-0.466
Secondary Metabolites		
ferulic acid (µg/g dw)	1205.75-2873.05[a]; 1011.40-2539.86[b]	291.93-4397.30
p-coumaric acid (µg/g dw)	94.77-327.39[a]; 66.48-259.68[b]	53.4-820.0
Forage Nutrients		
Proximates		
protein (% dw)	5.80-10.24[a]; 5.56-9.14[b]	2.37-16.32
total fat (% dw)	1.28-3.62[a]; 0.20-1.76[b]	0.296-6.755
ash (% dw)	2.67-8.01[a]; 4.59-6.9[b]	0.66-13.20
Carbohydrates By Calculation		
carbohydrates by calculation (% dw)	81.88-89.26[a]; 84.11-87.54[b]	73.3-92.9
Fiber		
ADF (% dw)	19.11-30.49[a]; 20.73-33.39[b]	5.13-47.39
NDF (% dw)	27.73-49.62[a]; 31.81-50.61[b]	18.30-67.80
Minerals		
calcium (% dw)	0.12-0.33[a]; 0.21-0.41[b]	0.04-0.58
phosphorus (% dw)	0.090-0.26[a]; 0.13-0.21[b]	0.07-0.44

[1]dw=dry weight; FA=Fatty Acid; mg/kg/ dw
[2]Literature range references: [a](Harrigan *et al.*, 2009) (see U.S. Field data);[b](Harrigan *et al.*, 2009) (see Chile field data);[c](Ridley *et al.*, 2011);[d](Egesel *et al.*, 2003)
[3]AFSI range is from AFSI Crop Composition Database, 2019 (Accessed January 25, 2019)

C. INFORMATION RELATED TO THE NUTRITIONAL IMPACT OF THE FOOD PRODUCED USING GENE TECHNOLOGY

There are no nutritional impacts on the food and feed derived from MON 95275. This product is developed to confer insect protection. It is not a nutritionally altered product.

D. OTHER INFORMATION

The data and information presented in this submission demonstrate that the food and feed derived from MON 95275 are as safe and nutritious as those derived from commercially-available, conventional maize for which there is an established history of safe consumption. No additional studies have been supplied to add value to the safety of MON 95275.

PART 3 STATUTORY DECLARATION – AUSTRALIA

I, Nina McCormick, declare the following points in this application:

The information provided in this application fully sets out the matters required.

The information provided in this application is true to the best of my knowledge and belief.

No information has been withheld that might prejudice this application, to the best of my knowledge and belief.

Signature: [redacted]

Declared before me ..... [redacted] .....

This ..... 14th ..... day of ..... SEPTEMBER ..... 2022.

[redacted]
Level 1, 8 Redfern Road, Hawthorn East VIC 3123
An Australian Legal Practitioner within the meaning of the Legal Profession Uniform Law (Victoria)

PART 4 REFERENCES

Akhtar, S. 2009. Oral delivery of siRNA and antisense oligonucleotides. Journal of Drug Targeting 17:491-495.

Akiba, T., Y. Abe, S. Kitada, Y. Kusaka, A. Ito, T. Ichimatsu, H. Katayama, T. Akao, K. Higuchi, E. Mizuki, M. Ohba, R. Kanai and K. Harata. 2009. Crystal structure of the parasporin-2 *Bacillus thuringiensis* toxin that recognizes cancer cells. Journal of Molecular Biology 386:121-133.

Anderson, J.E., J.M. Michno, T.J.Y. Kono, A.O. Stec, B.W. Campbell, S.J. Curtin and R.M. Stupar. 2016. Genomic variation and DNA repair associated with soybean transgenesis: A comparison to cultivars and mutagenized plants. BMC Biotechnology 16:41.

Babst, M., D.J. Katzmann, E.J. Estepa-Sabal, T. Meerloo and S.D. Emr. 2002. ESCRT-III: An endosome-associated heterooligomeric protein complex required for MVB sorting. Developmental Cell 3:271-282.

Bachman, P.M., R. Bolognesi, W.J. Moar, G.M. Mueller, M.S. Paradise, P. Ramaseshadri, J. Tan, J.P. Uffman, J. Warren, B.E. Wiggins and S.L. Levine. 2013. Characterization of the spectrum of insecticidal activity of a double-stranded RNA with targeted activity against Western Corn Rootworm (*Diabrotica virgifera virgifera* LeConte). Transgenic Research 22:1207-1222.

Bachman, P.M., K.M. Huizinga, P.D. Jensen, G. Mueller, J. Tan, J.P. Uffman and S.L. Levine. 2016. Ecological risk assessment for DvSnf7 RNA: A plant-incorporated protectant with targeted activity against western corn rootworm. Regulatory Toxicology and Pharmacology 81:77-88.

Barker, R.F., K.B. Idler, D.V. Thompson and J.D. Kemp. 1983. Nucleotide sequence of the T-DNA region from the *Agrobacterium tumefaciens* octopine Ti plasmid pTi15955. Plant Molecular Biology 2:335-350.

Barry, G.F., G.M. Kishore, S.R. Padgette and W.C. Stallings. 2001. Glyphosate-tolerant 5-enolpyruvylshikimate-3-phosphate synthases. Patent 6,248,876, U.S. Patent Office, Washington, D.C.

Baum, J.A., T. Bogaert, W. Clinton, G.R. Heck, P. Feldmann, O. Ilagan, S. Johnson, G. Plaetinck, T. Munyikwa, M. Pleau, T. Vaughn and J. Roberts. 2007a. Control of coleopteran insect pests through RNA interference. Nature Biotechnology 25:1322-1326.

Baum, J.A., C.A. Cajacob, P. Feldmann, G.R. Heck, I. Nooren, G. Plaetinck, W. Maddelein and T.T. Vaughn. 2007b. Methods for genetic control of insect infestations in plants and compositions thereof. Patent US 2007/0124836 A1, U.S. Patent Office, Washington, D.C.

Baum, J.A., T.B. Johnson and B.C. Carlton. 1999. *Bacillus thuringiensis*: Natural and recombinant bioinsecticide products. Pages 189-209 in Methods in Biotechnology: Biopesticides: Use and Delivery. Volume 5. F.R. Hall and J.J. Menn (eds.). Humana Press Inc., Totowa, New Jersey.

Betz, F.S., B.G. Hammond and R.L. Fuchs. 2000. Safety and advantages of *Bacillus thuringiensis*-protected plants to control insect pests. Regulatory Toxicology and Pharmacology 32:156-173.

Biron, D.G., C. Brun, T. Lefevre, C. Lebarbenchon, H.D. Loxdale, F. Chevenet, J.-P. Brizard and F. Thomas. 2006. The pitfalls of proteomics experiments without the correct use of bioinformatics tools. Proteomics 6:5577-5596.

Bokori-Brown, M., C.A. Hall, C. Vance, S.P. Fernandes da Costa, C.G. Savva, C.E. Naylor, A.R. Cole, A.K. Basak, D.S. Moss and R.W. Titball. 2014. *Clostridium perfringens* epsilon toxin mutant Y30A-Y196A as a recombinant vaccine candidate against enterotoxemia. Vaccine 32:2682-2687.

Bokori-Brown, M., M.C. Kokkinidou, C.G. Savva, S. Fernandes da Costa, C.E. Naylor, A.R. Cole, D.S. Moss, A.K. Basak and R.W. Titball. 2013. *Clostridium perfringens* epsilon toxin H149A mutant as a platform for receptor binding studies. Protein Society 22:650-659.

Bolognesi, R., P. Ramaseshadri, J. Anderson, P. Bachman, W. Clinton, R. Flannagan, O. Ilagan, C. Lawrence, S. Levine, W. Moar, G. Mueller, J.G. Tan, J. Uffman, E. Wiggins, G. Heck and G. Segers. 2012. Characterizing the mechanism of action of double-stranded RNA activity against western corn rootworm (*Diabrotica virgifera virgifera* LeConte). PLoS ONE 7:e47534.

Bowen, D., Y. Yin, S. Flasinski, C. Chay, G. Bean, J. Milligan, W. Moar, A. Pan, B. Werner, K. Buckman, A. Howe, T. Ciche, K. Turner, M. Pleau, J. Zhang, J.-L. Kouadio, B.E. Hibbard, P. Price and J. Roberts. 2021. Cry75Aa (Mpp75Aa) insecticidal proteins for controlling the western corn rootworm, Diabrotica *virgifera virgifera* LeConte (Coleoptera: Chrysomelidae), isolated from the insect-pathogenic bacterium *Brevibacillus laterosporus*. Applied and Environmental Microbiology 87:e02507-02520.

Bradshaw, R.A., W.W. Brickey and K.W. Walker. 1998. N-terminal processing: The methionine aminopeptidase and N^{α}-acetyl transferase families. Trends in Biochemical Sciences 23:263-267.

Brown, S.M. and C.G. Santino. 1997. Enhanced expression in plants. Patent 5,593,874, U.S. Patent Office, Washington, D.C.

Brune, P., S. Chakravarthy, G. Graser, C.A. Mathesius, S. McClain, J.S. Petrick, A. Sauve-Ciencewicki, B. Schafer, A. Silvanovich, K. Brink, K. Burgin, D. Bushey, M.L. Cheever, T. Edrington, H. Fu, V. Habex, R. Herman, E. Islamovic, E.A. Lipscomb, S. Motyka, L. Privalle, R. Ranjan, J. Roper, P. Song, G. Tilton, J. Zhang, S. Waters, A. Ramos, A.H. Culler, P. Hunst, R. Gast, D. Mahadeo and L. Goodwin. 2021. Core and supplementary studies to assess the safety of genetically modified (GM) plants used for food and feed. Journal of Regulatory Science 9:45-60.

Cade, R., K. Burgin, K. Schilling, T.-J. Lee, P. Ngam, N. Devitt and D. Fajardo. 2018. Evaluation of whole genome sequencing and an insertion site characterization method for molecular characterization of GM maize. Journal of Regulatory Science 6:1-14.

Caetano-Anollés, G., M. Wang, D. Caetano-Anollés and J.E. Mittenthal. 2009. The origin, evolution and structure of the protein world. Biochemical Journal 417:621-637.

Campbell, J.D., K.H. Clement, S.S. Wasserman, S. Donegan, L. Chrisley and K.L. Kotloff. 2007. Safety, reactogenicity and immunogenicity of a recombinant protective antigen anthrax vaccine given to healthy adults. Human Vaccines 3:205-211.

Cannon, R.J.C. 1993. Prospects and progress for *Bacillus thuringiensis*-based pesticides. Pesticide Science 37:331-335.

Casini, A., G. Christodoulou, P.S. Freemont, G.S. Baldwin, T. Ellis and J.T. MacDonald. 2014. R2oDNA designer: Computational design of biologically neutral synthetic DNA sequences. ACS Synthetic Biology 3:525-528.

Clem, A.S. 2011. Fundamentals of vaccine immunology. Journal of Global Infectious Diseases 3:73-78.

Codex Alimentarius. 2009. Foods derived from modern biotechnology. Second Edition. Codex Alimentarius Commission, Joint FAO/WHO Food Standards Programme, Food and Agriculture Organization of the United Nations, Rome, Italy.

Cole, A.R., M. Gibert, M. Popoff, D.S. Moss, R.W. Titball and A.K. Basak. 2004. *Clostridium perfringens* ε-toxin shows structural similarity to the pore-forming toxin aerolysin. Nature Structural & Molecular Biology 11:797-798.

Coruzzi, G., R. Broglie, C. Edwards and N.-H. Chua. 1984. Tissue-specific and light-regulated expression of a pea nuclear gene encoding the small subunit of ribulose-1, 5-bisphosphate carboxylase. EMBO Journal 3:1671-1679.

Crickmore, N., C. Berry, S. Panneerselvam, R. Mishra, T.R. Connor and B.C. Bonning. 2021. A structure-based nomenclature for *Bacillus thuringiensis* and other bacteria-derived pesticidal proteins. Journal of Invertebrate Pathology 186:107438.

Crickmore, N., D.R. Zeigler, J. Feitelson, E. Schnepf, J. Van Rie, D. Lereclus, J.A. Baum and D.H. Dean. 1998. Revision of the nomenclature for the *Bacillus thuringiensisi* pesticidal crystal proteins. Microbiology and Molecular Biology Reviews 62:807-813.

Curtis, A.K., C. Lamb, W.M. Hassan and J. Foxworth. 2020. *Brevibacillus laterosporus* bacteremia in an adult. Cureus 12:e10481.

Della Vedova, C.B., R. Lorbiecke, H. Kirsch, M.B. Schulte, K. Scheets, L.M. Borchert, B.E. Scheffler, U. Wienand, K.C. Cone and J.A. Birchler. 2005. The dominant inhibitory chalcone synthase allele *C2-Idf* (*Inhibitor diffuse*) from *Zea mays* (L.) acts via an endogenous RNA silencing mechanism. Genetics 170:1989-2002.

Depicker, A., S. Stachel, P. Dhaese, P. Zambryski and H.M. Goodman. 1982. Nopaline synthase: Transcript mapping and DNA sequence. Journal of Molecular and Applied Genetics 1:561-573.

Dickinson, B., Y. Zhang, J.S. Petrick, G. Heck, S. Ivashuta and W.S. Marshall. 2013. Lack of detectable oral bioavailability of plant microRNAs after feeding in mice. Nature Biotechnology 31:965-967.

Edgerton, M.D. 2009. Increasing crop productivity to meet global needs for feed, food, and fuel. Plant Physiology 149:7-13.

Egesel, C.O., J.C. Wong, R.J. Lambert and T.R. Rocheford. 2003. Gene dosage effects on carotenoid concentration in maize grain. Maydica 48:183-190.

Fling, M.E., J. Kopf and C. Richards. 1985. Nucleotide sequence of the transposon Tn*7* gene encoding an aminoglycoside-modifying enzyme, 3"(9)-*O*-nucleotidyltransferase. Nucleic Acids Research 13:7095-7106.

Frizzi, A. and S. Huang. 2010. Tapping RNA silencing pathways for plant biotechnology. Plant Biotechnology Journal 8:655-677.

FSANZ. 2013. Response to Heinemann et al on the regulation of GM crops and foods developed using gene silencing. Food Standards Australia New Zealand, Canberra, Australia.

Gilbertson, L. 2003. Cre-*lox* recombination: Cre-ative tools for plant biotechnology. Trends in Biotechnology 21:550-555.

Gill, S.S., E.A. Cowles and P.V. Pietrantonio. 1992. The mode of action of *Bacillus thuringiensis* endotoxins. Annual Review of Entomology 37:615-636.

Gowda, A., T.J. Rydel, A.M. Wollacott, R.S. Brown, W. Akbar, T.L. Clark, S. Flasinski, J.R. Nageotte, A.C. Read, X. Shi, B.J. Werner, M.J. Pleau and J.A. Baum. 2016. A transgenic approach for controlling *Lygus* in cotton. Nature Communications 7:12213.

Hammond, B. 2004. A review of the food/feed safety and benefits of *Bacillus thuringiensis* protein containing insect-protected crops. Pages 103-123 in Agricultural Biotechnology: Challenges and Prospects. M.K. Bhalgat, W.P. Ridley, A.S. Felsot, and J.N. Seiber (eds.). American Chemical Society, Washington, D.C.

Hammond, B.G. and J.M. Jez. 2011. Impact of food processing on the safety assessment for proteins introduced into biotechnology-derived soybean and corn crops. Food and Chemical Toxicology 49:711-721.

Hare, P.D. and N.-H. Chua. 2002. Excision of selectable marker genes from transgenic plants. Nature Biotechnology 20:575-580.

Harrigan, G.G., D. Lundry, S. Drury, K. Berman, S.G. Riordan, M.A. Nemeth, W.P. Ridley and K.C. Glenn. 2010. Natural variation in crop composition and the impact of transgenesis. Nature Biotechnology 28:402-404.

Harrigan, G.G., W.P. Ridley, K.D. Miller, R. Sorbet, S.G. Riordan, M.A. Nemeth, W. Reeves and T.A. Pester. 2009. The forage and grain of MON 87460, a drought-tolerant corn hybrid, are compositionally equivalent to that of conventional corn. Journal of Agricultural and Food Chemistry 57:9754-9763.

Hartung, M. and B. Kisters-Woike. 1998. Cre mutants with altered DNA binding properties. Journal of Biological Chemistry 273:22884-22891.

Haupenthal, J., C. Baehr, S. Kiermayer, S. Zeuzem and A. Piiper. 2006. Inhibition of RNAse A family enzymes prevents degradation and loss of silencing activity of siRNAs in serum. Biochmical Pharmacology 71:702-710.

Heinemann, J.A., S.Z. Agapito-Tenfen and J.A. Carman. 2013. A comparative evaluation of the regulation of GM crops or products containing dsRNA and suggested improvements to risk assessments. Environment International 55:43-55.

Hernandez-Garcia, C.M. and J.J. Finer. 2014. Identification and validation of promoters and *cis*-acting regulatory elements. Plant Science 217-218:109-119.

Herrmann, K.M. 1995. The shikimate pathway: Early steps in the biosynthesis of aromatic compounds. The Plant Cell 7:907-919.

Hileman, R.E., A. Silvanovich, R.E. Goodman, E.A. Rice, G. Holleschak, J.D. Astwood and S.L. Hefle. 2002. Bioinformatic methods for allergenicity assessment using a comprehensive allergen database. International Archives of Allergy and Immunology 128:280-291.

Hoess, R.H., A. Wierzbicki and K. Abremski. 1986. The role of the *lox*P spacer region in P1 site-specific recombination. Nucleic Acids Research 14:2287-2300.

Hong, H.A., L.H. Duc and S.M. Cutting. 2005. The use of bacterial spore formers as probiotics. FEMS Microbiology Reviews 29:813-835.

Huang, H., C.D. Davis and T.T.Y. Wang. 2018. Extensive degradation and low bioavailability of orally consumed corn miRNAs in mice. Nutrients 10:215.

Huang, Y.-F., W.R. Jordan, R.A. Wing and P.W. Morgan. 1998. Gene expression induced by physical impedance in maize roots. Plant Molecular Biology 37:921-930.

Hunt, A.G. 1994. Messenger RNA 3' end formation in plants. Annual Review of Plant Physiology and Plant Molecular Biology 45:47-60.

Illergård, K., D.H. Ardell and A. Elofsson. 2009. Structure is three to ten times more conserved than sequence - A study of structural response in protein cores. Proteins 77:499-508.

ILSI-CERA. 2011. Problem formulation for the environmental risk assessment of RNAi plants. International Life Sciences Institute, Center for Environmental Risk Assessment, Washington, D.C.

Iurlina, M.O. and R. Fritz. 2005. Characterization of microorganisms in Argentinean honeys from different sources. International Journal of Food Microbiology 105:297-304.

Ivashuta, S.I., J.S. Petrick, S.E. Heisel, Y. Zhang, L. Guo, T.L. Reynolds, J.F. Rice, E. Allen and J.K. Roberts. 2009. Endogenous small RNAs in grain: Semi-quantification and sequence homology to human and animal genes. Food and Chemical Toxicology 47:353-360.

Jain, K.K. 2008. Stability and delivery of RNA via the gastrointestinal tract. Current Drug Delivery 5:27-31.

Jensen, P.D., Y. Zhang, B.E. Wiggins, J.S. Petrick, J. Zhu, R.A. Kerstetter, G.R. Heck and S.I. Ivashuta. 2013. Computational sequence analysis of predicted long dsRNA transcriptomes of major crops reveals sequence complementarity with human genes. GM Crops and Food 4:90-97.

Jeon, J.-S., S. Lee, K.-H. Jung, S.-H. Jun, C. Kim and G. An. 2000. Tissue-preferential expression of a rice *α*-tubulin gene, *OsTubA1*, mediated by the first intron. Plant Physiology 123:1005-1014.

Jerga, A., D. Chen, C. Zhang, J. Fu, J.-L.K. Kouadio, Y. Wang, S.M.G. Duff, J.E. Howard, T.J. Rydel, A.G. Evdokimov, P. Ramaseshadri, A. Evans, R. Bolognesi, Y. Park and J.A. Haas. 2016. Mechanistic insights into the first Lygus-active β-pore forming protein. Archives of Biochemistry and Biophysics 600:1-11.

Juliano, R., J. Bauman, H. Kang and X. Ming. 2009. Biological barriers to therapy with antisense and siRNA oligonucleotides. Molecular Pharmaceutics 6:686-695.

Kamthan, A., A. Chaudhuri, M. Kamthan and A. Datta. 2015. Small RNAs in plants: Recent development and application for crop improvement. Frontiers in Plant Science 6:208.

Kang, W., C.H. Bang-Berthelsen, A. Holm, A.J.S. Houben, A.H. Müller, T. Thymann, F. Pociot, X. Estivill and M.R. Friedländer. 2017. Survey of 800+ data sets from human tissue and body fluid reveals xenomiRs are likely artifacts. RNA 23:433-445.

Klee, H.J., Y.M. Muskopf and C.S. Gasser. 1987. Cloning of an *Arabidopsis thaliana* gene encoding 5-enolpyruvylshikimate-3-phosphate synthase: Sequence analysis and manipulation to obtain glyphosate-tolerant plants. Molecular and General Genetics 210:437-442.

Knapp, O., R. Benz and M.R. Popoff. 2016. Pore-forming activity of clostridial binary toxins. Biochimica et Biophysica Acta 1858:512-525.

Koch, M.S., J.M. Ward, S.L. Levine, J.A. Baum, J.L. Vicini and B.G. Hammond. 2015. The food and environmental safety of *Bt* crops. Frontiers in Plant Science 6:283.

Kouadio, J.-L., S. Duff, M. Aikins, M. Zheng, T. Rydel, D. Chen, E. Bretsnyder, C. Xia, J. Zhang, J. Milligan, A. Evdokimov, J. Nageotte, Y. Yin, W. Moar, K. Giddings, Y. Park, A. Jerga and J. Haas. 2021a. Structural and functional characterization of Mpp75Aa1.1, a putative beta-pore forming protein from *Brevibacillus laterosporus* active against the western corn rootworm. PloS ONE 16:e0258052.

Kouadio, J.-L., M. Zheng, M. Aikins, D. Duda, S. Duff, D. Chen, J. Zhang, J. Milligan, C. Taylor, P. Mamanella, R. Timothy, C. Kessenich, T. Panosian, Y. Yin, W. Moar, K. Giddings, Y. Park, A. Jerga and J. Haas. 2021b. Structural and functional insights into the first *Bacillus thuringiensis* vegetative insecticidal protein of the Vpb4 fold, active against western corn rootworm. PLoS ONE 16:e0260532.

Kovalic, D., C. Garnaat, L. Guo, Y. Yan, J. Groat, A. Silvanovich, L. Ralston, M. Huang, Q. Tian, A. Christian, N. Cheikh, J. Hjelle, S. Padgette and G. Bannon. 2012. The use of next generation sequencing and junction sequence analysis bioinformatics to achieve molecular characterization of crops improved through modern biotechnology. The Plant Genome 5:149-163.

Kozak, M. 1989. Circumstances and mechanisms of inhibition of translation by secondary structure in eucaryotic mRNAs. Molecular and Cellular Biology 9:5134-5142.

Krantz, B.A., R.A. Melnyk, S. Zhang, S.J. Juris, D.B. Lacy, Z. Wu, A. Finkelstein and R.J. Collier. 2005. A phenylalanine clamp catalyzes protein translocation through the anthrax toxin pore. Science 309:777-781.

Krause, E., H. Wenschuh and P.R. Jungblut. 1999. The dominance of arginine-containing peptides in MALDI-derived tryptic mass fingerprints of proteins. Analytical Chemistry 71:4160-4165.

Kuluev, B.R. and A.V. Chemeris. 2007. Amplification and cloning of dahlia mosaic virus and carnation etched ring virus promoters. Russian Journal of Genetics 43:1413-1414.

Kusaba, M., K. Miyahara, S. Iida, H. Fukuoka, T. Takano, H. Sassa, M. Nishimura and T. Nishio. 2003. *Low glutelin content1*: A dominant mutation that suppresses the glutelin multigene family via RNA silencing in rice. The Plant Cell 15:1455-1467.

Kwan, T. and S.R. Thompson. 2019. Noncanonical translation initiation in eukaryotes. Cold Spring Harbor Perspectives in Biology 11:a032672.

Laubach, C.A. 1916. Studies on aerobic spore-bearing non-pathogenic bacteria. Part II: Spore-bearing bacteria in dust. Journal of Bacteriology 1:493-533.

Leath, M.N. and L.D. Hill. 1987. Economics of production, marketing, and utilization. Pages 210-219 in Corn: Chemistry and Technology. S.A. Watson and P.E. Ramstad (eds.). American Association of Cereal Chemists, St. Paul, Minnesota.

Lee, G. and I. Saito. 1998. Role of nucleotide sequences of *loxP* spacer region in Cre-mediated recombination. Gene 216:55-65.

Loy, D.D. and E.L. Lundy. 2019. Nutritional properties and feeding value of corn and its coproducts. Pages 633-659 in Corn: Chemistry and Technology. Third Edition. S.O. Serna-Saldivar (ed.). Woodhead Publishing and AACC International Press.

Mao, Y.-B., W.-J. Cai, J.-W. Wang, G.-J. Hong, X.-Y. Tao, L.-J. Wang, Y.-P. Huang and X.-Y. Chen. 2007. Silencing a cotton bollworm P450 monooxygenase gene by plant-mediated RNAi impairs larval tolerance of gossypol. Nature Biotechnology 25:1307-1313.

May, J.B. 1987. Wet milling: Process and products. Pages 377-397 in Corn: Chemistry and Technology. S.A. Watson and P.E. Ramstad (eds.). American Association of Cereal Chemists, St. Paul, Minnesota.

McClintock, J.T., C.R. Schaffer and R.D. Sjoblad. 1995. A comparative review of the mammalian toxicity of *Bacillus thuringiensis*-based pesticides. Pesticide Science 45:95-105.

McConnell, M., D. Liefert, D. Olson and T. Capehart. 2021. Feed outlook: FDS-21a. Lower corn supplies reduce use, raise prices for 2020/21. U.S. Department of Agriculture, Economic Research Service, Washington, D.C.

Melnyk, R.A. and R.J. Collier. 2006. A loop network within the anthrax toxin pore positions the phenylalanine clamp in an active conformation. Proceedings of the National Academy of Sciences 103:9802-9807.

Mendelsohn, M., J. Kough, Z. Vaituzis and K. Matthews. 2003. Are *Bt* crops safe? Nature Biotechology 21:1003-1009.

Metcalfe, D.D., J.D. Astwood, R. Townsend, H.A. Sampson, S.L. Taylor and R.L. Fuchs. 1996. Assessment of the allergenic potential of foods derived from genetically engineered crop plants. Critical Reviews in Food Science and Nutrition 36:S165-S186.

Moar, W.J., C. Berry and K.E. Narva. 2017a. The structure/function of new insecticidal proteins and regulatory challenges for commercialization. Journal of Invertebrate Pathology 142:1-4.

Moar, W.J., A.J. Evans, C.R. Kessenich, J.A. Baum, D.J. Bowen, T.C. Edrington, J.A. Haas, J.-L.K. Kouadio, J.K. Roberts, A. Silvanovich, Y. Yin, B.E. Weiner, K.C. Glenn and M.L. Odegaard. 2017b. The sequence, structural, and functional diversity within a protein family and implications for specificity and safety: The case for ETX_MTX2 insecticidal proteins. Journal of Invertebrate Pathology 142:50-59.

Nivetha, L. and H. Jayachandran. 2017. Isolation and identification of *Brevibacillus lactosporum* from soil and evaluation of their antibiotic properties. International Journal of Advanced Research in Biological Sciences 4:93-98.

NZ EPA. 2022. Approval: Lateral (*Brevibacillus laterosporus* strain 1951). Environmental Protection Authority, Wellington, New Zealand.

O'Neill, M.J., L. Bourre, S. Melgar and C.M. O'Driscoll. 2011. Intestinal delivery of non-viral gene therapeutics: Physiological barriers and preclinical models. Drug Discovery Today 16:203-218.

Odell, J.T., F. Nagy and N.-H. Chua. 1985. Identification of DNA sequences required for activity of the cauliflower mosaic virus 35S promoter. Nature 313:810-812.

OECD. 2002a. Report of the OECD workshop on the toxicological and nutritional testing of novel foods. SG/ICGB(1998)1/FINAL. Organisation for Economic Co-operation and Development, Paris, France.

OECD. 2002b. Consensus document on compositional considerations for new varieties of maize (*Zea mays*): Key food and feed nutrients, anti-nutrients and secondary plant metabolites. ENV/JM/MONO(2002)25. Series on the Safety of Novel Foods and Feeds, No. 6. Organisation for Economic Co-operation and Development, Paris, France.

Padgette, S.R., D.B. Re, G.F. Barry, D.E. Eichholtz, X. Delannay, R.L. Fuchs, G.M. Kishore and R.T. Fraley. 1996. New weed control opportunities: Development of soybeans with a Roundup Ready™ gene. Pages 53-84 in Herbicide-Resistant Crops: Agricultural, Environmental, Economic, Regulatory and Technical Aspects. S.O. Duke (ed.). CRC Press, Inc., Boca Raton, Florida.

Panda, A.K., S.S. Bisht, S. DeMondal, N. Senthil Kumar, G. Gurusubramanian and A.K. Panigrahi. 2014. *Brevibacillus* as a biological tool: A short review. Antonie van Leeuwenhoek 105:623-639.

Parrott, W., B. Chassy, J. Ligon, L. Meyer, J. Petrick, J. Zhou, R. Herman, B. Delaney and M. Levine. 2010. Application of food and feed safety assessment principles to evaluate transgenic approaches to gene modulation in crops. Food and Chemical Toxicology 48:1773-1790.

Petrick, J.S., B. Brower-Toland, A.L. Jackson and L.D. Kier. 2013. Safety assessment of food and feed from biotechnology-derived crops employing RNA-mediated gene regulation to achieve desired traits: A scientific review. Regulatory Toxicology and Pharmacology 66:167-176.

Petrick, J.S., G.E. Frierdich, S.M. Carleton, C.R. Kessenich, A. Silvanovich, Y. Zhang and M.S. Koch. 2016. Corn rootworm-active RNA DvSnf7: Repeat dose oral toxicology assessment in support of human and mammalian safety. Regulatory Toxicology and Pharmacology 81:57-68.

Pigott, C.R. and D.J. Ellar. 2007. Role of receptors in *Bacillus thuringiensis* crystal toxin activity. Microbiology and Molecular Biology Reviews 71:255-281.

Prado, J.R., G. Segers, T. Voelker, D. Carson, R. Dobert, J. Phillips, K. Cook, C. Cornejo, J. Monken, L. Grapes, T. Reynolds and S. Martino-Catt. 2014. Genetically engineered crops: From idea to product. Annual Review of Plant Biology 65:769-790.

Rademacher, T.W., R.B. Parekh and R.A. Dwek. 1988. Glycobiology. Annual Review of Biochemistry 57:785-838.

Rausch, K.D., D. Hummel, L.A. Johnson and J.B. May. 2019. Wet milling: The basis for corn biorefineries. Pages 501-535 in Corn: Chemistry and Technology. Third Edition. S.O. Serna-Saldivar (ed.). Woodhead Publishing, Duxford, United Kingdom.

Raybould, A., P. Kilby and G. Graser. 2013. Characterising microbial protein test substances and establishing their equivalence with plant-produced proteins for use in risk assessments of transgenic crops. Transgenic Research 22:445-460.

Ridley, W.P., G.G. Harrigan, M.L. Breeze, M.A. Nemeth, R.S. Sidhu and K.C. Glenn. 2011. Evaluation of compositional equivalence for multitrait biotechnology crops. Journal of Agricultural and Food Chemistry 59:5865-5876.

Rigden, D.J., L.V. Mello and M.Y. Galperin. 2004. The PA14 domain, a conserved all-β domain in bacterial toxins, enzymes, adhesins and signaling molecules. TRENDS in Biochemical Sciences 29:335-339.

Rochester, D.E., J.A. Winer and D.M. Shah. 1986. The structure and expression of maize genes encoding the major heat shock protein, hsp70. EMBO Journal 5:451-458.

Rodrigues, T.B. and J.S. Petrick. 2020. Safety considerations for humans and other vertebrates regarding agricultural uses of externally applied RNA molecules. Frontiers in Plant Science 11:407.

Román-Blanco, C., J.J. Sanz-Gómez, T.-M. López-Díaz, A. Otero and M.-L. García-López. 1999. Numbers and species of *Bacillus* during the manufacture and ripening of Castellano cheese. Milchwissenschaft 54:385-388.

Rooney, L.W. and S.O. Serna-Saldivar. 2003. Food uses of whole corn and dry-milled fractions. Pages 495-535 in Corn: Chemistry and Technology. Second Edition. P.J. White and L.A. Johnson (eds.). American Association of Cereal Chemists, St. Paul, Minnesota.

Rose, A.B. 2008. Intron-mediated regulation of gene expression. Current Topics in Microbiology and Immunology 326:277-290.

Ruiu, L. 2013. *Brevibacillus laterosporus*, a pathogen of invertebrates and a broad-spectrum antimicrobial species. Insects 4:476-492.

Ruiu, L., A. Satta and I. Floris. 2014. Administration of *Brevibacillus laterosporus* spores as a poultry feed additive to inhibit house fly development in feces: A new eco-sustainable concept. Poultry Science 93:519-526.

Russell, S.H., J.L. Hoopes and J.T. Odell. 1992. Directed excision of a transgene from the plant genome. Molecular and General Genetics 234:49-59.

Salomon, S. and H. Puchta. 1998. Capture of genomic and T-DNA sequences during double-strand break repair in somatic plant cells. EMBO Journal 17:6086-6095.

Sarkar, P.K., B. Hasenack and M.J.R. Noun. 2002. Diversity and functionality of *Bacillus* and related genera isolated from spontaneously fermented soybeans (Indian Kinema) and locust beans (African Soumbala). International Journal of Food Microbiology 77:175-186.

Schnepf, E., N. Crickmore, J. van Rie, D. Lereclus, J. Baum, J. Feitelson, D.R. Zeigler and D.H. Dean. 1998. *Bacillus thuringiensis* and its pesticidal crystal proteins. Microbiology and Molecular Biology Reviews 62:775-806.

Shida, O., H. Takagi, K. Kadowaki and K. Komagata. 1996. Proposal for two new genera, *Brevibacillus* gen. nov. and *Aneurinibacillus* gen. nov. International Journal of Systematic Bacteriology 46:939-946.

Sidorov, V. and D. Duncan. 2009. *Agrobacterium*-mediated maize transformation: Immature embryos versus callus. Pages 47-58 in Methods in Molecular Biology: Transgenic Maize - Methods and Protocols. M.P. Scott (ed.). Humana Press, Inc, Totowa, New Jersey.

Silvanovich, A., M.A. Nemeth, P. Song, R. Herman, L.Tagliani and G.A. Bannon. 2006. The value of short amino acid sequence matches for prediction of protein allergenicity. Toxicological Sciences 90:252-258.

Snow, J.W., A.E. Hale, S.K. Isaacs, A.L. Baggish and S.Y. Chan. 2013. Ineffective delivery of diet-derived microRNAs to recipient animal organisms. RNA biology 10:1107-1116.

Stalker, D.M., C.M. Thomas and D.R. Helinski. 1981. Nucleotide sequence of the region of the origin of replication of the broad host range plasmid RK2. Molecular and General Genetics 181:8-12.

Sutcliffe, J.G. 1979. Complete nucleotide sequence of the *Escherichia coli* plasmid pBR322. Cold Spring Harbor Symposia on Quantitative Biology 43:77-90.

Thomas, K., M. Aalbers, G.A. Bannon, M. Bartels, R.J. Dearman, D.J. Esdaile, T.J. Fu, C.M. Glatt, N. Hadfield, C. Hatzos, S.L. Hefle, J.R. Heylings, R.E. Goodman, B. Henry, C. Herouet, M. Holsapple, G.S. Ladics, T.D. Landry, S.C. MacIntosh, E.A. Rice, L.S. Privalle, H.Y. Steiner, R. Teshima, R. van Ree, M. Woolhiser and J. Zawodny. 2004. A multi-laboratory evaluation of a common in vitro pepsin digestion assay protocol used in assessing the safety of novel proteins. Regulatory Toxicology and Pharmacology 39:87-98.

Thomas, K., G. Bannon, S. Hefle, C. Herouet, M. Holsapple, G. Ladics, S. MacIntosh and L. Privalle. 2005. In silico methods for evaluating human allergenicity to novel proteins: International Bioinformatics Workshop Meeting Report, 23-24 February 2005. Toxicological Sciences 88:307-310.

Tuteja, J.H., S.J. Clough, W.-C. Chan and L.O. Vodkin. 2004. Tissue-specific gene silencing mediated by a naturally occurring chalcone synthase gene cluster in *Glycine max*. The Plant Cell 16:819-835.

U.S. EPA. 1988. Guidance for the reregistration of pesticide products containing *Bacillus thuringiensis* as the active ingredient. 540/RS-89-023. U.S. Environmental Protection Agency, Washington, D.C.

U.S. EPA. 2001a. Exemption from the requirement of a tolerance under the Federal Food, Drug, and Cosmetics Act for residues of nucleic acids that are part of plant-incorporated protectants (formerly plant-pesticides). Federal Register 66:37817-37830.

U.S. EPA. 2001b. Biopesticides registration action document - *Bacillus thuringiensis* plant-incorporated protectants. U.S. Environmental Protection Agency, Washington, D.C. http://www.epa.gov/pesticides/biopesticides/pips/bt_brad.htm [Accessed July 24, 2013].

U.S. EPA. 2005. *Bacillus thuringiensi*s Cry3Bb1 protein and the genetic material necessary for its production (Vector ZMIR13L) in event MON 863 corn & *Bacillus thuringiensis* Cry1Ab delta-endotoxin and the genetic material necessary for its production in corn (006430, 006484) fact sheet. U.S. Environmental Protection Agency, Washington, D.C. http://www.epa.gov/pesticides/biopesticides/ingredients_keep/factsheets/factsheet_006430-006484.htm [Accessed September 23, 2013].

U.S. FDA. 1992. Statement of policy: Foods derived from new plant varieties. Federal Register 57:22984-23005. U.S. Food and Drug Administration, Washington, D.C.

U.S. FDA. 2001. Premarket notice concerning bioengineered foods. Federal Register 66:4706-4738.

USDA-FAS. 2022. Grain: World markets and trade. August 2020. U.S. Department of Agriculture, Foreign Agricultural Service, Washington, D.C. https://apps.fas.usda.gov/psdonline/circulars/grain-corn-coarsegrains.pdf [Accessed February 25, 2022].

Venkatesh, T.V., M.L. Breeze, K. Liu, G.G. Harrigan and A.H. Culler. 2014. Compositional analysis of grain and forage from MON 87427, an inducible male sterile and tissue selective glyphosate-tolerant maize product for hybrid seed production. Journal of Agricultural and Food Chemistry 62:1964-1973.

Viswanathan, V.K., K. Krcmarik and N.P. Cianciotto. 1999. Template secondary structure promotes polymerase jumping during PCR amplification. BioTechniques 27:508-511.

Wang, C., K.C. Glenn, C. Kessenich, E. Bell, L.A. Burzio, M.S. Koch, B. Li and A. Silvanovich. 2016. Safety assessment of dicamba mono-oxygenases that confer dicamba tolerance to various crops. Regulatory Toxicology and Pharmacology 81:171-182.

Watson, S.A. 1988. Corn marketing, processing, and utilization. Pages 881-940 in Corn and Corn Improvement. Third Edition. G.F. Sprague and J.W. Dudley (eds.). American Society of Agronomy, Inc., Crop Science Society of America, Inc., Soil Science Society of America, Inc., Madison, Wisconsin.

Wesche, J., J.L. Elliott, P.O. Falnes, S. Olsnes and R.J. Collier. 1998. Characterization of membrane translocation by anthrax protective antigen. Biochemistry 37:15737-15746.

WHO. 1999. Microbial pest control agent: *Bacillus thuringiensis*. Environmental Health Criteria 217. World Health Organization, Geneva, Switzerland. http://www.inchem.org/documents/ehc/ehc/ehc217.htm [Accessed May 14, 2009].

Witwer, K.W., M.A. McAlexander, S.E. Queen and R.J. Adams. 2013. Real-time quantitative PCR and droplet digital PCR for plant miRNAs in mammalian blood provide little evidence for general uptake of dietary miRNAs: Limited evidence for general uptake of dietary plant xenomiRs. RNA Biology 10:1080-1086.

Xing, A., B.P. Moon, K.M. Mills, S.C. Falco and Z. Li. 2010. Revealing frequent alternative polyadenylation and widespread low-level transcription read-through of novel plant transcription terminators. Plant Biotechnology Journal 8:772-782.

Xu, C., U. Chinte, L. Chen, Q. Yao, Y. Meng, D. Zhou, L.-J. Bi, J. Rose, M.J. Adang, B.-C. Wang, Z. Yu and M. Sun. 2015. Crystal structure of Cry51Aa1: A potential novel insecticidal aerolysin-type β-pore-forming toxin from *Bacillus thuringiensis*. Biochemical and Biophysical Research Communications 462:184-189.

Yang, L., C. Wang, A. Holst-Jensen, D. Morisset, Y. Lin and D. Zhang. 2013. Characterization of GM events by insert knowledge adapted re-sequencing approaches. Scientific Reports 3:2839.

Yin, Y., S. Flasinski, W. Moar, D. Bowen, C. Chay, J. Milligan, J.-L. Kouadio, A. Pan, B. Werner, K. Buckman, J. Zhang, G. Mueller, C. Preftakes, B.E. Hibbard, P. Price and J. Roberts. 2020. A new *Bacillus thuringiensis* protein for Western corn rootworm control. PLoS ONE 15:e0242791.

Zambryski, P., A. Depicker, K. Kruger and H.M. Goodman. 1982. Tumor induction by *Agrobacterium tumefaciens*: Analysis of the boundaries of T-DNA. Journal of Molecular and Applied Genetics 1:361-370.

Zastrow-Hayes, G.M., H. Lin, A.L. Sigmund, J.L. Hoffman, C.M. Alarcon, K.R. Hayes, T.A. Richmond, J.A. Jeddeloh, G.D. May and M.K. Beatty. 2015. Southern-by-sequencing: A robust screening approach for molecular characterization of genetically modified crops. The Plant Genome 8:1-15.

Zhang, L., D. Hou, X. Chen, D. Li, L. Zhu, Y. Zhang, J. Li, Z. Bian, X. Liang, X. Cai, Y. Yin, C. Wang, T. Zhang, D. Zhu, D. Zhang, J. Xu, Q. Chen, Y. Ba, J. Liu, Q. Wang, J. Chen, J. Wang, M. Wang, Q. Zhang, J. Zhang, K. Zen and C.-Y. Zhang. 2012a. Exogenous plant MIR168a specifically targets mammalian LDLRAP1: Evidence of cross-kingdom regulation by microRNA. Cell Research 22:107-126.

Zhang, L., X.-Z. Li and K. Poole. 2001. SmeDEF multidrug efflux pump contributes to intrinsic multidrug resistance in *Stenotrophomonas maltophilia*. Antimicrobial Agents and Chemotherapy 45:3497-3503.

Zhang, W., S. Subbarao, P. Addae, A. Shen, C. Armstrong, V. Peschke and L. Gilbertson. 2003. Cre/*lox*-mediated marker gene excision in transgenic maize (*Zea mays* L.) plants. Theoretical and Applied Genetics 107:1157-1168.

Zhang, Y., B.E. Wiggins, C. Lawrence, J. Petrick, S. Ivashuta and G. Heck. 2012b. Analysis of plant-derived miRNAs in animal small RNA datasets. BMC Genomics 13:381.

Zhou, J., G.G. Harrigan, K.H. Berman, E.G. Webb, T.H. Klusmeyer and M.A. Nemeth. 2011. Stability in the composition equivalence of grain from insect-protected maize and seed from glyphosate-tolerant soybean to conventional counterparts over multiple seasons, locations, and breeding germplasms. Journal of Agricultural and Food Chemistry 59:8822-8828.